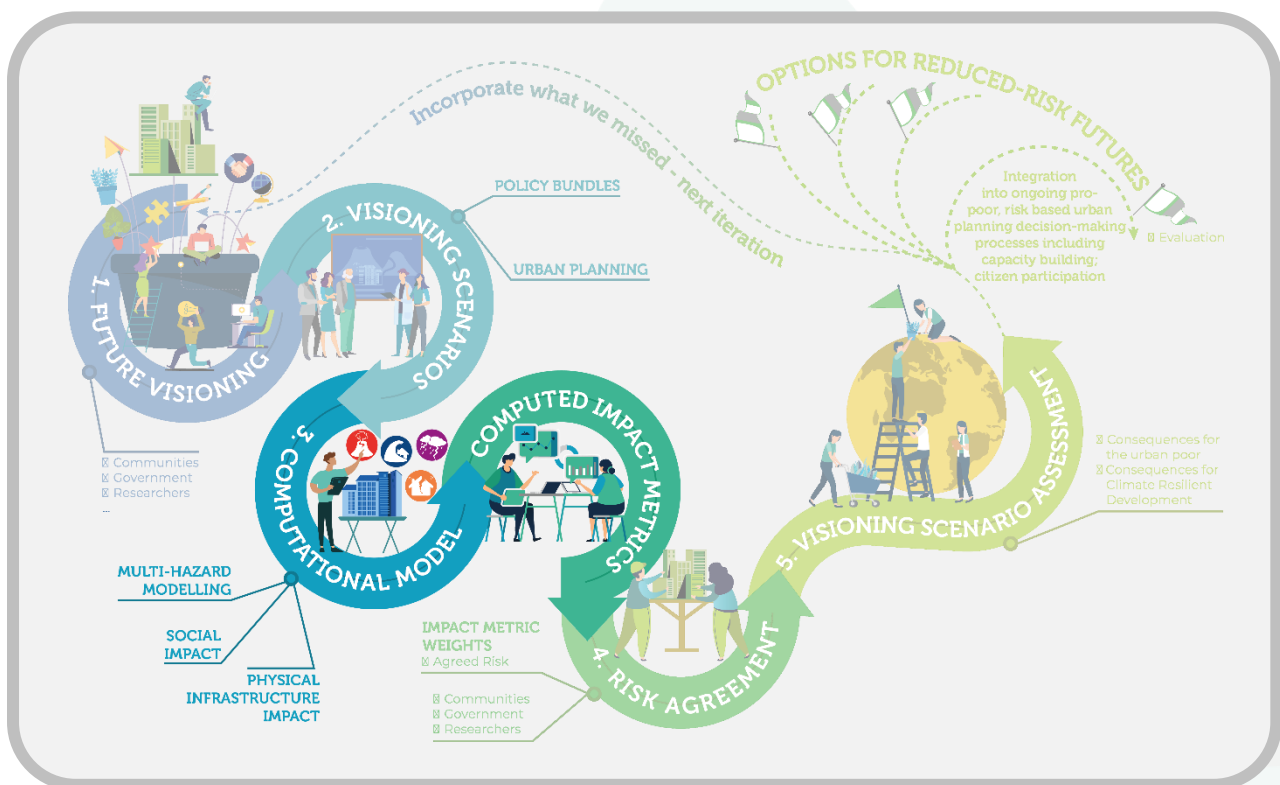


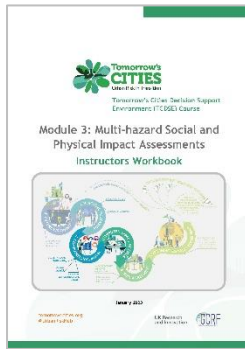


Tomorrow's Cities Decision Support Environment (TCDSE) Course

Module 3: Multi-hazard Physical and Social Impact Assessments Workbook



March 2024



Workbook

Module 3: Multi-hazard Physical and Social Impact Assessments

Authors

Mr. Vibek Manandhar, Research Associate (Module 3 Lead)

Dr. Gemma Cremen, Work Package 3 Lead

Dr. Jeremy Phillips, Work Package 3 Lead

Mr. Prayash Malla, Research Associate

Dr. Prashant Rawal, Post Doctoral Researcher

Dr. Vishnu Prasad Pandey, Professor, Tribhuvan University

Ms. Januka Gyawali, Researcher

Dr. Maggie Creed, Lecturer, University of Glasgow

Dr. C. Scott Watson, Post Doctoral Researcher

Dr. Luke Jenkins, Post Doctoral Researcher

Dr. Camilo Zapata, Researcher

Dr. Elizabeth Holcombe, Co-investigator-Quito

Dr. Basanta Raj Adhikari, City Co-ordinator-Kathmandu

Ms. Sneha Bhatta, Researcher

Ms. Dibya Laxmi Subedi, Researcher

Ms. Rojina Haiju, Researcher

Dr. Fabrizio Nocera, Post Doctoral Researcher

Dr. Leandro Iannacone, Post Doctoral Researcher

Dr. Ryerson Christie, Researcher

Dr. Emin Yahya Mentese, Work Package 2 Lead

Dr. Hüseyin Kaya, Researcher

Reviewers

Dr. Gemma Cremen, Work Package 3 Lead

Dr. Jeremy Phillips, Work Package 3 Lead

Dr. Ramesh Guragain, Capacity Strengthening Lead

Ms. Rajani Prajapati, Capacity Strengthening Expert

Guidance & Support

Tomorrow's Cities' Senior Management Team (SMT)

Work Package 3: Multi-hazard Physical and Social Impact Assessments Development teams from learning cities: Kathmandu, Istanbul, Nairobi and Quito

Graphic Design

Chandan Dhoj Rana Magar, NSET

Date of Publication: August 2024

Publication Series No.: NSET-161-2024

This material has been developed and published by NSET under UKRI GCRF Urban Risk Hub: Tomorrow's Cities, a research project.

Citation: Manandhar et al. (2024). Workbook of Module 3: Multi-hazard Physical and Social Impact Assessments. Tomorrow's Cities Disaster Risk Hub.

PREFACE

This workbook on Module M3: “Multi-hazard Physical and Social Impact Assessments of Tomorrow’s Cities Decision Support Environment (TCDSE) course” has been developed under the Capacity Strengthening program on Tomorrow’s Cities Decision Support Environment (TCDSE) Course of the Tomorrow’s Cities (TC) project. This course aims to enhance the capacity of professionals from the Tomorrow’s Cities and urban areas in utilizing the TCDSE and expand its reach so that the cities or urban areas can then adapt the framework based on scenarios specific to them and ultimately self-sustain.

This workbook serves as a training manual for Module 3: Multi-hazard Physical and Social Impact Assessments of Tomorrow’s Cities Decision Support Environment (TCDSE) course. The module is aimed to enable the participants to interpret the components of the computational model and to familiarize them with the developed TC Computational Platform aided by a demonstration, which is a crucial component of the Module.

The components of the computational model under TCDSE includes hazard modelling, physical and social impact assessment, and their interpretation through impact metrics. The target audiences of this module are city officials, academicians, government and non-government personnel, private sector, TC members or other stakeholders associated with building and macro infrastructure, utility and service infrastructure, housing, hazard assessment, physical infrastructure impact assessment, social impact assessment etc.

The module consists of 15 sessions on various hazard modelling like earthquake, flood, debris flow, landslide, fire and climate change, physical impact assessments, social impact assessment, characterization of impact metrics and demonstration of computational platform, which were developed based on learnings from the TCDSE implementing cities. Sessions on hazard modelling which are only relevant for the city can be delivered selectively in the training of this module. For this the module lead shall consult with the city lead on prevalent hazards which can pose risk and on the need for hazard studies in the city.

The course includes an overview on the objectives and processes of the key components of Work Package 3 of the TCDSE, Multi-hazard Physical and Social Impact Assessments, describing how it takes its inputs from TCDSE Work Package 2 - Visioning Scenario and feeds its to the next step, TCDSE Work Package 4 - Risk Agreement. The module will be using various examples from TCDSE cities, including different methods used for multi-hazard Physical and Social impact assessment process in different cities. Apart from theoretical sessions, there are exercises, group discussions, demonstration, case-studies, process-mapping, learnings and experiences in the hub cities, and learnings from Tomorrow Ville facilitating skill development of the participants.

The goal of this module is to empower participants with the tools and expertise needed to interpret the process of Multi-hazard Physical and Social Impact Assessments. Whether participants are professionals seeking to deepen their understanding or a newcomer eager to explore new horizons, this module offers something valuable for everyone.



Table of Content

PREFACE	IV
ABBREVIATIONS	XVII
SESSION 1: INTRODUCTION	1
1.1 Objectives.....	1
1.2 Structure of Session 1	1
1.3 Purpose, Objective and content of Module 3: Multi-hazard Physical and Social Impact Assessment	2
1.3.1 Introduction to Tomorrow’s Cities Decision Support Environment (TCDSE)....	2
1.3.2 Purpose of M3	4
1.3.3 Objectives of M3.....	4
1.3.4 Target Audience of M3.....	4
1.3.5 Contents of M3.....	4
1.4 Prerequisite Concepts for the Module	5
1.4.1 Concept of Risk	5
1.5 Components of Module 3	6
1.5.1 Prerequisites for the Computational Model	6
1.5.2 Illustration through Tomorrowville	6
1.5.3 The Computational Model.....	7
1.5.4 Computed Impact Metrics.....	10
1.5.5 Outputs of the Computational Model.....	11
SESSION 2: SEISMIC HAZARD MODELLING	12
2.1 Objectives.....	12
2.2 Structure of Session 2	12
2.3 Understanding Earthquakes	12
2.3.1 Structure of the Earth	12
2.3.2 Cause of Earthquakes: Plate Tectonics	13
2.3.3 Global Seismic Hazard	13
2.3.4 Terminologies Related to the Source of Earthquakes	14
2.3.5 Types of Seismic Waves	14
2.4 Seismic Hazard Analysis and Its Use in Risk Assessment	17
2.4.1 Seismic Hazard Analysis (SHA).....	17
2.4.2 Use of Seismic Hazard Analysis in Risk Assessment	23
2.5 Scenario Based Seismic Hazard Analysis (SSHA).....	25
2.5.1 Introduction	25
2.5.2 Scenario Based Seismic Hazard Analysis in Openquake Engine.....	25
2.5.3 Seismic Risk Calculation in Openquake Engine	30
2.5.4 An Overview of Preparing Input in Openquake	30
2.6 Physics Based Seismic Hazard Analysis	38
2.6.1 Advantages of Physics-based Simulations.....	38
2.6.2 Data and Models Required for Physics-based Simulations.....	39



2.6.3	Example of Physics-based Seismic Model in Tomorrowville	40
SESSION 3: FLOOD HAZARD MODELLING		42
3.1	Objectives.....	42
3.2	Structure of Session 3	42
3.3	Concept of Hazard, Vulnerability and Risk	42
3.3.1	Flood Hazards	42
3.3.2	Drivers of Flood Hazards	42
3.3.3	Hazard, Vulnerability and Risk Associated with Flood.....	42
3.4	Flood Hazard Modelling	43
3.4.1	Approaches for Flood Mapping	43
3.4.2	Community Based Flood Mapping	44
3.4.3	Empirical Modelling	45
3.4.4	Physics-based Modelling.....	45
3.5	Physics-Based Modelling in Tomorrow’s Cities	46
3.5.1	Data Collection and Model Input Requirements:	47
3.5.2	Pre-processing:	47
3.5.3	Model Runs:	47
3.5.4	Post-processing:	47
3.6	Impact Of Data Resolution of Flood Modelling	48
3.6.1	DEMs	48
3.7	Validation of Flood Hazard Maps	52
SESSION 4: DEBRIS FLOW MODELLING		53
4.1	Objectives.....	53
4.2	Structure of Session 4	53
4.3	Introduction.....	53
4.3.1	Characteristics of Debris Flow.....	53
4.3.2	Initiation of Debris Flow.....	54
4.4	Components of Debris Flow Modelling.....	54
4.4.1	Model Source Conditions	54
4.4.2	Model Ingredients and Assumptions	56
4.4.3	Model Inputs.....	57
4.4.4	Model Outputs.....	58
SESSION 5: LANDSLIDE HAZARD MODELLING		59
5.1	Objectives.....	59
5.2	Structure of Session 5	59
5.3	Landslide Hazard Assessment: Scope of Landslide Problem and Local Capacity	59
5.3.1	Landslides and Diagnosis on Its Types and Interactions	59
5.3.2	Landslide Assessment Methods	62
5.3.3	Decision-Support and Research Gaps.....	66
5.4	City-Wide Landslide Hazard Assessment: Landslide Problem Definition	67
5.4.1	GIS-based Landslide Assessment in Kathmandu: Methodology and Input.....	67
5.4.2	Susceptibility Models/ GIS Tools Used	70



5.4.3	Expected Outputs	70
5.4.4	Uncertainties	71
5.5	Examples of Physics-Based Modelling for Quantifying the Local Hazard	71
5.5.1	Everyday Landslide Hazards	71
5.5.2	Representing Urban Slopes and Dynamic Hydrology	73
5.5.3	Modelling Urban Landslide Scenarios with Limited Data	74
SESSION 6: FIRE HAZARD MODELLING.....		78
6.1	Objectives.....	78
6.2	Structure of Session 6	78
6.3	Fire Dynamics.....	78
6.3.1	Small scale physics of fire.....	78
6.3.2	Causes of fire	79
6.3.3	Measurement of fire	80
6.3.4	Stages of fire	80
6.3.5	Heat transfer	81
6.3.6	Fire development.....	82
6.4	Fire Modelling	83
6.4.1	Compartment fire	83
6.4.2	Approaches of fire modelling	84
6.4.3	Physics-based fire modelling	86
6.4.4	Uses of fire spread modelling	88
6.5	Wildland-Urban Interface Fire	88
6.5.1	Factors affecting wildfires	89
6.6	A Case Study on Fire Hazard Assessment	89
6.6.1	Fire hazard assessment in Tamakoshi Rural Municipality, Nepal using Analytic Hierarchy Process (AHP) approach.....	89
6.7	General Provisions for Fire Safety.....	91
6.7.1	Layers of fire safety in buildings and settlements	91
6.7.2	Wildland-Urban Interface (WUI) fire safety provisions	92
SESSION 7: CLIMATE CHANGE.....		93
7.1	Objectives.....	93
7.2	Structure of Session 7	93
7.3	Climate Change and Climate Extremes.....	93
7.3.1	Introduction	93
7.4	Case Study: Climate Change Effects on Rainfall Extremes in Kathmandu Valley Catchment	96
7.4.1	Description of Kathmandu Valley Catchment	96
7.4.2	Approach: Rainfall Extremes under Future Climate Change with Implications for Urban Flood Risk.....	96
SESSION 8: VULNERABILITY MODELLING - SINGLE HAZARD		100
8.1	Objectives.....	100
8.2	Structure of Session 8	100



8.3	Introduction.....	100
8.3.1	Vulnerability within Catastrophe Risk.....	102
8.4	Fragility Analysis	102
8.4.1	Uncertainties	103
8.4.2	Random Variables	104
8.4.3	Capacity and Demand.....	106
8.4.4	Reliability Analysis	106
8.4.5	Monte Carlo Simulations.....	107
8.4.6	Fragility Curves	107
8.4.7	Damage/ Vulnerability Curves.....	108
8.4.8	Portfolio Assessment.....	108
8.5	Fragility/ Vulnerability Curves for Earthquakes	109
8.5.1	Steps in Probabilistic Seismic Hazard Analysis (PSHA).....	109
8.5.2	Ground Motion Prediction Equation (GMPE).....	110
8.5.3	Exposure	111
8.5.4	Building Damage Estimation	112
8.5.5	Damage State Definition	113
8.5.6	Analytical Method of Development of Fragility Curves.....	115
8.6	Fragility/ Vulnerability Curves for Floods.....	119
8.6.1	Analytical Method of Development of Fragility Curves.....	119
SESSION 9: VULNERABILITY MODELLING – MULTI HAZARD.....		123
9.1	Objectives.....	123
9.2	Structure of Session 9	123
9.3	Introduction.....	123
9.3.1	Hazard Interactions	123
9.4	Hazard Interactions: Level I Interactions	129
9.4.1	Mathematical Modelling	129
9.5	Hazard Interactions: Level II Interactions	141
9.5.1	Mathematical Modelling	141
SESSION 10:VULNERABILY MODELLING – MODEL SELECTION		145
10.1	Objectives.....	145
10.2	Structure of Session 10.....	145
10.3	Physical Impact Models for Different Hazards.....	145
10.3.1	Earthquake Induced Ground Shaking	145
10.3.2	Flooding and Mass Movement Hazards	145
10.4	Characterization Procedure for Physical Impact Models	146
10.4.1	Preliminary phase: defining the exposure taxonomy string of the considered asset classes.....	147
10.4.2	Screening Phase: Selecting Candidate Physical Impact Models	149
10.4.3	Scoring and Ranking Phase: Selecting the Most Suitable Models.....	151
10.5	Example- Application on Tomorrowville	157
10.5.1	Description of the case study.....	157
10.5.2	Exposure Characterization	158



10.5.3 Modelling Choices and User Requirements for the Procedure.....	161
10.5.4 Selected Physical Impact Models.....	162
SESSION 11: NETWORK ANALYSIS.....	165
11.1 Objectives.....	165
11.2 Structure of Session 11.....	165
11.3 Network Representation of Infrastructure.....	165
11.3.1 Motivations	165
11.3.2 Graphs and Networks	165
11.3.3 Infrastructure Modelling Definitions.....	165
11.3.4 Need for Network Reliability	167
11.4 Types of Infrastructure Analysis.....	168
11.4.1 Topology-based Approaches	169
11.4.2 Flow-based Approaches	170
11.5 Infrastructure Performance Assessment in Post-Hazard Conditions	171
11.6 Exercises	171
11.6.1 Exercise 1: Infrastructure Representation - Adjacency matrix	171
11.6.2 Exercise 2: Topology Metrics - Computing Diameter and Efficiency	172
11.6.3 Exercise 3: Infrastructure Performance Assessment in Post-hazard conditions - Changes in Network Performance	172
SESSION 12: SOCIAL IMPACT	174
12.1 Objectives.....	174
12.2 Structure of Session 12.....	174
12.3 Social Vulnerability	174
12.3.1 Factors Shaping Social Vulnerabilities	174
12.3.2 Capturing Social Impact	174
12.3.3 Process to Assess Social Impact	175
12.4 Quantitative Methodology for Social Data Capture and Input	176
12.4.1 Impact of Urban Planning on Social Vulnerability.....	177
12.4.2 Keys Ideas and Example Methodology.....	177
12.4.3 Identification of Data Inputs and Impacts	179
12.4.4 Gap Identification and Address through Modelling.....	180
12.5 Utilising Development Proxies to Inform Social Vulnerability and Impact.....	182
12.5.1 Assessing Changes to Vulnerability over Time	182
12.5.2 Assessing Social Impact using Changes to the Built Environment as Proxies	182
12.5.3 Applying the Built Environment Proxies	183
SESSION 13: CHARACTERISING IMPACT METRICS	184
13.1 Objectives.....	184
13.2 Structure of Session 13.....	184
13.3 Determining Relevant Natural Hazard Impacts for the City	184
13.3.1 Methods to Identify the Potential Natural Hazards	184



13.3.2 Possible Data Sources to Understand the Socio-economic and Demographic Context.....	184
13.3.3 List of Potential Impacts	185
13.4 Characterisation of Relevant Impact Metrics.....	185
13.4.1 Impact Metric	185
13.4.2 Characterising Impact Metrics.....	186
13.5 Use of Computational Platform to Compute Impact Metrics.....	186
SESSION 14:END-TO-END DEMONSTRATION OF COMPUTATIONAL PLATFORM.....	187
14.1 Objectives.....	187
14.2 Structure of Session 14.....	187
14.3 Introduction.....	187
14.3.1 Background on the Computational Platform	187
14.3.2 Installation Requirements.....	187
14.3.3 Process of Computing Impact using the Platform	187
14.4 Computing Impact Using the Platform	188
14.4.1 Main Screen.....	188
14.5 TUTORIAL	196
SESSION 15:LINKAGE OF MODULE 3 WITH OTHER MODULES	199
15.1 Objectives.....	199
15.2 Structure of Session 15.....	199
15.3 Introduction.....	199
15.3.1 Recap of Module 3.....	199
15.3.2 Computed Impact Metrics.....	201
15.4 Linkage Of Module 3 With Other Modules.....	201
15.4.1 Linkage with Module 2	201
15.4.2 Linkage with Module 4.....	202
REFERENCE	203



LIST OF FIGURES

Figure 1: Summary of Tomorrow’s Cities Decision Support Environment	2
Figure 2: Prerequisites and results of the computational model.....	6
Figure 3: Visioning scenarios of future Tomorrowville	7
Figure 4: Scenarios for different hazards in Tomorrowville.....	8
Figure 5: Development of earthquake fragility curves for various building system in Nepal	9
Figure 6: Illustration of how one sample of a Computed Impact Metric is determined ...	10
Figure 7: Inputs and outputs of the computational model	11
Figure 8: Movements and velocities of tectonic plates	13
Figure 9: Global seismic hazard map	14
Figure 10: Source of earthquake	14
Figure 11: Particle motion in P-wave	15
Figure 12: Particle motion in S-wave.....	15
Figure 13: Particle motion in Love wave	16
Figure 14: Particle motion in Rayleigh wave.....	16
Figure 15: Seismic waves recorded in seismogram.....	17
Figure 16: Evolution of fault models in California from 1988 to 2014	21
Figure 17: Path and site effects on ground motion	21
Figure 18: Spectral acceleration of a structure as a function of the distance from the earthquake source	22
Figure 19: Local site effect: amplification in ground motion intensity measure PGA can be seen due to soil deposit	23
Figure 20: Fragility curve for non-engineered RC building (HAZUS).....	24
Figure 21: Vulnerability curves for stone in mud masonry buildings and non-engineered RC buildings.....	24
Figure 22: Components of seismic hazard and risk assessment	25
Figure 23: Rupture parameters	26
Figure 24: Rupture model for Mw 7.9 Gorkha earthquake (April 25, 2015) in Nepal based on Yagi and Okuwaki 2015	27
Figure 25: Rupture model for Mw 7.4 Izmit earthquake (Aug 17, 1999) in Turkey based on Reilinger et al. (2000)	28
Figure 26: Rupture model for Mw 8.4 Tokachi-Oki earthquake (Mar 04, 1952) in Japan based on Kobayashi et al 2021	28
Figure 27: Rupture model for Mw 9.2 Sumatra-Andaman earthquake (Dec 26, 2004) in the Indian Ocean based on Rhie et al 2007	29
Figure 28: Seismic hazard maps for various scenarios - Tamakoshi	36
Figure 29: Building damage (extensive) distribution - Tamakoshi.....	36
Figure 30: Number of buildings damaged (wardwise) - Tamakoshi.....	37



Figure 31: Building damage distribution (typology) - Tamakoshi 37

Figure 32: Human casualties - Tamakoshi 38

Figure 33: Physics-based simulation of ground motion..... 39

Figure 34: Rupture directivity effect..... 39

Figure 35: Effect of asperity..... 39

Figure 36: Physics-based simulation in Tomorrowville 41

Figure 37: Community Risk Mapping..... 44

Figure 38: Numerical model output of flood map..... 46

Figure 39: Volcanic debris flow in Semeru, Indonesia 53

Figure 40: Erosion and deposition in debris flow 56

Figure 41: Outputs of debris flow model 58

Figure 42: Types of landslides..... 60

Figure 43: Photographs of landslides..... 60

Figure 44: Collage of pictures about the process of community-based mapping in Quito-Ecuador..... 62

Figure 45: Landslide susceptibility map of Kathmandu 63

Figure 46: Rocscience SLIDE 6.0 64

Figure 47: Newmark displacements zonation in ravine considered a hotspot of landslide occurrence..... 65

Figure 48: Hazard zonation of earthquake-induced landslides by a deterministic seismic event with epicenter in the local fault system ($M_w = 5.9$) during the dry season 66

Figure 49: Kathmandu DEM (2 * 2 m) 68

Figure 50: Landslide Inventory, Kathmandu 69

Figure 51: Methodology of GIS-based Landslide Assessment. 69

Figure 52: Area Under Curve (AUC) for Model Validation 71

Figure 53: Variation in results from different models, a) Heuristic Model, b) IV Model, c) FR Model..... 71

Figure 54: Landslide inventory and urban growth map from 1900 to 2020 in Quito. 72

Figure 55: Side view of an informal neighborhood located in the pro-landslide zone. 73

Figure 56: Inputs and outputs of Combined Hydrology and Slope Stability Model. 74

Figure 57: Modelling scenario of urban slopes 74

Figure 58: Rainfall intensity with returned periods..... 75

Figure 59: Landslide sources for debris flow hazard assessment, considering several rainfalls scenarios 76

Figure 60: Debris flow simulation using rainfall with retuned period of 50 years 77

Figure 61: Illustration of fire triangle..... 78

Figure 62: Stages of fire..... 81

Figure 63: Conduction of heat..... 81



Figure 64: Convection of heat..... 82

Figure 65: Radiation of heat..... 82

Figure 66: Multi-scale fire triangles describing the elements of wildland fire at the scale of the flame, a wildfire, and a fire regime 82

Figure 67: Typical curve of the Heat Release Rate in a fuel-limited fire 84

Figure 68: In a building, a fire can A) spread through openings, B) burn through combustible walls, C) leapfrog from one window to the next, D) spread over combustible cladding..... 86

Figure 69: In urban settings, fire can spread through direct flame contact, thermal radiation, firebrands of a combination of all three mechanisms. 87

Figure 70: Annual average fire density 2000-2020 89

Figure 71: Methodology flowchart for fire hazard assessment using AHP method 90

Figure 72: Fire hazard map developed for Tamakoshi Rural Municipality, Nepal..... 91

Figure 73: Emission scenarios in the future with each Representative Concentration Pathways (RCPs) 94

Figure 74: Hazard Map..... 100

Figure 75: Global insured natural catastrophe losses by peril (left) and flood losses by decade (right)..... 101

Figure 76: Examples of fragility curves for different damage states 103

Figure 77: Probability Mass Function associated with the result of the two dice roll..... 104

Figure 78: Probability Density Function of the height of a person 105

Figure 79: Cumulative Distribution Function (CDF) 105

Figure 80: 2D Probability Density Function 106

Figure 81: Joint PDF of capacity and demand, and definition of failure and safe domain 107

Figure 82: Fragility curves 107

Figure 83: Example of damage curve for wind hazard 108

Figure 84: Portfolio Assessment..... 109

Figure 85: Path and site effects on ground motion 110

Figure 86: Spectral acceleration of a structure as a function of the distance from the earthquake source 111

Figure 87: Damage scales across various standards..... 113

Figure 88: Typical pushover analysis 116

Figure 89: Thresholds between different damage states 116

Figure 90: Recorded ground motion and Peak Ground Acceleration (PGA) 117

Figure 91: Procedure to obtain the response spectrum..... 118

Figure 92: Determination of maximum displacement 118

Figure 93: Generation of fragility curves..... 119

Figure 94: Determination of demand due to flooding hazard 120

Figure 95: Hydrograph calculation..... 120



Figure 96: Content inventory for a household	121
Figure 97: Component based flood damage estimation	122
Figure 98: Spatial and temporal scale of several hazards	124
Figure 99: Performance measure of the system over time	124
Figure 100: Performance measure of the system over time for independent hazard	125
Figure 101: Site effects and physical impact of hazards	128
Figure 102: Types of interaction	129
Figure 103: Interactions through the nature of the hazard (level I interactions)	130
Figure 104: Simplified interaction matrix.....	131
Figure 105: Gutenberg-Richter law	132
Figure 106: An occurrence curve	132
Figure 107: Earthquake hazard curve.....	133
Figure 108: Hazard surface for a rainfall event (intensity measures are the rainfall height and duration).....	133
Figure 109: Poisson process for simulation of a sequence of events	134
Figure 110: Generation of CDF of the event characteristic/ intensity measure M.....	135
Figure 111: An example for modelling of concurrent hazard for wind-snow.....	136
Figure 112: Probability of a secondary hazard given a specific type of volcanic eruption (left), and variability of the characteristics of the secondary hazard (right). 137	137
Figure 113: Flowchart summarizing the scenario simulation	139
Figure 114: Data for the numerical example. Occurrence curves of primary hazards, interaction taxonomy, and conditional occurrence curves for each of the interactions.	140
Figure 115: One scenario realization was obtained using the procedure in Figure and data above.	140
Figure 116: Example of transition probability matrix.....	142
Figure 117: FEMA damage scales and measurable consequences	143
Figure 118: Damage states following flood	144
Figure 119: Methodology to score and select physical impact models for a given asset class	146
Figure 120: Considerations in Multi-hazard taxonomy string (GED4ALL).....	147
Figure 121: Organization into hierarchical structure	151
Figure 122: Hierarchical organization for selecting suitable daily meal package	152
Figure 123: Graph showing criteria weightage calculated from AHP	154
Figure 124: TOPSIS decision-making	155
Figure 125: Methodology to score and select physical impact models for a given asset class	158
Figure 126: Building-class attributes of the TV50_total scenario in Tomorrowville: a) Occupancy type; b) Material and lateral load resisting system; c) Height; d) Code level	160



Figure 127: Structure of process to assess social impact..... 175

Figure 128: Impact modelling for gap identification..... 181

Figure 129: Process for computing impact..... 188

Figure 130: Main screen of the application..... 188

Figure 131: Computational modeling page 189

Figure 132: Exposure data requirements for every layer..... 190

Figure 133: Exposure data validity for every layer..... 190

Figure 134: Exposure data sample dataset for every layer 191

Figure 135: Vulnerability data requirements..... 191

Figure 136: Vulnerability data examples..... 192

Figure 137: Hazard data requirements..... 192

Figure 138: Hazard data examples..... 193

Figure 139: Other buttons 193

Figure 140: Policy page 194

Figure 141: Numerical results example 195

Figure 142: Disaggregation example..... 195

Figure 143: Map illustration example..... 196

Figure 144: Loading exposure data from the corresponding path 196

Figure 145: Loading data, and validate all 197

Figure 146: Policies screen..... 198

Figure 147: Summary of Tomorrow’s Cities Decision Support Environment 199

Figure 148: Scenarios for different hazards in Tomorrowville..... 200

Figure 149: Typical Fragility Curve 201

Figure 150: Computed impact metrics for a visioning scenario 201

LIST OF TABLE

Table 1: Contents of Module 3: Multi-hazard Physical and Social Impact Assessment 5

Table 2: Typical DEM characteristics. Note that minimum order sizes usually apply to costings..... 49

Table 3: Runoff coefficients for land use types..... 55

Table 4: Example parameters..... 57

Table 5: Types of landslide movements..... 59

Table 6: Methodology and input parameters of GIS-based Landslide Assessment in Kathmandu 68

Table 7: ETCCDI extreme value indices 95

Table 8: Precipitation related indices calculated in terms of intensity, frequency and duration 97



Table 9:	Characteristics of different methods on fragility functions development	112
Table 10:	Qualitative description of building-specific damage states (FEMA P-58).....	114
Table 11:	Qualitative description of damage states (Eurocode)	114
Table 12:	Qualitative description of damage states (Dolsek and Fajfar, 2008 [14]).....	115
Table 13:	GED4ALL attributes for buildings exposed to various hazards	148
Table 14:	GED4ALL attributes for bridges exposed to various hazards	148
Table 15:	Examples of GED4ALL taxonomy strings	149
Table 16:	Model screening criteria: minimum thresholds for acceptance [N_{ds} , R_{im} , N_{hp} are defined by the user; example values: $N_{ds}= 1$, $R_{im}=20$, $N_{hp}= 80$]	150
Table 17:	Available interactive databases.....	150
Table 18:	Available non-interactive databases and model compendia	151
Table 19:	Scale of relative importance	152
Table 20:	Calculated criteria weightage.....	154
Table 21:	Adopted Exposure Taxonomy Attributes, considering the GED4ALL and the Simplified Ad-hoc Taxonomies	158
Table 22:	Adopted Weights for TOPSIS.....	161
Table 23:	Values Assigned to Scores.....	161
Table 24:	Model Ranking for the CP+CIP/LFINF+CDM/H:6/YBET: 1994:2015 (RCi+MC+6s+Res) building class	163
Table 25:	Description of infrastructure modelling terms	166



ABBREVIATIONS

DRR	Disaster Risk Reduction
TCDSE	Tomorrow's Cities Decision Support Environment
SHA	Seismic Hazard Analysis
SSHA	Scenario-based Seismic Hazard Analysis
PSHA	Probabilistic Seismic Hazard Analysis
GMPE	Ground Motion Prediction Equation
GCM	General Circulation Models
RCM	Regional Climate Models
CMIP	Coupled Model Inter-comparison Project
RCP	Representative Concentration Pathways
SSP	Shared Socioeconomic Pathways
ETCCDI	Expert Team on Climate Change Detection and Indices
AUC	Area Under Curve
DEM	Digital Elevation Model
DSM	Digital Surface Model
SC	Source Condition
DSE	Decision Support Environment
GIS	Geographic Information System
CHASM	Combined Hydrology and Stability Model
FS	Factor of Safety
LPG	Liquid Petroleum Gas
HRR	Heat Release Rate
CFD	Computational Fluid Dynamics
FDS	Fire Dynamics Simulator
AHP	Analytic Hierarchy Process
WUI	Wildland-Urban Interface
DS	Damage State
CDF	Cumulative Distribution Function
PDF	Probability Distribution Function
MVI	Multi-dimension Vulnerability Index
SoVI	Social Vulnerability Indexing
IM	Impact Metrics





SESSION 1: INTRODUCTION

1.1 Objectives

The major objective of this session is to introduce the M3: Multi-hazard Physical and Social Impact Assessment.

By the end of the session, the participants will be able to:

- Discuss the Tomorrow's Cities Decision Support Environment (TCDSE) and its key components
- List the Purpose, Objective and content of Module 3: Multi-hazard Physical and Social Impact Assessment
- Discuss terminologies related to the module such as hazards, vulnerability and risk.
- Broadly outline the case study of Tomorrowville.
- Discuss the inputs required for the Computational Model and its linkage to previous steps in the TCDSE.
- Discuss the outputs of the Computational Model and its linkage to Risk Agreement.

1.2 Structure of Session 1

Structure
1. Purpose, Objective, Target audience, course content and evaluation methods of Module 3: Multi-hazard Physical and Social Impact Assessment
2. Introduction of module 3 and TCDSE
3. Components of module 3



1.3 Purpose, Objective and content of Module 3: Multi-hazard Physical and Social Impact Assessment

1.3.1 Introduction to Tomorrow's Cities Decision Support Environment (TCDSE)

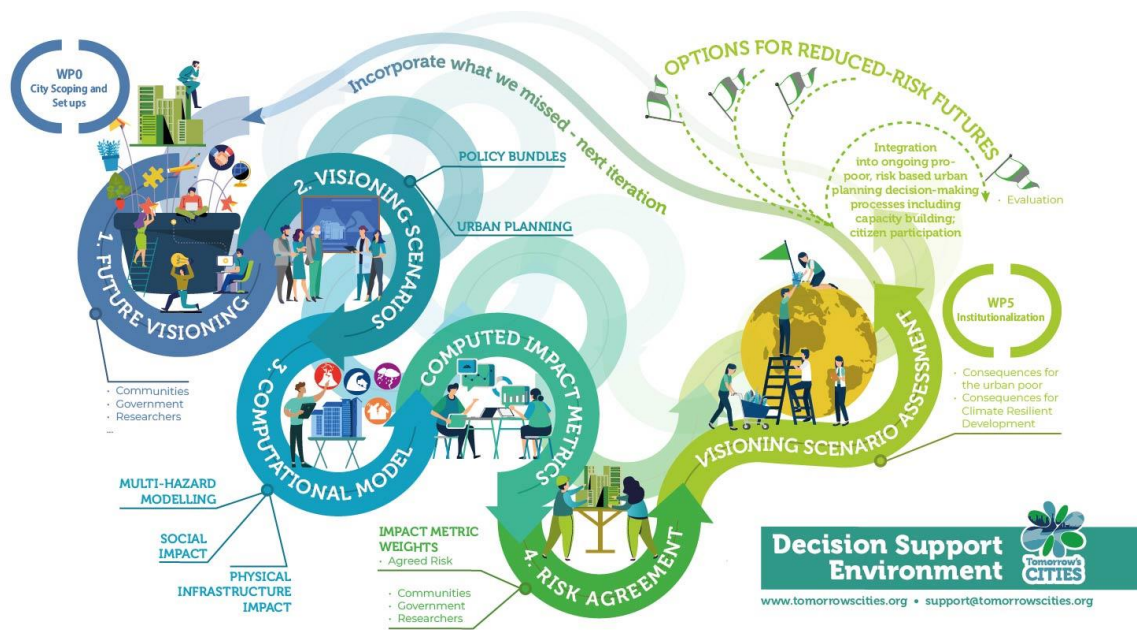


Figure 1: Summary of Tomorrow's Cities Decision Support Environment

Source: Tomorrow's Cities Communication Team.

The Capacity Strengthening program of Tomorrow's Cities is based on Tomorrow's Cities Decision Support Environment (TCDSE). The TCDSE is a flexible framework to support inclusive and evidence-based decision making, leading to a low-disaster-risk and more equitable urban development. As the name suggests, this is a process that supports informed decision making rather than making or enforcing decisions. Drawing on Tomorrow's Cities primary mission to reduce disaster risk for the urban poor, the TCDSE creates equitable and interactive spaces which allow multiple stakeholders and urban groups (whether institutional actors or urban residents) to think differently about risk. This is a space for learning; about the objective impacts of hazards on people, nature and the built environment, about different perceptions and experiences of hazardous events, and about how risk could be a negotiated concept. In a nutshell, the TCDSE articulates technical and political spaces of decision making by engaging in a systematic methodology composed of five stages: (1) Future Visioning, (2) Visioning Scenarios Development, (3) Multi-Hazard Physical and Social Impact Assessment, (4) Risk Agreement and (5) Institutionalization. It is important to note that, before the kick-off of the TCDSE, there is a preparatory stage (covered by Module 0 in this course) which deals with the assessment of existing data, a critical mapping and selection of stakeholder groups (on the basis of power imbalances in planning), besides other technical and logistical arrangements that allow the TCDSE to function.

- **Future Visioning** (Stage 1) encompasses a series of participatory engagements that explore desired urban futures with different city stakeholders, incorporating



expectations for land uses and critical urban assets, as well as expected policies to tackle the negative impacts of future natural hazards.

- **Visioning Scenarios Development** (Stage 2) renders these desired futures into detailed virtual representations that make Future Visions more realistic and connected to data-driven trends. Expected land uses are adjusted to meet planning standards, and a modelling of future exposure is incorporated. The latter means forecasting who the future urban residents will be, and where they will live and work. Further, Visioning Scenarios include a detailed refinement of policies discussed during Future Visioning workshops.
- **Multi-Hazard Physical and Social Impact Assessment** (Stage 3) subjects Visioning Scenarios to earthquake, flood and landslide events. This leads to an understanding of the consequences of the decisions made during future visioning and scenario building before a brick is laid. Maps of damage states combined with different impact metrics (number of casualties, of displaced households, etc) enable a clear visualisation of the spatial distribution of impact and help diagnose risk drivers back through complex causal chains in urban decision-making.
- **Risk Agreement** (Stage 4) opens up a collective definition of risk that accounts for the objective impact of hazards and the subjective priorities of key community and institutional groups that engaged with the TCDSE. Using digital tools, stakeholders unpack the consequences of spatial and policy decisions and how they increase or decrease disaster risk. They also assess the equity of the distribution of risk across space and the impacts of planning decisions on poor and disadvantaged communities in the event of natural hazard events, earthquakes, landslides or floods. Critical learning about risk, which results from our decisions, leads to an opportunity to modify our plans based on a clear understanding of the risk they imply.
- **Iteration** (Stages 1 to 4 repeated) is one of the key innovations of the TCDSE. Having developed a vision, translated this into a detailed visioning scenario and exposed its risk consequences, stakeholders now revisit problematic aspects of their vision that have led to the risk uncovered by this analysis. The city team then repeats Stage 1, modifying some aspects of the future vision. These modifications then lead to changes in the visioning scenarios. The new visioning scenarios are now exposed to the same hazard events and the impacts metrics are recalculated. This leads to both a refined understanding of critical decisions leading to risk, and to discussions about how to transfer that learning into the actual decision environment of cities. This helps to promote policy uptake by institutions. The process can be repeated as often as required so that these new insights into decisions and their consequences lead to safer development planning and better decision making.
- **Institutionalisation** (Stage 5) happens once stakeholders have learned enough from the process of iteration. Cities could take concrete lessons and outputs from the TCDSE (e.g., actual plans and policy ideas) and the very tools and processes of Tomorrow's Cities into their institutional environments for a process of pro-poor risk reduction that is meaningful and long-lasting.

It is important to always keep in mind that this is a Decision Support Environment - not a Decision Making Environment - which means that the outputs of iterations are only informing planning discussions within cities. That is, the TCDSE offers a way to think differently about planning, in which risk is central. Although concrete solutions could be used, it is less of a prescription and more of a process of stimulating critical urban thinking.



1.3.2 Purpose of M3

Module 3: Multi-hazard Physical and Social Impact Assessment is based on the WP3: Multi-hazard Physical and Social Impact Assessment of Tomorrow's Cities Decision Support Environment TCDSE process. The module is aimed to enable the participants to interpret the components of the computational model and to familiarize them with the developed TC Computational Platform aided by a demonstration, which is a crucial component of the Module.

1.3.3 Objectives of M3

By the end of the module, the participants will be able to:

- Perform basic tasks in seismic hazard and risk analysis and communicate with relevant experts on the use of seismic hazard models within the TCDSE.
- Discuss the capacity of and requirements for physics-based numerical modelling of flood hazards.
- Communicate with relevant experts on the use of debris flow models within the TCDSE.
- Discuss broadly on different landslide hazard assessment scales, associated model types and data requirements, and the resulting information for decision support.
- Discuss the concept of fire hazards and its modelling requirements within the TCDSE.
- Discuss climate change impact assessment and the linkage of climate change analysis to TCDSE.
- Explain the basic concept of vulnerability analysis of buildings for earthquake and flood and its integration under TCDSE.
- Assess the importance of multi-hazard analysis as more than just the sum of single hazard analyses and recognize the input required for a proper multi-hazard analysis.
- Describe the concept of scoring, selecting and ranking physical impact models for multi hazard risk agreement.
- Apply infrastructure performance assessment before and after the occurrence of a future hazard.
- Identify the relevant inputs for social representation of vulnerability and identify gaps in the social inputs for the TCDSE and explain ways in which these can be filled using qualitative and qualitative methods.
- Discuss possible methods that can be used to identify the potential natural hazards and list out different impacts of the natural hazards.
- Discuss how the computational platform computes impact metrics and loads appropriate data (related to visioning scenarios, hazard, and physical and social impact) into the computational platform.

1.3.4 Target Audience of M3

The target audiences of this module are city officials, academicians, government and non-government personnel, private sector, TC members or other stakeholders associated with building and macro infrastructure, utility and service infrastructure, housing, hazard assessment, physical infrastructure impact assessment, social impact assessment etc.

1.3.5 Contents of M3

The M3 course is a 5-day course (16 hrs.) with 15 major sessions. It covers 14 theoretical sessions including short exercises and one demonstration session. The structure of M3 is as follows:



Table 1: Contents of Module 3: Multi-hazard Physical and Social Impact Assessment

S.N.	Structure	Duration
1	Session 1: Opening and Introduction to module 3	60 min
2	Session 2: Seismic hazard modelling	60 min
3	Session 3: Flood hazard modelling	60 min
4	Session 4: Debris flow modelling	60 min
5	Session 5: Landslide hazard modelling	60 min
6	Session 6: Fire hazard modelling	60 min
7	Session 7: Climate Change	60 min
8	Session 8: Vulnerability analysis - single hazard	60 min
9	Session 9: Vulnerability analysis - multi hazard	60 min
10	Session 10: Vulnerability analysis - model selection	60 min
11	Session 11: Network analysis	60 min
12	Session 12: Social impact	60 min
13	Session 13: Characterising impact metrics	60 min
14	Session 14: End to end demonstration of Computational Platform	120 min
15	Session 15: Linkage of Module 3 With Other Modules and Closing	60 min

1.4 Prerequisite Concepts for the Module

1.4.1 Concept of Risk

In the field of Disaster Risk Reduction, the concept of risk is very important. Risk can be defined as the probability or likelihood of impact or damage that can occur to a system, society or community as a result of exposure to hazard. It is often expressed as a function of hazard, exposure, and vulnerability along with capacity as shown below.

$$\text{Risk} = \frac{\text{Hazard} \times \text{Vulnerability} \times \text{Exposure}}{\text{Capacity}}$$

Below are brief explanations of each component of risk:

A. Hazard:

It is the characteristics, intensity and probability of damaging natural events occurring at the site of interest. Hazards can include earthquakes, floods, landslides, debris flows, fire, infectious diseases and others.

Vulnerability:

Vulnerability is the characteristics and circumstances of a community, system or asset that make it susceptible to the damaging effects of a natural hazard. Vulnerability can be socio-economic and physical.

B. Exposure:

Exposure includes community, system or asset exposed to natural hazard.



C. Capacity:

Capacity means strengths, attributes and resources available within an organization, community or society to manage and reduce disaster risks and strengthen resilience. Capacity can be influenced by access to resources, education, awareness, training, social networks and cultural norms.

D. Disaster Risk Reduction

Disaster risk reduction is aimed at preventing new and reducing existing disaster risk and managing residual risk, all of which contribute to strengthening resilience and therefore to the achievement of sustainable development.

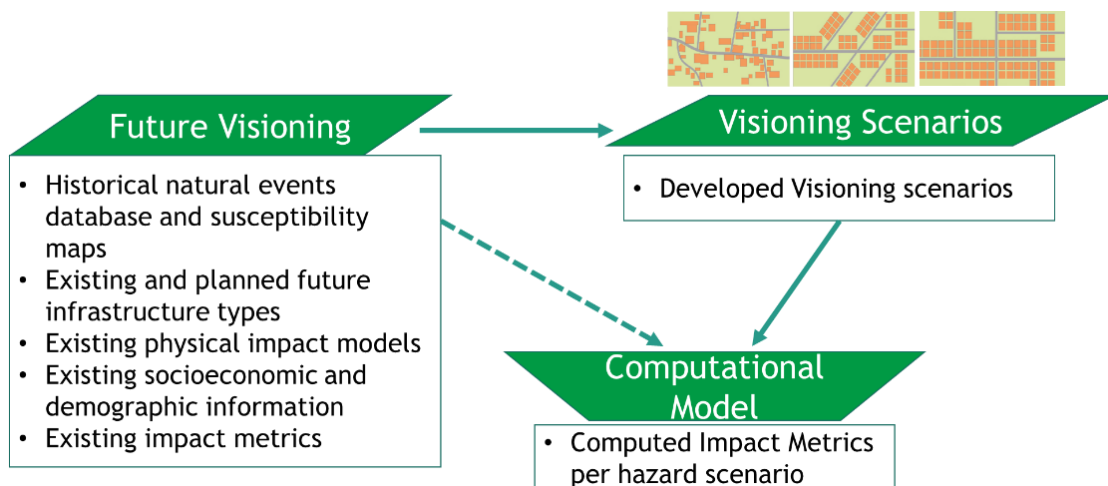
E. Multi-hazards

A multi-hazard approach considers more than one hazard in a given place (ideally progressing to consider all known hazards) and the interrelations between these hazards, including their simultaneous or cumulative occurrence and their potential interactions.

1.5 Components of Module 3

1.5.1 Prerequisites for the Computational Model

The computational model takes the developed visioning scenarios of the city from Stage 2: Visioning Scenarios as shown through direct linkage in Figure below. In addition, data gathered on historical natural events, susceptibility maps, existing and planned future infrastructure types, existing physical impact models, existing socio-economic and demographic information, and existing impact metrics collected in Stage 0: Preparatory stage and Stage: Future visioning stage also feeds into its calculation.



Source: Tomorrow's Cities

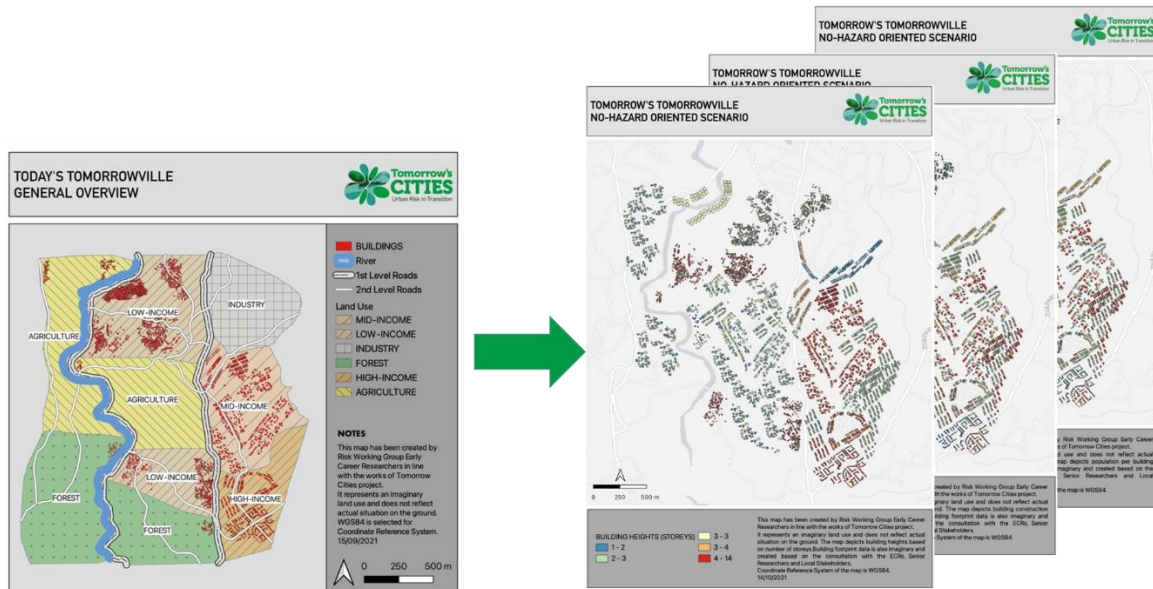
Figure 2: Prerequisites and results of the computational model

1.5.2 Illustration through Tomorrowville

Tomorrowville, a virtual urban test-bed is used to illustrate this framework of the computational model. It is a synthetic urban settlement based on digital elevation model of a real 500 ha area situated south of Kathmandu. Tomorrowville incorporates the typical demographic, socio-economic and physical features of urban landscapes in the Global South, specifically those of Kathmandu and Nairobi. It is susceptible to hazards such as earthquakes, floods and debris flows. Tomorrowville is defined by a spatially distributed information of its urban features, which



includes land-use polygon information, building (physical) attributes, household (social) attributes, and individual (social) attributes. In order to explore the risk implications of different future urban scenarios (conditional urban plans) in the context of TCDSE, various building layout have been created for Tomorrowville based on constraints imposed by current development, as well as future population and demographic projections. The first scenario (TV0_b0) refers to the present-day Tomorrowville. The TV50_total scenario is also considered, representing one possible configuration of Tomorrowville 50 years in the future and including TV0_b0. This spatial information/ attributes down to the level of the individuals will feed into the computational model along with consideration of the identified hazards [1].



Source: Tomorrow's Cities

Figure 3: Visioning scenarios of future Tomorrowville

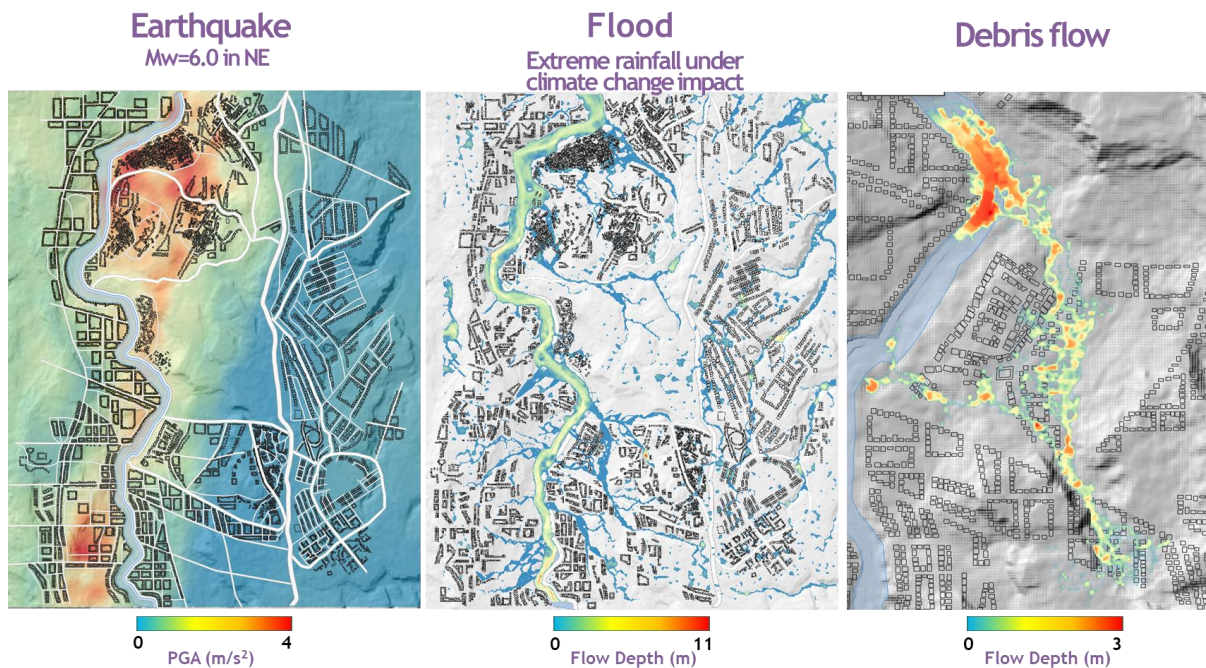
1.5.3 The Computational Model

The computational model within the TCDSE consists of three modules:

A. Multi-hazard modelling

In this component of the computational model, the natural hazards that are identified in Stage 0 and 1 are taken for selecting multi-hazard scenarios. Various data are collected on site and from various secondary sources for hazard study. This module can represent different single hazards in a place but can also incorporate realistically contrived interrelationships between different hazards (e.g., earthquake triggering a tsunami and/or liquefaction, wildfire followed by landslide) to represent a reasonable future multi-hazard experience. The hazards are then simulated for the future urban setting of the city and distributed spatially and temporally based on their relevant intensity measures. As shown in figure below for Tomorrowville, earthquake hazard zonation maps are produced in terms of Peak Ground Acceleration (PGA), and flood hazard maps and debris flow hazard map are zoned in terms of flood depth. These outputs serve as an input for the Physical Infrastructure Impact module.





Source: Tomorrow's Cities

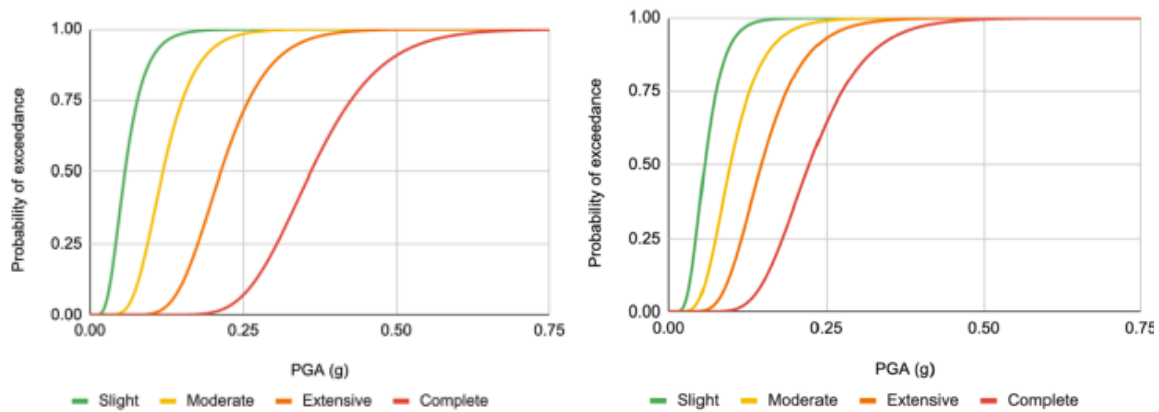
Figure 4: Scenarios for different hazards in Tomorrowville

B. Physical infrastructure impact

In the physical infrastructure impact module, the attributes of buildings and infrastructures are identified first for future-built environment as developed in the Visioning Scenario Development Module and then the associated fragility or vulnerability models are gathered. Fragility models relate probability of exceeding certain sets of damage level with relevant hazard intensity measures whereas vulnerability model relate loss with relevant hazard intensity measures. Earthquake fragility models developed for some building systems prevalent in Nepal is shown in figure below. It can be seen that for the same level of earthquake intensity i.e. PGA, brick in cement mortar buildings have lesser probability of suffering damage as compared to brick in mud mortar buildings. Fragility models are generally preferred over vulnerability models, since estimating damage enables greater flexibility in subsequently characterising a wide array of impact metrics that can also draw on social information as part of the social impact module. If the fragility functions are not available, they are developed. The spatially distributed hazard intensity measures in the urban settlement are then translated into physical damage/ impact they can most likely cause in a particular building/ infrastructure using these fragility/ vulnerability models. For example, in Tomorrowville, the building attributes are generated synthetically to be consistent with relevant statistical distributions of Nairobi and Kathmandu building data. The attributes include various occupancy, material + lateral load resisting system, code level and height. Based on these building attributes, the best physical impact models for earthquake, flood and debris flow are selected from various available databases and using the hazard intensity as calculated in hazard modelling module, the physical impact is calculated using these models.

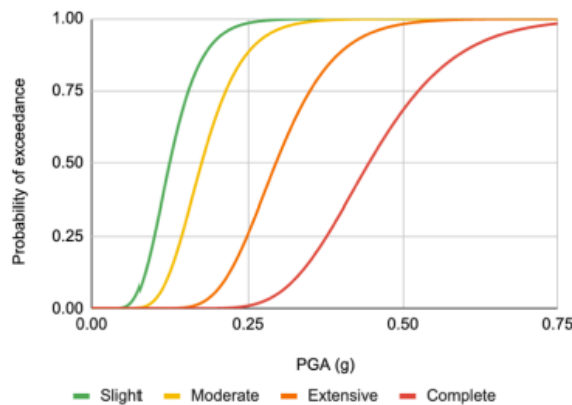
In addition, network level losses (such as infrastructure downtime) are also included in this module and are estimated as part of a systemic approach for characterising impact. Network analysis techniques are used to aggregate asset-specific losses accounting for inter-asset functionalities.





Brick in cement mortar with flexible floor

Brick in mud mortar with flexible floor



Brick in cement mortar with rigid floor

Source: Guragain (2015). Development of seismic risk assessment system for Nepal. PhD dissertation, <http://doi.org/10.15083/00007589> [2]

Figure 5: Development of earthquake fragility curves for various building system in Nepal

C. Social impact

The social impact module facilitates a community-based “bottom-up” component in impact characterisation for risk-informed decision support. The aim of this module is to determine the differential impact on different social groups that the future multi-hazard scenarios might have in the city, particularly those most marginalised quantitatively and qualitatively. It does so by:

1. Disaggregating outputs from the Physical Infrastructure Impact module based on overlapping inequalities (derived from relevant categories of demographic and socioeconomic differentiation from the Visioning Scenario Development module, e.g., gender, race, age, income). This is done through quantitative approaches to intersectionality.
2. Assessing the influence of outputs from the Physical Infrastructure Impact module on disruption/improvement of mobility patterns and other flows of people, services, and commodities for individual and intersecting social groups that are specified in the Visioning Scenario Development module. Examples include access to work, education, and food/essential items due to transport infrastructure damage (e.g., \pm variation in commuting time for workers to workplace, children to school, and consumers to markets)

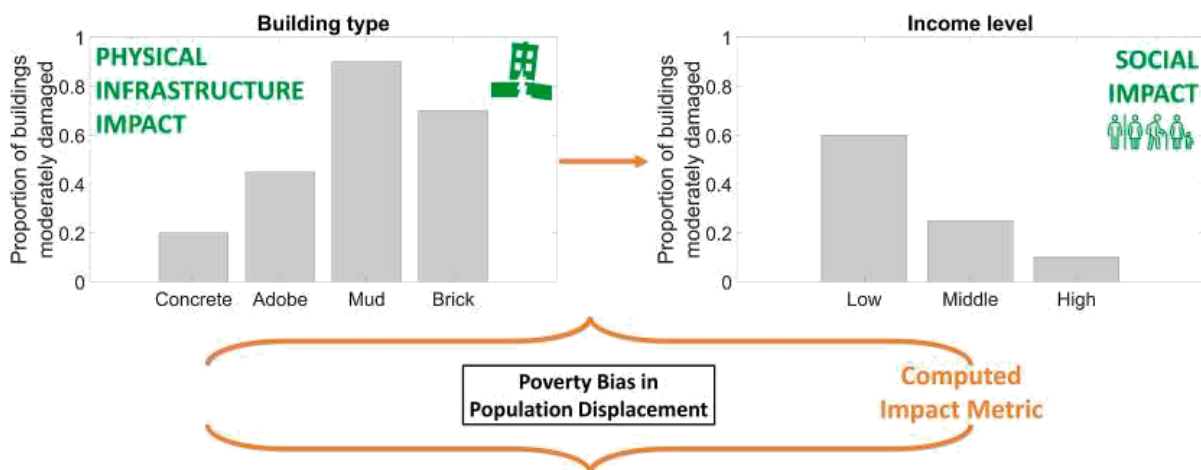


The quantitative part of this module assesses how social categories affect multi-hazard impacts individually and jointly. The quantitative part of this module is further enforced through qualitative part:

1. Contextualising multi-hazard impacts by understanding the root causes and underlying drivers of vulnerabilities as well as the conditions that enable/constrain the capacities of different social groups in each city.
2. Incorporating intangible impacts (e.g., on social relations, mental health, happiness, spirituality, aesthetic, heritage) that are derived from a qualitative enquiry.

1.5.4 Computed Impact Metrics

Computed Impact Metrics are the formal quantitative and/ or qualitative summaries of the Social Impact Module outputs. These impact metrics are used to compare and assess developed Visioning Scenarios in Stage 4: Risk Agreement of the TCDSE. The development of these metrics must be transparent and well documented to enable participatory assessment of the risk characterisation process. Impact metrics may also be temporal e.g. the number of displaced populations within six months of the event. Figure below shows the determination of one sample of a Computed Impact Metric. In this case, the Social Impact module first outputs the proportion of households with moderate damage across different income groups for the sample, which is based on relevant building damage information provided by the Physical Infrastructure Impact module. The output of the Social Impact module is further converted into the number of low-income households displaced (because of moderate damage) relative to the average number of displacements across all income groupings to produce the sample value of the “Poverty Bias in Population Displacement” Computed Impact Metric.



Source: Cremen et. al (2022), A state-of-the-art decision-support environment for risk-sensitive and pro-poor urban planning and design in Tomorrow’s cities, IJDRR, <https://doi.org/10.1016/j.ijdr.2022.103400> [3]

Figure 6: Illustration of how one sample of a Computed Impact Metric is determined

Some examples of potential impact metrics are:

- A **poverty bias indicator**, which measures the extent to which low-income people are disproportionately affected by some type of disaster-induced loss. This metric is shaped by a consequence measurement like economic loss, related infrastructure damage, unemployment, social network disruption etc. That is disaggregated by income.
- Infant mortality, which would be shaped based on estimates of fatality by age.
- Population displacement, which could depend on socio-demographic factors, the extent of housing damage (i.e., loss of functionality), and the strength of social networks.
- Education inaccessibility, which measures the extent to which the school-going population are inhibited from participating in educational activities, as a result of



damage/loss to (1) school buildings; (2) relevant transport infrastructure between schools and residences of school-going children; and (3) critical service-related infrastructure associated with schools.

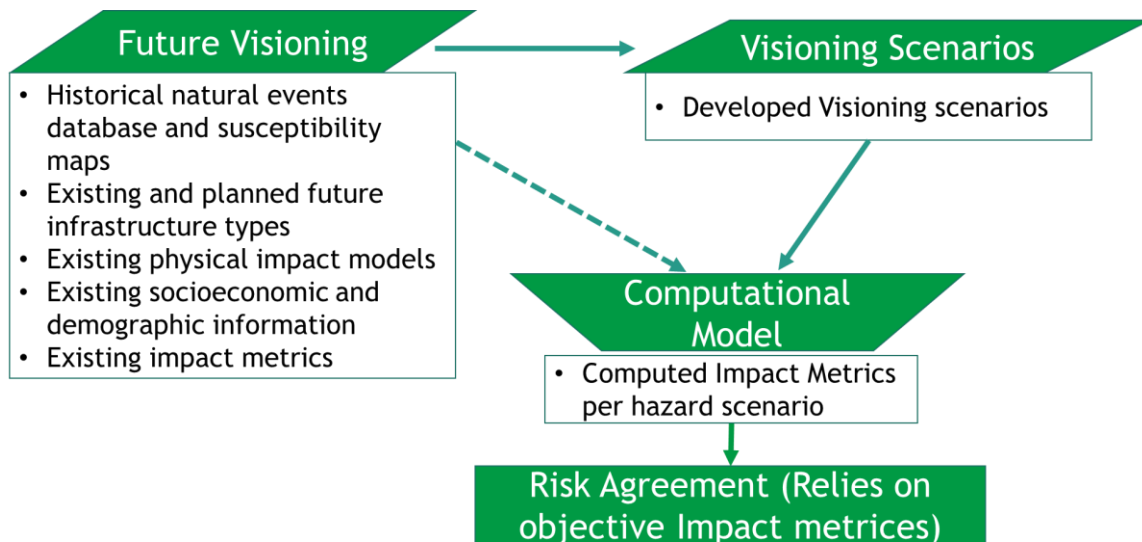
The metrics are computed through Monte-Carlo Simulation to capture uncertainties in:

1. The urban planning component of the Visioning Scenario
2. Multi-hazard modelling scenarios (hazard intensities)
3. Quantification of physical infrastructure impact (e.g., damage states)
4. Quantification of social impact (e.g., casualties leading to breakdown of social groups)

Therefore, quantitative impact metrics are expressed in the form of a probability distribution. In case there are insufficient availability of data to quantitatively define an impact metric or when it is unlikely to measure a consequence explicitly, qualitative indicators that contain discrete distributions of consequences (such as “high”, “medium”, and “low”) are used.

1.5.5 Outputs of the Computational Model

The qualitative and/or quantitative multi-hazard impacts derived from the computational model are used in the Risk Agreement module in Stage 4. Risk agreement consists of decision mechanisms that follow a democratized approach allowing different actors with diverse knowledge to lead and influence conversations about disaster risk. It is specifically designed to determine priorities around multi-hazard impacts through multi-attribute decision-making processes such as Analytic Hierarchy Process.



Source: Tomorrow's Cities

Figure 7: Inputs and outputs of the computational model



SESSION 2: SEISMIC HAZARD MODELLING

2.1 Objectives

By the end of the session, the participants will be able to:

- Discuss various terms used in Seismic Hazard Analysis (SHA).
- Perform basic tasks in seismic hazard and risk analysis using Openquake tool.
- Discuss the advantages offered by physics based deterministic seismic hazard analysis over conventional methods.

2.2 Structure of Session 2

Structure
1. Understanding Earthquakes
2. Seismic Hazard Analysis and Its Use in Risk Assessment
3. Scenario Based Seismic Hazard Analysis (SSHA)
4. Physics Based Seismic Hazard Analysis

2.3 Understanding Earthquakes

2.3.1 Structure of the Earth

The Earth is made up of three layers: core, mantle and crust.

Crust (Lithosphere):

The crust is the outer surface layer of the earth. It varies in composition and thickness in its oceanic and continental parts. The thinnest parts under the oceans (oceanic crust) are basaltic and go to a depth of approximately 10 km. The thickest parts are the continents (continental crust) extending down to 35 km on average and consist of two layers: granitic in the upper portion and basaltic in the lower with a thickness of about 30 to 60 km. Continents float in the form of thin hard plates called tectonic plates on the viscoelastic mantle. The landmasses are constantly drifting.

Mantle (Asthenosphere):

The mantle is the intermediate layer beneath the crust about halfway to the centre. It is made of solid rock and behaves like an extremely viscous liquid. The temperature of the earth increases with depth. Through the action of heat convection from the centre of the Earth, the movement of the tectonic plates.

Core (Centrosphere):

The core of the earth is further divided into two layers: outer core and inner core. The outer core is the layer beneath the mantle and is 2270 km in depth. The core temperature is believed to be swapping 5000-6000°C. It is composed of liquid iron and nickel. Complex convection currents give rise to dynamo effect, responsible for the Earth's magnetic field. The inner core is solid due to the massive pressure. It lies at the centre and is 1216 km in depth. It is made of solid iron and nickel.



2.3.2 Cause of Earthquakes: Plate Tectonics

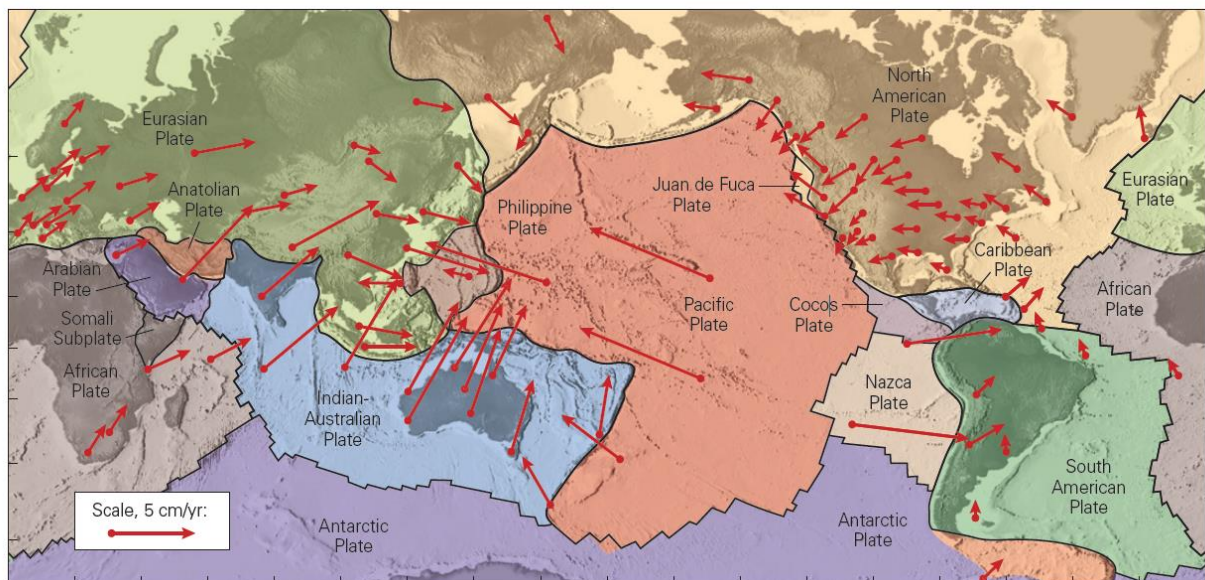
The phenomena of earthquakes are explained by the theory of plate tectonics. According to this theory, the earth's crust (lithosphere) consists of several large and fairly stable landmasses called plates. There are 7 major tectonic plates: Pacific, North American, Eurasian, African, Antarctic, Indo-Australian and South American Plate. In addition to these plates, there are several other minor plates that are contained within or near the major plates.

These plates move with average speed ranging from 1 to 6 cm/year over the underlying mantle (asthenosphere) driven by the convection current in this layer. The source of heat driving the convection currents is radioactive decay occurring deep within the Earth. As these massive plates move, diverging (pulling apart) or converging (coming together) along their borders, tremendous energies are released resulting in tremors that transform Earth's surface. Thus, the boundaries of these plates are the sites of intense geologic activities such as earthquakes, volcanoes and mountain formation.

The data in earthquake occurrence have further validated and refined the concept of plate tectonics, showing that the seismic activity is confined to regions near the plate boundaries as shown in figure below. Even in the regions close to tectonic plate boundaries, the direction of plate movement determines which regions experience greater seismic activities.

2.3.3 Global Seismic Hazard

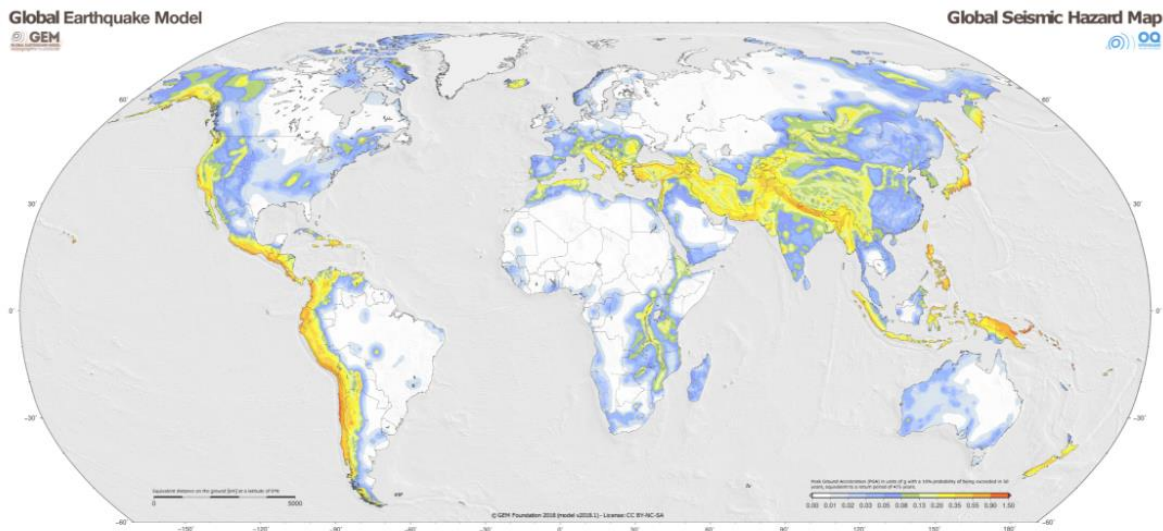
The global distribution of earthquakes and seismic hazard closely follows the tectonic movement.



Source: Stephen Marshak - Earth: Portrait of a Planet

Figure 8: Movements and velocities of tectonic plates





Source: GEM Global Seismic Hazard Map

Figure 9: Global seismic hazard map

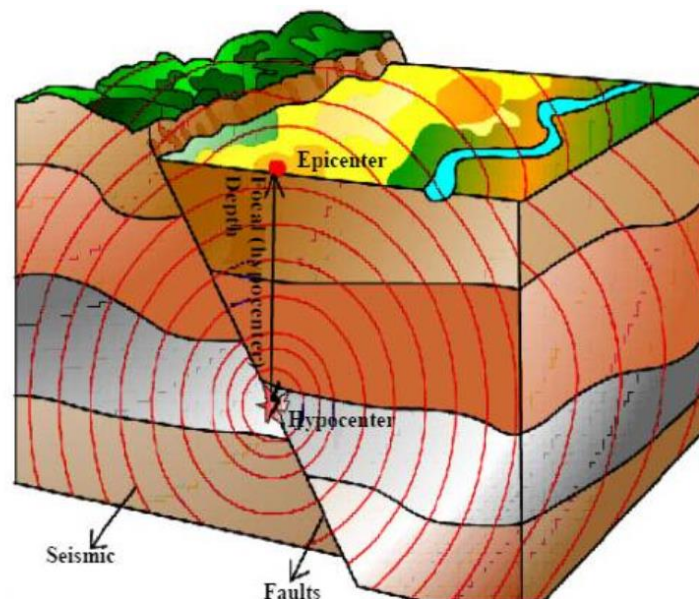
2.3.4 Terminologies Related to the Source of Earthquakes

The location or the source of earthquakes is characterized in terms of hypocenter and epicenter.

Hypocenter (Focus): It is the point under the surface, from where rupture begins. It can also be defined as the location from where seismic waves originate.

Epicenter: It is the point on the surface of the earth, vertically above the place of origin (hypocenter) of an earthquake.

Focal depth: It is the distance between the focus (hypocenter) and the epicenter.



Source: <https://scweb.cwb.gov.tw/en-US/Guidance/FAQdetail/179>

Figure 10: Source of earthquake

2.3.5 Types of Seismic Waves

Seismic waves are waves of energy generated by the sudden slippage/ breakage of rocks within the earth. They originate at the focus and propagate erratically and non-uniformly through the



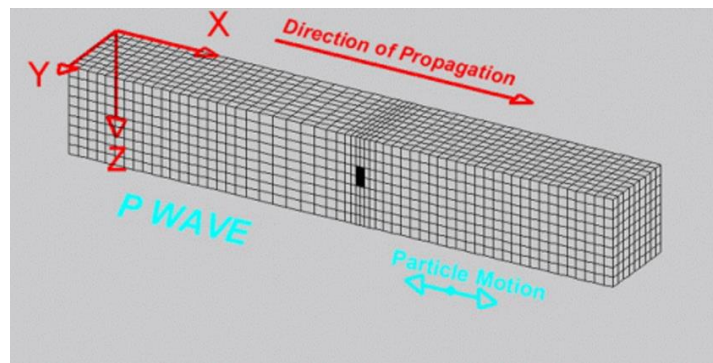
earth. The two main types of seismic waves are **body waves** and **surface waves**. Body waves can travel through the earth's inner layers and are faster to arrive at the station whereas surface waves can travel along the earth's surface and slower than body waves.

A. Body Waves

Body waves traveling through the earth's interior are of higher frequency than surface waves. And they arrive before the surface waves. There are two types of body waves: P (Primary or pressure) and S (Secondary or shear) waves.

P (Primary or Pressure) Waves:

P (Primary or Pressure) waves are the fastest seismic waves which are first to arrive at a seismic station. These waves can move through solid rocks and fluids, like water or liquid layers of the earth. It pushes and pulls the rock it moves through similar to sound waves. So, these waves are also called compressional waves. Particles move in the same direction that the wave is propagating in.

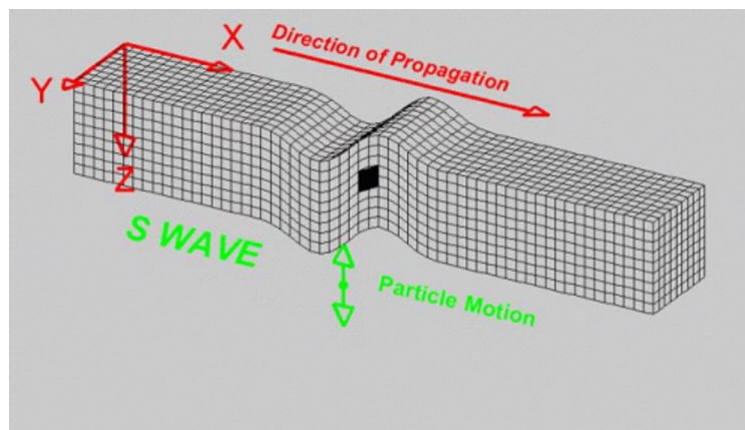


Source: <https://www.mtu.edu/geo/community/seismology/learn/seismology-study/body-wave/>

Figure 11: Particle motion in P-wave

S (Secondary or Shear) Waves:

S (Secondary or Shear) waves are slower than P waves and can move only through solid rock i.e., they cannot move through liquid medium. S waves move rock particles up and down or sideways in the direction perpendicular to the direction that the wave is traveling in.



Source: <https://www.mtu.edu/geo/community/seismology/learn/seismology-study/body-wave/>

Figure 12: Particle motion in S-wave

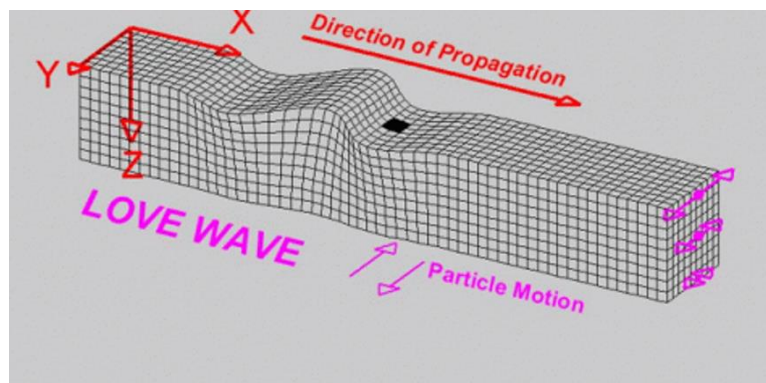


B. Surface Waves

Surface waves are of lower frequency than that of body waves and are slower than body waves. They only travel through the earth's crust. Surface waves cause greater ground motion and tend to be more destructive. There are two types of surface waves: Love waves and Rayleigh waves.

Love Waves:

Love waves are named after A.E.H Love, a British mathematician who worked out the mathematical model for this type of wave. It is the fastest surface wave and moves the surface sideways. Just confined to the earth's surface, it entirely produces horizontal motion in a plane parallel to the direction of wave propagation.

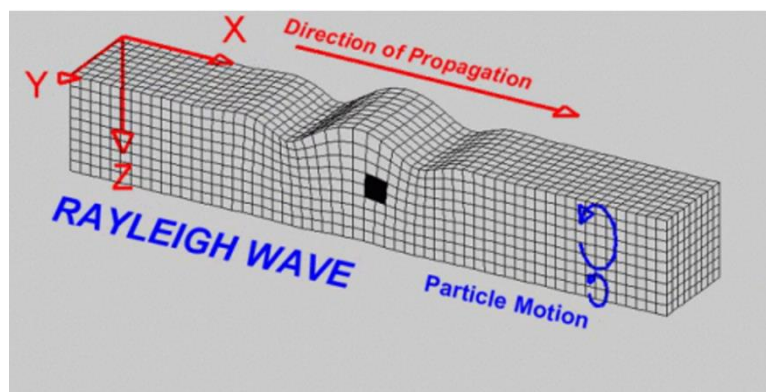


Source: <https://www.mtu.edu/geo/community/seismology/learn/seismology-study/body-wave/>

Figure 13: Particle motion in Love wave

Rayleigh Waves:

Rayleigh waves are named after John William Strutt, Lord Rayleigh, who mathematically predicted the existence of this type of wave. Rayleigh waves travel along the ground surface similar to the ripples across a water body. It moves the ground up and down and sideways in the plane perpendicular to the direction of wave propagation in a kind of rolling (circular) motion.



Source: <https://www.mtu.edu/geo/community/seismology/learn/seismology-study/body-wave/>

Figure 14: Particle motion in Rayleigh wave

The following figure shows a typical seismograph recorded. P-waves are the first to arrive followed by S-wave and then surface waves.



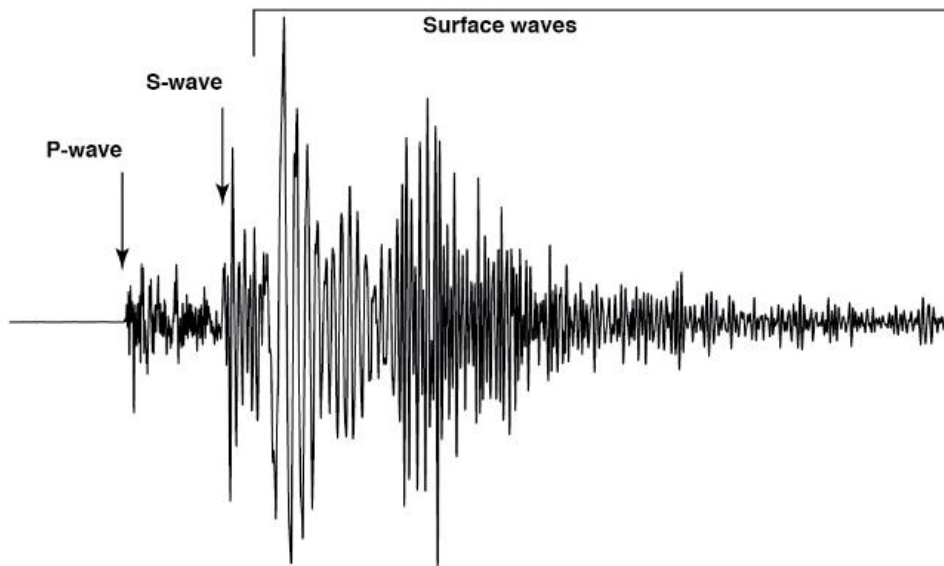


Figure 15: Seismic waves recorded in seismogram

2.4 Seismic Hazard Analysis and Its Use in Risk Assessment

2.4.1 Seismic Hazard Analysis (SHA)

Earthquakes can cause threat to human life and properties as evident from the impacts of numerous past seismic events. So, their careful consideration is required in the design of structures and several facilities. The aim of **earthquake-resistant design** is to design a structure or facility which can resist a certain level of shaking without suffering from excessive damage. This level of shaking is given by a **design ground motion**, characterized by **design ground motion parameters**. Specification of design ground motion parameters is one of the most challenging and important problems in seismology.

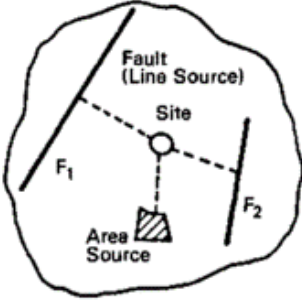
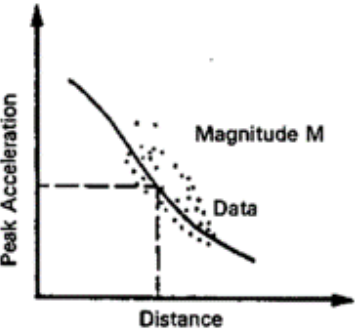
Seismic Hazard Analyses gives quantitative estimation of ground-shaking hazards for a region of interest. Seismic hazards can be analyzed deterministically, in which a particular earthquake scenario is taken, or probabilistically, in which uncertainties in the occurrence of earthquakes are explicitly considered.

A. Deterministic Seismic Hazard Analysis (DSHA)

A Deterministic Seismic Hazard Analysis (DSHA) evaluates ground motion hazard (intensity measures) based on a particular seismic scenario. The scenario on the occurrence of an earthquake of a specified size occurring at a specified location is postulated. DSHA yields a single value of ground motion measure. Scenario-based Seismic Hazard Analysis (SSHA) and Physics-based Seismic Hazard Analysis are also the form of DSHA. These will be discussed later.

A DSHA typically is done through following four steps:



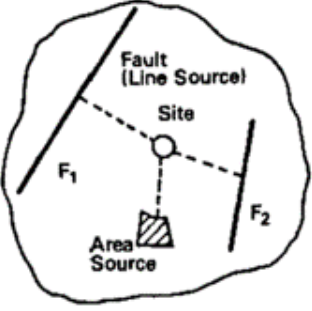
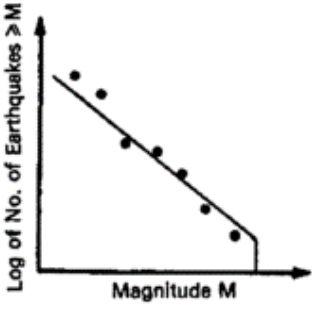
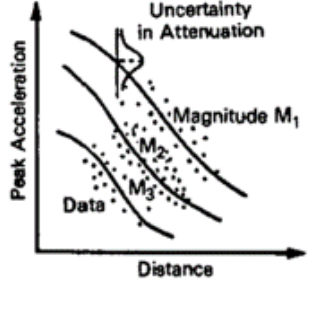
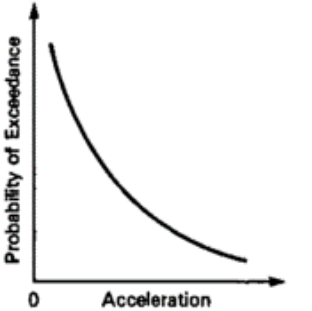
<p>1.</p>	<p>Identification and characterization of all earthquake sources in the region of interest. Characterization of source means definition of sources' geometry (point, line or area) and their earthquake potential.</p>	 <p style="text-align: center;">Step 1 SOURCES</p>
<p>2.</p>	<p>Selection of distance from source to site for each source. Mostly, the shortest distance is selected, and it can be expressed as epicentral or hypocentral distance, depending on the parameter used in the predictive equations used in step 3.</p>	<p style="text-align: center;">FIXED DISTANCE R FIXED MAGNITUDE M</p> <p style="text-align: center;">Step 2 SELECT CONTROLLING EARTHQUAKE</p>
<p>3.</p>	<p>Selection of the controlling earthquake (the earthquake that is expected to produce strongest shaking level) at the site. It is described in terms of its size (usually magnitude) and distance from the site.</p>	 <p style="text-align: center;">Step 3 GROUND MOTION</p>
<p>4.</p>	<p>Definition of hazard at site, usually in terms of the ground motions at the site by the controlling earthquake. Peak Ground Acceleration (PGA), Peak Ground Velocity (PGV) and Response Spectrum are commonly used.</p>	<p style="text-align: center;">FIXED PEAK ACCELERATION OR OTHER GROUND MOTION MEASURES</p> <p style="text-align: center;">Step 4 HAZARD AT THE SITE</p>

B. Probabilistic Seismic Hazard Analysis (PSHA)

Uncertainties in the size, location and rate of recurrence of earthquakes along with variation of ground motion characteristics with earthquake size and location needs to be explicitly considered in seismic hazard analysis. Probability theory is utilized in Probabilistic Seismic Hazard Analysis (PSHA) to identify, quantify and combine all these uncertainties to define seismic hazard (ground motion intensity measure) at a site.



A PSHA is done through following four steps:

<p>1.</p>	<p>Identification and characterization of all earthquake sources in the region of interest. The probability distribution of potential earthquake locations within the source is also characterized.</p>	 <p style="text-align: center;">Step 1 SOURCES</p>
<p>2.</p>	<p>Characterization of seismicity or temporal distribution of earthquake recurrence. Seismicity of each source zone is characterized using a recurrence relationship, which gives the average rate at which an earthquake of some size will be exceeded.</p>	 <p style="text-align: center;">Step 2 RECURRENCE</p>
<p>3.</p>	<p>Determination of ground motion produced at the site by earthquakes of any possible size occurring at any possible point in each source zone using predictive relationships. The uncertainty present in the predictive relationship is also considered.</p>	 <p style="text-align: center;">Step 3 GROUND MOTION</p>
<p>4.</p>	<p>Combination of the uncertainties in location, size and prediction of ground motion parameter of the earthquake. It is done to obtain the probability that the ground motion parameter will be exceeded during a particular period.</p>	 <p style="text-align: center;">Step 4 PROBABILITY OF EXCEEDANCE</p>



C. Characterization of Earthquake Source

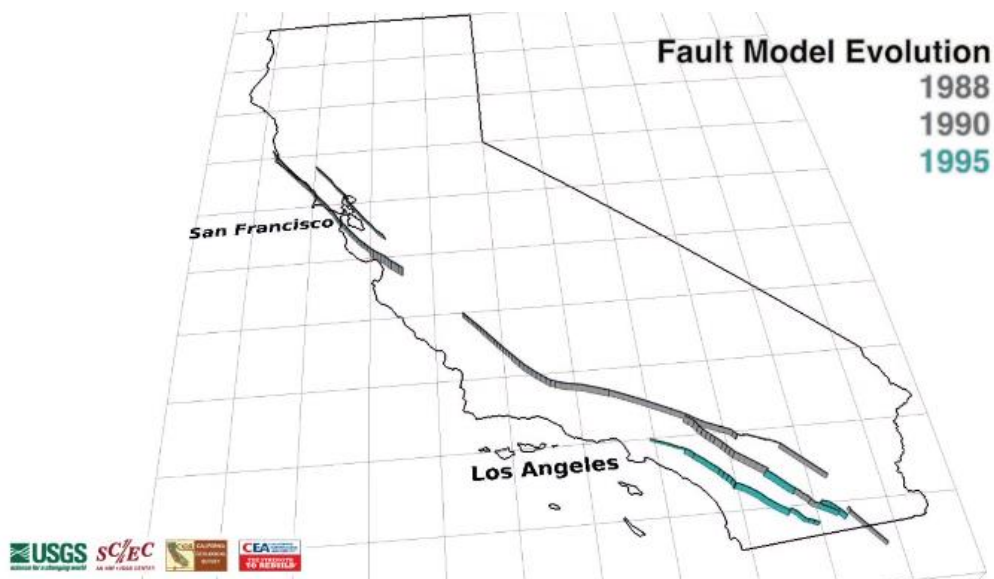
Source Geometry:

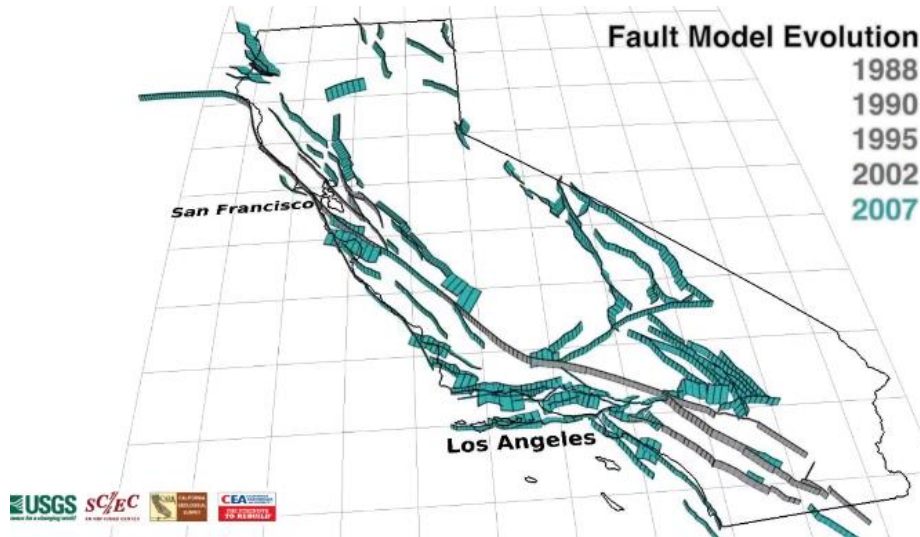
The geometry of earthquake sources can be quite complex in the real field which depends on the tectonic processes leading to their formulation. They are generally idealized as having simple geometry for the purpose of seismic hazard analysis. A fault that is small enough to allow them to be characterized as point source, since the distance between any point along its length and the site is nearly constant. In a similar way, if the fault is sufficiently shallow such that the hypocentral distance is nearly constant, it can be assumed as a linear source. If there is a well-defined fault plane on which earthquake can occur in any location can be considered as areal source. In areas where there is insufficient data on earthquakes and have extensive faults making it hard to distinguish individual faults, it can be taken as volumetric source.

Earthquake Size:

All the source zones have a maximum earthquake magnitude that cannot be exceeded. This maximum magnitude is dependent on the size of the fault which produces it. Generally speaking, the source zone will produce earthquakes of different sizes up to the maximum earthquake magnitude, with smaller ones occurring more frequently than the larger ones. Many faults tend to produce earthquakes of a certain magnitude or magnitude range (with about one-half magnitude unit) at fairly regular intervals. Such earthquakes are said to be “characteristic earthquake” of that particular fault or fault segment.

Seismology is a science which requires constant research and advancement. To perform a reliable and well-informed seismic hazard analysis, the researcher/ analyst must stay up to date with the latest findings in the seismic hazard research literature. An example on the evolution of fault model in California from 1988 to 2014 is shown in the following figure. This clearly portrays how the knowledge regarding the location, type and number of faults have evolved there and how it needs to be considered in seismic hazard analysis.





Source: <https://www.youtube.com/watch?v=L0vHyHLMN8&list=PLfSGTUJx7YsZ-wAQH9XXtQZKFyQ6LBZDx&index=4>

Figure 16: Evolution of fault models in California from 1988 to 2014

D. Ground Motion Prediction Equation (GMPE) [and Selection]

Ground Motion Prediction Equations (GMPEs) are the predictive relationships that are used to translate the earthquake characteristics into ground motion intensity measures at the site of interest. Mathematically, they describe the rate of decay in ground motion with distance. This decay is the cause of path effects (due to the soil through which the waves propagate) and site effects (due to the soil at the site of interest). Thus, they are also termed as **Attenuation relations**.

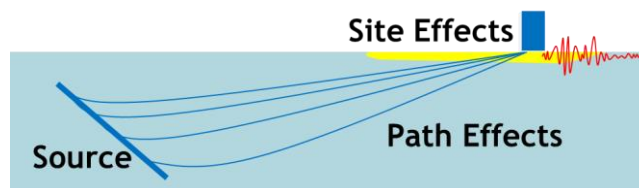


Figure 17: Path and site effects on ground motion

A typical GMPE is expressed as below:

$$\log(Y) = c_1 + c_2 * M + c_3 * (M_{ref} - M)^2 + (c_4 + c_5 * M) * \log(R) + c_6 * R + \text{site effects} + \text{faulting mechanisms} + \text{basin effects} \dots + \text{error}$$

Where, Y is the ground motion measure (PGA/ PGV/ Spectral acceleration)

M is the magnitude of the earthquake

R is the source-to-site distance

M_{ref} is a reference magnitude.

$c_1 - c_6$ are coefficients obtained empirically from the real or simulated ground motion data

The equation has additional terms to account for site effects, fault mechanisms and basin effects.

The error term is taken to account for aleatory uncertainty in the earthquake phenomenon.



These equations are developed by regression analysis of recorded strong motion databases and are typically updated with additional strong motion data available. They are updated approximately every 5 years using statistical methods such as Bayesian updating. They can also be generated using physics-based stochastic simulations. To perform seismic hazard analysis using method that requires the use of GMPE, it is essential to have a GMPE developed specifically for the geographic region of interest. In the absence of site specific GMPEs, it is a common practice to use GMPEs developed for other places with similar site characteristics.

The figure below shows an example of predicted spectral acceleration as a function of the distance of the structure from the source.

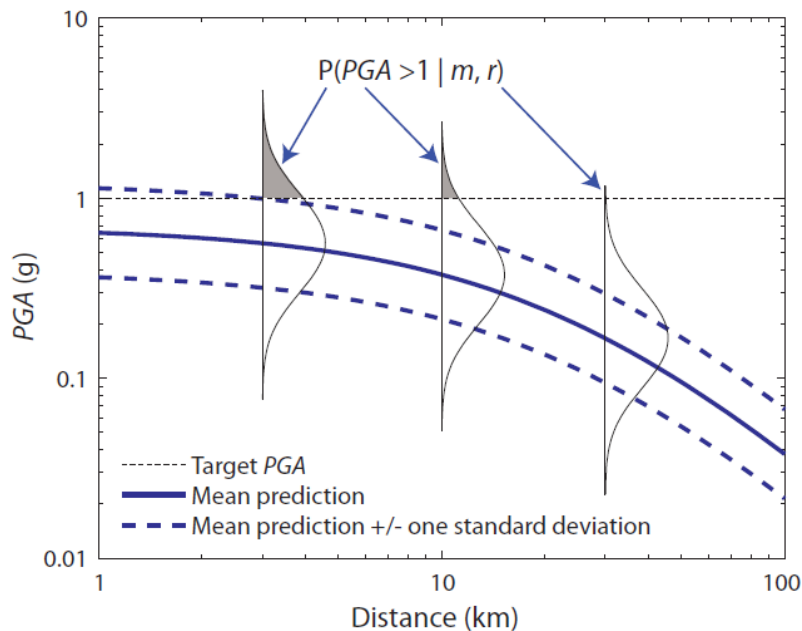


Figure 18: Spectral acceleration of a structure as a function of the distance from the earthquake source

Even if we fix the distance from the source, there is still some uncertainty associated with the resulting spectral acceleration. The uncertainty arises because we are trying to predict a highly complex phenomenon i.e., ground shaking intensity at a site using very simplified predictive parameters such as magnitude, distance, and a few other parameters.

Local Site Effects:

The ground motion predicted at a site using GMPE estimates the ground motion at the bedrock located in that site. However, if there is a thick layer of soil deposited over the bedrock, the ground motion at the surface can be significantly different. This effect of local soil deposit conditions is usually estimated using V_s30 .



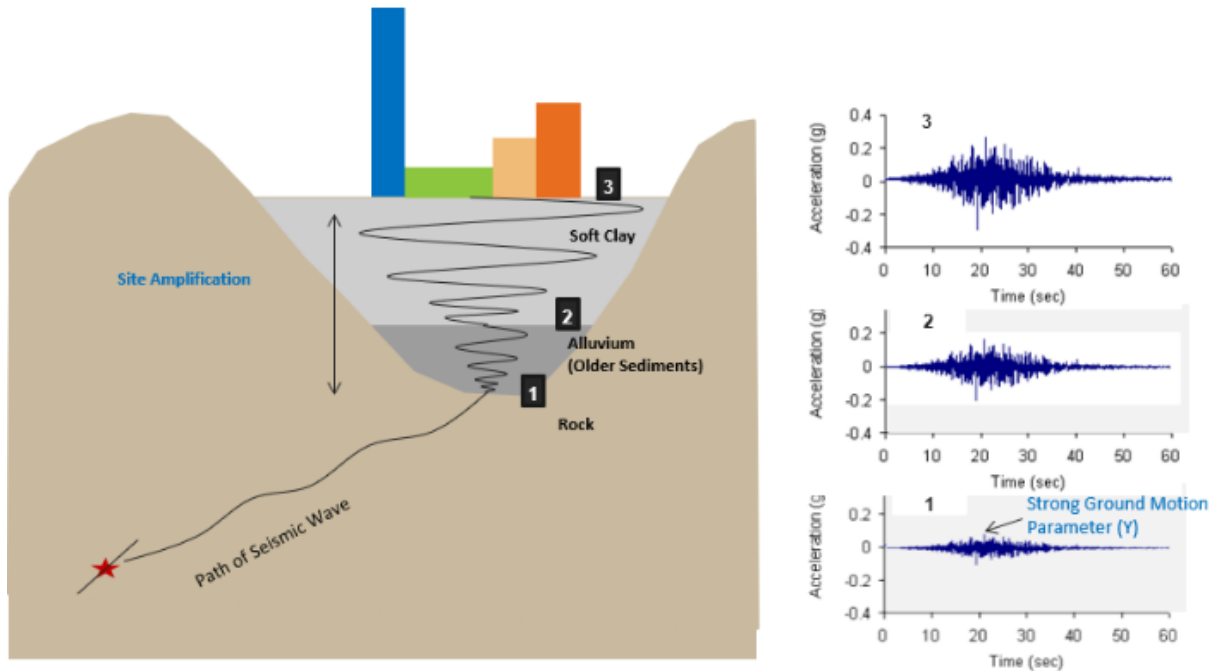


Figure 19: Local site effect: amplification in ground motion intensity measure PGA can be seen due to soil deposit

V_{S30} is defined as the time averaged shear wave velocity to a depth of 30 m from the ground surface. It is used widely as a parameter to characterize local site response for a wide range of applications such as simplified earthquake resistant design procedures in building codes and seismic hazard mapping. Mathematically it can be determined from the travel time (tt_{S30}) required for a shear wave to travel from the surface to a depth of 30m or vice versa i.e.

$$V_{S30} = 30m/tt_{S30}$$

V_{S30} has been correlated with strong-motion spectral amplification measurements, empirical amplifications taken from GMPE, V_{SZ} at other depths establishing it as a robust sole parameter for site response characterization. V_{S30} was initially introduced to provide unambiguous definitions of site classes and coefficients for a simplified estimation of site-dependent response spectra for use in the NEHRP building code 1994. However, due to limitations of a single parameter to fully characterize the response of a site, it was recommended to provide the option to use complete and detailed V_s profiles with corresponding modulus degradation and damping ratio curves to improve estimates of site response. Similarly, V_{S30} correlated with physical properties, geologic layer and topographic features provide representations useful in mapping V_{S30} as a parameter to distinguish broad variations in site response in a region of interest. Such maps are useful in preparing Seismic Hazard maps.

In the absence of field measurement of V_{S30} , approximation based on topographic slope can be used. This is because high V_{S30} value occurs at stiff or rocky surfaces, which tend to maintain steep slopes whereas, soft soils tend to be deposited on plain surface or maintain a gradual slope.

2.4.2 Use of Seismic Hazard Analysis in Risk Assessment

Various methods of Seismic Hazard Analysis estimate the intensity of ground motion experienced at a region of interest. This intensity measure is used in fragility or vulnerability function to determine the damage or loss incurred by the building, infrastructure and population. Fragility curves provide the probability of exceedance of damage corresponding to different intensity measures. On the other hand, vulnerability curves provide loss ratios for different intensity



measures. Thus, for the purpose of risk assessment, fragility curves estimate damage and vulnerability curves estimate loss caused due to a certain intensity measure of earthquake.

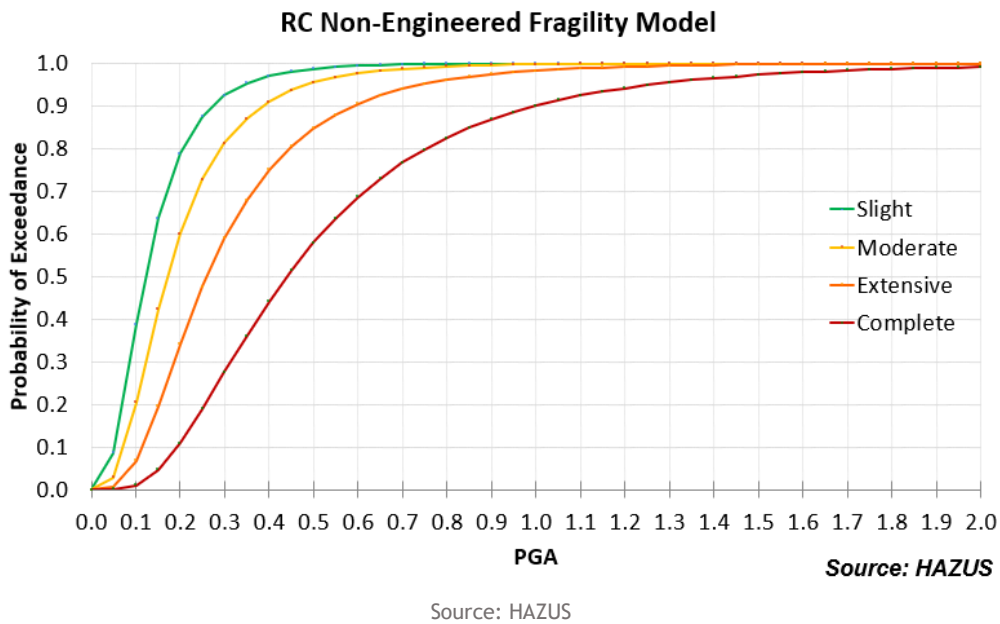


Figure 20: Fragility curve for non-engineered RC building (HAZUS)

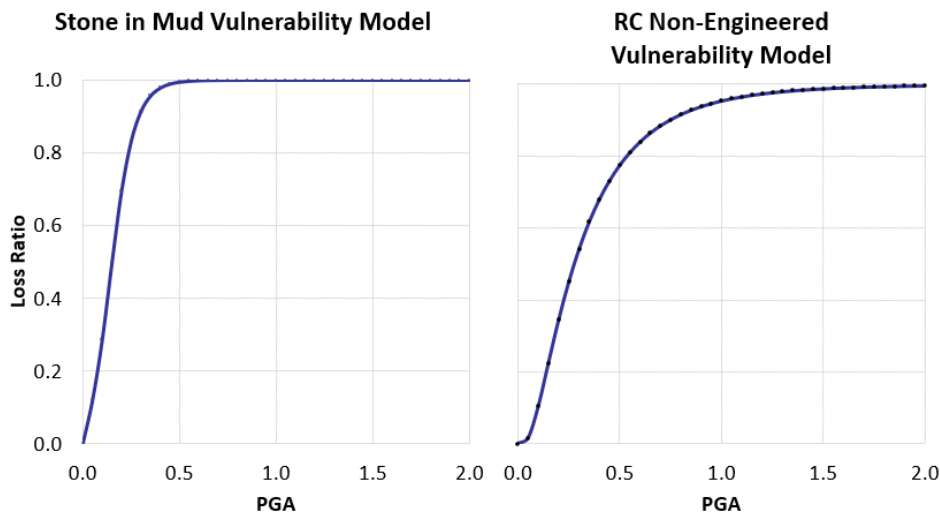
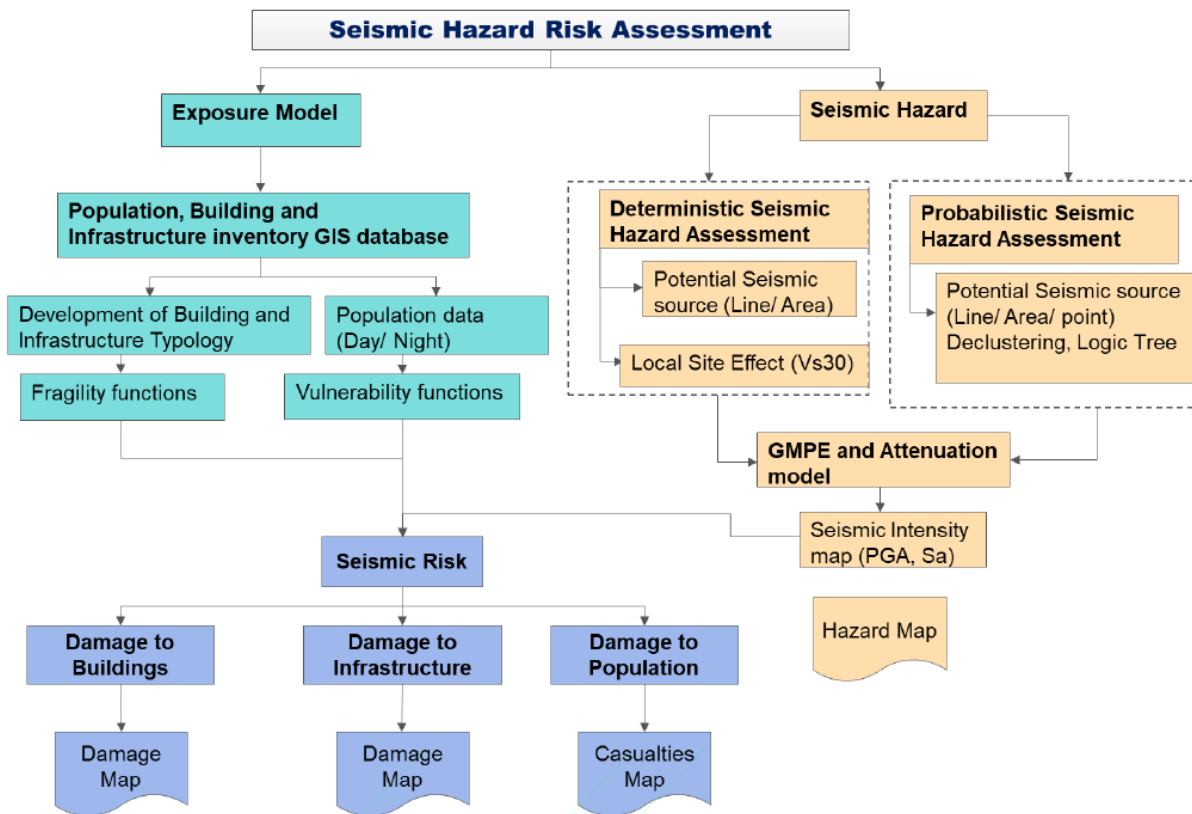


Figure 21: Vulnerability curves for stone in mud masonry buildings and non-engineered RC buildings

In summary, using methods such as PSHA or DSHA along with the knowledge of local site conditions and ground motion attenuation, the ground motion intensity at desired locations is estimated. Then, the impact of this ground motion on building, infrastructure and population, termed as exposure, is estimated in terms of damage and loss with the help of fragility and vulnerability functions.





Source: NSET 2022 Multi-hazard and Multi-Risk Assessment Guidelines for Municipalities of Nepal

Figure 22: Components of seismic hazard and risk assessment

2.5 Scenario Based Seismic Hazard Analysis (SSHA)

2.5.1 Introduction

Scenario based seismic hazard analysis considers a range of potential earthquake scenarios that could occur in a given region of interest. Scenarios on multiple hypothetical earthquake scenarios are developed with varying magnitudes, source-to-site distances and locations. These scenarios are based on the knowledge of active faults, historical seismic events and geological composition at the site. Ground motion prediction equations are then used to estimate the potential ground motion intensities for each scenario. It also incorporates the probabilities of occurrence of different scenarios, enabling the consideration of uncertainties and variability in earthquake occurrences.

2.5.2 Scenario Based Seismic Hazard Analysis in Openquake Engine

A. Introduction to Openquake

Openquake is an open-source software developed by Global Earthquake Model (GEM) Foundation collaboratively for earthquake hazard and risk modelling. It is compatible for operating systems such as Linux, macOS and Windows. Along with Openquake Engine, QGIS should also be installed to facilitate the visualisation of the analysis results. An openquake plugin is available within QGIS to link it with the engine. Detailed instructions on how to install Openquake Engine and its related software can be found in the video in the link: <https://www.training.openquake.org/oq-introduction>



Openquake has two components: hazard and risk. Under the hazard component it mainly performs three types of seismic hazard analysis:

1. Classical PSHA

Under this approach, the Openquake Engine allows calculation of hazard curves and hazard maps following the classical integration procedure (Cornell 1968, McGuire 1976) as formulated by (Field, Jordan, and Cornell 2003).

2. Event based PSHA

Under Event based PSHA, the engine allows calculation of ground-motion fields from sets of stochastic events. By post-processing the set of computed ground-motion fields, traditional results such as hazard curves can be obtained.

3. Scenario based SHA

This allows the calculation of ground motion fields from a single earthquake rupture scenario taking into consideration the ground motion aleatory uncertainties.

We will discuss here in more detail the scenario based seismic hazard analysis.

In the case of Scenario Based SHA, the engine requires a single earthquake rupture model and one or more ground-motion models (GSIMs). Multiple realizations of ground motions can be computed, each realization sampling the aleatory uncertainties in the ground-motion model. It is also possible to condition the ground motion to observed values, if available, such as ground motion recordings and macroseismic intensity observations. The simulated ground motion fields are cross-spatially correlated.

B. Earthquake Scenarios

Firstly, multiple historical and/or hypothetical seismic events are selected to create seismic scenarios. The source of historical seismic events is defined through the knowledge of active faults, historical seismic events and geological composition at the site or hypothetical assumptions. Sufficient information is needed to parameterise the location (as a 3D surface), the magnitude and the style-of-faulting of the rupture. The parameters that are required to define a rupture are:

1. Strike: It is the angle between the intersection of the fault plane with a horizontal surface (relative to the North).
2. Dip: It is the angle between the fault and a horizontal plane.
3. Rake: It is the direction in which the hanging wall moves during a rupture.

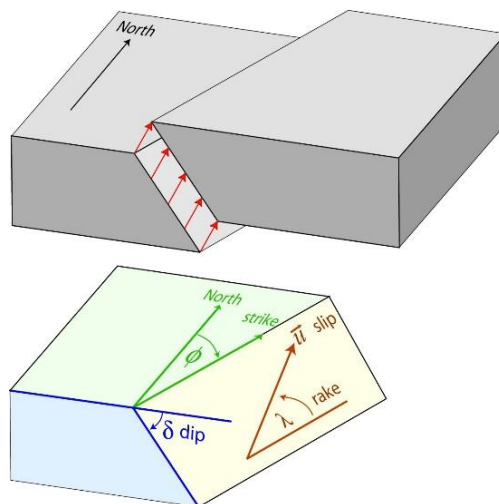


Figure 23: Rupture parameters

A rupture model can be defined in the following ways:



1. Simple Fault Rupture

Geometry is defined by the trace of the fault rupture, the dip and the upper and lower depth values limiting the seismogenic interval.

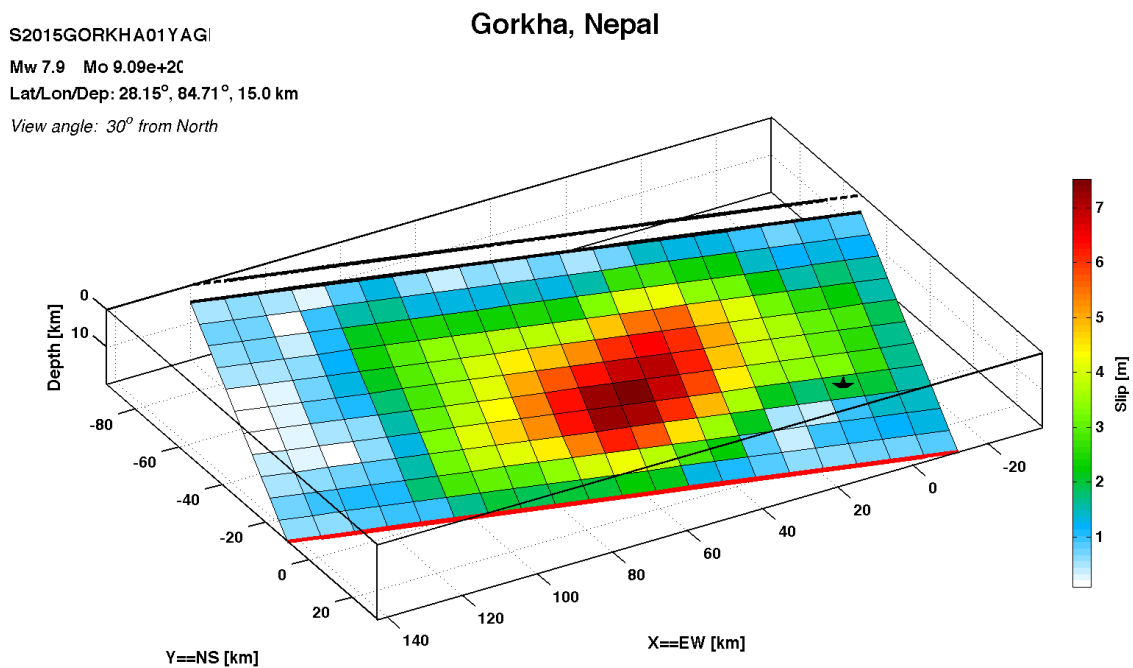
2. Planar and Multi-Planar Rupture

Geometry is defined as a collection of one or more rectangular planes, each defined by four corners.

3. Complex Fault Rupture

The geometry is defined by the upper, lower and intermediate edges (if applicable) of the fault rupture.

<http://equake-rc.info/srcmod/> is a useful online repository compiling rupture models for various past historical earthquakes. Some of the rupture models present in the repository are shown in the following figures:



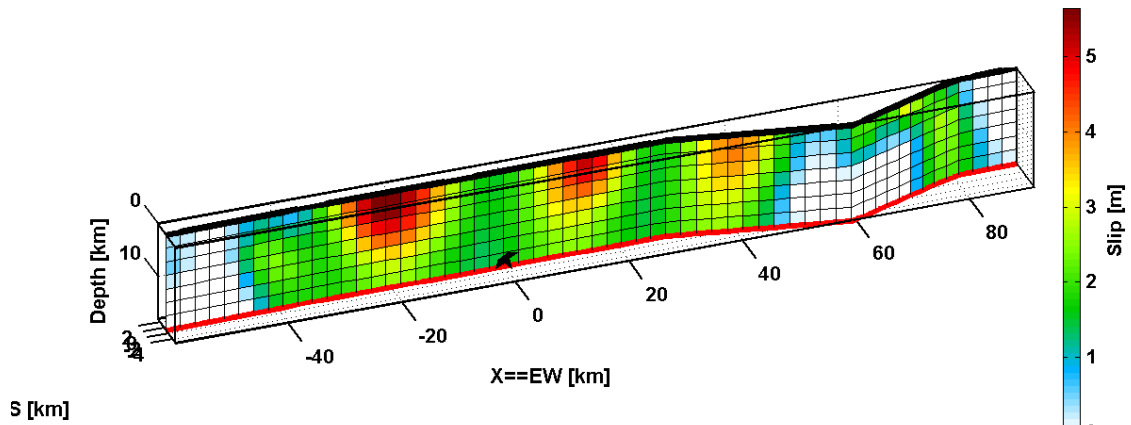
Source: <http://equake-rc.info/SRCMOD/searchmodels/viewmodel/s2015GORKHA01YAGI/>

Figure 24: Rupture model for Mw 7.9 Gorkha earthquake (April 25, 2015) in Nepal based on Yagi and Okuwaki 2015



Izmit (Turkey)

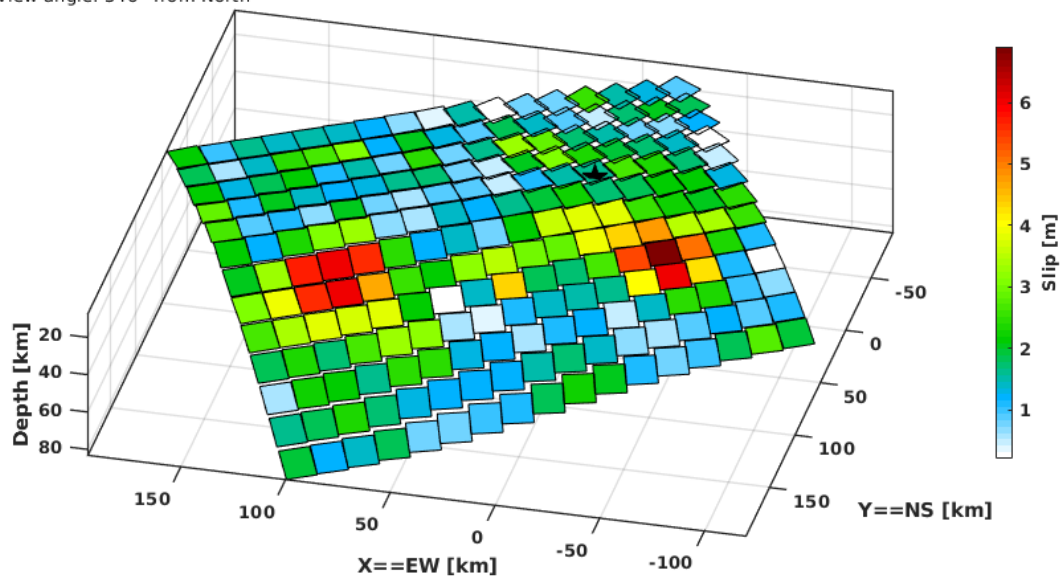
s1999IZMITTrell
Mw 7.4 Mo 1.54e+020
Lat/Lon/Dep: 40.76°, 29.97°, 17.0 km
View angle: 200° from North



Source: <http://equake-rc.info/SRCMOD/searchmodels/viewmodel/s1999IZMITT01REIL/>

Figure 25: Rupture model for Mw 7.4 Izmit earthquake (Aug 17, 1999) in Turkey based on Reilinger et al. (2000)

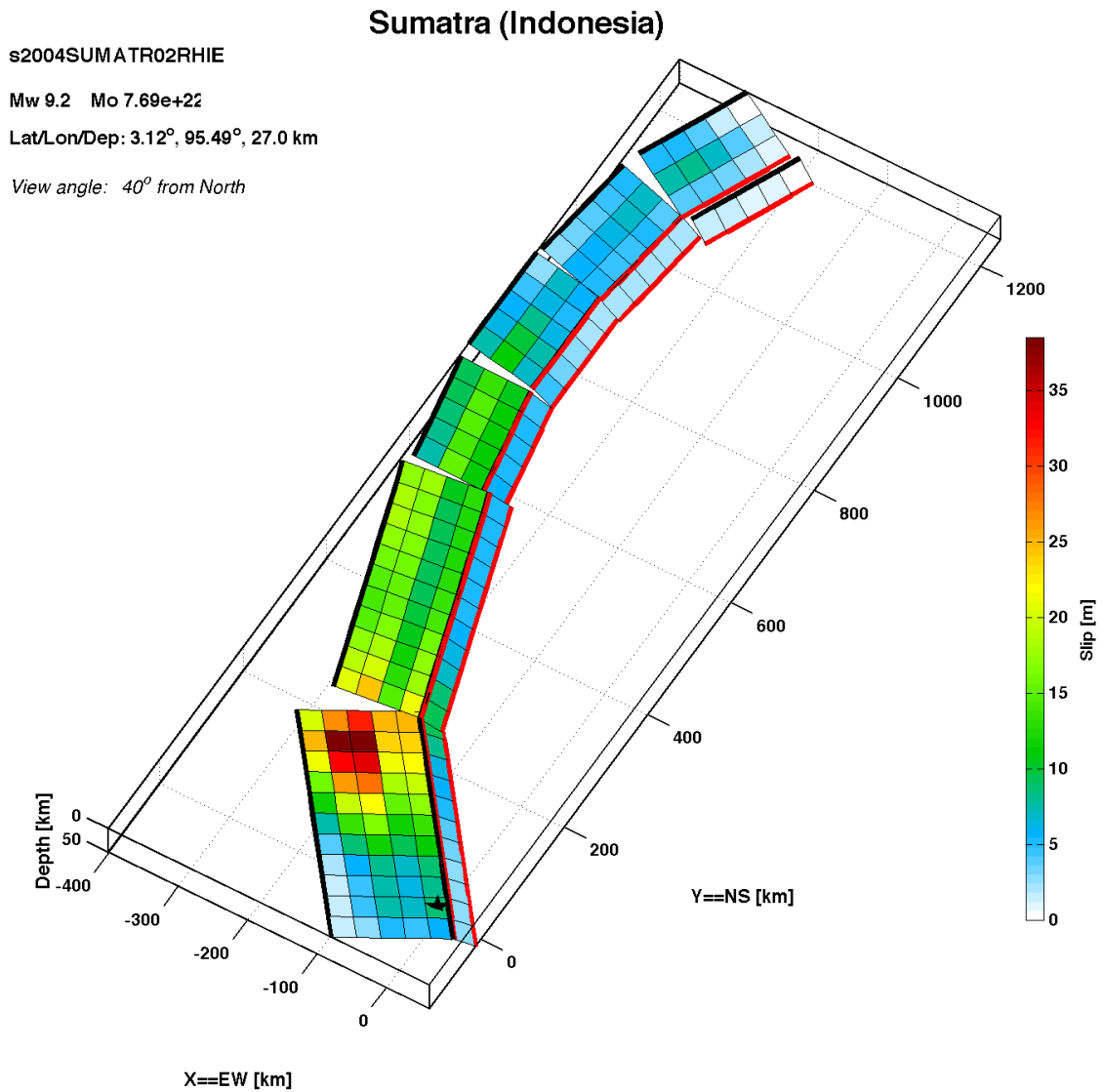
S1952TOKACH01KOB
Tokachi-Oki, Japan
Mw 8.4 Mo 4.80e+21
Lat/Lon/Dep: 41.71°, 144.15°, 17.6 km
View angle: 346° from North



Source: <http://equake-rc.info/SRCMOD/searchmodels/viewmodel/s1952TOKACH01KOB/>

Figure 26: Rupture model for Mw 8.4 Tokachi-Oki earthquake (Mar 04, 1952) in Japan based on Kobayashi et al 2021





Source: <http://equake-rc.info/SRCMOD/searchmodels/viewmodel/s2004SUMATR01RHIE/>

Figure 27: Rupture model for Mw 9.2 Sumatra-Andaman earthquake (Dec 26, 2004) in the Indian Ocean based on Rhie et al 2007

The explanation for fault geometry measurement convention for the preceding figures can be found in <http://equake-rc.info/SRCMOD/fileformats/geometry/>

Likewise, GEM foundation has also maintained a GitHub repository for earthquake scenarios which can be accessed through <https://github.com/gem/earthquake-scenarios/tree/main>.

C. Calculating Ground Motion Fields

Using the parameters of the rupture and one or more ground motion prediction models, the engine calculates the Ground Motion Field. The ground motion prediction equations have been already discussed in previous section. Multiple realizations of ground shaking are computed, each realization sampling the aleatory uncertainties in the ground-motion model.



2.5.3 Seismic Risk Calculation in Openquake Engine

A. Exposure Models

Exposure models quantifies the level of exposure and potential impact of disasters on various physical and social elements such as buildings, infrastructures, populations, natural resources and environmental assets that could be affected by various disasters, such as earthquakes, floods, landslides and fire. An exposure model provides spatial distribution of various elements at risk.

In Openquake Engine, exposure models comprise general information about the exposure, followed by a cost conversions section that describes how the different areas, costs and occupancies for the assets will be specified, followed by data regarding each individual asset in the portfolio. The Exposure model can be provided using csv files listing the asset information, along with an xml file containing the metadata section for the exposure model.

The following resources contain global exposure data used for seismic risk analysis (loss calculation):

1. METEOR project data download page:
<https://meteor-project.org/data/>
<https://maps.meteor-project.org/>
2. GEM foundation GitHub repository for earthquake scenarios and global exposure data
https://github.com/gem/global_exposure_model

B. Fragility/ Vulnerability Models

In order to perform scenario-based damage calculations, it is necessary to define a Fragility Function for each building typology or infrastructure in the Exposure Model. A Fragility Model contains a set of fragility functions, describing the probability of exceeding damage limit or states. Vulnerability Models are similar to fragility models, but different in that these relates hazard intensity measure with loss parameters.

Online interactive and non-interactive sources for various fragility and vulnerability functions are discussed along with criteria and methods to select these are explicitly discussed in upcoming session.

Combining hazard models, exposure models and fragility/vulnerability models, Openquake calculates risk in the form of damage or losses.

2.5.4 An Overview of Preparing Input in Openquake

After installing the Openquake Engine, you open its web interface using two ways:

1. By clicking on the console icon , and typing `> oq webui start`
2. By clicking on the webui icon  (it directs to the web interface)

You can prepare your input file by clicking on the Tools tab.



Here you can glide through various tabs for preparing your exposure models, fragility models, vulnerability models and earthquake rupture models.



INPUT PREPARATION TOOLKIT

Exposure Fragility Consequence Vulnerability Earthquake Rupture Configuration File

1. Use this form to modify the table header.

Description:

Structural Costs:

Nonstructural Costs:

Contents Costs:

Business Interruption Costs:

Occupants: Day
 Night
 Transit

Tags:

Select type of exposure:
 CSV Exposure (one XML plus one or more CSV files) | XML Exposure (all in one file)

CSV Header Description

id	lon	lat	taxonomy	number
----	-----	-----	----------	--------

Exposure CSV file[s]

Along with these tabs, there sits a configuration file tab. This tab is used to combine all of these inputs to form a single compressed file with configuration information.



INPUT PREPARATION TOOLKIT

Exposure Fragility Consequence Vulnerability Earthquake Rupture **Configuration File**

Earthquake Scenarios **Classical Probabilistic** Stochastic Event-Based Volcano Scenarios

The OpenQuake scenario calculators can be used for the calculation of damage distribution statistics or individual asset and portfolio loss statistics for a portfolio of buildings from a single earthquake rupture scenario, taking into account aleatory and epistemic ground-motion variability.

Choose components of your configuration file and fill related fields.

Hazard Risk

Description:

Scenario calculation

Rupture information

Rupture model file [?]:

Rupture mesh spacing (km) [?]:

Hazard Sites

Choose a method to input hazard sites:

Region grid List of sites Exposure model [?]

Region grid

Grid spacing (km) [?]:

Region coordinates Infer region coordinates from exposure model

Coordinates [?]:

Longitude	Latitude



Site conditions

Select a method to specify site conditions:

Use uniform site parameters Site conditions file

Reference vs30 value (m/s) [?]:

Reference vs30 type [?]: Inferred Measured

Minimum depth (m) at which vs30 ≥ 1.0 km/s (z1.0) [?]:

Minimum depth (km) at which vs30 ≥ 2.5 km/s (z2.5) [?]:

Calculation parameters

GMPE [?]:

Specify IMT [?]:

Custom IMTs:

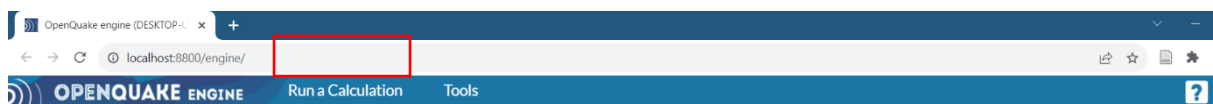
Ground Motion Correlation Model [?]:

Level of truncation [?]:

Maximum source-to-site distance (km) [?]:

Number of ground motion fields [?]:

This compressed file is then uploaded by clicking on Run a Calculation button in the initial page of the web interface.

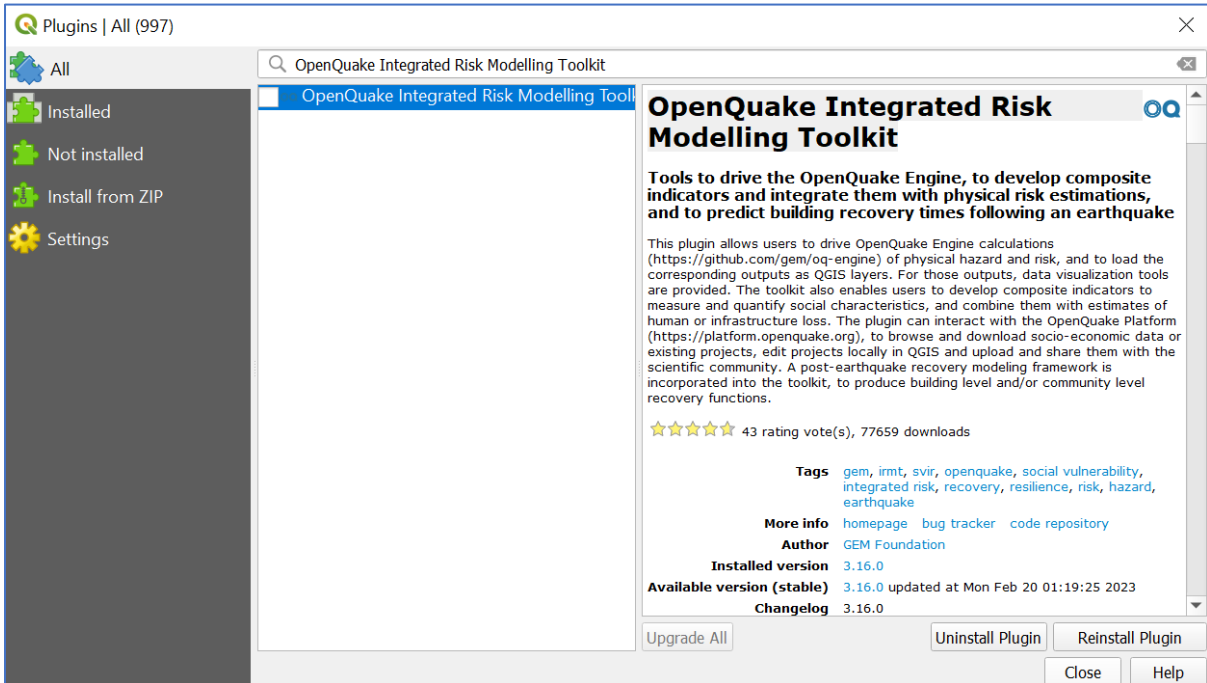
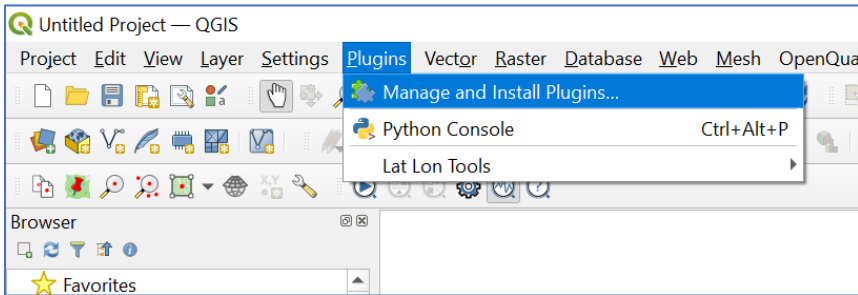


The Engine runs the analysis and produces outputs which can be visualized in QGIS through an integrated Openquake plugin.

In order to install the Openquake plugin in QGIS,

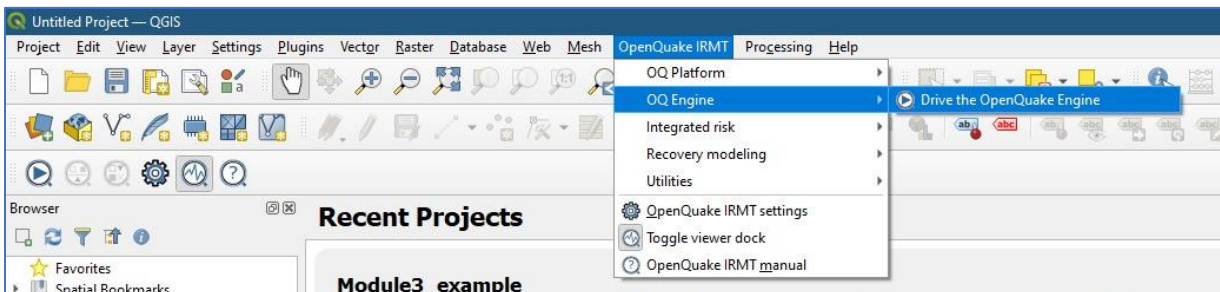
- Open QGIS software
- Go to Plugins in the Menu bar and click on Manage and Install Plugins....
- Click on the search bar and search for Openquake Integrated Risk Modelling Toolkit
- Click on Install Plugin





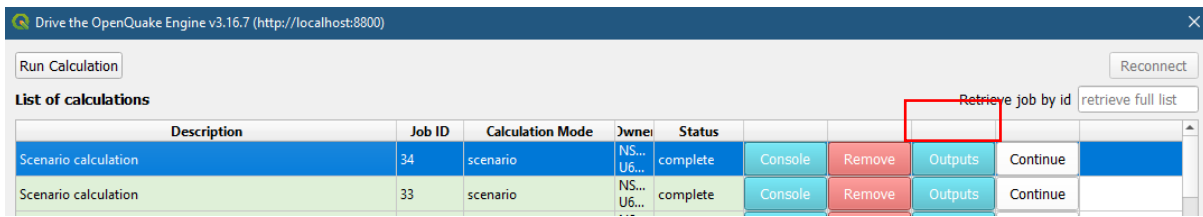
After installing the plugin, the plugin can be accessed,

- through menu bar by clicking Openquake IRMT > OQ Engine > Drive the Openquake Engine
- Or, simply clicking on shortcut icon 



It opens a dialog box similar to the Openquake Risk Calculation Webpage. There you click on Outputs on your calculation,





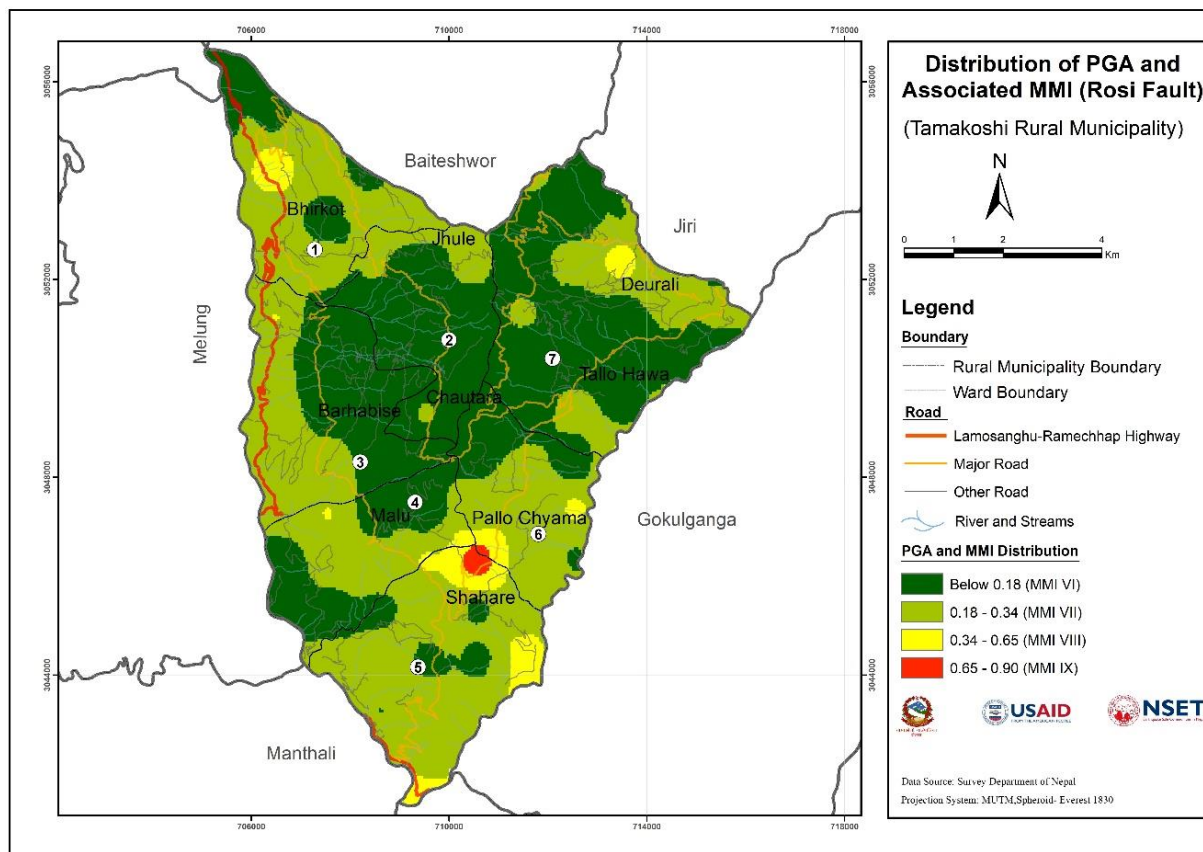
And click on load layer under your calculation type, in this case ground motion fields for example.

List of outputs for calculation 34

Id	Name			
43	Events	Load table	Download csv	
44	Full Report	Show	Download rst	
45	Ground Motion Fields	Load layer	Download csv	Download hdf5

This generates seismic hazard map showing ground motion fields or spatial distribution of intensity measures in the domain. [4]

Following figures show refined maps related to seismic hazard and risk assessment for Tamakoshi Rural Municipality in Nepal for various scenarios.



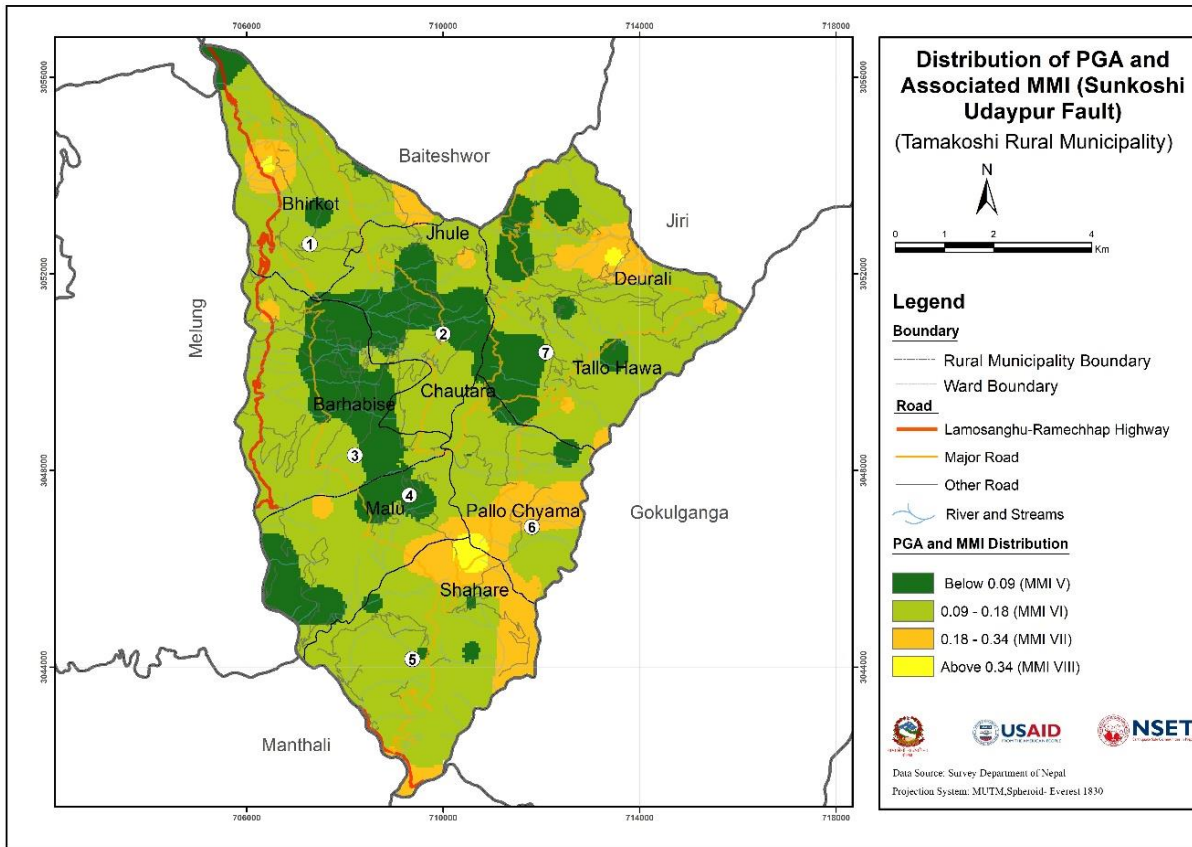


Figure 28: Seismic hazard maps for various scenarios – Tamakoshi

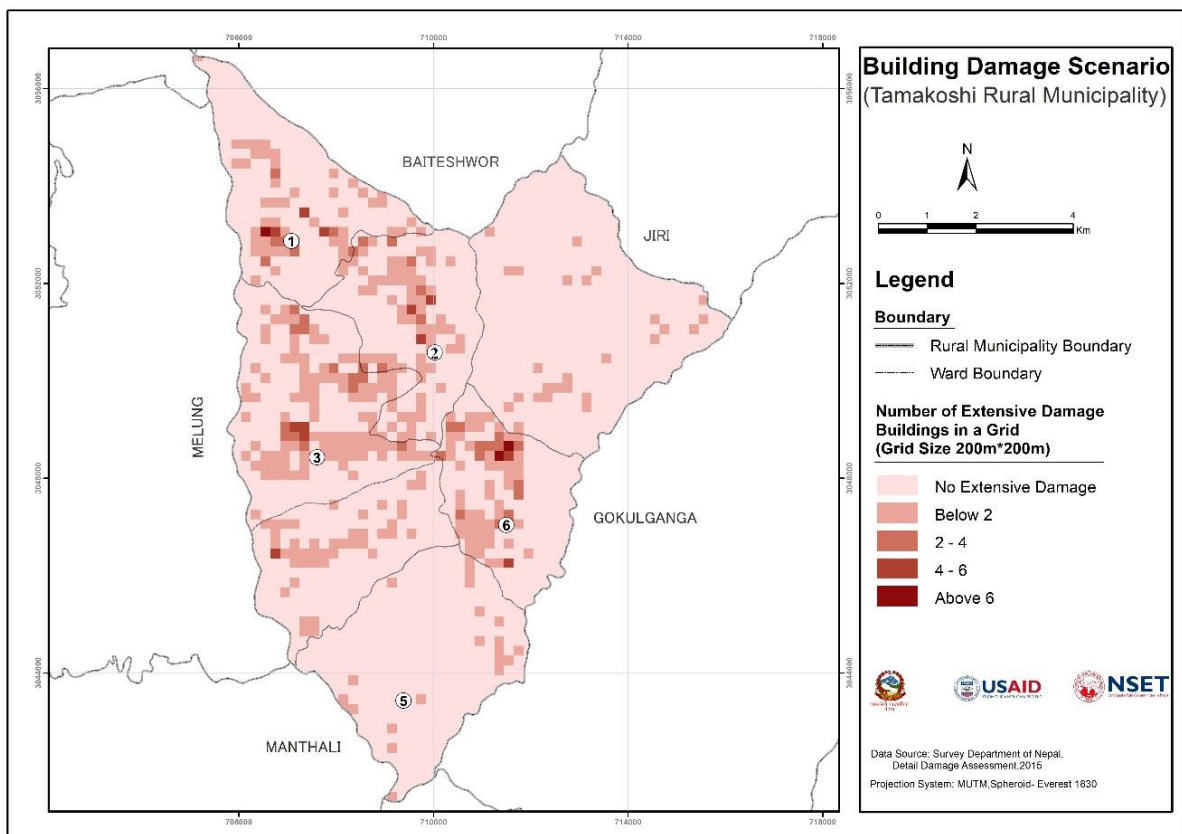


Figure 29: Building damage (extensive) distribution – Tamakoshi



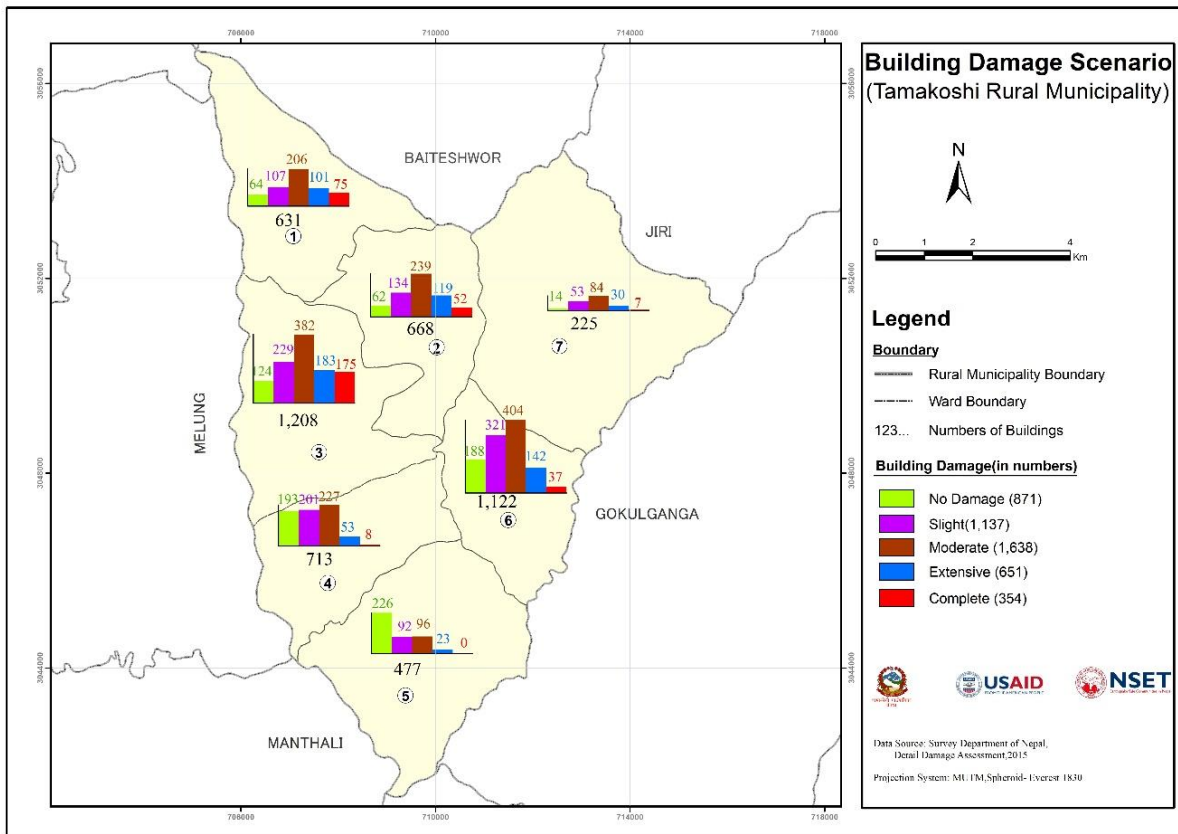


Figure 30: Number of buildings damaged (wardwise) – Tamakoshi

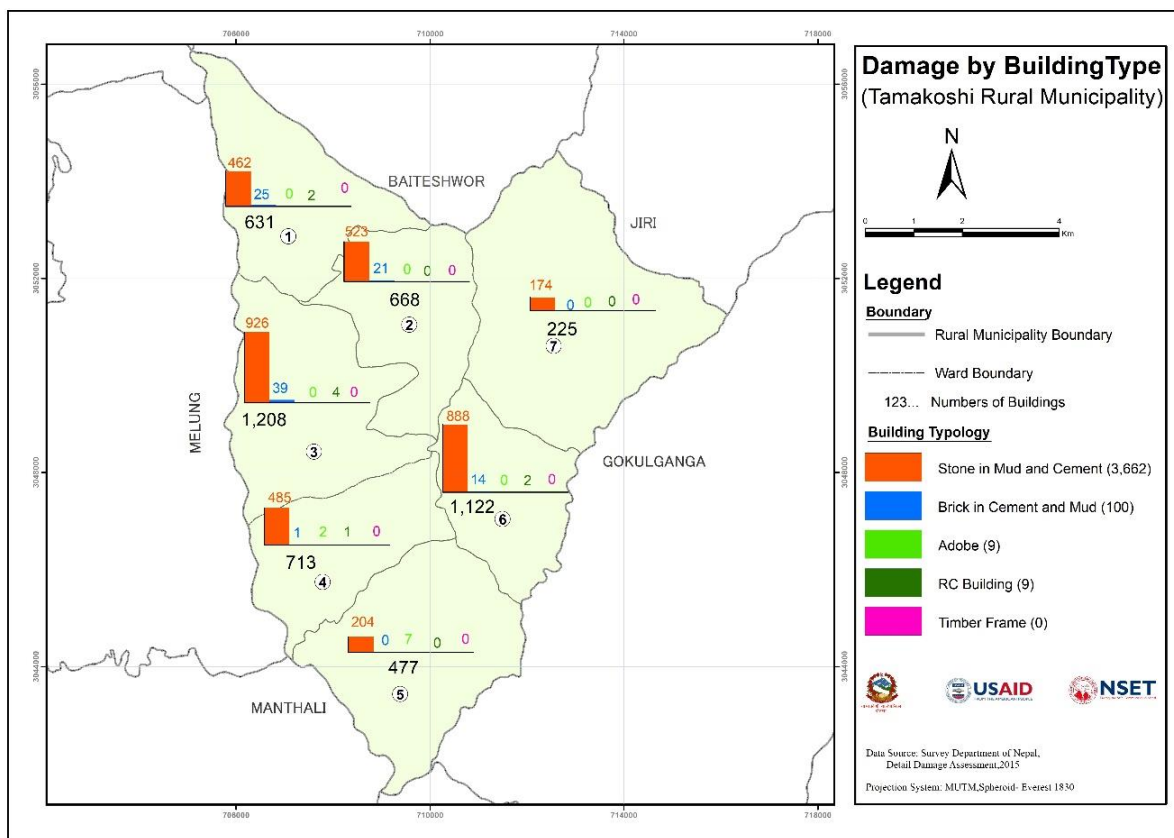


Figure 31: Building damage distribution (typology) - Tamakoshi



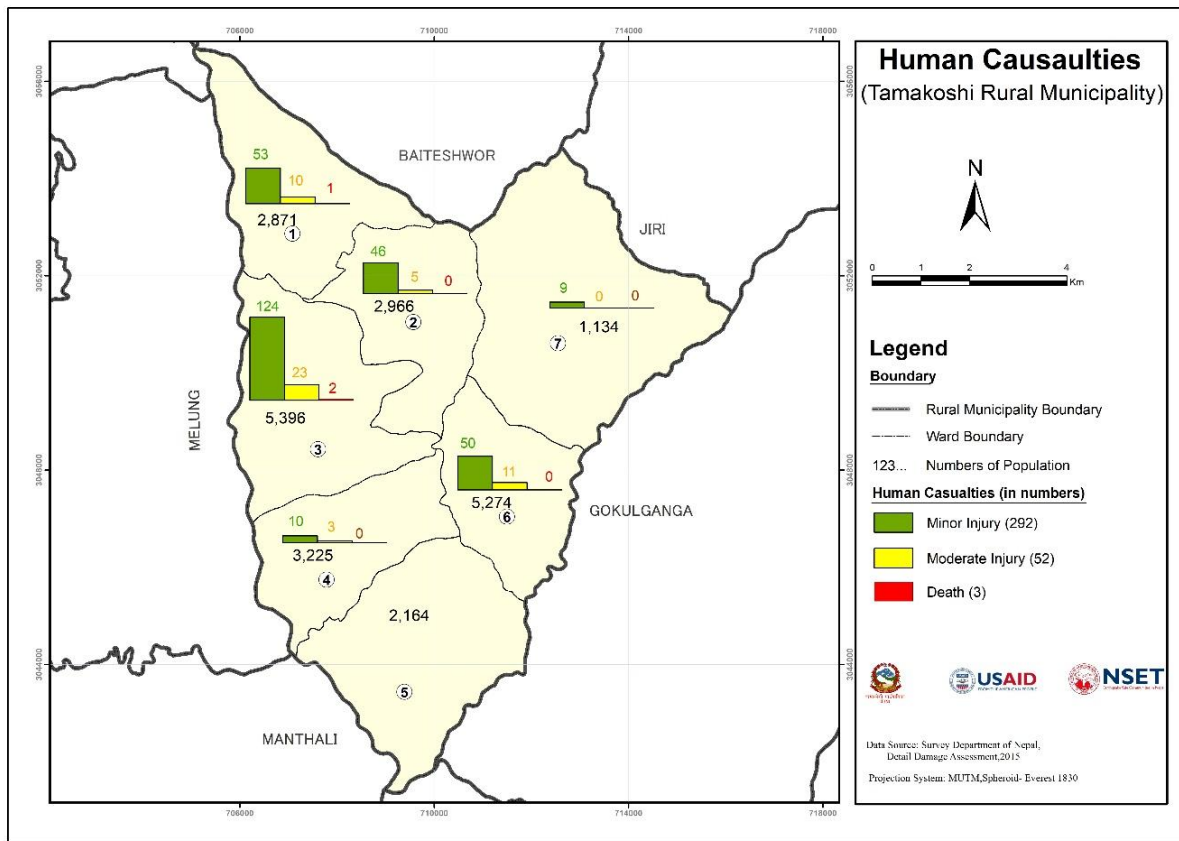


Figure 32: Human casualties - Tamakoshi

2.6 Physics Based Seismic Hazard Analysis

Physics-based seismic hazard analysis is an approach to seismic hazard analysis which uses the fundamental principles of physics, geophysics and seismology. The method uses mathematical and computational simulations to predict the behavior of fault mechanisms and the resulting ground motions. Physics-based methods are continually evolving as scientific knowledge is increasing, resulting in more accurate predictions of earthquake hazards and risks.

SPECFEM 3D is one of the software used to simulate 3D seismic wave propagation based on the spectral-element method. You can follow the link: <https://github.com/SPECFEM/specfem3d> for more details on the software and the seismic modelling process.

2.6.1 Advantages of Physics-based Simulations

Some of the advantages of physics-based seismic hazard analysis over other conventional methods previously discussed are:

1. Physics-based models can simulate the complex local ground motion better capturing the effects of local amplification and realistic rupture propagation



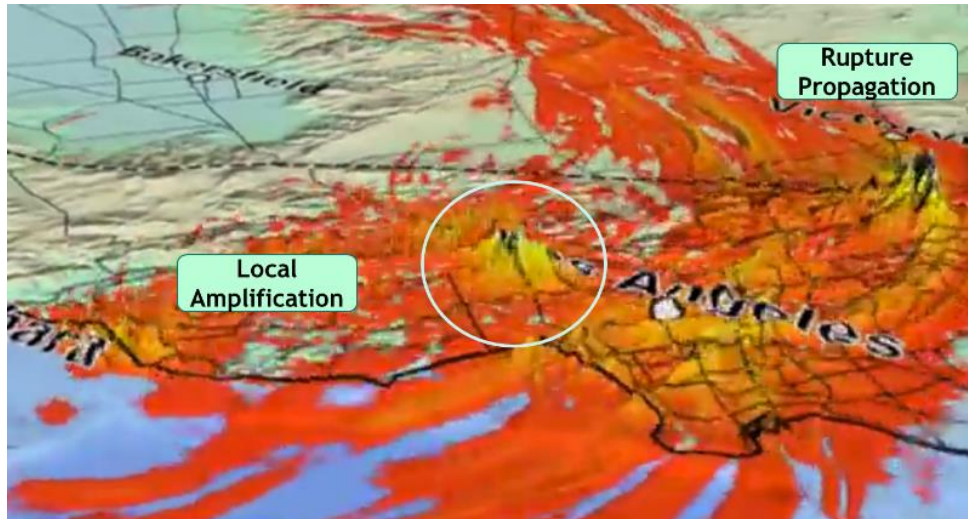


Figure 33: Physics-based simulation of ground motion

2. It can capture the effect of rupture directivity and basin response, which can increase the hazard level in some sites as compared to that predicted by the conventional methods.

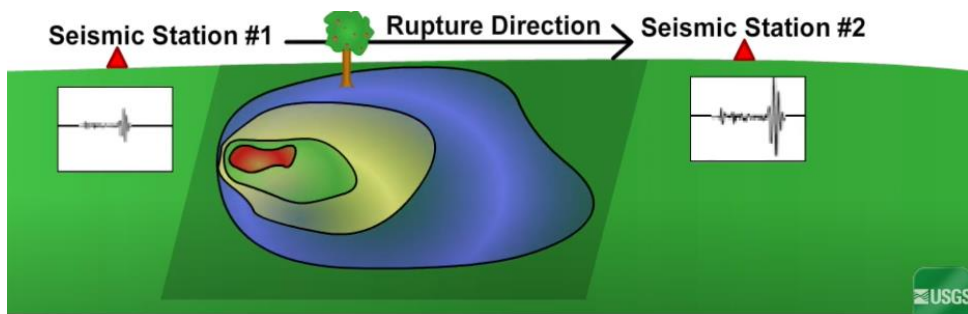


Figure 34: Rupture directivity effect

3. It can simulate the presence of asperities (stuck path) along the fault. Release of stress at an asperity under sliding of faults can intensify ground motion.

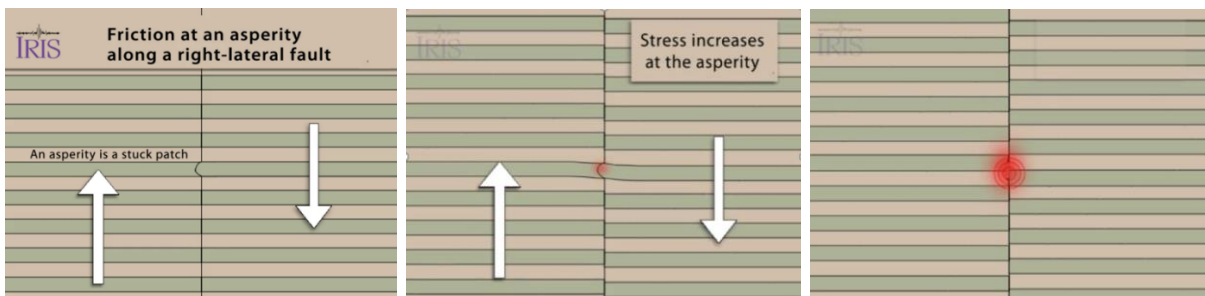


Figure 35: Effect of asperity

2.6.2 Data and Models Required for Physics-based Simulations

Physics-based models rely on detailed data on:

1. Earthquake source



Identification and characterisation of potential earthquake sources, such as faults, tectonic plate boundaries and seismic zones (spatial and temporal evolution of the rupture).

2. Velocity structure

Characterisation of the geometry of the geological features and their wave propagation properties for predicting the intensity, duration and frequency content of ground shaking at specific locations due to seismic events.

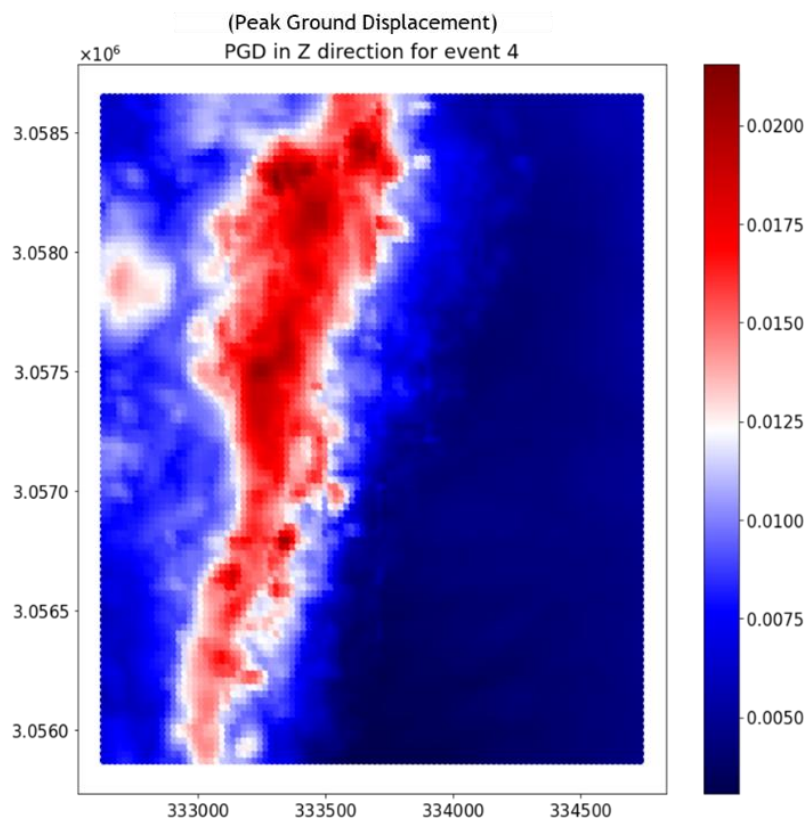
3. Near-surface soil behaviour

Characterisation of the shear modulus, damping, average shear waves, etc. for localized site response analysis.

Physics-based simulations cannot be done if there is unavailability of these data.

2.6.3 Example of Physics-based Seismic Model in Tomorrowville

The figures show the output of physics-based seismic simulation in Tomorrowville. Propagation of earthquake intensity at incremental time steps are shown in the second figure with colder colour denoting higher intensity. We can see here that higher intensity seismic shaking is concentrated along the river basin.



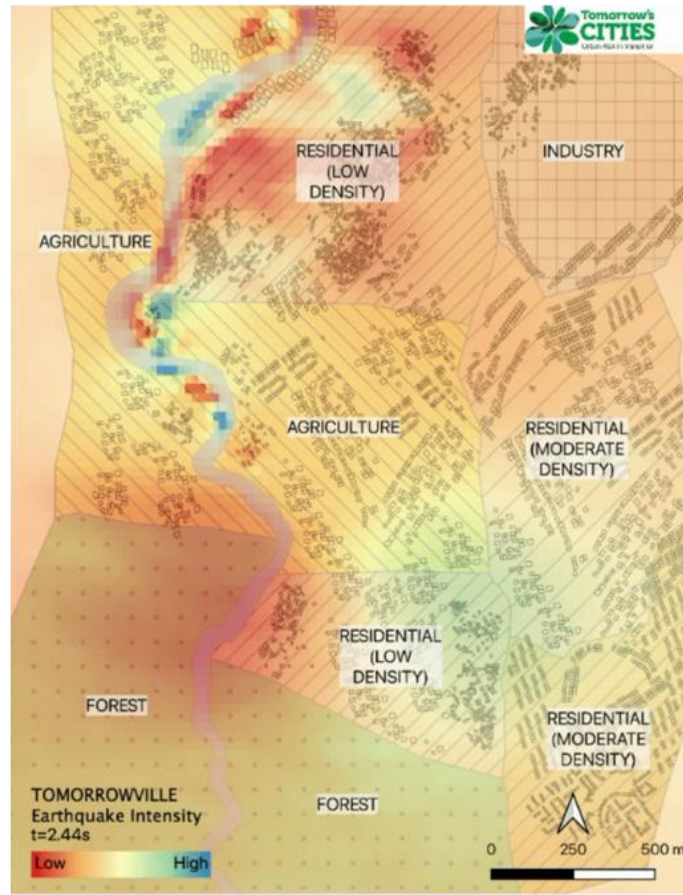


Figure 36: Physics-based simulation in Tomorrowville



SESSION 3: FLOOD HAZARD MODELLING

3.1 Objectives

By the end of the session, the participants will be able to:

- Explain the concept of flood hazard, vulnerability and risk.
- Differentiate between different flood hazard mapping methods.
- Discuss the capacity of and requirements for physics-based numerical modelling of flood hazards.
- Recognize the implications of input data resolution and quality.
- Identify methods for validating flood hazard maps.

3.2 Structure of Session 3

Structure
1. Concept of Hazard, Vulnerability and Risk
2. Flood Hazard Modelling
3. Physics-Based Modelling in Tomorrow's Cities
4. Impact of Data Resolution of Flood Modelling
5. Validation of Flood Hazard Maps

3.3 Concept of Hazard, Vulnerability and Risk

3.3.1 Flood Hazards

A flood hazard can be defined as a temporary inundation of land due to rainfall, storm surges, or overbank flow from rivers, lakes or reservoirs, for example. Floods can be beneficial by depositing nutrient rich sediments on agricultural land. However, floods are also responsible for widespread destruction of life, property, infrastructure, agriculture, and the environment.

3.3.2 Drivers of Flood Hazards

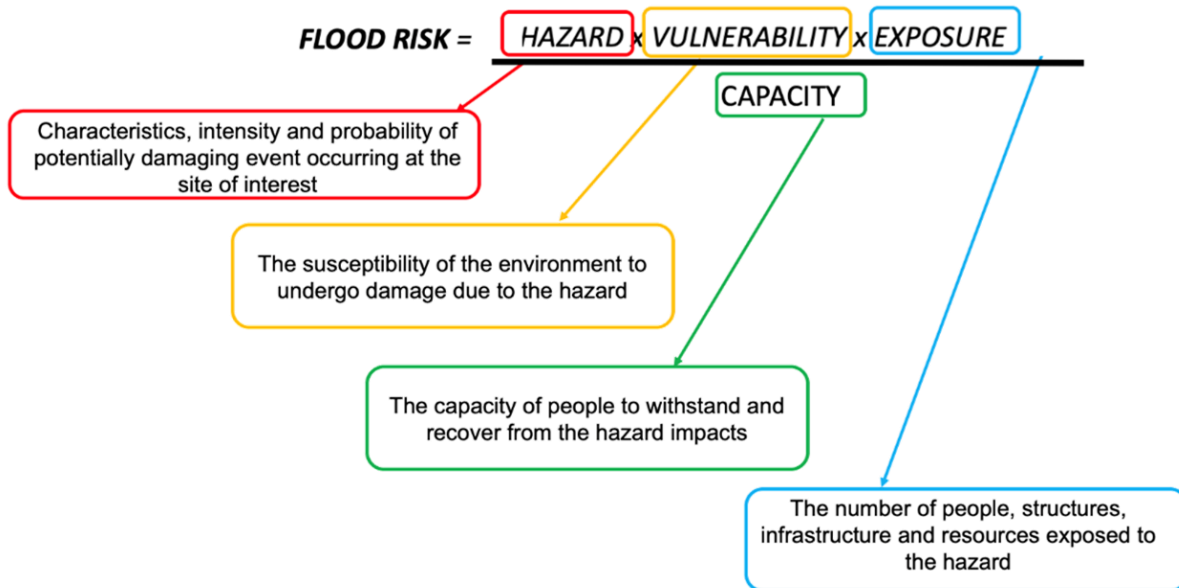
The drivers of floods can vary depending on geographical location and climate. Human drivers include land use change, urbanization, deforestation, dam breaches, blocked urban drainage systems, modification of rivers. Natural drivers of floods include flash floods and heavy rainfall, snow melt, storm surges and tsunamis, heavy sedimentation. In some parts of the world, climate change is increasing the frequency and intensity of extreme weather events, leading to more frequent flood hazards and flood disasters.

3.3.3 Hazard, Vulnerability and Risk Associated with Flood

Flood risk can be defined as the probability of flood event and its potential adverse consequences (UNISDR, 2009). As both aspects of risk - hazard and vulnerability - are non-stationary, flood risk is a “dynamic entity” (Merz et al. (2010) [5]; Loschner et al. (2016) [6]). Flood risk is generally expressed as a function of hazard, vulnerability and exposure as did by Kang et al. (2005) [7], Romali et al. (2020) [8], etc. The hazard is the intensity and duration of a given flood event within a given region. It can be defined in combination with the probability of occurrence in a given period. Vulnerability is the degree of loss sustained by a particular element or group of elements exposed to risk due to a natural phenomenon of certain intensity. Exposure is the element at risk such as population, property or other human activities. This definition of risk



can be extended to include the capacity of the people affected by the flood hazard to withstand and recover from the hazard impacts, such that the risk reduces as the capacity to rebuild and recover increases.



Within the current version of the TCDSE, flood hazards are measured by the depth and duration of a flood event. The outputs from the flood hazard modelling are combined with flood depth-damage functions in session on vulnerability modelling for single hazard to determine the level of damage intensity of the flood in any given location. In this module you will learn about:

- different approaches that can be used to generate the flood hazard information,
- key information about pre-processing input data to ensure reliable results from numerical flood models
- methods for post-processing the outputs of flood models for better visualisation and for use within the impact module of the TCDSE
- Sources of uncertainty in model results and limitations and appropriate use of flood models.

3.4 Flood Hazard Modelling

Flood hazard mapping and modelling are methods of estimating the intensity of a flood hazard in a given location. They can be used as a tool for flood forecasting and flood warning systems and can support the design and evaluation of flood risk reduction systems. In the context of the TCDSE and urban design, flood modelling can generate spatial information about flood intensity and duration for future flood events with different probabilities of occurrence.

Flood hazard mapping and modelling can be used together or separately to generate visual maps of flood intensities in a given region. The maps can be used to classify flood hazard prone regions as low, medium or high hazard zones.

3.4.1 Approaches for Flood Mapping

Different methods for developing flood hazard maps exist, all with their own pros and cons. For example, in the context of less data availability and/or unavailability of hydraulic modelling expertise, community-based approaches can be useful. If hydraulic modelling expertise is available in a region where there is reliable data available to calibrate the model, detailed numerical modelling of flood hazards may be more useful.



3.4.2 Community Based Flood Mapping

Method:

A community has local/traditional knowledge and that can be capitalized to develop flood hazard map. In this approach, various rounds of consultations are carried out with the community so that they will be able to plan before, during and after the flood event. It includes identifying safe shelters to stay during flood events to save their lives and livelihoods, and valuable belongings. Then a sketch of the study area is prepared, and the community is asked to locate major locations prone to flood hazard. A detailed hand-drawn map including safer and risky areas, hospitals or health posts, road network, sources of drinking water, households with differently abled etc. are prepared. A sample map product could be something like shown in the following figure below.

Challenge:

A community consists of different social structures (ethnic, class, religion, language, minority groups, etc.); cultural arrangements; socio-economic well-being; & spatial characteristics. They are too diverse to reflect in output. Representing/Reflecting their spirit in the best possible way is a great challenge. These are hand-drawn without scale, and often useful only to few people in the communities.

Strength:

It engages and makes the community aware and gets ready for planning and preparedness by internalizing the flood-related issues and consequences.

Suitability:

This approach is generally suitable in the context of less data availability and/or unavailability of hydraulic modelling expertise. This approach can also be applied even if modelling expertise is available, to complement the model-based results. However, when this local information is combined with novel digital mapping technologies such as Open Street Mapping, these maps become more accurate and easier to understand to both communities and decision makers.



Figure 37: Community Risk Mapping.



Note: these maps are not drawn to scale and give a brief overview of safe shelters, rivers and rivulets, road, at-risk houses, hospitals/health posts and sources of drinking water.

3.4.3 Empirical Modelling

Empirically modelling approach uses black-box models. Such models contain parameters that may have physical characteristics that allow the modelling of input-output patterns based on empiricism. Such models are classified as: Machine learning/AI; Statistical; Multi-criteria decision making (MCDM).

3.4.4 Physics-based Modelling

Method:

Flood inundation maps of an area are developed using hydrological and/or hydraulic modeling tools. There is a wide variety of commercial and open-source software available to develop such maps, for example, HEC-RAS, Caesar-Lisflood, TUFlow, Delft3D, etc. The choice of model depends on the type of flood event being modelled and the availability and quality of input data. Basic input data for most 1D or 2D models include input from rain gauges (hydrological data) or river discharge gauges (hydraulic), and a map of the bathymetry or topography, such as a Digital Elevation Model (DEM). Additional data is required for some models, for example, river channel description (including cross-section data), specific inlet and outlet boundary conditions, and information on hydraulic structures such as bridges, culverts, embankments etc.

Challenge:

This method requires existing expertise and capacity in numerical modelling to set up the model and interpret the results correctly. It requires reliable data for model calibration. Sources of uncertainty include the input data quality, uncertainty in the various parameters in the model, model complexity and the expertise of the model user.

Strength:

Detailed flood maps for large areas can be produced in a relatively short amount of time for a range of different flood intensities, including large floods which have not been recorded in the historical record by combining the flood modelling with return period analysis.

Suitability:

Only suitable where numerical modelling expertise is available and the input data available is of a reliable quality.



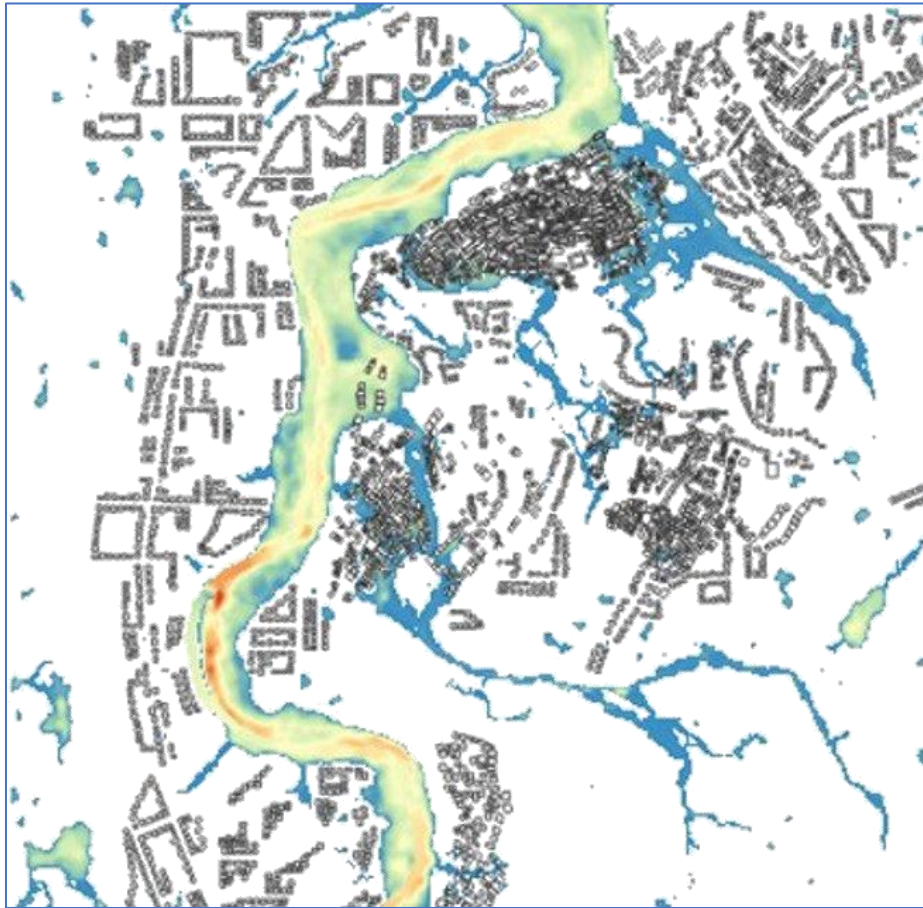


Figure 38: Numerical model output of flood map

3.5 Physics-Based Modelling in Tomorrow's Cities

Physics-based models are numerical models which can simulate the dynamic nature of flood hazards in time and space. Many types of physics-based flood models exist but they can be broadly divided into three categories: 1D models, 2D models and 2D water-sediment models. 1D models are fast and efficient to model flow within a river channel and can be useful to assess the time it takes for a flood wave to travel from upstream to downstream, or when time and computational resources are limited. 2D models are useful to model flow in rivers and floodplains, or coastal regions. They can produce more accurate spatial flood data when more computational time and expertise is available for the project. Lastly, 2D models which combine flow information and sediment dynamics (erosion and deposition of sediment) can be useful when modelling flood hazards around sensitive structures, or in regions where there is a lot of sediment activity.

Every physics-based flood model requires four main steps to generate flood hazard maps from a physics-based model: 1) Data collection; 2) Data pre-processing; 3) Model run and model calibration; and 4) Output data post-processing and data visualisation.

Within Tomorrow's Cities flood hazard mapping, two main models have been used: HEC-RAS and HAIL-CAESAR. HEC-RAS is a well-documented and widely used flood model. It has many parameters that require calibration and can be slow to run on large catchments. HAIL-CAESAR is based on the Lisflood algorithm.



3.5.1 Data Collection and Model Input Requirements:

The data required will depend on the specifics of the numerical model being used. Most 2D hydraulic and hydrological models, such as those used within the TCDSE, the data required includes a digital elevation model (DEM) of the region to define the topography and river network, land use/cover classification maps to define the Manning's roughness coefficient, rainfall and discharge timeseries files, soil infiltration details and information about important infrastructure such as bridges. For models which include sediment dynamics, sediment grainsize data are also required. Boundary conditions must be assigned at upstream and downstream locations and depend on the particular context. In the absence of detailed downstream boundary information, an open boundary can be assigned using the energy (or bed) slope condition.

For example, HAIL-CAESAR - High-performance Architecture Independent LISFLOOD-CAESAR (HAIL-CAESAR) is an adaptation of Caesar-Lisflood model to simulate streamflow and sediment erosion in a river catchment. The model doesn't have Graphical User Interface (GUI) and runs from scripts. The DEM file, parameter file and rainfall time series text file must be placed in the same folder and formatted correctly. Both catchment average rainfall and spatially varied rainfall can be used as input files. Details of the model can be found [here](#).

For Hail-CAESAR, the outlet point of the catchment should be at one side of the DEM file - touching DEM edged so that water will be able to leave the model domain without unrealistic pooling. Details on preparing DEM to input in HAIL-CAESAR can be found in the [documentation](#), and the methodology and necessity of removing DEM artefacts can be found in the module

3.5.2 Pre-processing:

It involves preparing DEM and rainfall files. Selecting proper resolution of DEM and removing artefacts are necessary before running the model.

Any anomalies in rainfall records and data consistency should be checked prior to preparing rainfall input files.

3.5.3 Model Runs:

The selected model is set-up properly by preparing inputs complying with the model's input data structure/template. All required inputs, such as DEM, rainfall, land use/cover, soil, etc. are set up well for the selected model. Then test run is implemented. Once it becomes successful, the model is ready for calibration/validation. During calibration/validation stage, observed and simulated discharge/floods are compared and performance of model to simulated observed discharge is evaluated. In addition, flood extent depth and extent map is generated for the selected flood and the flood extent is compared with actual flood extent (to be confirmed either from field observation or community consultation, or based on satellite images). Once the acceptable level of accuracy is achieved, the model parameters can be finalized and now the model is ready for extracting outputs, interpretation, and scenario analysis (if any).

3.5.4 Post-processing:

The model outputs water flow velocity and water depth files. They are in raster file format for each time step. For example, HAIL-CAESAR doesn't have GUI and runs from scripts. Model generated outputs are timeseries text file of water discharge, sediment fluxes, raster files for water depths, elevations, and erosion amount. ArcGIS, QGIS, or any other data visualization software such as R and python can be used for postprocessing model outputs.



3.6 Impact Of Data Resolution of Flood Modelling

Hydrological models are developed using spatial and temporal data. DEM and land-use/landcover are spatial data while hydro-meteorological data such as rainfall, discharge, water-depth are temporal data. Spatial data resolution refers to the area of land represented by a single grid cell in the field. For example, a 30 m DEM means one grid cell represents 30X30 meter area of land surface. Higher resolution DEM refers to the smaller area covered in the field and vice versa.

Similarly, temporal data resolution refers to the time interval of data and is fixed by the frequency of data collection such as minute, hour, day, month etc.

In flood modelling, data resolution has a significant impact on quality of model outputs. When ran with lower resolution of spatial and temporal data, it overestimates flooding extent, miss peak discharge and peak arrival time while higher resolution increases computation time. Thus, a trade-off between data resolution, accuracy and computation time must be ascertained prior to running the hydro-morphological models.

3.6.1 DEMs

A. Summary

Flow hazard models, including floods and landslides, are applied using topographic models (DEMs) that simplify reality. Key considerations when using DEMs include the spatial resolution, the acquisition sensor (e.g. optical, radar, lidar), the date of acquisition, post-processing (e.g. filtering or smoothing), and the relative (pixel to pixel) and absolute (with respect to an established vertical datum) model accuracy. The choice of DEM should be specific to the characteristics of the study site and not simply guided by data availability. Poor DEM choice creates poor quality results, which can propagate through further analysis to create outputs that are misinterpreted or fundamentally incorrect. The 'best' DEM is rarely applied in a given application due to accessibility and processing constraints. However, this guidance will show the reader how to select appropriate DEMs and interpret common artefacts.

B. Background

- DEMs are produced at a broad range of spatial resolutions, depending on the acquisition source. Here we focus on the type of models applicable for Tomorrow's Cities hazard models: typically, bespoke models produced at ≤ 2 m resolution, and global open-access models available at 30-90 m resolution (Table 2).
- Bespoke DEMs are produced with a defined time stamp and could be produced for annual or sub-annual time periods, whereas global DEMs are typically produced for a single date, although this often spans multiple years due to a composite of data that were used to produce the final product.
- DEMs are sometimes supplied with a quality layer that indicates how many valid observations were used to derive the final elevation value, or if a pixel was interpolated due to a data gap.
- Elevation values are usually referenced to either the ellipsoid (used by Global Navigation Satellite Systems) or a Earth Gravitational Model (EMG) geoid (e.g. EGM96 or EGM 2008).
- Accounting for different vertical referencing is required when comparing DEMs. Similarly, DEMs should be coregistered horizontally before comparing elevation values, or the outputs of multiple simulations run on different DEMs. Coregistration involves iterative shifting of the DEM in XYZ directions to minimise differences until the DEMs are aligned.



Table 2: Typical DEM characteristics. Note that minimum order sizes usually apply to costings.

Source	Typical spatial resolution	Temporal resolution	Typical cost	Considerations
Lidar (terrestrial or airborne)	Centimetres	As required	Variable (\$1,000s)	<ul style="list-style-type: none"> Will pass through vegetation to produce accurate DSM and DTMs. Surface features such as buildings, walls, and vegetation are well resolved.
UAV/ aerial photogrammetry	Centimetres to decimetres	As required	Variable (\$1,000s)	<ul style="list-style-type: none"> Cannot resolve below vegetation. UAV surveys have low cost but low spatial coverage. Aerial surveys are expensive and not always available. Surface features such as buildings, walls, and vegetation are well resolved.
Optical satellite (e.g. Pleiades or WorldView)	1-2 m	Daily depending on cloud cover.	\$31/km ²	<ul style="list-style-type: none"> Products are DSMs and cannot resolve below vegetation. Resolving the ground amongst high-rise buildings may require tri-stereo (three images) acquisitions or greater. Surface features such as buildings vegetation are reasonably well resolved.
ALOS World 3D - 2.5 m	2.5 m	2006-2011 (window)	\$7/km ²	<ul style="list-style-type: none"> Product is a DSM and cannot resolve below vegetation.
TanDEM-X DEM	12 m	2010-2015 (window)	\$6/km ²	<ul style="list-style-type: none"> Radar will partially pass through vegetation. Elevation values represent an average of surface and ground features.
Shuttle Radar Topography Mission (SRTM)	30 m	2000	Open-access	
Advanced Spaceborne Thermal Emission and Reflection Radiometer (ASTER) Global Digital Elevation Model (GDEM)	30 m	2000-2013 (window)	Open-access	<ul style="list-style-type: none"> Global open-access DEMs are generally produced from a composite of data, meaning the elevation of individual pixels is within a window of several years. Elevation values represent an average of surface and ground features.
ALOS World 3D - 30m (AW3D30)	30 m	2006-2011 (window)	Open-access	<ul style="list-style-type: none"> Products are DSMs and cannot resolve below vegetation. Elevation values represent an average of surface and ground features.
Copernicus (COP30)	30 m	2011-2015 (window)	Open-access	
Multi-Error-Removed Improved-Terrain (MERIT)	90 m	2000-2011 (window)	Open-access	



C. DEM type:

Digital Surface Model (DSM):

- DSMs represent the resolvable ground surface and surface features such as buildings and vegetation.
- Whether the ground or a surface feature is resolvable is dependent on the spatial resolution relative to the feature of interest.
- In the case of a global 30-90 m DSM, the elevation values representing the urban environment are some average of the ground surface, buildings, and vegetation, so flow models will not capture routing through streets and between buildings.
- Vegetation that is resolved in a DSM will act as an undesirable barrier to flow, therefore removing it is necessary to improve flow routing.

Partial DSMs and Digital terrain models (DTMs):

- A partial DSM, where vegetation is removed but buildings are retained, is desirable for flow routing since buildings act as barriers to flow in most cases, though is dependent on construction type.
- Creating a partial DSM usually first requires a DTM, where all surface features are removed from the model, before re-adding building elevations to the DTM.
- Several tools existing for creating DTMs usually involve a moving window of a size that is large enough to cover the largest size of buildings present in the model.
 - An algorithm with a given window size is usually passed over the raw 3D point cloud if available (i.e. before the DSM gridding) to identify ground point vs. surface feature points, the latter of which are removed, and the data gaps interpolated over to create a ground surface model (DTM).
- The DTM generation approach can produce undesirable outputs in several cases, particularly in dense urban areas where no ground pixels are found, on steeply sloping areas, and in breaks of slope such as riverbanks or ridges, which are usually truncated by the algorithms.
 - Smaller moving window sizes reduce these effects but are subsequently only capable of removing smaller surface features (e.g. smaller buildings).
 - Consideration should be given to the topographic changes introduced in the DTM generation step when evaluating model outputs.
 - Differencing the DSM and DTM is an easy way to reveal these changes.

F. DEM processing:

Sinks

- Flow models should specifically consider the location of sinks in the DEM, which act to accumulate water until they are overtopped, and the location of the drainage network.
- Sinks may be natural depressions in the landscape, artefacts of the DEM, or related to the DEM resolution. A medium resolution DEM is more likely to have sinks caused by poor representation of topography, for example in a river valley or gorge, which means the true valley floor is not resolved and acts as a damming feature in a flow model.
- Common methods to remove sinks in a process called hydrological correction, include 'filling' or raising the elevation values of the upstream topography until the height of the sink is matched and water would continue to flow downstream.
 - For large sinks, this can cause extensive artificial modification of the topography, leading to large areas of flat topography upstream of the sink.



- An alternative method is to breach through the sink using a ‘cutting’ algorithm. In this case, the true valley floor remains unknown, but the algorithm will cut a channel through the topography until water can flow. A method called ‘cut and fill’ incorporates both these methods to minimise the overall topographic modification required for hydrological correction.
- Generally, ‘filling’ algorithms should be avoided in medium resolution DEMs where they can cause extensive undesirable effects.
- Similarly, not applying post-processing would lead to the same damming effect and incorrect flow hazard mapping.

Drainage network

- It may be necessary to ‘burn-in’ or enforce the drainage network within a DEM to remove artefacts caused by poor representation of the water surface, which causes spikes or undulations in the elevation profile, or to breach damming features such as bridges.
- Ideally, the river channel bed (accounting for river width and depth) is burnt into the DEM. However, in most cases this information is unavailable, so the channel will represent the water surface in the DEM.

DEM uncertainties and model outputs:

- DEM uncertainties should be considered before and after application of a flow model so that the level of interpretability of outputs beyond background noise can be determined, and to check for areas where DEM artefacts may propagate through to cause incorrect flow model results.
- Common methods to quantify DEM uncertainties include comparisons of elevation values with independent ground control points or altimetry datasets such as ICESAT-2.
 - DEM differencing with other models of similar resolution is also used to characterise the spatial distribution of errors, for example using a semivariogram, in addition to revealing areas of topographic change.
- Once the flow model outputs are produced, they should be inspected alongside the input topographic data to check that the results look reasonable, especially in areas where the DEM was modified during hydrological correction or other post-processing.
- The user should consider how DEM errors compare to the magnitude of modelled flow depth and if stochastic DEM simulations can better quantify the DEM-related uncertainties, since DEM errors are known to be spatially correlated.
 - Stochastic simulations produce multiple model DEM inputs and therefore probabilistic outputs by adding a spatially distributed error model to the DEM.
 - The limitation of such an approach is that typical flow models using high-resolution elevation models are not designed to efficiently iterate over multiple topographic datasets.
- Evaluation of model outputs should also consider features that are not present in the topographic input such as potential for drains and subterranean flow in an urban environment. In some cases, it may be reasonable to assume that these features are overwhelmed or blocked during large magnitude flow events

Example: impact of resolution of rainfall data:

- Show hydrographs from the daily and hourly rainfall model of 2021 event



3.7 Validation of Flood Hazard Maps

Validating flood hazard map is a challenge, primarily because of limited (or no) availability of observed data on flood hazard or its components. Generally, flood hazard maps are validated based on field observation of flood marks or observed flood depths at gauging stations or comparing flood extent map with satellite imageries.

- Validation from field observation and flood marks: flood marks, flood inundation extent, and depth related information can be collected from field study, by observation as well as consultation with community. Such information can be considered as a reference for validating results from flood inundation modeling.
- Validation with observed flood depth: Simulated flood depth at hydrological station can be compared with observed flood depth to evaluate capability of flood models to map flood hazards. In one of the case study locations of Tomorrow's Cities Project, Kathmandu, flood hazard maps are validated by comparing simulated flood depth with the observed depth at gaging station.
- Validation from satellite imagery: depending upon resolution of data, some satellite imageries can provide at least flood extent map for specific events. If results from model-simulation matches with that of satellite imagery, it helps to validate the results.



SESSION 4: DEBRIS FLOW MODELLING

4.1 Objectives

By the end of the session, the participants will be able to:

- Explain the properties of debris flows that control their dynamics and impacts.
- Explain how debris flow initiates, and that knowledge is used to determine idealized source conditions for debris flow modelling.
- Summarize qualitatively how debris flow properties and source conditions are encoded into mathematical models for their dynamics and hazard.
- Recognize the three components of a debris flow model - the mathematical model, source conditions and topography on which the flows are computed.
- Communicate with relevant experts on the use of debris flow models within the TCDSE.

4.2 Structure of Session 4

Structure
1. Introduction to debris flow
2. Components of Debris Flow Modelling

4.3 Introduction

4.3.1 Characteristics of Debris Flow

Debris flow consists of a rapid moving mass of loose soil, rock, and water down a slope under the action of gravity. It can travel typically 10s km from their source, up to 100s km for the largest (volcanic debris flows). It carries significant volume of sediment and can increase their volume by up to 10 times due to erosion and the dynamics of debris flow is characterised by fronts and shocks.



Source: <https://www.youtube.com/watch?v=bt05FIIZPgM>

Figure 39: Volcanic debris flow in Semeru, Indonesia

Debris flows are destructive which cause significant threats to life in various settlements. The routing of urban debris flows is typically controlled by the topography of buildings, roads and other urban infrastructure. This means that future urban designs need to be incorporated into



digital surface models on which debris flow models are computed, in order to properly assess the potential impacts of urban debris flows in future cities.

4.3.2 Initiation of Debris Flow

Understanding the physical processes that control the sourcing of sediment is key to predicting the behavior and damage caused by debris flows. The two end member mechanisms that trigger sediment mobilization are:

A. Shallow landsliding

Rainfall can trigger debris flows by causing shallow landsliding (due to increased substrate pore pressure destabilising slopes) or by surface rainfall runoff entraining soils or other materials to create a debris flow. Failure of inclined material can mobilise large volumes of concentrated sediment. Further routing/ fluidisation is required for this material to be incorporated within a debris flow. Landslides occur when the shear strength of a hillslope can no longer support shear stresses. This is expressed as a 'Safety Factor'.

$$\text{Safety Factor} = \frac{\text{Shear Strength}}{\text{Shear Stress}}$$

Several mechanisms that can trigger shallow landsliding by increasing shear stress or decreasing shear strength are:

- Earthquakes - increases stress acting on hillslope
- Slope modification (e.g. cutting slopes for roads)
- Infiltration of water following heavy rainfall, snowmelt, anthropogenic sources -> increase in pore pressure

B. Erosion and entrainment

Erosion (adding of substrate into the flow) increases the downslope component of weight which is the force that drives the flows downhill under the action of gravity. This increase of weight causes the flow to be able to travel further and faster. Debris flows are episodic flows of water and sediment in ephemeral channels. Loose material is remobilised provided that hydrodynamic pressure exerted on debris exceeds resistive forces (e.g. friction). This is often parameterised using the Shields Number (θ_s):

$$\theta_s - \theta_{crit} = \frac{\tau_b}{(\rho_s - \rho_w)gd} - \theta_{crit} > 0$$

Material is entrained when,

$$\frac{\text{Shear stress } (\tau_b)}{\text{Debris buoyancy } [(\rho_s - \rho_w)gd]} > \text{Critical threshold } (\theta_s)$$

4.4 Components of Debris Flow Modelling

When we refer to a 'debris flow model' we are referring to three components: the numerical calculations of the flow dynamics, the source conditions for the flow that are needed to start this calculation, and the topography over which the flow calculations are being made.

4.4.1 Model Source Conditions

A realistic source condition for the model must be chosen that:

- Ensures the resulting debris flow is realistic
- Develops channelised flow in the desired area only



- Is based on physically plausible past or future scenarios
- Obeys modelling assumptions
- Stable (i.e. small perturbations to SC does not significantly impact model performance as outputs)

There are two principal source conditions:

A. Cap source

It is a sudden collapse of materials, typically either solid materials such as a sudden collapse of the surface which might be relevant to landslides that transition to debris flow or instantaneous release of fluid such as dam break.

B. Flux source

And then there is the more commonly used flux source, which is a release of a flow rate of water and sediment. And this is commonly used for rainfall driven debris flows.

Source Condition:

The flux source is typically represented by what we call a hydrograph, which is a plot of source flux or source volumetric flow rate as a function of time. In a debris flow model, it might include components such as the fluid or water flux shown in blue and also some variable concentration of sediment which is released at the source. So, these are idealisation of how materials are set into motion within the model scenario.

Estimating peak hydrograph discharge:

In order to prescribe time series for future debris flow scenarios, we can make and estimate the peak discharge which is the peak of the hydrograph. We can do that, for example for a rainfall event in a very simple empirical way using the expression shown,

$$Q \sim A \cdot I_r \cdot C$$

Where, A = upstream catchment area (from the source location)

I_r = rainfall intensity (mm/s, inches/hour, etc.)

C = Runoff coefficient (proportion of rainfall converted to surface runoff)

Table 3: Runoff coefficients for land use types

Land Use/ Type of Surface	Range of "C" Values*
Downtown business	0.70 to 0.95
Heavy industrial	0.60 to 0.90
Multi-residential units, attached	0.60 to 0.75
Light industrial	0.50 to 0.80
Neighborhood businesses	0.50 to 0.70
Cultivated lands with loamy soils	0.40 to 0.45
Suburban residential	0.25 to 0.40
Playgrounds	0.20 to 0.35
General unimproved lands	0.10 to 0.40
Parks and cemeteries	0.10 to 0.25
Woodlands with sandy soils	0.10 to 0.15

* C is a unitless coefficient



This table shows the range of typical C values, and those related to how permeable the surface is. For example, in urbanised settings, C can be quite close to 1 because with hard urban surfaces nearly all of the rainfall runs off. In more rural areas or the urban green spaces this coefficient can be much lesser. We could also multiply this peak flux by estimating sediment concentration as well to give us some initial source condition. So, this is a way we can create an idealised hydrograph for future events if we know the catchment area and rainfall intensity in the future.

Other Considerations:

Location	Flow source should generate flow in target channel only.
Size	Flow in source area must obey shallow layer approximation ($h/r \ll 1$).
Duration and magnitude	Based on current/ projected climate data.
Ramping on/ off	Promotes stability and prevents development of artificial fronts in flow.
Simplicity	Simple hydrograph structure allows for easier interpretation of downstream dynamics.

4.4.2 Model Ingredients and Assumptions

There are range of standard models that are applied to debris flow with their underlying principles and assumptions:

- Conserves mass and momentum
- Shallow layer approximation
- Vertical averaged quantities (density, concentration, etc.)
- Rheology/ drag that can account for flow concentration
- Often neglect erosion and simplify deposition

A. Debris Flow Model Ingredients

Here we have a flowing layer of water and solid material on the slope. This layer is accelerated downslope as a consequence of its downslope component of weight which is resisted by the basal stress. And if the model includes processes of erosion which is adding the underlying surface to the flow or deposition which is removing solids from the flow and increasing the height of underlying surface then those local changes due to erosion and deposition change both the downslope component of the weight and deposition and the basal resistance. These processes are all coupled in the computation of the properties of this flowing layer.

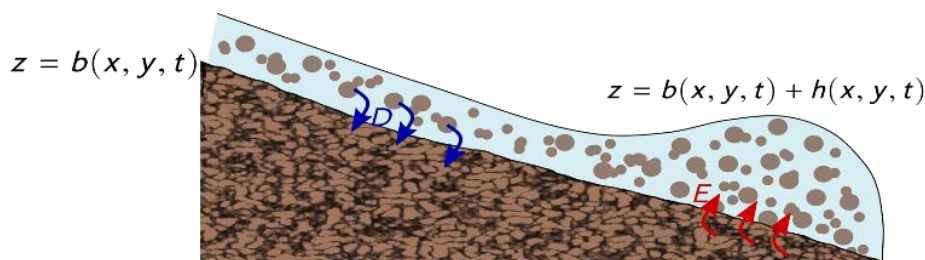


Figure 40: Erosion and deposition in debris flow

And some models use quite sophisticated basal drag laws, that might account for concentration-dependence of that drag. Here’s an example which is used in the model I am going to show later, where you have fluid drag component and granular drag component, which is relevant to higher particle concentrations and you might want to switch between these two components in a way that can be calibrated in the model.



Where erosion and deposition are included, they are often parameterised in a standard way. In this case, erosion is parameterised based on excess Shields stress that we talked about in the initiation for these flows and deposition is parameterised by an analogy with sedimentation rate of individual particle which creates rate of deposition. If erosion and deposition are included, adding solids from the bed to the flow increases the solid concentration in the bed but it reduces the surface height. If deposition occurs, it decreases the solid concentration and increases the surface height. These topographical changes due to erosion and deposition can be computed in a simple way.

4.4.3 Model Inputs

A. Parameters

Table 4: Example parameters

Parameters	Value
Water density	1000 kgm ⁻³
Sediment density	2000 kgm ⁻³
Solids diameter	0.01 m
Bed porosity	0.65
Maxm packing fraction	0.65
Maxm erosion depth	1 m
Critical Shields Number	0.055
Fluid Erosion Rate	10 ⁻⁴
Granular erosion rate	0.1
Chézy drag coefficient	0.04
Pouliquen Minm Slope	0.1
Pouliquen Maxm Slope	0.4
Voellmy switch rate	3.0
Voellmy switch value	0.2

Source: Jenkins et al., 2023

Some of these parameters can be chosen based on information that is available within the city or within academic literature. It can be based on municipal geotechnical data, data from the scientific literature, some of these quantities can be measured in the field and the lab, and overall, the model needs to be calibrated for all of these parameters by matching the predictions of the models against past/ analogous events where's there has been good observations.

B. DEM/ DSM

Topographical artefacts in DEMs (e.g. trees, cars, bridges, etc.) introduce errors in flow routing. Artefacts must be removed via interpolation.

Accurate flow routing through urban landscape requires:

- High resolution drone surveys (< 1 m resolution)
- Future building elevations must be incorporated into a Partial Digital Surface Model (DSM)



4.4.4 Model Outputs

The model outputs are typically the dynamic properties of the flow: the maximum depth of the flow as a function of time and position, the maximum velocity and if your model also includes erosion and deposition, you can also compute the topographical changes. We take these maps of flow intensity or hazard intensity and combine them with engineering and social calculations to compute impacts.

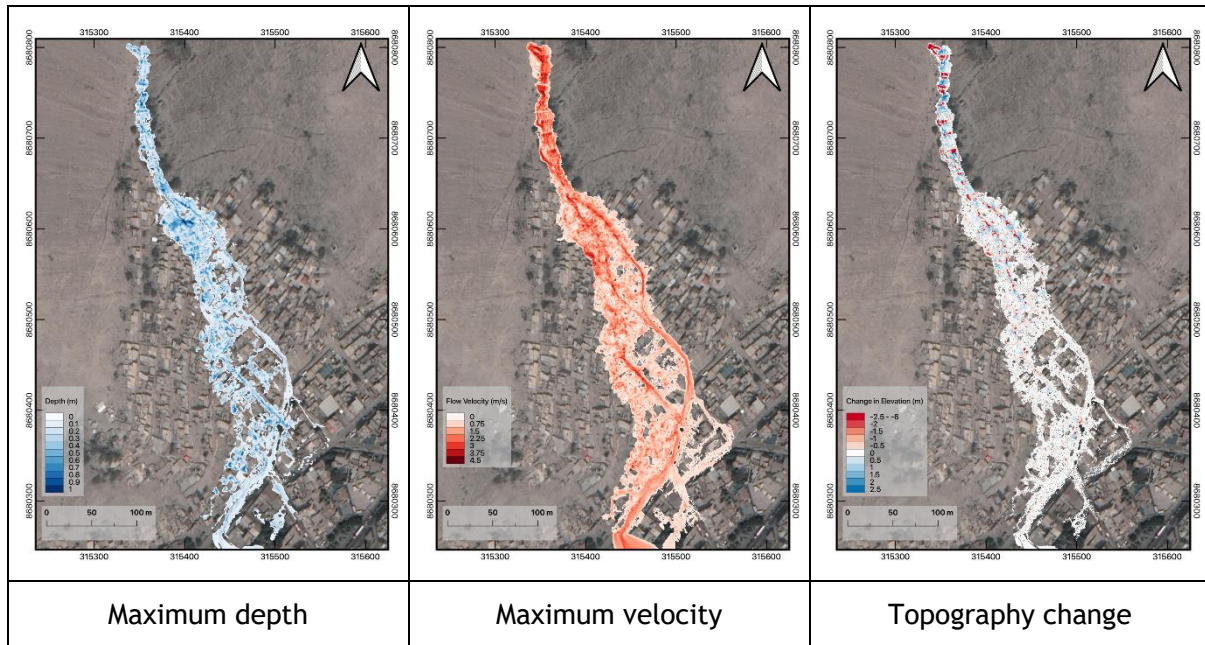


Figure 41: Outputs of debris flow model

Debris flow causes damage in multiple different mechanisms, which means sophisticated fragility functions are needed. The flow,

- exerts pressure on structures as a result of its dynamic properties which can cause the structure to fail,
- as the flow carries debris the individual boulders can impact the structures causing damage to it,
- erosion at the base of the flow can scour out the foundations of the structures, and deposition of sediment can bury the structures and the roads.

And essentially, by taking the intensity maps from the model and combining it with vulnerability functions we end up with some estimate of the impact that can be used to inform different urban development choices.



SESSION 5: LANDSLIDE HAZARD MODELLING

5.1 Objectives

By the end of the session, the participants will be able to:

- Identify broad landslide types and causes (including interactions with dynamic urban environments and climate).
- Discuss broadly on different landslide hazard assessment scales, associated model types and data requirements, and the resulting information for decision support.
- Diagnose local capacity for landslide hazard assessment (people and organizations, technical skills, data, models).
- Define the scope of the local landslide hazard problem and select an appropriate modelling approach.
- Identify the types of information required to study landslides in the city and case study scales.
- Explain the empirical-statistical methodologies used to study the landslide hazard at the city level, examples from Kathmandu and Quito.
- Interpret the results obtained at the city scale and their use in the TCDSE.

5.2 Structure of Session 5

Structure
1. Landslide Hazard Assessment: Scope of Landslide Problem and Local Capacity
2. City-Wide Landslide Hazard Assessment: Landslide Problem Definition
3. Examples of Physics-Based Modelling for Quantifying the Local Hazard

5.3 Landslide Hazard Assessment: Scope of Landslide Problem and Local Capacity

5.3.1 Landslides and Diagnosis on Its Types and Interactions

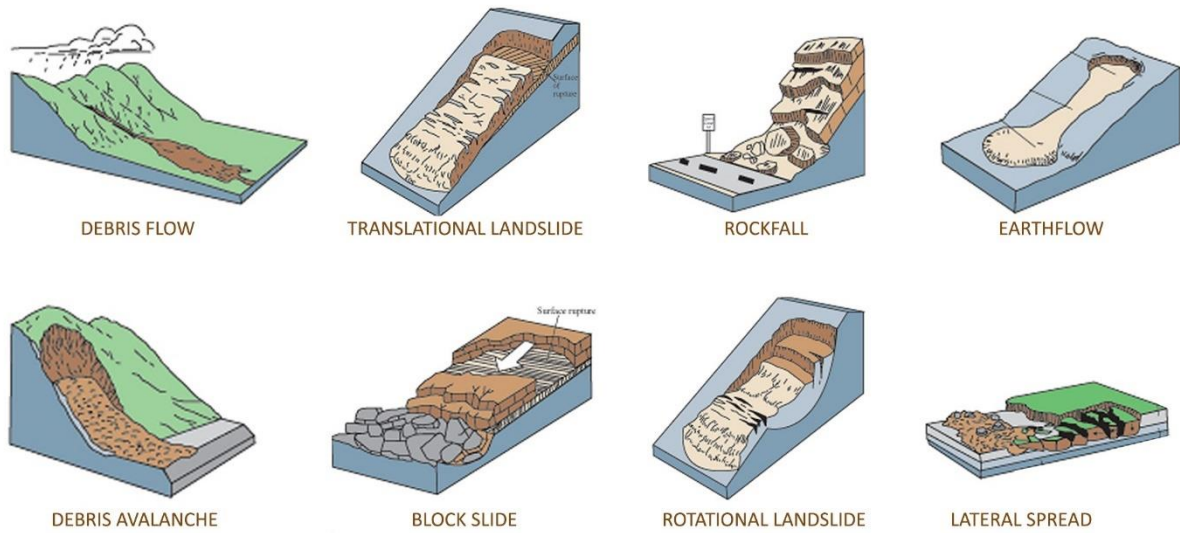
Landslide is the movement of mass of rock, earth or debris down a slope under the influence of gravity. The types of landslides that we are dealing with is shown in table below:

Table 5: Types of landslide movements

Type of Movement (Failure and Runout Mechanism)	2. Type of Material		
	Bedrock	Engineering Soils	
		Mainly coarse	Mainly fine
Falls	Rock fall	Debris fall	Earth fall
Topples	Rock topple	Debris topple	Earth topple
Slides	Rock slide	Debris slide	Earth slide
Rotational			
Translational			
Lateral spreads	Rock spread	Debris spread	Earth spread
Flows	Rock flow	Debris flow	Earth flow
	(deep creep)	(soil creep)	
Complex	Combination of two or more movement types		

Source: USGS Fact Sheet 2004-3072, July 2004: <http://pubs.usgs.gov/fs/2004/3072/pdf/fs2004-3072.pdf>





Source: <https://nggindia.com/blogs/landslide-typologies-causes-detection-of-prone-areas/>

Figure 42: Types of landslides

Real examples:



Rotational landslide



Rock fall



Debris flow

Source: Basanta Raj Adhikari and Camilo Zapata

Figure 43: Photographs of landslides



For further information on the classification and characterization of mass movements according to type and material, we recommend the paper by Hungr, O., Leroueil, S., y Picarelli, L. 2014. The Varnes classification of landslide types, an update. *Landslides*, 11(2), 167-194.[9]

A. Urban Landslides Predisposing Factors and Triggers, Frequencies and Magnitudes

Physical preparatory factors	<ul style="list-style-type: none"> • Topography (slope angle, height, convergence), • Material (strength, hydrology, strata, depth), • Drainage, vegetation
Human interactions	<ul style="list-style-type: none"> • Change the above preparatory factors (increase hazard?), • Often most vulnerable are most exposed to LS hazards
Triggers	<ul style="list-style-type: none"> • Rainfall, earthquakes, excavation (mining, construction)
Scale, frequency	<ul style="list-style-type: none"> • From small rotational slides to high-velocity, long-runout debris flows; and from frequent individual landslides (everyday hazards) to multiple concurrent landslides

B. Multi-disciplinary and Co-Developed Data, Knowledge and Actions

Collaborative work between researchers and community members allows sharing of information and knowledge in two ways. Researchers can collect relevant data from the experience of the local inhabitants. On the other hand, it allows the inhabitants to understand the environment in a systematic manner.





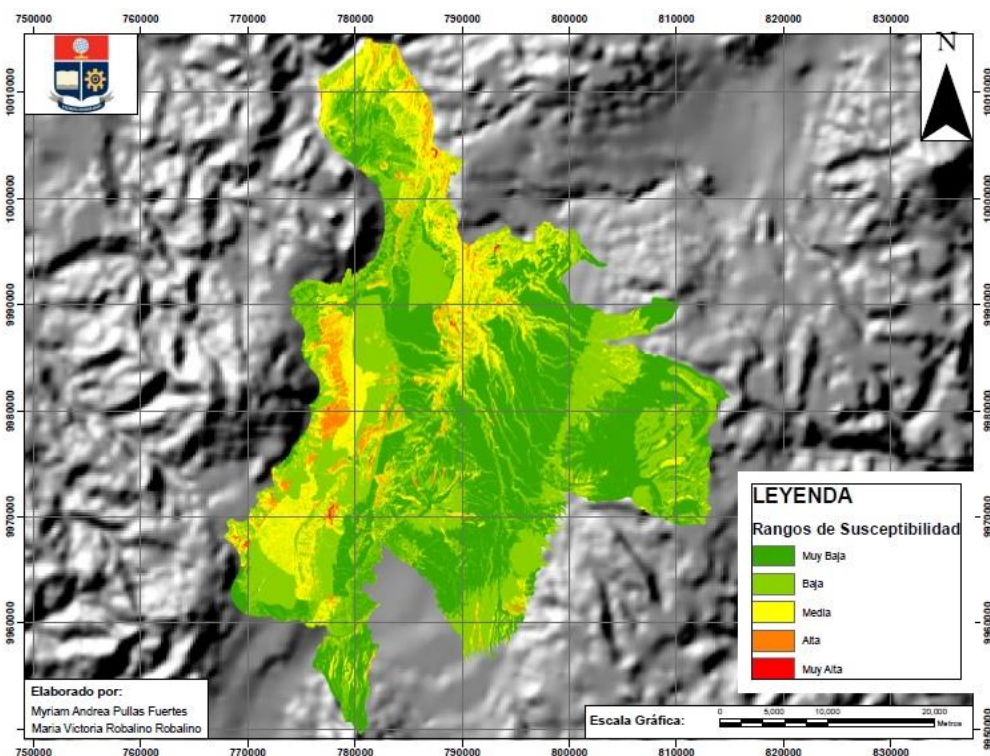
Source: Camilo Zapata

Figure 44: Collage of pictures about the process of community-based mapping in Quito-Ecuador

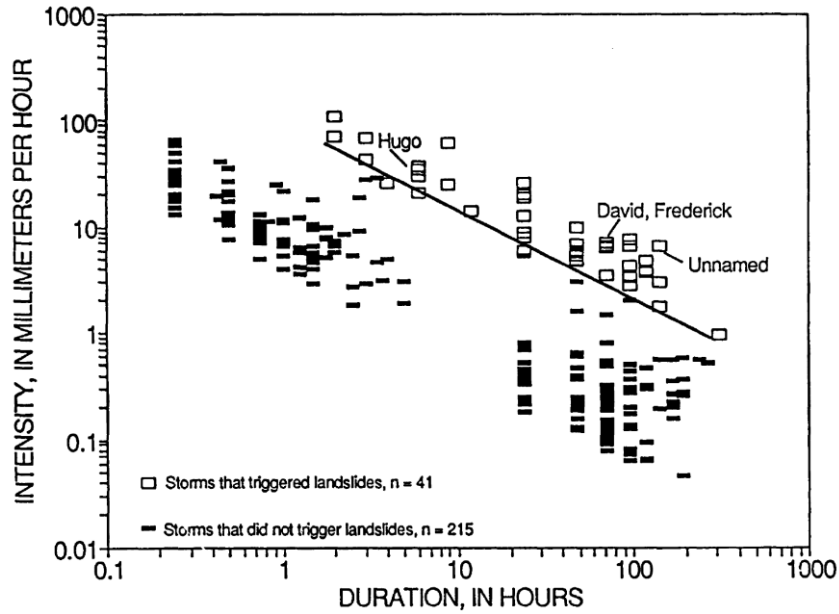
5.3.2 Landslide Assessment Methods

A. Some Empirical- Statistical Methods of Landslide Assessment

Methods	Examples
Inventories and landslide triggering thresholds	<ul style="list-style-type: none"> Larson and Simon, 1993 Puerto-Rico rainfall intensity-duration threshold for landslides
Statistical analysis of landslide sizes, frequencies, length-width ratios, etc.	<ul style="list-style-type: none"> Taylor, Malamud, Witt and Guzzetti, 2018. doi: 10.1002/esp.4479
Spatially distributed (Geographical Information System, GIS-based) susceptibility and hazard maps	<ul style="list-style-type: none"> Central Nepal, inventory of 22,000 landslides post-2015 (Durham, BGS) used in landslide hazard mapping Quito inventory of 1,300 landslides used in bivariate statistical analysis of landslide susceptibility mapping

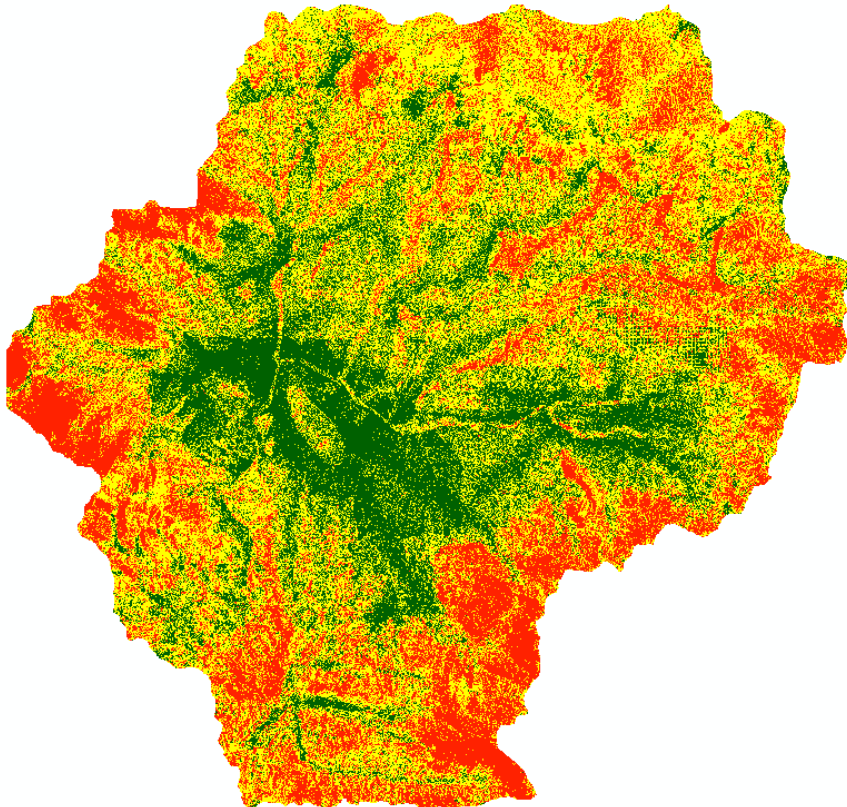


Source: Pullas A, Robalino MV, 2018. Geological Engineering Thesis, EPN Quito-Ecuador



Source: Larsen, M.C. & Simon, A. (1993). Geogr. Ann. Ser. A, Phys. Geogr., 75(1-2), 13-23 [10]

Landslide Susceptibility Map: Kathmandu:



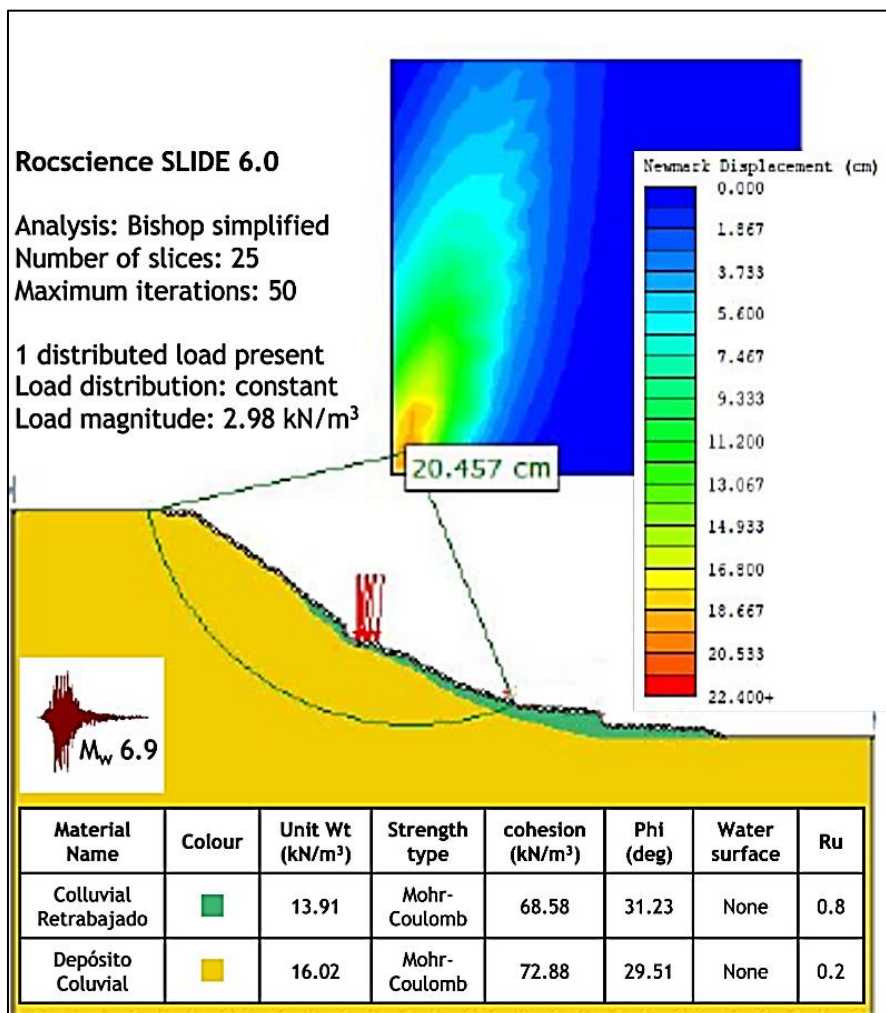
Source: Bhatta & Adhikari draft article

Figure 45: Landslide susceptibility map of Kathmandu



B. Some Physics-Based Methods

Analytical	<ul style="list-style-type: none"> • Static Limit Equilibrium Analysis- wedge analysis, methods of slices
Dynamic LEM	<ul style="list-style-type: none"> • Slope hydrology and stability over time (CHASM); or seismic trigger (Newmark displacement)
Analysis of Continua	<ul style="list-style-type: none"> • Stress-strain analysis based on rheological equations (Discontinuous Deformation Analysis allows detachment of failed mass)
2-Phase Flows	<ul style="list-style-type: none"> • Fluid dynamics models representing solid and liquid phases of the failed material (often for debris flows or lahars)
Discrete Element Models	<ul style="list-style-type: none"> • Movement of individual rigid elements, from grain scale to blocks of material



Source: Camino D., 2019. Geological Engineering Thesis, EPN Quito-Ecuador

Figure 46: Rocscience SLIDE 6.0

Physics-based and Spatially Distributed Hazard Maps:

GIS-based with 1D infinite slope assumption. E.g.,

- Shallow Landsliding Stability Model, SHALSTAB (Montgomery and Dietrich, 1994)
 - Stability Index Mapping, SINMAP (Pack et al., 1998)
 - Transient Rainfall Infiltration and Grid-based Regional Slope-Stability Model, TRIGRS (Baum et al., 2002)
- ... with Newmark Displacement (EPN, Quito)



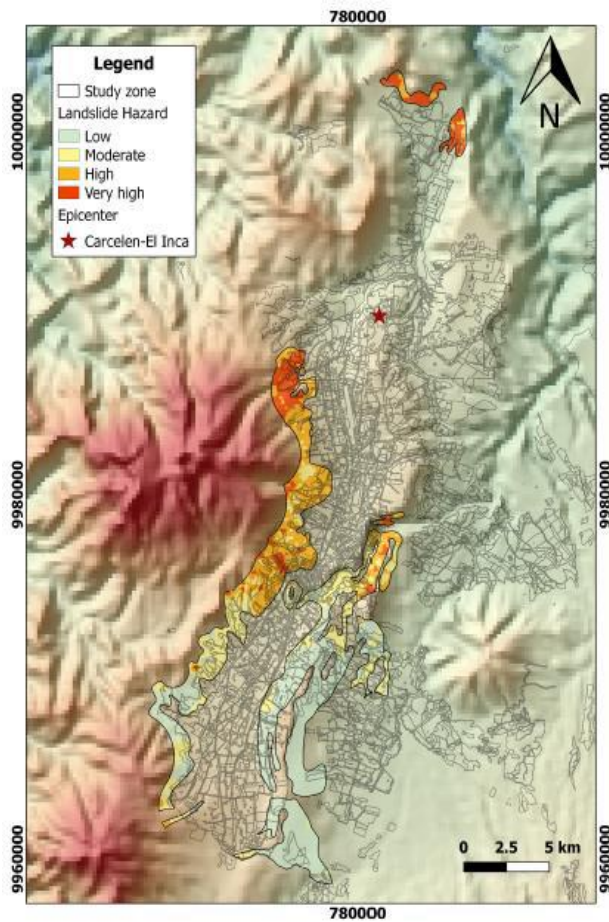


Source: Chamba C., 2022. Geological Engineering Thesis, EPN Quito-Ecuador

Figure 47: Newmark displacements zonation in ravine considered a hotspot of landslide occurrence

- ... 2D irregular slip search
- OpenLISEM Hazard (ITC, Twente, 2019)
 - ... 3D Bishop circular method
- Scoops3D (USGS, 2015)
 - ... Quito seismic microzonation info. as a Landslide trigger



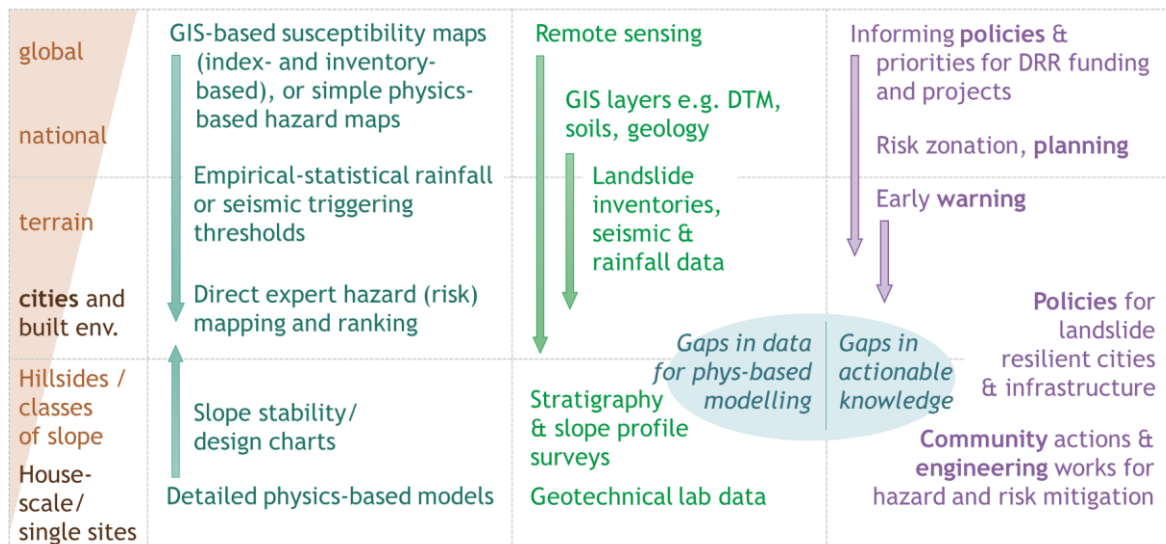


Source: Zapata C. Master Thesis 2018

Figure 48: Hazard zonation of earthquake-induced landslides by a deterministic seismic event with epicenter in the local fault system ($M_w = 5.9$) during the dry season

5.3.3 Decision-Support and Research Gaps

A. Landslide Hazard Scales, Methods, Data and Purposes



B. Quito Examples of Data Collation/ Collection

Hillslope hydrological hazard models (e.g. for landslides, debris flows and floods) require similar datasets. In many cities this data is incomplete and is not detailed enough for the physics-based modelling of local hazard drivers. An important task is to collate existing data and fill in the gaps using multiple methods.

	City-scale Data for Susceptibility Mapping in GIS	Slope Class (Case Study) Data for Physics-based Modelling
LS observations	Inventory of past events	Local knowledge and drone mapping
Land cover	Urbanization over time	Participatory mapping and drone mapping
DEM	Start with available satellite data	
Geology/ lithology	Existing maps	Observations, expert knowledge, new database applied to stability assessment (Hen-Jones et al. 2022), Citizen Science
Soil geotechnics	Literature review -> new database (Othman et al. 2022)	
Rainfall	Regional intensity-duration-frequency information	Local IDF data and design storms

An important task is to collate existing data and fill in the gaps using multiple methods.

C. Drone Method and Geotech Database (And Citizen Science)

In data scarce regions, collecting data from previous studies is crucial, some of them show extensive databases. In this section is shown two examples of data gathering using databases:

- Developing a geotechnical database to improve slope stability assessments in Quito, Ecuador. Hen-Jones et al. 2022
- The SAFER geodatabase for the Kathmandu Valley: Geotechnical and geological variability. Gilder et al. 2019

Databases allow the use of statistically processed information to show the most representative values of different parameters.

5.4 City-Wide Landslide Hazard Assessment: Landslide Problem Definition

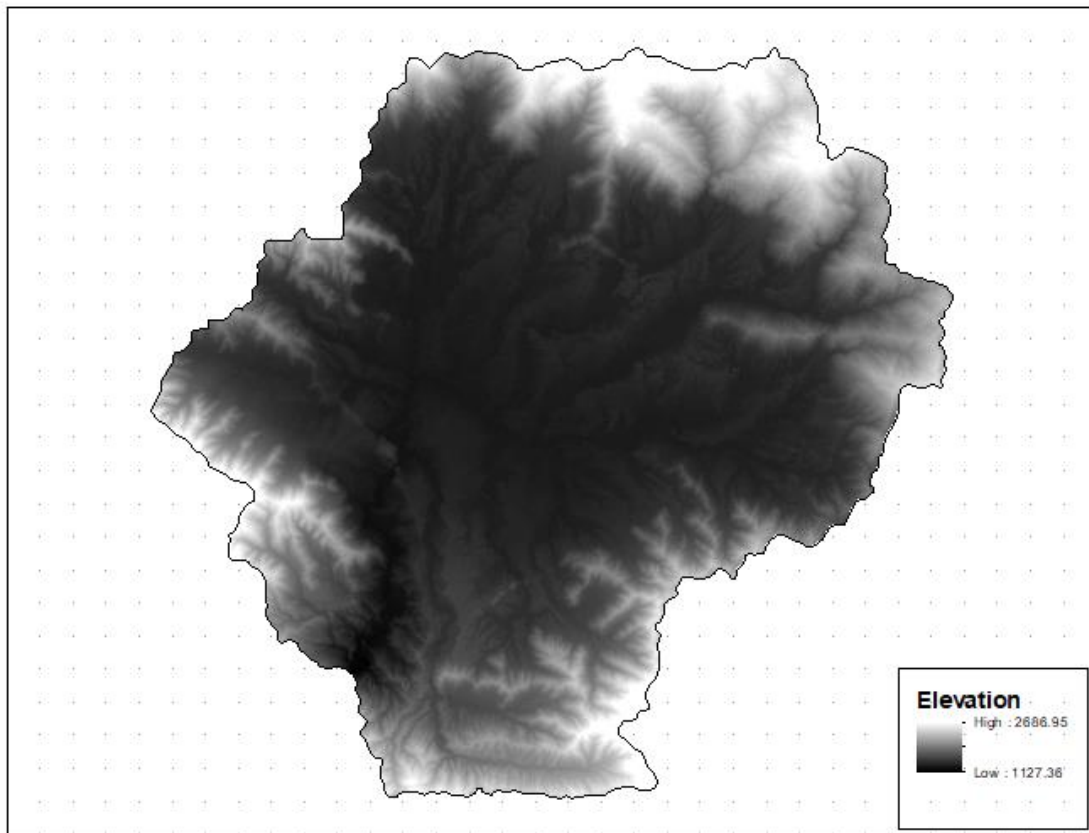
5.4.1 GIS-based Landslide Assessment in Kathmandu: Methodology and Input

This study aims to perform a GIS-based Landslide Susceptibility Mapping of Kathmandu Basin using bivariate statistical approaches (Frequency Ratio and Information Value) and Heuristic approach. The landslide inventory was generated by identifying the landslide areas from years 2010 to 2021 through Google Earth Pro. 105 Landslide areas were identified and ten predisposing factors categorized into different classes (Aspect, Slope, Geology, Curvature, Landuse, Distance to road, Distance to drainage, Rainfall, NDVI, and Relative relief) have been used in the study. The research has utilized a 2m resolution Digital Elevation Model (DEM), land cover map, satellite images (Landsat 8), rainfall data, and geological map to generate the predisposing factor maps. The resulting maps have been used to set up the respective susceptibility models and subsequently perform Landslide Susceptibility Mapping of the area. The landslide susceptibility classes for all three methods were divided into three classes as low, medium, and high. Furthermore, the Frequency ratio and Information Value methods have been validated through Area Under Curve (AUC) approach.



Table 6: Methodology and input parameters of GIS-based Landslide Assessment in Kathmandu

Input Parameters	Source	Purpose
DEM	ALOS Palsar	Slope, Aspect, Relative Relief, Curvature
Road and Stream data	Government website	Stream/ Road Buffer
Rainfall data	Department of Hydrology and Meteorology	Rainfall/ Thiessen polygon
Landsat 8 images	EarthData website	Vegetation Index/ NDVI
Land cover	National Land Cover Monitoring System	Landuse
Geology map	Department of Mines and Geology	Geological information
Google Earth Pro Images	Google Earth Pro	Landslide Inventory
Field study results	Field visit	Landslide Inventory

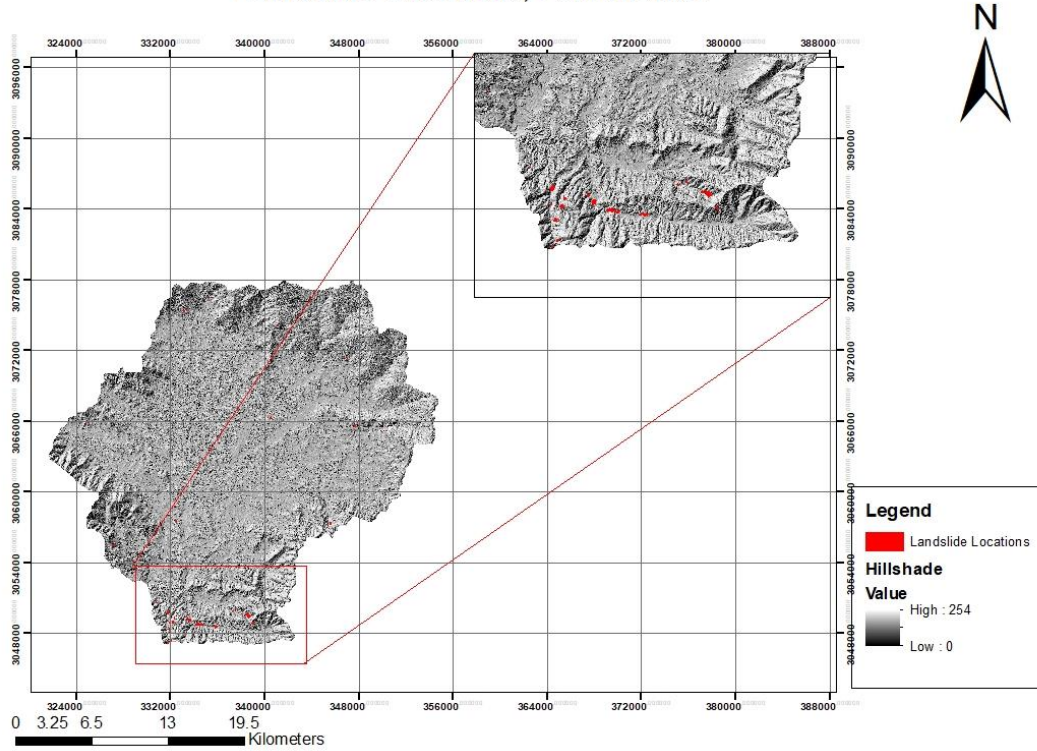


Source: Bhatta & Adhikari draft article

Figure 49: Kathmandu DEM (2 * 2 m)

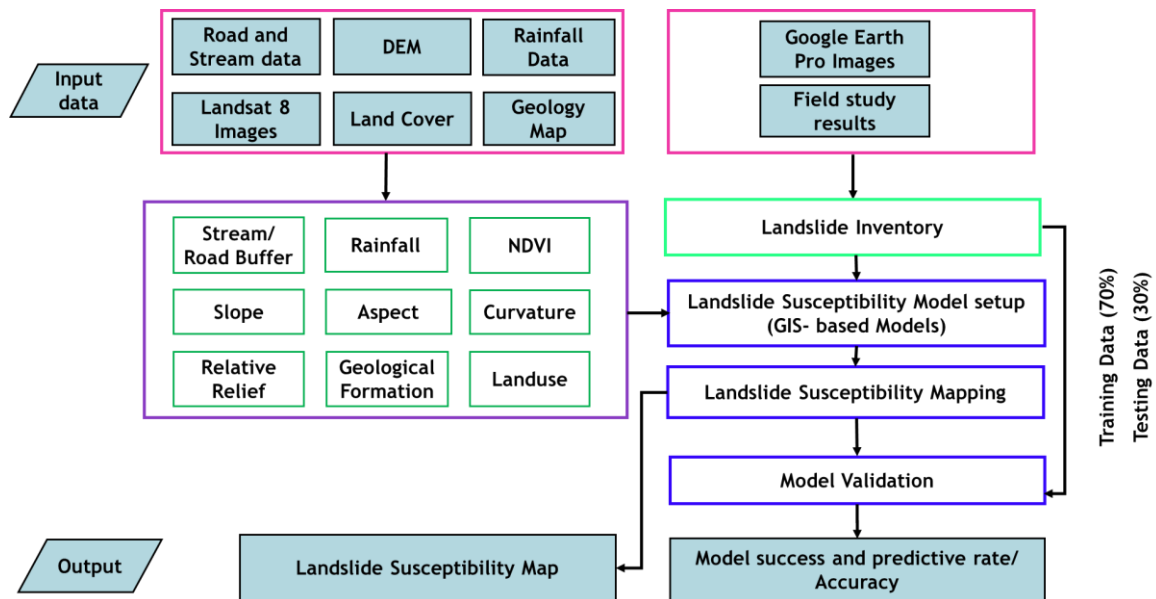


Landslide Locations, Kathmandu



Source: Bhatta & Adhikari draft article

Figure 50: Landslide Inventory, Kathmandu



Source: Bhatta & Adhikari draft article

Figure 51: Methodology of GIS-based Landslide Assessment.



5.4.2 Susceptibility Models/ GIS Tools Used

A. Heuristic Approach (Qualitative)

The heuristic model is built based on expert knowledge and experience. The premise of Heuristic model is to provide a certain weightage to the predisposing factor maps for the landslides.

B. Statistical Approach

Bi-variate Statistical Approach:

The bi-variate statistical analysis for landslide hazard zonation compares each data layer of causative factor to the existing landslide. Weights to the landslide causative factors are assigned based on landslide density.

E.g. Frequency Ratio approach, Information Value Model (IVM), Weights of Evidence Model, Weighted Overlay Model)

Multi-variate Statistical Approach:

Multi-variate statistical analysis for landslide hazard zonation considers the relative contribution of each thematic data layer to the total landslide susceptibility. These methods calculate percentage of landslide area for each pixel and landslide absence-presence data layer is produced followed by the application of multivariate statistical method for reclassification of hazard for the given area.

E.g. Logistic regression model, Discriminant analysis, Multiple regression models, Conditional analysis, Artificial Neural Networks (ANN))

C. Deterministic Approach (Deterministic Landslide Hazard Zonation)

Deterministic models are based on physical laws of conservation of mass, energy or momentum. In the case of deterministic landslide hazard zonation, distributed hydrological and slope stability programs are used to calculate the spatial distribution of groundwater levels, pore pressures and safety factors. The deterministic calculations can be performed within the GIS.

D. Probabilistic Approach (Hazard Curve)

Probabilistic method quantifies, for a given slope location, the exceedance probability of being affected by a landslide with a specific local intensity within a reference time interval i.e., the hazard curve. Probabilistic landslide hazard analysis has the advantage of providing hazard curves and maps, and to be applicable to all typologies of landslides.

E. Multi-Criteria Decision-Making Process (Analytical Hierarchy Process Approach)

AHP in landslide susceptibility evaluation utilizes expert knowledge to decide the factors affecting the landslide process. It then determines the relative importance of all the criteria (predisposing factors) and sub criteria (classes) that contribute to landslide susceptibility to compute its weight.

5.4.3 Expected Outputs

- Landslide Susceptibility Map– reclassify to classify the area into low, medium, and high susceptible areas
- Model success and predictive rate– Validation of the model



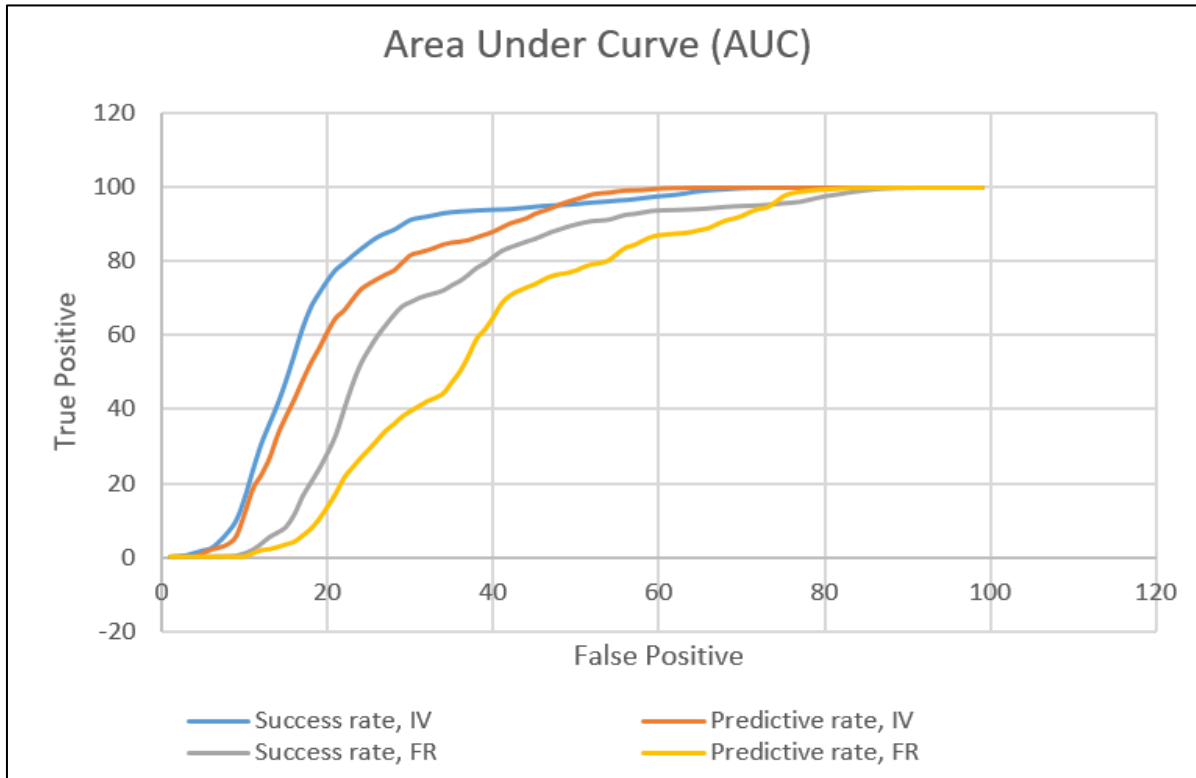
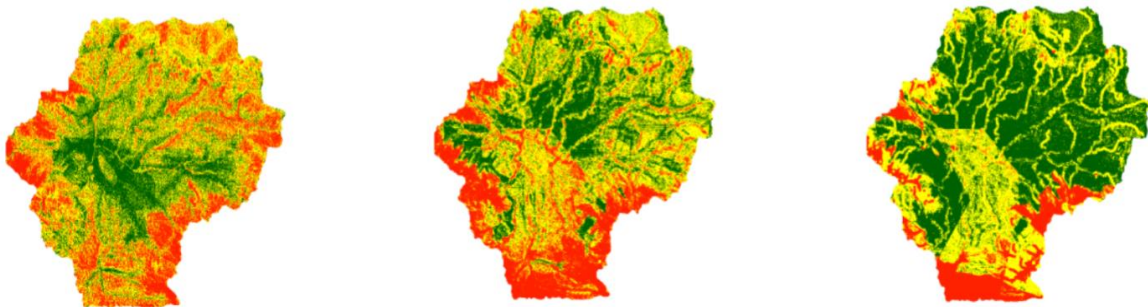


Figure 52: Area Under Curve (AUC) for Model Validation

5.4.4 Uncertainties

- Identification of Landslides— landslide areas intensively modified by farming activity or covered by dense vegetation cannot readily be identified and correctly classified
- Use of different Susceptibility Models— gives varying results



Source: Bhatta & Adhikari draft article

Figure 53: Variation in results from different models, a) Heuristic Model, b) IV Model, c) FR Model.

5.5 Examples of Physics-Based Modelling for Quantifying the Local Hazard

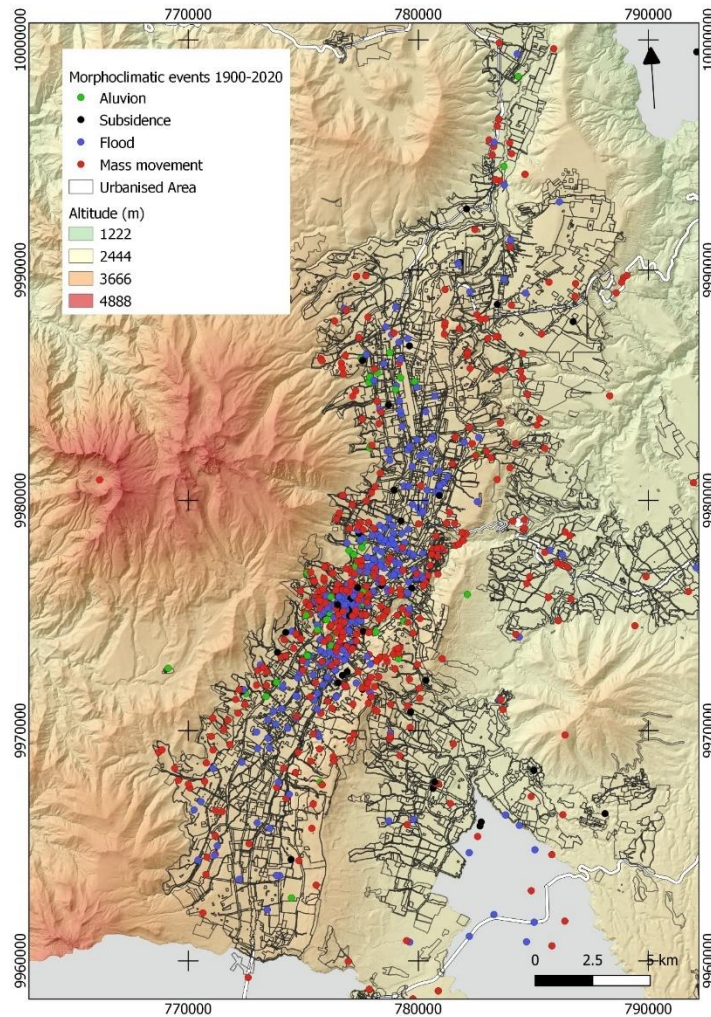
5.5.1 Everyday Landslide Hazards

A. Example of Landslide Problem Diagnosis

- Volcanic deposits, consolidated and unconsolidated material
- Seismic and rainfall trigger with human interaction



- Rotational/ translational earth slides and debris flows
- Multi-hazards: runoff, erosion, floods/ volcanos and quakes
- Household-scale to mountainsides and ravines



Source: reducirriesgosenquito.com

Figure 54: Landslide inventory and urban growth map from 1900 to 2020 in Quito.

B. Existing data and methods

- GIS data, Landslide inventories, soil tests
- Hazard maps and site-specific studies
- Static hydrology, Earthquake triggers

C. Decision-support and research gaps

- Everyday rainfall-triggered landslide
- Slide-flow mechanisms and runout
- Rainfall, soils and urban influences: dynamic, localised, highly variable
- Challenges:
 1. Model?
 2. Data and scenarios?
 3. Holistic approach?





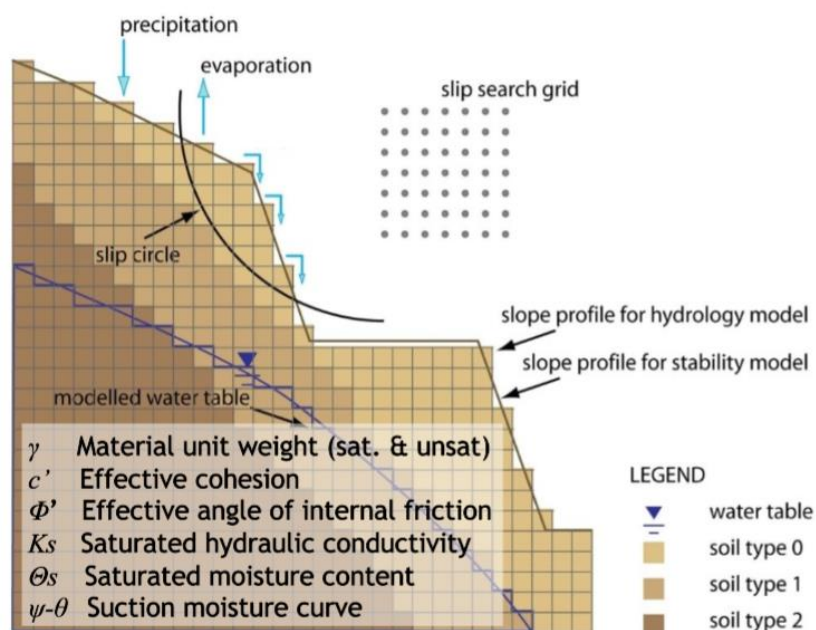
Source: Eliana Jimenez Ph.D. Thesis (on review)

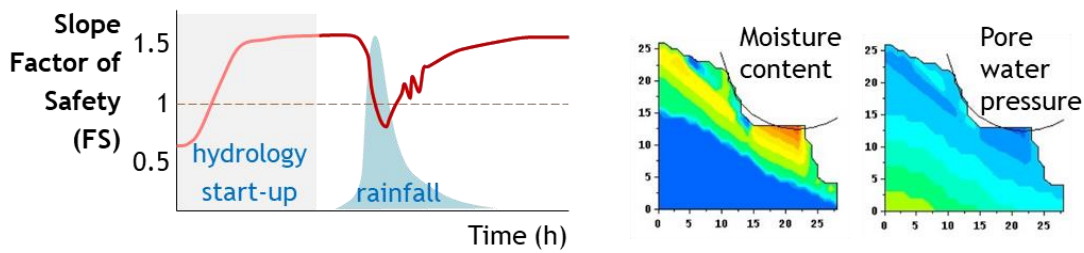
Figure 55: Side view of an informal neighborhood located in the pro-landslide zone.

5.5.2 Representing Urban Slopes and Dynamic Hydrology

A. Combined Hydrology and Stability Model (CHASM)

- Unsaturated and saturated zone pore water pressure calculated every timestep (Richard's Equation, Darcy's Law)
- Factor of Safety calculated every hour (Bishop circular method of slices with search algorithm for min FS slip surface)
- Data requirements: slope cross-section, strata, soil effective strength, unit weights, hydrological properties, rainfall
- Track record: 72.5% correct classification of stable vs failed for cut slopes along roads in Hong Kong (Anderson, M.G., GEO Report, 1990)



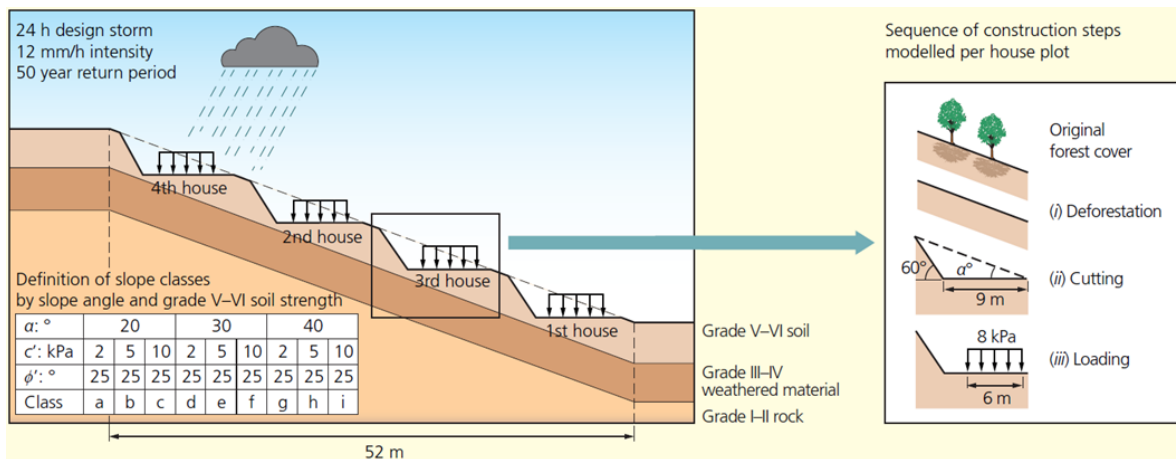


Source: Malcolm & Holcombe 2013

Figure 56: Inputs and outputs of Combined Hydrology and Slope Stability Model.

5.5.3 Modelling Urban Landslide Scenarios with Limited Data

Method 1. Parametric analysis: Explore selected combinations of slope, rainfall and urban properties and look for patterns.



Source: Holcombe, E. A., Beesley, M. E. W., Vardanega, P. J. and Sorbie, R. (2016) Urbanisation and landslides: hazard drivers and better practices, Proc. ICE Civ. Eng., 169(3), 137-144, <https://doi.org/10.1680/jcien.15.00044> [11]

Figure 57: Modelling scenario of urban slopes

A. Drone Approach to Collect Data

Cartography with drones allows obtaining digital terrain models and high-quality aerial photos, reaching 5cm/pixel.

This detailed information of the site allows the researcher to carry out plenty interpretations and information gathering according to his interest, s interest, e.g. to locate active landslides, filled zones, and slope geometry, surface cover, housing location and structural typologies, drainage system and more.

B. Outputs from Landslide Hazard Analysis- CHASM

- CHASM can be used to evaluate changes in a slope (defined geometry) when its parameters vary, e.g. if soil properties change and effects of less infiltration, or if the slope experiences different precipitation regimes (current conditions and climate change), them a driving the hazard in difference scenarios.
- Also, the safety factor of a slope can also be evaluated if its geometry changes, e.g.: cut height, cutting angles, useful approach to urban development plans.
- CHASM can give indications of the typical sizes of rotational/translational failure planes within a certain slope type, and hence 2D cross-sectional areas of landslides for specific scenarios (cut slopes, different slope angles and soil types)

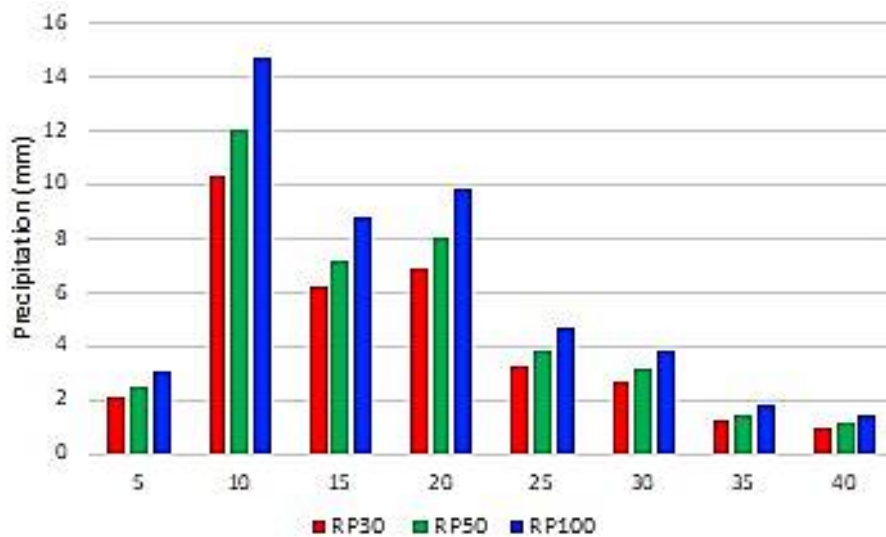


C. Example Outputs and Interpretation of DSE

CASCADE EFFECT: From Rain to Debris Flows (Quito Example):

Precipitation

- Santa Rosa is a dry area as well as their ravines.
- Wind permanently erodes the steep slopes of the surrounding hills triggering landslides. The loose material fills the ravines (boulders and sand).
- Often, convective storms occur triggering landslides.
- Eventually heavy rain removes the loose material on the ravines and forms debris flows.
- We analysed precipitation based on climate change for a return period of 30, 50 and 100 years.



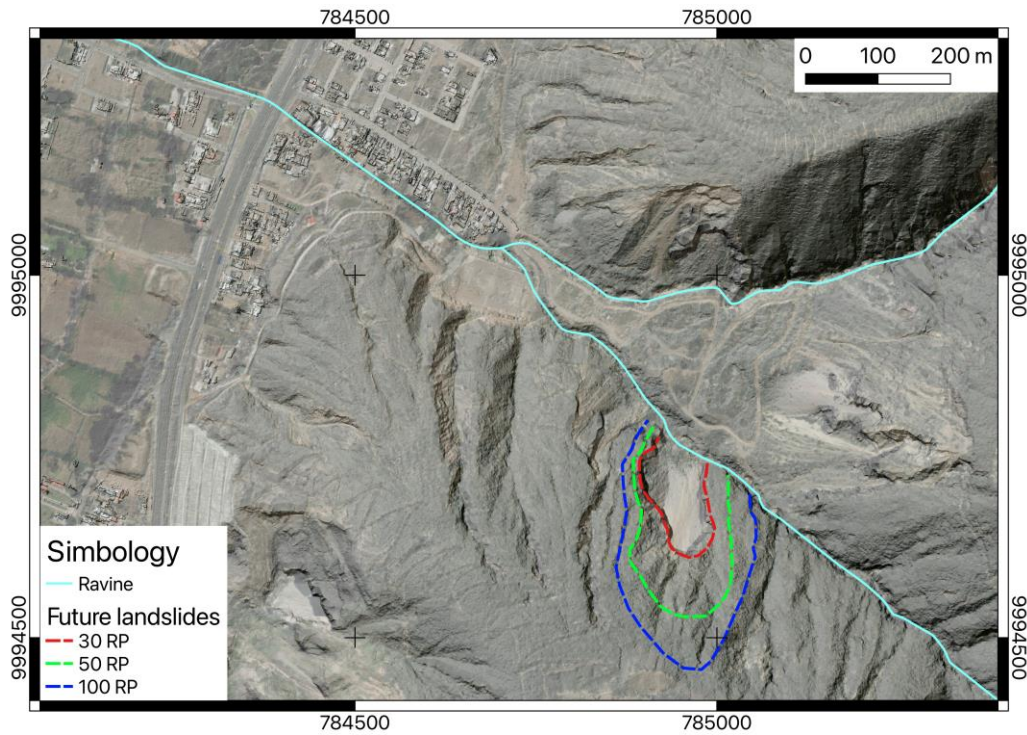
Source: Francisco Vásquez

Figure 58: Rainfall intensity with returned periods

Landslides based on precipitation (return periods)

Based on climate change (precipitation), we defined the most prone areas to slide in return periods of 30, 50 and 100 years. Consequently, future hazard scenarios were defined.

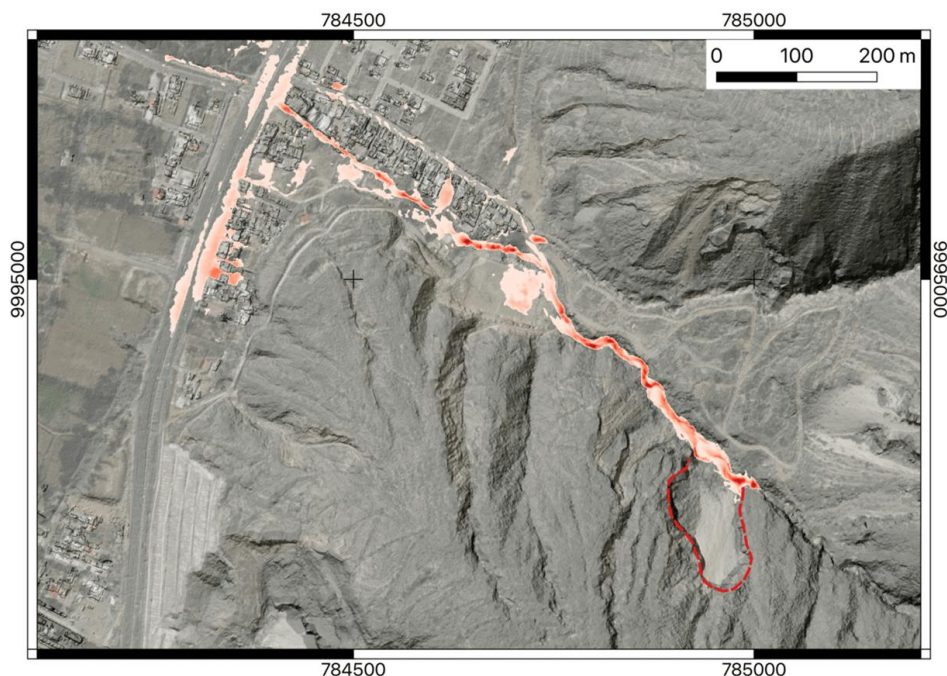


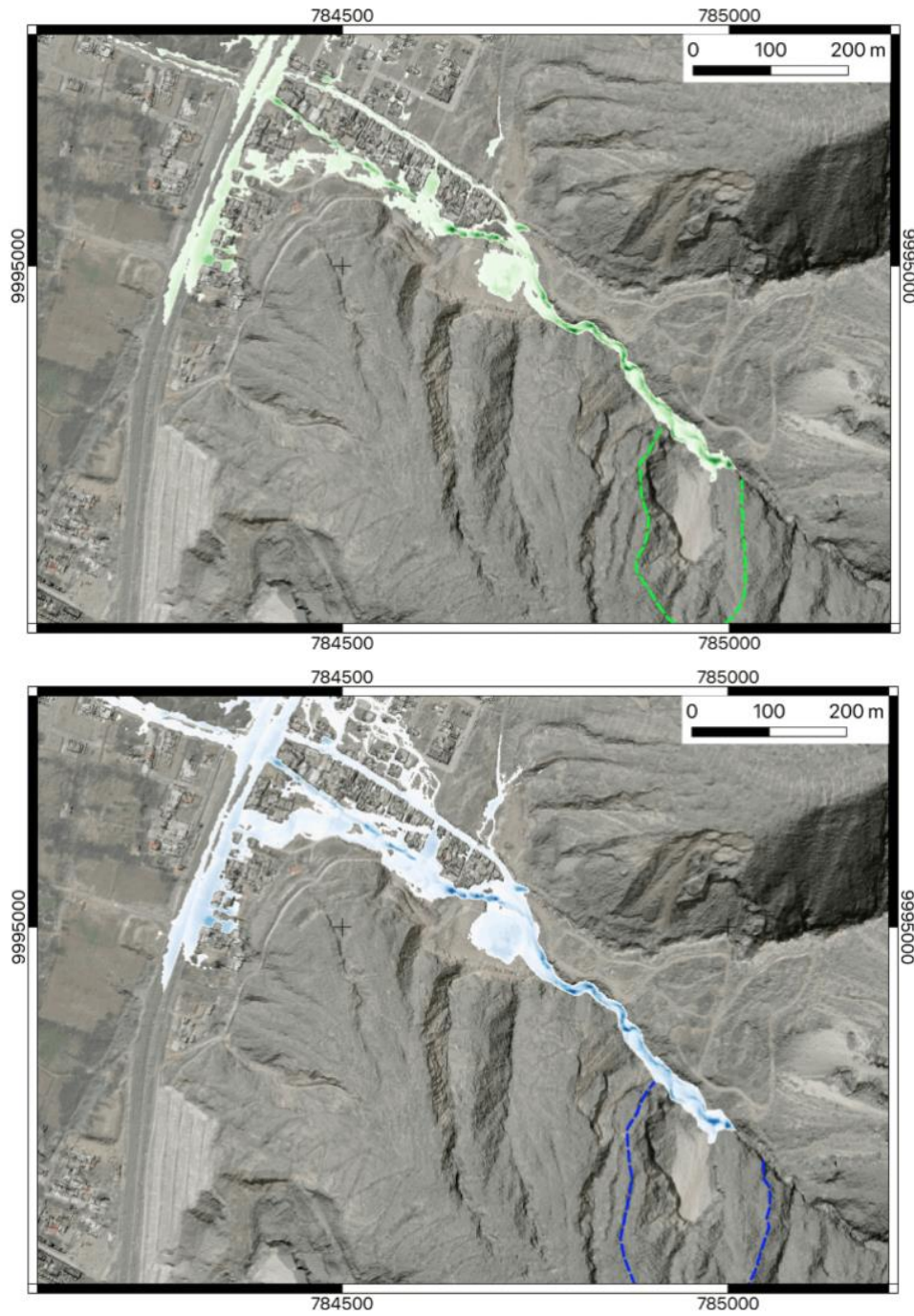


Source: Francisco Vásquez

Figure 59: Landslide sources for debris flow hazard assessment, considering several rainfalls scenarios

- As an example, we simulated the three hazard scenarios based on climate change and return periods of 30, 50 and 100 years.
- Time increases as precipitation. Consequently, the scenario for a 100-year period is larger than 30 years scenario. However, the probability for a 100-year scenario is lower than for the 30 years.
- Our analysis includes uncertainties based on climate change.





Source: Francisco Vásquez

Figure 60: Debris flow simulation using rainfall with returned period of 50 years



SESSION 6: FIRE HAZARD MODELLING

6.1 Objectives

At the end of the session, the participants will be able to:

- Explain the basics of fire dynamics.
- Outline the prerequisites, processes and outputs of fire modelling.
- Discuss fire hazards and related issues in urban planning.
- Discuss Wildland-Urban Interface Fire.
- Outline the case study of Fire Hazard Assessment using AHP approach.
- Discuss general provisions for fire safety in building codes and policies.

6.2 Structure of Session 6

Structure
1. Fire Dynamics
2. Fire Modelling
3. Wildland-Urban Interface Fire
4. A Case Study on Fire Hazard Assessment
5. General Provisions for Fire Safety

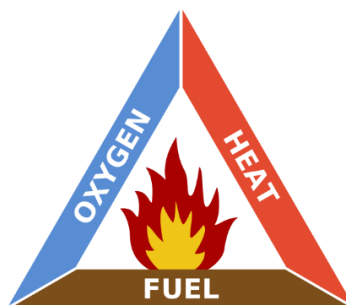
6.3 Fire Dynamics

Fire dynamics is a relatively new science, which utilizes the understanding of physical and chemical processes in the study of how fires initiate, spread and behave. By understanding fire dynamics, fire modelers and engineers can develop better fire prevention, suppression and mitigation strategies against fire hazards.

6.3.1 Small scale physics of fire

Fire is simply the rapid oxidation of objects at elevated temperature producing heat, smoke and light. Various materials undergo oxidation at various rates. For example, metals are also oxidizing but at a slower rate taking years to fully oxidize. A burning candle on the other hand undergoes rapid oxidation producing heat and light which we call fire.

Fire is commonly described through the “Fire Triangle”, as shown in figure below, to illustrate the relationship between the three elements a flame needs to be sustained: heat, fuel, and an oxidizing agent, usually oxygen.



Source: https://en.wikipedia.org/wiki/Fire_triangle

Figure 61: Illustration of fire triangle



As fuel degrades under the influence of heat, it releases gas which can ignite when mixed with oxygen from the surrounding environment in a reaction of combustion. This reaction releases heat, which can create a self-sustained feedback loop where more combustible gas is released. In the simple example of a candle, the fuel is the molten wax that flows in the wick, generates hot combustible gas (this process is called as pyrolysis) which mixes with the oxygen of the air in a hot buoyant plume, reacts and transfers enough heat back to the wick when it burns to sustain the flame until all the candlewax is consumed.

To stop a combustion reaction and thus quench a fire, one of the three elements of the fire triangle must be removed. For instance, covering a fire with a fire blanket blocks oxygen, adding water absorbs the heat, and creating fire-resistant partitions in a building can block access to the fuel in the next room, all leading to extinction of a fire. These mechanisms can be very efficient on a small fire, however problematic firefighting situations can occur if the fire grows to a large size.

A. Relation between fire size and scale of destruction

The size of a fire is driven by the availability of the three elements of the fire triangle. In contrast to other hazards where the energy is initially released by a single source (for instance the epicenter of an earthquake), most fires gradually grow in size with time as they burn through available fuel. Because of this specificity, fire creates the illusion of being controllable, unlike other natural hazards such as hurricanes, earthquakes, and tornadoes.

In addition, this means that the intensity of a fire is never known at the beginning of the event but can only be assessed afterwards. As fire burns through more combustible elements, the fire intensity increases which can in turn create additional destruction.

The complexity of this unique feedback loop requires an understanding of the initial situation far beyond what is accessible. When an uncontrolled fire grows, a lot of chemistry and physics happen simultaneously. Butterfly effects are regularly observed even in well-controlled experiments, where a slight variation in the spacing of elements, initial temperature, intensity of the initial flame, or ventilation conditions can lead to dramatically different outcomes¹.

6.3.2 Causes of fire

The causes of fire can be categorized into two: Natural and Manmade.

Natural:

Fires have been occurring for more than 400 million years and continue to naturally occur in the wild due to the sun's heat and lightning. As such, fires in the natural habitat, also called wildfires, are classified as natural hazards by most environmental agencies worldwide². In contrast, the invention of the lightning rod in the 18th century has almost eliminated the risk of natural fire in cities and buildings.

Manmade:

- Negligence/ Accidents. E.g. due to unattended frying pan/candles, due to overheating of power equipment, improper use of LPG or Propane gas stoves, etc.
- Electrical equipment. E.g. overloading of extension cords, arcing of electrical currents in faulty concealed wirings, etc.
- Intentional lighting/ smoking of fuels. E.g. arson, bombing, etc.

¹ The great fire of London which destroyed over 13,000 in 1666 initially started as a model bakery kitchen fire, which were quite common at the time.

² See the list of natural hazards at <https://hazards.fema.gov/nri/natural-hazards>



The vast majority of fires start through accidents, negligence, or criminal activity. In the US, the National Fire Protection Association has identified that cooking fires are the most common types of house fires, causing around 49% of all residential fires as overheated grease starts burning. Heating appliances, electrical failures, candles, and smoking follows as other leading causes of house fires in the past years³.

Fires in electrical wiring systems and electrical equipment are often the result of arcing or overheating associated with electrical conductors. Therefore, any defects to the electrical supply, meters, fuses, wiring, sockets or switches add to the risk of a fire occurring. Electrical appliances and supply systems contain considerable amounts of plastic materials so when arcing or overheating occurs adjacent to any insulation, combustion can occur.

Because it is impossible to locate the exact position of an incipient accidental fire and know the exact layout of the room where it happens, it is commonly assumed that a fire can start at any location and that the fire can spread to the neighbouring items until the fire is fully developed in the room. In the process, attention is paid to the rate at which the intensity of the fire grows to capture how fast the fuel is burnt and heat is generated.

6.3.3 Measurement of fire

In order to understand how fire initiates, spreads and behaves, we must learn some of the measurements related to fire and its transfer.

- **Heat Energy:** It is a form of energy characterised by vibration of molecules and capable of initiating and supporting chemical changes and changes of state (NFPA 921). It can also be defined as the energy needed to change the temperature of an object.
- **Temperature:** It is a measure of the degree of molecular activity of a material to a reference point.
- **Heat Release Rate (HRR):** It is the rate at which fire releases energy. It is also known as the power/ intensity of fire. HRR of some of the burning items are provided below:

Candle	100W
A tree on fire	1MW
A cigarette	10W
A room fully on fire	10MW

- **Heat flux:** It is the rate of heat energy transferred per surface unit area.

6.3.4 Stages of fire

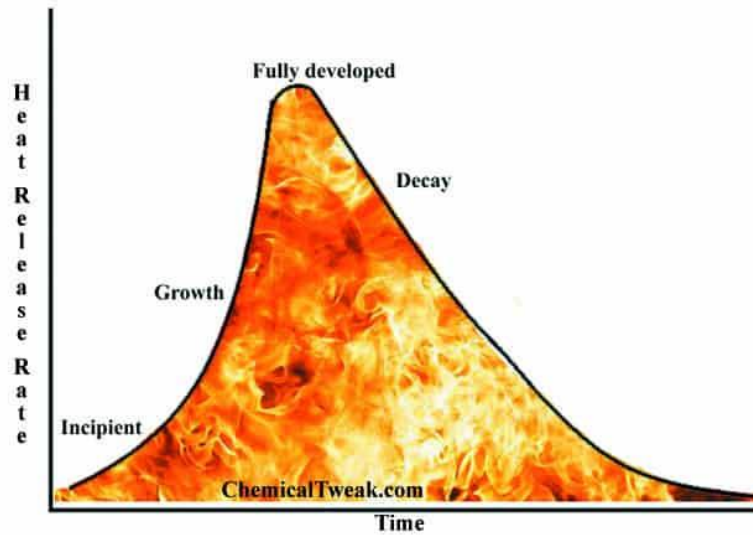
Generally, there are four stages of fire:

1. **Incipient/ Ignition stage**
It is the initial stage where the fire is ignited and is the smallest. This is the critical phase in order to suppress a fire.
2. **Growth stage**
If the fire is not controlled, it grows exponentially. It is the shortest and the most dangerous stage of fire, also known as pre-flashover stage.
3. **Fully developed stage**
After growth stage has reached its maximum potential, the fire is considered fully developed. The temperature at this stage is maximum.
4. **Decay stage**

³ See <https://www.nfpa.org/Public-Education/Fire-causes-and-risks>



Decay stage is the last and the longest stage at which the fire subsides. Decay may be due to limited fuel supply or presence of oxygen.



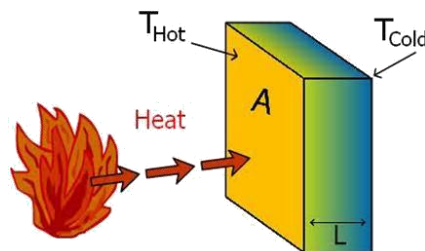
Source: ChemicalTweak.com

Figure 62: Stages of fire

6.3.5 Heat transfer

Heat transfer is a major factor in the ignition, growth, spread, decay and extinction of a fire. Heat is always transferred from the hotter object to the cooler object, i.e. heat energy transferred to an object increases its temperature and heat energy transferred from an object decreases its temperature. Heat transfer can occur through any of the following modes:

1. Conduction: Conduction is heating transfer within solids or between contacting solids. E.g., heating thick metal on one side gets transferred to the other side.

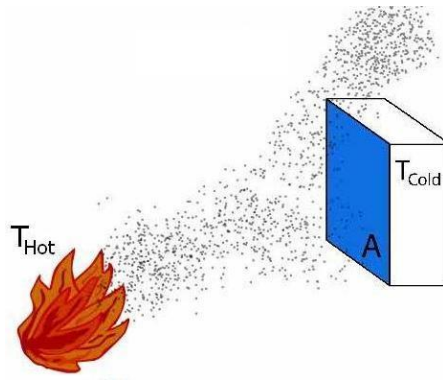


Source: <https://www.nist.gov/el/fire-research-division-73300/firegov-fire-service/fire-dynamics>

Figure 63: Conduction of heat

2. Convection: Convection is heat transfer by the movement of liquids or gases. E.g. Rising of hot gas or smoking heating other surfaces.

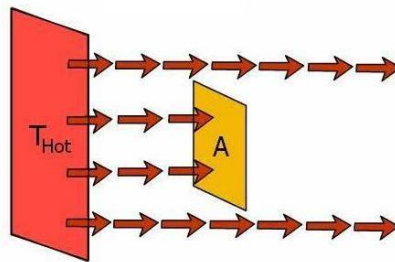




Source: <https://www.nist.gov/el/fire-research-division-73300/firegov-fire-service/fire-dynamics>

Figure 64: Convection of heat

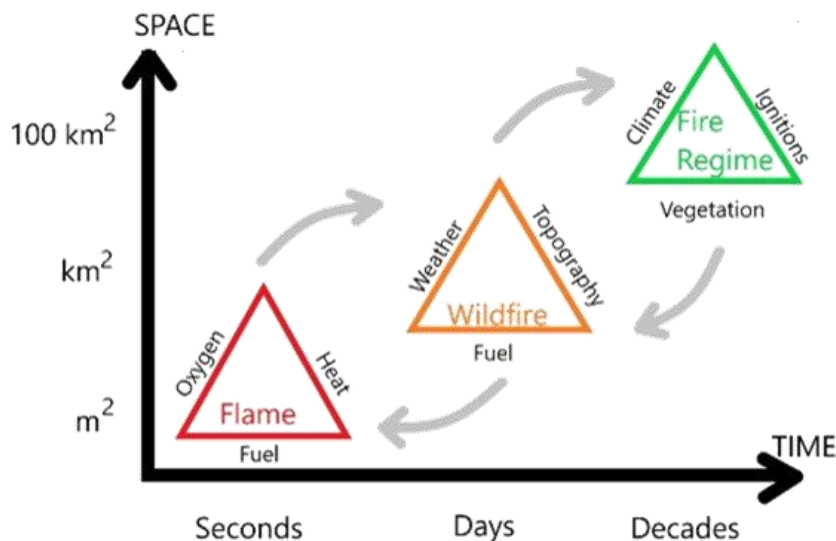
3. Radiation: Radiation is heat transfer by electromagnetic waves. E.g., Heat waves from sun.



Source: <https://www.nist.gov/el/fire-research-division-73300/firegov-fire-service/fire-dynamics>

Figure 65: Radiation of heat

6.3.6 Fire development



Source: Moritz et al. (2005) [12]

Figure 66: Multi-scale fire triangles describing the elements of wildland fire at the scale of the flame, a wildfire, and a fire regime

The chart in figure above shows an extended scale of fire triangles describing the elements of open fire at the scale of the flame, a wildfire and a fire regime. In the initial stage of open fire, depicted by the flame fire triangle, fuel particles are ignited at a critical temperature and fire transfers to the nearest surroundings. The fire triangle can be scaled up for the context of



wildfire, to apply to fire spread over landscapes (in the scale of days and several kilometres) and recurrence of fire over time (scales of decades and hundreds of kilometres).

The type, amount and arrangement of fuel can significantly affect the behavior of fire. Different fuels have different ignition temperatures and burn rates. In addition, their arrangement can affect the spread and intensity of the fire. Fuels that vary over larger space and time is called vegetation. Fire requires oxygen to burn and the amount of oxygen available can affect the rate and intensity of the fire. Heat is the energy source that ignites and sustains the fire, and the amount of heat generated can affect the temperature of the fire and the rate of its spread. In the scale of a wildfire, weather can also affect the behavior of fire. Wind can spread the fire more quickly, while rain or high humidity can dampen it. The longer pattern of weather is termed as climate, which influences the behavior of large-scale fire regime. The topography of the surrounding area also plays a role in wildfires. Fire tends to burn more rapidly uphill than downhill, and it can be influenced by topographical factors such as slope, aspect and elevation. Apart from this, human intervention and several other ignition sources can also affect the spread and intensity of fire.

6.4 Fire Modelling

Fire modelling refers to the use of various tools to simulate and understand the spread and behavior of fires. In this session, we will be particularly focused on discussions about modelling fire in an enclosed scenario such as in a room or a building and in a closely spaced settlement. A fire behaves differently and there are several other factors that affect fires if it is freely occurring or open such as a wildfire.

6.4.1 Compartment fire

A. Overall mechanism

Rapid fire spread occurs when the flames come into contact with new sources of fuel such as plastics, untreated fabrics, timber etc. This fuel will itself start to generate flammable gases very quickly and eventually ignite. The hot gases in the plume, until they have cooled down by mixing with enough fresh air, can also cause combustible material located above the initial fire to start giving off flammable gases. Overall, as little as 1/3 of the heat from a room fire will leave a room as hot smoke. As the room temperature rises, less and less heat from the plume can be absorbed by the room's walls and contents. The plume gets hotter, and this increases the efficiency of the combustion process. It also furthers heats up unburnt fuel, increasing the rate at which the gases are generated. Thus, increasing room temperature will result in increased combustion rate, as long as there is an adequate supply of oxygen.

The heat release rate (HRR), which is the rate at which fire generates energy, is then commonly used as an efficient way to evaluate the development of the room fire in time. If unattended, such a fire would burn until all the fuel in the room has been consumed.

B. Typical single room fire scenario

A fire in a room can be characterized by three phases, illustrated in figure below.

The fire **growth phase** relates to the sequence where a fire grows in size from a small incipient fire to its maximum size. As the room heats up, it is possible to observe a very rapid increase in the HRR as the fire spreads unrestrictedly. The maximum HRR can be controlled either by the amount of fuel present or the amount of air available through ventilation openings (remember the fire triangle at the beginning). In the former case, the fire is labeled **fuel limited**, whereas in the latter case it is called **oxygen limited**. Indoor fires tend to develop in oxygen limited conditions.



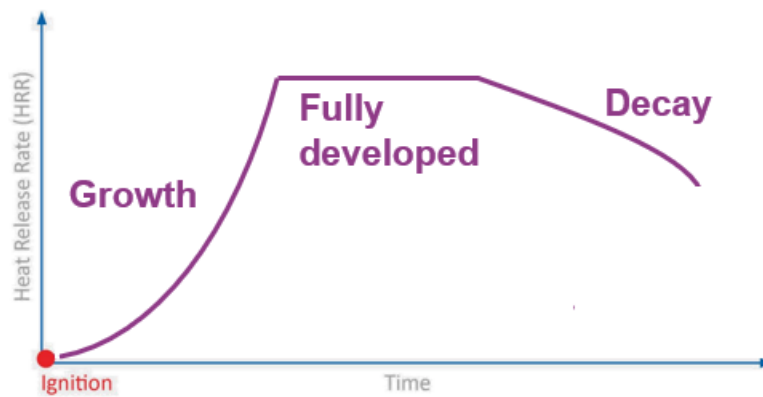


Figure 67: Typical curve of the Heat Release Rate in a fuel-limited fire

Once the entire room is set ablaze termed as flashover, the fire intensity will plateau in the fully developed phase. As all of the fuel is consumed, the fire will decrease in size in the decay phase. The fully developed fire is affected by (a) the size and shape of the enclosure, (b) the amount, distribution and type of fuel in the enclosure, (c) the amount, distribution and form of ventilation of the enclosure and (d) the form and type of construction materials comprising the walls, ceiling, and floor of the room. Most of these parameters are set at the beginning of the fire, and ventilation is the one parameter which can change dramatically as a door or window opens, due to firefighting action or destruction by the fire itself.

In the growth stage, the fire is fuel-controlled, with its rate of growth limited by the availability of fuel around. The HRR of the growing fire time depends on how heat is transferred from the incipient fire to its surrounding area. This then dictates the amount of heat generated by the fire as well as the temperature distribution in the enclosure.

Convection is the primary mode of heat transfer during the early stage of fire growth. The hot gases exchange heat by convection as they flow upwards and across the ceiling, heating it and any other surfaces with which they come into contact.

As it accumulates under the ceiling, the hot smoke that is collecting near the ceiling is also emitting thermal radiation to its surroundings. The radiations from the ceiling walls, and accumulated hot gases increase combine with the radiation from the fire itself to increase the fire intensity as the surfaces preheat, begin to pyrolyze and produce fuel vapour from any combustible items in the room. Radiation becomes gradually dominant as the fire continues to grow.

In a fire situation, conduction occurs in the gas phase in the vicinity of the flame, but also in solids, especially in the presence of metallic structures of high thermal conductivity, to preheat objects far from the initial fire source.

Ignition of objects in a room happens via a combination of radiation, convection and conduction. Direct impingement of the flame plume onto any secondary flammable surface will cause it to ignite and become involved in the fire. Alternately, the burning plastic items can melt and then drip burning hot material to ignite secondary items.

6.4.2 Approaches of fire modelling

Fire modelling aims at simulating or visualizing fire behavior and its spread in different scenarios. Fire modelling can be classified into two categories:



1. **Physical model:** Physical models are the experimental models developed with certain fire scenarios. They can be developed to scale or in full scale in terms of materials, dimensions and environments.
2. **Mathematical model:** Mathematical models are idealized representation/ simulation of fire scenarios to study its behavior and spread mechanisms using the knowledge based on physics for representing fire scenarios. Mathematical models are further categorized into:
 - a. **Probabilistic:** Probabilistic approaches of modelling are based on observations of the consequences of similar past fires. A prediction is made based on the most relevant past fire scenarios. However, as two fire situations are never identical, these models carry an inherent level of uncertainty. Still, these stochastic models form the basis of many codes and regulations due to their adequate performance in worst-case scenarios. More information on stochastic fire modelling can be found in the dedicated fire session.
 - b. **Deterministic:** Deterministic approaches are straightforward methods in which a definite set of inputs will have a definite set of outputs. There are primarily three methods under it:
 - i. **Analytical or Hand Calculations:** Under this method, various correlations are used to idealise real world physics of fire. They are often developed from empirical methods.

Applicability:

- are simple to use and gives relatively quick results.
 - are limited to fire involving one or two combustibles and objects in the fire plume.
- ii. **Two zone model:** Two zone models are the models simplified using theories of physics and are based on specific fire scenarios. Most commonly, these models are developed for analysing early development of compartment fire where two distinct layers of hot smoke and cold bottom are present. The condition within each layer is assumed to be consistent.

Applicability:

- can be used for multiple burning items and objects in multiple rooms.
- are limited to geometry without any obstructions.
- are more suitable for pre-flashover situations, where two zone assumption holds true.

- iii. **Physics-based/ CFD simulation:** Physics-based model aims at representing the laws of nature in their most general forms. In the case of fire modelling at a building scale, a particular emphasis is made to accurately represent how heat is transferred. However, this does not mean that the uncertainties disappear. Instead, they are carried to the initial and boundary conditions, or to sub-models which have exceptional variability.

Applicability:

- are used for detailed simulation of fire scenarios for complex geometry.
- provides good visual outputs for fire.
- are computationally intensive.

The subsequent session overviews the inputs, processes and outputs of physics-based modelling.



6.4.3 Physics-based fire modelling

A. Evolution of fire within a room or roof

The overall mechanism of evolution and spread of fire within a room is explained in section above. It is impossible to locate the exact position of an incipient accidental fire and know the exact layout of the room where it happens, so it is commonly assumed that a fire can start at any location and that the fire can spread to the neighbouring items until the fire is fully developed in the room. In the process, attention is paid to the rate at which the intensity of the fire grows to capture how fast the fuel is burnt and heat is generated.

B. Room to room spread

Five mechanisms of fire spread between rooms and apartments inside a building can be considered.

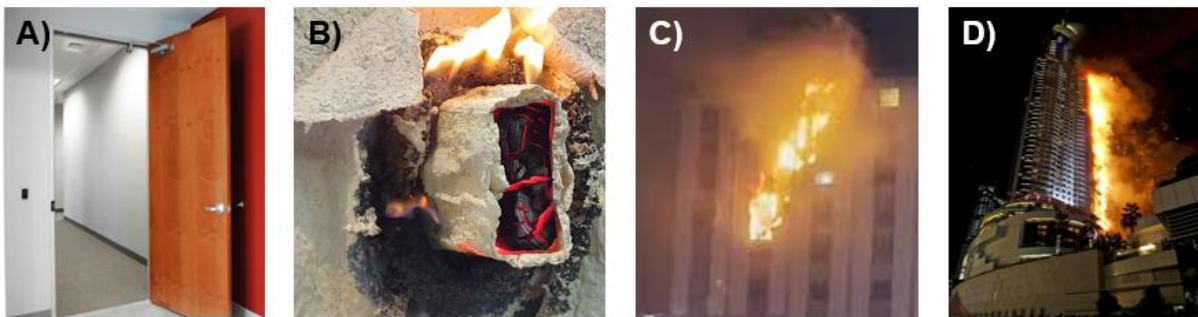


Figure 68: In a building, a fire can A) spread through openings, B) burn through combustible walls, C) leapfrog from one window to the next, D) spread over combustible cladding

Direct spread:

Direct spread occurs when an internal partition has an opening, such as a door, which is left open during the fire. Considering a fire burning over a number of buildings, it is not possible to keep track of which openings exist and as such a probabilistic approach is adopted. Different doors will be considered open or closed depending on the characteristics of the local architecture, modes of habitation, and possible records of building use.

Burn through:

As an intense fire develops in a room, it can burn through walls, floors, and ceilings if the fabric is combustible. Contrasting the incipient fire HRR from beginning to end with the material and geometric properties of the partitions will give an initial assessment of the likelihood and possible timing for the burn-through of the structure, propagation the fire to a neighboring room. Because detailing of the building services can generate weaknesses in both combustible and non-combustible partitions, additional considerations will capture these features, when available. If unknown, considerations towards the architectural properties of the building will be introduced to adopt a probabilistic approach in a dedicated sub-model.

Direct ignition by flame impingement:

During a fire, flow occurs through openings because of vertical pressure differences in the opening as the hot smoke layer builds. When the pressure is higher inside than outside the room, smoke will flow out of the enclosure. Conversely, cooler air will flow into the room in places where the opposite is true. Across a doorway, ambient air will flow back into the room through the bottom of the opening to replace the gases that have exited it. In this way, the flow of hot smoke in a room fire will be affected by natural and mechanical ventilation (windows, the opening and closing of doors). It is common to see fresh air entering a room on fire through the



openings located close to the floor, and a hot mix of air, fuel, and combustion products exiting the room through the openings closest to the ceiling.

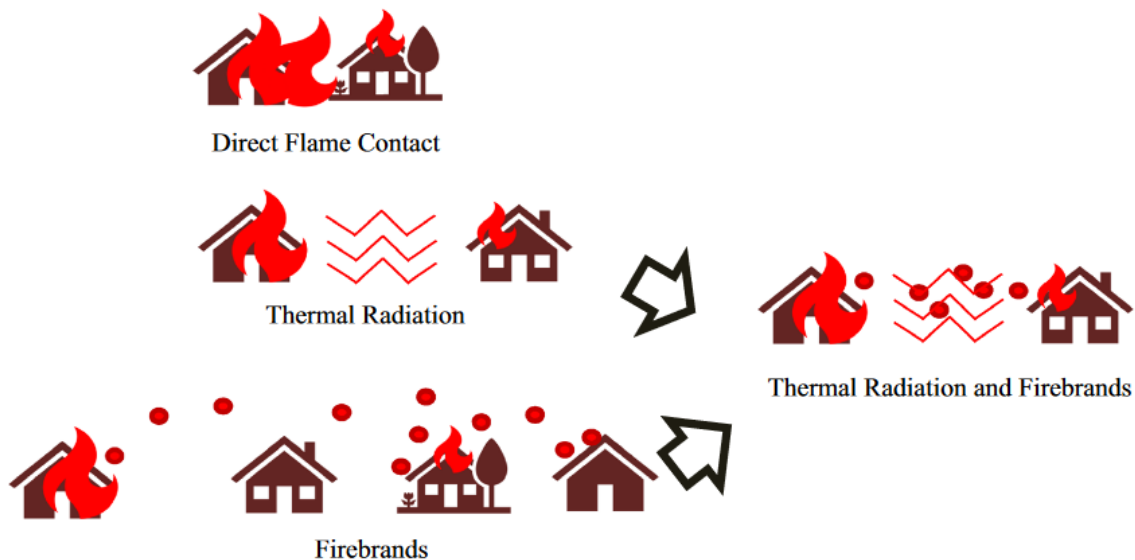
When the fire reaches the fully developed phase, flames carried by the hot plume can extend far out of the openings. Depending on the weather conditions and local winds, these flames can impinge on the openings of surrounding rooms and apartments. As a result, the fire can break back in the building through a combination of conduction, convection and radiative heat transfer, starting a new fire in a secondary room. A situation where a fire can spread from floor to floor through this process is called leapfrogging.

Façade fire:

A problem regularly identified in modern construction is the development of combustible cladding elements on building façade for insulation purposes⁴. If the building information highlights the existence of such combustible material and a flame extending out of an opening can reach a sufficient HRR, then the surface of the cladding can ignite and fire spreads over the façade. The fire will spread vertically until the top of the building is reached, and a possible horizontal spread can be integrated, driven by wind conditions. The existence of barriers in the cladding can be considered, though most recent façade fires have highlighted their lack of efficiency. A façade fire rapidly multiplies the number of direct impingement cases that lead to more fires starting in the upper floors.

C. Building to building spread

Once a building is on fire, three major mechanisms of fire spread can spread the fire to the surrounding structures. These mechanisms do combine, and their effects are cumulative.



Source: Suzuki and Manzello, Fire Technology 2021

Figure 69: In urban settings, fire can spread through direct flame contact, thermal radiation, firebrands or a combination of all three mechanisms.

Direct flame contact:

If not enough space is provided between structures in city planning, flames can extend from a building on fire to its neighbors. The resulting convective, radiative, and conductive heat transfer can be enough to ignite a combustible façade or break through windows and vent openings. This situation can also happen when combustible material accumulates between

⁴ See the tragic example of the Grenfell fire https://en.wikipedia.org/wiki/Grenfell_Tower_fire



buildings, such as vegetation, trash, or vehicles, and the fire spreads on these intermediate elements.

As previously, flame extension can be evaluated from the properties of the initial fire, the buildings floorplans, and the weather conditions to identify the surrounding openings at risk.

Thermal radiation:

Because a flame does not extend all the way to an adjacent building does not mean the fire cannot propagate. In large-scale fires, the amount of heat radiated can reach values high enough to ignite a combustible element meter ahead of the fire front. Combustible elements can spontaneously ignite under the influence of an external radiative heat source powerful enough. As the fire in a building can extend through multiple openings, radiation from several fires can add up to reach a critical threshold leading to ignition.

Evaluating the cumulative radiative heat flux from a series of fires to a potential fuel element requires the evaluation of the HRR of each visible flame combined with a geometric view factor to understand how much of a given flame “sees” the fuel element and consequently transfers part of its energy through radiations.

Firebrands:

When combustible elements burn and degrade, they can generate small particles light enough to be carried away by the buoyant plume. These are called ambers or firebrands and can be easily visualized in any wood fire. Once detached, the burning particles are transported through a complex flow motion and can land far away from the initial fire. If they are still burning or smoldering, the heat they generate can ignite the surface they land on. Modelling the generation, transport, and ignition at landing of all particles is beyond the state of knowledge, so statistical models have been developed to capture the likelihood of the ignition of a secondary fire due to branding based on smaller-scale experiments. Cumulative branding is an issue in corners and small openings, where the hot particles can accumulate until a new fire starts.

This mechanism is particularly important in wildfires but has also been reported in urban fire configurations.

6.4.4 Uses of fire spread modelling

Fire spread modelling can be a critical tool in simulating and understanding the behaviour of fires in urban or wildfire spread scenarios. Some of the most common uses are:

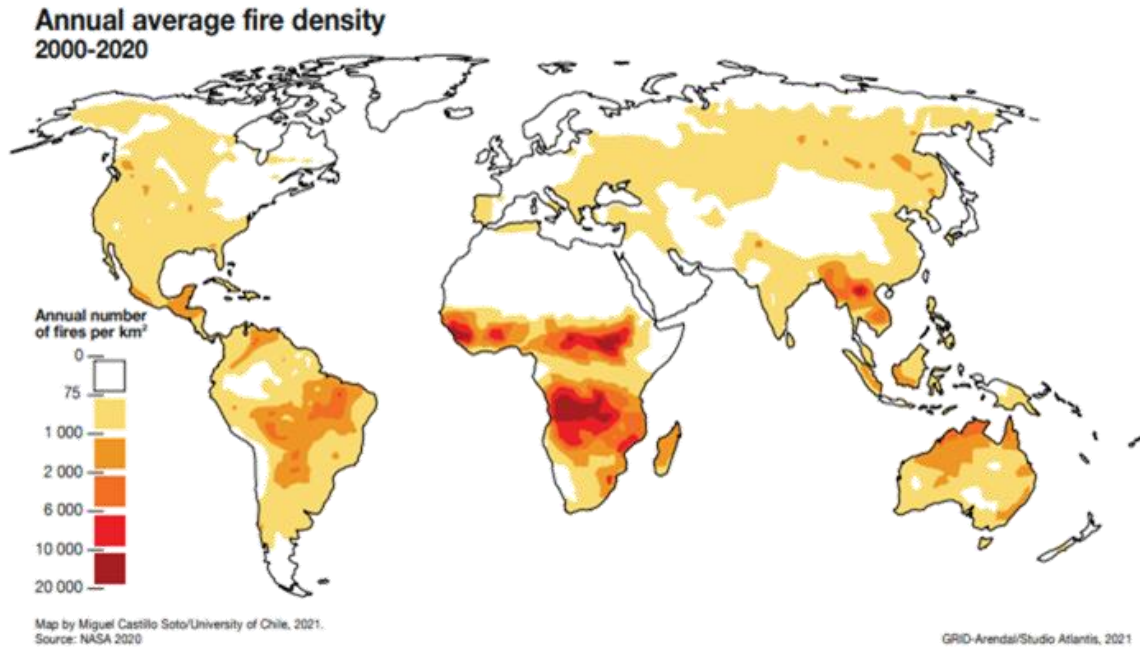
1. Building and urban planning
2. Fire risk assessment
3. Firefighting tactics
4. Fire suppression planning
5. Evacuation planning
6. Wildfire management
7. Raising awareness

6.5 Wildland-Urban Interface Fire

Wildland-urban interface (WUI) is the zone where urban setting meets or gets intermixed with wildland vegetations or fuels. These are often characterised by an increased risk of wildfire threatening both human lives and property as well as natural resources and ecosystems.

There has been an increase in the frequency and intensity of wildfire across the globe. This has been attributed to climate change. Global warming has been a contributing factor in increased wildfires.





Source: Miguel Castillo Soto. University of Chile, 2021

Figure 70: Annual average fire density 2000-2020

6.5.1 Factors affecting wildfires

There are primarily three factors that affect the development and spread of wildfires:

1. **Weather:** Drought, heat waves and low humidity can increase the probability of wildfires. Wind direction and speed can affect how quickly and in which direction a wildfire spreads.
2. **Fuel:** Amount and type of fuel available can affect the intensity and development of wildfires. Fuel includes vegetation, such as trees and grasses and manmade materials such as buildings, and other structures.
3. **Topography:** Shape, slope and aspect of the land can affect the speed at which the fire spreads. Wildfires travel faster on steep slopes and uphill direction.

Apart from these factors, human interventions also play a major role in initiating as well as managing or suppress a wildfire. Wildfire management strategies, prevention efforts, fire suppression planning, and fuel reduction can influence the severity and frequency of wildfires.

6.6 A Case Study on Fire Hazard Assessment

Fire hazard assessment is done to identify and prioritize fire hazard and risk so that the cities/ municipalities can determine which risk to address and how to address those. It also allows to ensure levels of service, programs and activities for public fire safety education, formulation and enforcement of fire codes and emergency response plan.

6.6.1 Fire hazard assessment in Tamakoshi Rural Municipality, Nepal using Analytic Hierarchy Process (AHP) approach

A. Spatial data collected and collated

1. **Primary data:** These are the data collected through building inventory and infrastructure survey at municipal level. Data on building information, critical infrastructure profile



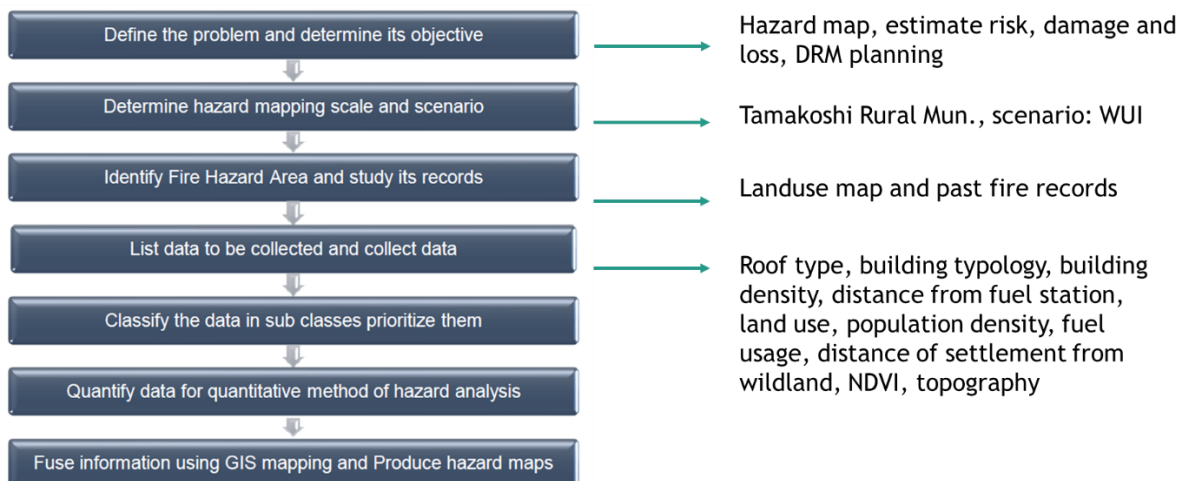
(location of petrol pump or chemical industries), availability of fire sources, and fire-fighting scenarios were collected.

2. Secondary data: These data are collected through municipal profile, department of survey, census and disinventar. Demographic data, land use data, past loss and fire event data were collected and used.

B. Methodology/ Approaches used

There are several approaches for fire hazard assessment based on availability of data and technology involved such as,

- Probability risk assessment
- Event tree and fault tree analysis
- Semi-quantitative method
- Multi-criteria decision-making approach (AHP)
- As a flexible while strong method is required to work with qualitative data and update current information with the availability of new information, the best with its feasibility in Nepal is the Analytic Hierarchy Process (AHP) model developed by Thomas Saaty in 1997. According to this AHP principle, derivation of weights for a set of activities according to priority is a fundamental logic of decision. This priority is judged according to several criteria based on the activities or objectives (Saaty, 1977). The AHP, introduced by Thomas Saaty is a mathematical method or a quantitative method which analyses complex decision problems under multiple criteria (a series of pair-wise comparisons), and helps the decision makers to set priorities and make the best decision. Moreover, the AHP incorporates a useful technique for checking the consistency of the decision maker’s evaluations, which in turn help in reducing the bias in the decision-making process (Saaty, 1977). AHP has been applied in many and diverse areas of decision-support in environmental management such as wildfire risk map, forest fire risk map, urban fire risk map, landslide susceptibility mapping etc.
- The steps followed in the overall process of fire hazard assessment is shown using the flowchart below.

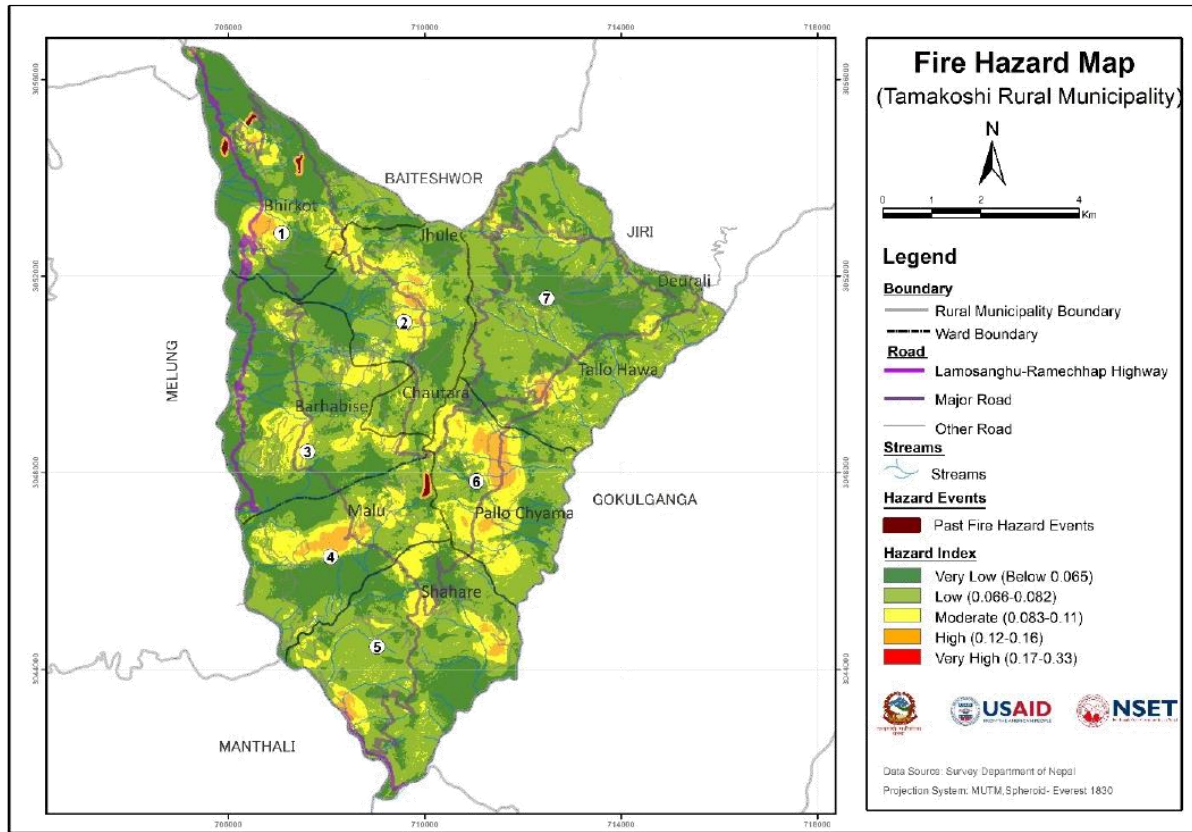


Source: Multi-hazard and multi-risk assessment guidelines for rural municipalities of Nepal, NSET, 2022

Figure 71: Methodology flowchart for fire hazard assessment using AHP method



C. Hazard Mapping



Source: Multi-hazard and multi-risk assessment guidelines for rural municipalities of Nepal, NSET, 2022

Figure 72: Fire hazard map developed for Tamakoshi Rural Municipality, Nepal

6.7 General Provisions for Fire Safety

6.7.1 Layers of fire safety in buildings and settlements

- Building codes and policies for fire are crucial to ensure that buildings are designed and constructed to minimize the risk of fire and to protect occupants in the event of a fire. Generally, seven layers of fire safety considerations are done to minimize fire risk in a building/ settlement:
 1. Prevention: E.g. electrical safety, awareness and education
 2. Detection: E.g. Smoke detectors and alarms their regular maintenance
 3. Early suppression: E.g. Automatic fire sprinklers, fire extinguishers
 4. Evacuation: E.g. Emergency escape route plan, regular evacuation drills, means of egress, exits
 5. Compartmentation: E.g. Fire walls and floors, fire doors and fireproof sealing of joints
 6. Structural safety: E.g. Standard fire resistance test, engineering methods to improve fire performance of structural systems
 7. Firefighting: E.g. Firefighting tactics, specific water supply and firefighting access ways



6.7.2 Wildland-Urban Interface (WUI) fire safety provisions

For the effective management and mitigation of wildfires, following measures are commonly deployed:

4. Limit settlement density and location
5. Create defensible zone/ barrier around the settlement
6. Use fire-resistant building materials
7. Vegetation management
8. Fire suppression techniques
9. Evacuation planning
10. Firefighting access and egress



SESSION 7: CLIMATE CHANGE

7.1 Objectives

By the end of the session, the participants will be able to:

- Describe the climate change impact assessment and interpretation of future climate data (GCMs/ RCMs) and extreme precipitation indices.
- List the methods of selection of GCMs, bias correction and statistical downscaling of selected GCMs to the required scale.
- Discuss the spatial and temporal variation of past extreme events, their importance for flood analysis, and their application to define extreme precipitation under climate change.
- Interpret projected changes in future precipitation and extreme precipitation indices.
- Discuss the linkage of climate change analysis to TCDSE.
- Discuss about rainfall extremes under future climate change with implications for urban flood risk, from Kathmandu Valley case study.
- Download and view GCM data.

7.2 Structure of Session 7

Structure
1. Climate Change and Climate Extremes
2. Case Study: Climate Change Effects on Rainfall Extremes in Kathmandu Valley Catchment

7.3 Climate Change and Climate Extremes

7.3.1 Introduction

The Intergovernmental Panel on Climate Change (IPCC) identifies climate change as “the change in the state of the climate that can be identified by changes in the mean and/or the variability of its properties and that persists for an extended period, typically decades or longer”.

In recent years, the increase in magnitude and frequency of extreme events has been quite evident. A major takeaway from the IPCC AR6 report was that human-induced climate change is causing more frequent and intense extreme events and has led to adverse and irreversible impacts.

This session aims to understand the effects of climate change on extreme precipitation and subsequently its effects on floods. The Kathmandu Valley catchment done for the Tomorrow’s Cities-Kathmandu project is taken as the case study for this session. We will begin by introducing some terminologies.

A. General Circulation Models (GCMs)

Also known as Global Circulation Models, GCMs are the mathematical models that represent the physical processes in the atmosphere, ocean, cryosphere and land surface. GCMs have a coarse resolution, varying between 250 and 600 km, and consist of vertical layers representing the atmosphere and oceans. These models are a means to understand and predict climate change in future, with modelled values for various variables such as precipitation, temperature, surface radiation, humidity and temperature.



B. Regional Climate Models (RCMs)

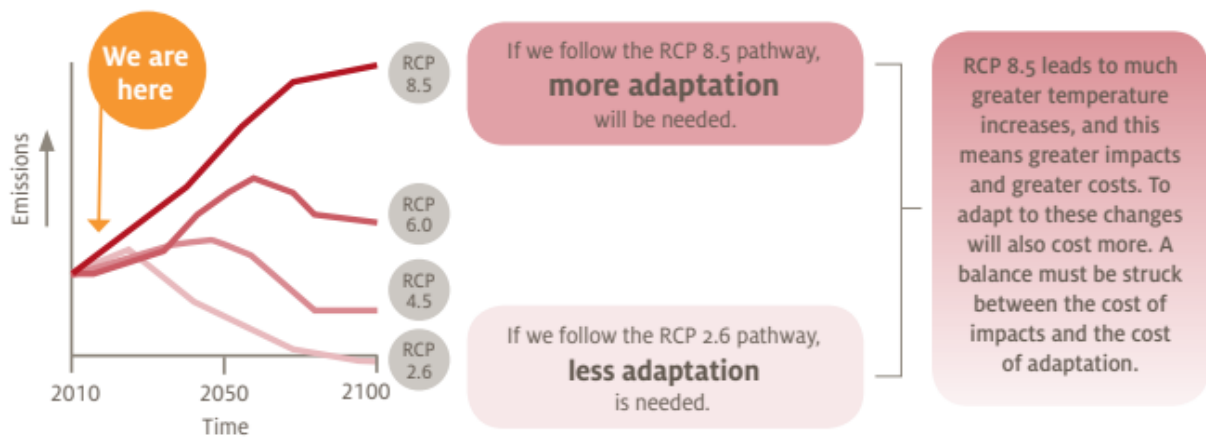
RCMs are the finer resolution and smaller area edition of GCMs and are obtained by dynamically downscaling the GCMs. The mathematical equations used for RCMs are the same as for GCMs. RCMs provide climate change information on regional and local level. RCMs provide better representation of spatial variations (topography, lakes, land, sea etc.), smaller-scale weather systems.

C. Coupled Model Intercomparison Project (CMIP)

CMIP is a framework for climate model experiments coordination. CMIP lets scientists analyze, validate, improve and update GCMs. CMIP allows the climate models to be improved by 7 comparing multi model simulations to observations and to each other. CMIP also ensures the public availability of multi-model output in standardized format. CMIP has done six large model intercomparison projects since its initiation. The sixth CMIP-CMIP6 is used in the IPCC AR6 (assessment report).

D. Representative Concentration Pathways (RCPs)

RCPs are the future scenarios of changes in greenhouse gases in the atmosphere as a result of human activities. The four RCP scenarios are RCP2.6, RCP4.5, RCP6.0 and RCP8.5. 2.6, 4.5, 6.0 and 8.5 are the radiative forcing in W/m² resulting from greenhouse gases concentration. Total radiative forcing is the difference between the incoming and outgoing radiation at the top of the atmosphere. RCP2.6 is the most optimistic scenario with a future adapting to renewable sources of energy, sustainable modes of transportation and low-level adaptations required for low cost. RCP8.5 is the scenario with the future still dependent on fossil fuels, higher temperature increase, higher sea level rise and high-level adaptations required at high cost.



Source: www.coastadapt.com.au

Figure 73: Emission scenarios in the future with each Representative Concentration Pathways (RCPs)

E. Shared Socioeconomic Pathways (SSPs)

SSPs are used to set future emission scenarios with and without climate policies. SSPs are used as inputs for the CMIP6 climate models. SSPs consider the changes in socioeconomic factors (such as education, economic growth, technological development, population, and urbanization). 5 socioeconomic narratives for future scenario have been considered. SSP1: Sustainability-taking the green road (low challenges to mitigation and adaptation), SSP2: Middle of the road (Medium challenges to mitigation and adaptation), SSP3: Regional Rivalry—a rocky road (High challenges to mitigation and adaptation), SSP4: Inequality-a Road divided (Low challenges to mitigation,



high challenges to adaptation) and SSP5: Fossil-fueled development-taking the highway (High challenges to mitigation, low challenges to adaptation).

F. ETCCDI Extreme Value Indices

These are the set of descriptive indices of extremes set by the Expert Team on Climate Change Detection and Indices (ETCCDI). These indices help to understand climate variability and trends. There are 27 temperature and precipitation based extreme indices.

Table 7: ETCCDI extreme value indices

ID	Indicator Name	Definitions	Units
SU25	Summer days	Annual count when TX (daily maximum) > 25 °C	Days
ID0	Ice days	Annual count when TX (daily maximum) < 0 °C	Days
TR20	Tropical nights	Annual count when TN (daily minimum) > 20 °C	Days
FDO	Frost days	Annual count when TN (daily minimum) < 0 °C	Days
TXx	Max Tmax	Annual maximum value of daily maximum temp	°C
TXn	Min Tmax	Annual minimum value of daily maximum temp	°C
TNx	Max Tmin	Annual maximum value of daily minimum temp	°C
TNn	Min Tmin	Annual minimum value of daily minimum temp	°C
TX90p	Warm days	Percentage of days when TX > 90 th percentile	%
TX10p	Cool days	Percentage of days when TX < 10 th percentile	%
TN10p	Cool nights	Percentage of days when TN < 10 th percentile	%
TN90p	Warm nights	Percentage of days when TN > 90 th percentile	%
GSL	Growing season length	Annual (1 Jan-31 Dec in NH) count between first span of at least 6 days with TG > 5 °C and first span after 1 July of 6 days with TG < 5 °C	Days
DTR	Diurnal temperature range	Annual mean difference between TX and TN	°C
WSDI	Warm spell duration indicator	Annual count of days with at least 6 consecutive days when TX > 90 th percentile	Days
CSDI	Cold spell duration indicator	Annual count of days with at least 6 consecutive days when TN < 10 th percentile	Days
RX1day	Max 1-day precipitation amount	Annual maximum 1-day precipitation	mm
RX5day	Max 5-day precipitation amount	Annual maximum consecutive 5-day precipitation	mm
SDII	Simple daily intensity index	Annual total precipitation divided by the number of wet days (defined as PRCP >= 1.0 mm) in the year	mm day ⁻¹
R10	Number of heavy precipitation days	Annual count of days when PRCP >= 10 mm	Days
R20	Number of very heavy precipitation days	Annual count of days when PRCP >= 20 mm	Days
R25	Number of days above 25 mm	Annual count of days when PRCP >= 25 mm, 25 is user-defined threshold	Days
CDD	Consecutive dry days	Maximum number of consecutive days with RR < 1 mm	Days
CWD	Consecutive wet days	Maximum number of consecutive days with RR >= 1mm	Days



ID	Indicator Name	Definitions	Units
R95p	Very wet days	Annual total PRCP when RR > 95 th percentile	mm
R90p	Extremely wet days	Annual total PRCP when RR > 99 th percentile	mm
PRCPTOT	Annual total wet-day precipitation	Annual total PRCP in wet days (RR >= 1 mm)	mm

7.4 Case Study: Climate Change Effects on Rainfall Extremes in Kathmandu Valley Catchment

7.4.1 Description of Kathmandu Valley Catchment

Kathmandu valley basin lies in the Bagmati province in central Nepal, with the catchment area of 654 km². This is an upstream catchment of Bagmati basin. Bagmati river originates from Shivapuri hills in northern Kathmandu and is joined by the tributaries: Manohara, Bishnumati, Hanumante, Dhobi Khola, Tukucha, Balkhu and Nakhu along its path. The average annual precipitation in Kathmandu Valley is approximately 1660 mm. Bagmati river at Khokana has an average annual discharge of 16 m³/s, while it has average monsoon discharge of 36 m³/s.

7.4.2 Approach: Rainfall Extremes under Future Climate Change with Implications for Urban Flood Risk

We start our analysis by selecting GCMs, which will provide us with future precipitation projections. We progress with bias correction and statistical downscaling of the selected GCMs for them to be ready to use at local scale. The next step is to analyze the rainfall extremes in changing climate. We focus on RX1day. The rainfall frequency analysis and studying spatial and temporal variation of rainfall patterns and its influence on discharge based on historical context provides us a basis to study flood behavior in a changing climate.

A. GCM Selection for Future Climate Scenario

GCM selection is based on an envelope based approach by Lutz et al. (2016) [13] where from a pool of GCMs. The selection is done based on:

- Projected average annual changes in mean temperature and precipitation sum.
- Changes in precipitation and temperature extremes.
- Validation of remaining models' past performance.

B. Extreme Value Indices

The Expert Team on Climate Change Detection and Indices (ETCCDI), a group of experts co-sponsored by the World Meteorological Organization (WMO), commission for Climatology (CCI), the World Climate Research Program (WCRP), and the Joint Technical Commission for Oceanography and Marine Meteorology (JCOMM) are the main player for the development of extreme indices. ETCCDI developed 27 internationally recognized sets of indices in order to detect the changes in extreme events due to climate change. Out of 27 indices, 16 are temperature related and 11 are precipitation related and derived from daily/annual rainfall as well as minimum/maximum temperature.

The precipitation indices are calculated based on the annual wet day, consecutive dry days, and days above or below a certain threshold value, and are mostly used in climate science in order to assess the trends of climate change projections caused due to extreme precipitation globally and regionally. Following are the 9 precipitation related indices that are calculated in terms of intensity, frequency and duration.



Table 8: Precipitation related indices calculated in terms of intensity, frequency and duration

S.No.	Name of Index	Description
1	Annual maximum 1-day (or 24 hour) precipitation (RX1day) (mm)	Most intense rainfall event in 1 day (or 24 hours) for a given year
2	Annual maximum consecutive 5-day precipitation (RX5day) (mm)	Most intense rainfall event in 5 consecutive days for a given year
3	Heavy rainfall days (R10mm) (days)	Annual count of days when precipitation > 10 mm
4	Very heavy rainfall days (R20mm) (days)	Annual count of days when precipitation > 20 mm
5	Consecutive dry days (CDD) (days)	Maximum number of consecutive days with daily precipitation (RR) less than 1 mm
6	Consecutive wet days (CWD) (days)	Maximum number of consecutive days with daily precipitation >= 1 mm
7	Very wet days precipitation (R95pToT) (mm)	Annual total precipitation when RR > 95 percentile of reference period
8	Annual total wet day precipitation (PRCPTOT) (mm)	Total wet-day precipitation
9	Simple precipitation intensity index (SDII) (mm/day)	Simple daily intensity

These indices can be represented in different climate conditions that ultimately are related with the catchment runoff in terms of water availability and extreme rainfall events. The 24-hour maximum rainfall represented as RX1day and 5-day maximum annual rainfall represented as RX5day, provides information about the climate conditions that can trigger floods and landslides. Highly wet days are also indicated by very wet day precipitation represented as R95PToT. Consecutive Dry days, CDD, are linked to dry spells of water availability or even droughts. Also, Consecutive Wet Days, CWD, refers to increased wet conditions. Intense Rainfall Days represented by R10mm and R20mm are related to frequency of the rainfall and flow in the catchment. For the study in Kathmandu, 24-hour maximum rainfall, RX1day, was assessed and analyzed to have a direct relationship with the flood events.

C. Bias Correction

Global Climate Models (GCMs) and Regional Climate Models (RCMs) during the model simulation can possess large systematic biases compared to the observed data. The GCMs and RCMs datasets are used as inputs to process the simulation therefore, algorithms have been developed to correct and minimize the biases that exist during the modeling. The errors in GCM precipitation field occur due to i) unrealistic large-scale variability or response to climate forcing ii) unpredictable internal variation that are different than the observed data iii) errors in convective parameters and difference in grid scales of different models.

Therefore, biases in rainfall magnitude in GCMS during the observed/historical period against the observation are corrected using the empirical quantile mapping method. Empirical quantile mapping method is a technique of mapping the probability distribution function of rainfall of the selected GCMs with that of the observed rainfall.

$$X_{future,t}^{corr} = \text{inverse } ecdf_{reference}^{obs} \left(ecdf_{reference}^{Model} (X_{future,t}^{Model}) \right)$$

Where,

ecdf is the empirical cumulative distribution function for the reference time period,



$X_{future,t}^{Model}$ is the raw GCM at time t for the future, $ecdf_{reference}^{Model}$ is the empirical cumulative distribution function of GCM for the certain reference period,

$inverse\ ecdf_{reference}^{obs}$ is the inverse empirical cumulative distribution function of the observed rainfall for a certain reference period,

$X_{future,t}^{corr}$ is the corrected estimate of $X_{future,t}^{Model}$.

Generally, distribution mapping by using the empirical formula functions well for the given normal range of rainfall values. In case of extreme values or future projected values beyond the observed values, extrapolation techniques such as linear scaling based on the upper quantiles are used. This can cause inflation, hence, to reduce such inflation, distribution mapping with the theoretical distribution is used rather than the empirical method for the extreme values. Here, extreme values are the rainfall values greater than or equal to 99th percentile during the reference period.

Generalized Pareto Distribution (GPD) is normally used as such theoretical distribution for the modeling of the extreme values above the threshold.

D. Spatial and Temporal Variation of Rainfall Events

Rainfall variation in the hydrologic cycle is affected by spatial and temporal changes. A detailed knowledge of the spatial and temporal distribution of rainfall is necessary for flood modeling. Therefore, the spatial variation of rainfall events is analyzed to understand the distribution of extreme rainfall events and their role in generating the highest flow that results in flood events. Analysis of spatial variations of rainfall events is based on the historical spatial distribution of the rainfall events.

Climate modeling in small catchments is more complex as in small catchments flows are sensitive to variations at small time intervals. Also, daily rainfall observations are not sufficient for accurate flood modeling in small catchments. Therefore, analysis of temporal variation is important to understand the fast hydrological response and time of concentration in the catchment.

Following steps are usually followed for temporal disaggregation:

- At first ratio of the catchment average rainfall of each 3-hourly time window to the catchment average rainfall of the whole day is calculated.
- Then the future extreme rainfall of a certain period is multiplied by the ratio to obtain rainfall clause for a specific 3 hourly time window.

After the temporal disaggregation, spatial disaggregation of rainfall for each time window is obtained.

- The grid values covering the basin are divided by the catchment average rainfall for a specific time to get a factor.
- Temporarily disaggregated value for a specific time is then multiplied by the factor to obtain spatially disaggregated rainfall values for the selected basin.

E. Rainfall Frequency Analysis

Stationary rainfall frequency analysis is the idea that the systems do not change with the change in time and human behavior and is mostly used to evaluate and manage the risks associated with water supplies in the given probability. But in reality, it is evident that due to substantial human activities the Earth's climate is significantly changing, and the extreme precipitation events, evaporation and discharge rates of the rivers are constantly increasing. Therefore, the theory of stationarity in water and climate systems is no longer valid or considered questionable. To include the changing processes in the natural system, a non-stationarity approach is introduced.



Non-stationarity climate models with time-dependent probability distribution functions (pdfs) were introduced to calculate the frequency analysis. Non-stationarity rainfall frequency is recommended by the Committee on Adaptation to a Changing Climate for analysis of climate change conditions.

A non-parametric Mann-Kendall trend test is usually performed firsthand to test if the trend exists in time series. Generalized extreme Value (GEV) is widely used for non-stationary frequency analysis of annual maximum rainfall. GEV is defined by following equation:

$$G(z) = \exp \left\{ - \left[1 + \xi \left(\frac{z - \mu}{\sigma} \right) \right]^{-\frac{1}{\xi}} \right\}$$

where μ , σ and ξ are location, scale and shape parameters, respectively. Here, the parameters satisfy $-\infty < \mu < \infty, \sigma > 0$ and $-\infty < \xi < \infty$. If $\xi \rightarrow 0$, which thus leads to Gumbel distribution given by the following equation:

$$G(z) = \exp \left\{ - \exp \left[- \left(\frac{z - \mu}{\sigma} \right) \right] \right\}$$

and the T- year return level value (X_T) for extreme rainfall is estimated as,

$$X_T = \mu + \frac{\sigma}{\xi} \left[1 - \left\{ - \log \left(1 - \frac{1}{T} \right) \right\}^{-\xi} \right]$$

GEV assumes that extreme values are independent and identically distributed and that any presence of a trend causes a violation of this assumption. Hence, the non-stationary case is introduced by adopting the parameters of GEV as a function of time. In general, the location and scale parameters are considered as the function of time.

Case	Description	Notation used
A	Location parameters is function of time for 2006-2100. Distribution is given by: $GEV(\mu(t), \sigma, \xi)$ $\mu(t) = \beta_0 + \beta_1 \times t$ where, β_0 and β_1 are parameters.	NS-GEV-M1
B	Location and scale parameters are functions of time for 2006-2100. Distribution is given by: $GEV(\mu(t), \sigma(t), \xi)$ $\mu(t) = \beta_0 + \beta_1 \times t$ $\sigma(t) = C_0 + C_1 \times t$ where, β_0 and β_1 and C_0 and C_1 are parameters.	NS-GEV-M2
C	Parameters are constant in time 2006-2100	S-GEV
D	Parameters are constant in time during given time period (near future, mid future and far future)	S-GEV (near-future NF or mid-future MF or far-future FF)

Note: NS and S represent non-stationary and stationary approaches, respectively. GEV represents Generalized extreme value.



SESSION 8: VULNERABILITY MODELLING - SINGLE HAZARD

8.1 Objectives

By the end of the session, the participants will be able to:

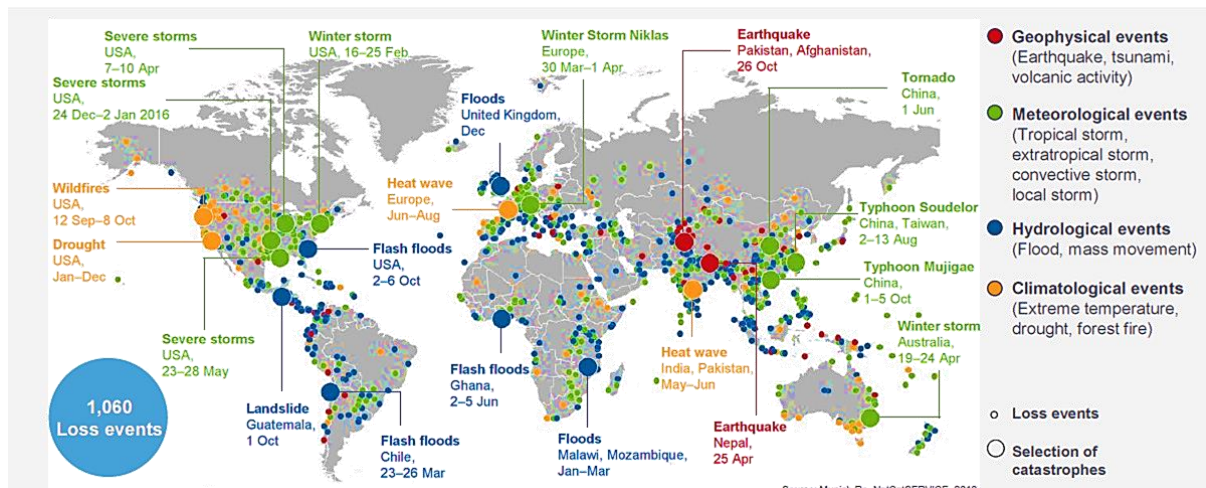
- Define the concept of fragility and vulnerability.
- Identify the concept of probability and uncertainty in the domain of fragility.
- List the different types of fragility curves based on their method of development.
- Name the parameters required for formulation of fragility curves.
- Explain the basic concept of vulnerability analysis of buildings for earthquake and flood.

8.2 Structure of Session 8

Structure
1. Introduction
2. Fragility Analysis
3. Fragility/ Vulnerability Curves for Earthquakes
4. Fragility/ Vulnerability Curves for Floods

8.3 Introduction

On a global scale, there are thousands of loss events caused by the occurrence of natural hazards. The map shown in Figure below displays the loss events in the year 2015. In one year alone, there were 1,060 loss events. Such events could fall into Geophysical events (such as earthquakes), Meteorological events (such as hurricanes), Hydrological events (such as floods), and Climatological events (such as droughts). There is a need to estimate the losses caused by these hazards. In particular, some hazards might be especially rare but be associated with significant consequences.



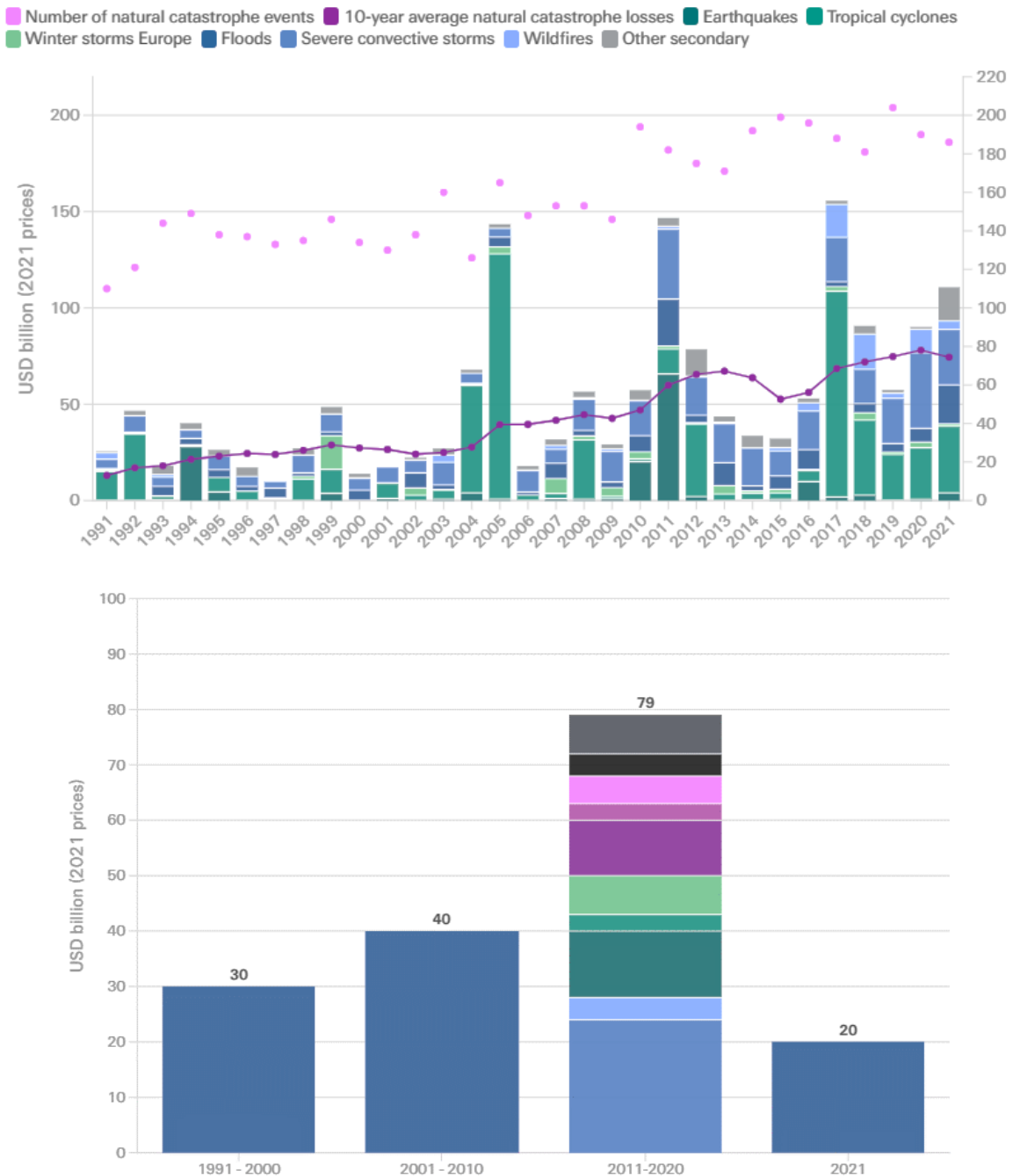
Source: Munchener Ruckversicherungs-Gesellschaft, Geo Risks Research, NatCatSERVICE

Figure 74: Hazard Map

The economic losses due to hazards have seen an increase over the past few years. Figure above on the left shows the global insured natural catastrophe losses by peril. A clear upward trend in these losses can be observed. On the right of the figure, flood losses by decade are shown. This



graph is updated to 2021. In 2021 alone, 20 billion USD losses have been estimated. This is comparable to the losses that were recorded in the whole decade 1991-2000 (30 billion losses).



Source: Swiss Re Institute

Figure 75: Global insured natural catastrophe losses by peril (left) and flood losses by decade (right)

While economic losses have been used in the past as a proxy for the consequences of natural hazards, in reality, they might be unsuited to account for the social consequences of these hazards. In particular, they might misrepresent the effect that such hazards have on poorer communities. In fact, the damage to a fancy, secondary house for a rich person would end up being more significant than the damage to a not-so-expensive primary house in a poor community. Newer formulations for risk assessment are gradually shifting to quantifying consequences based on the actual impact of the hazards. Either way, there is a need to quantify



the physical damage to the structures and infrastructure affected. This is when risk analysis comes in.

8.3.1 Vulnerability within Catastrophe Risk

Catastrophe risk is the estimation of the losses due to hazard events within a given time frame (e.g., the lifetime of a structure). Risk assessment is made up of three components,

$$\text{Risk} = \frac{\text{Hazard} \times \text{Vulnerability} \times \text{Exposure}}{\text{Capacity}}$$

- **Hazard:** This part accounts for the potentially damaging events occurring at the site of interest. The previous sessions on the different hazards have mostly focused on the quantification of this component.
- **Vulnerability:** It accounts for the susceptibility of the built environment to undergo damage due to the hazard. This component is accounted for using fragility and damage curves, which will be discussed in this session.
- **Exposure:** It accounts for the number of people, buildings and structures that are exposed to the hazard. The fragility and vulnerability curves just give an indication of how the hazard would affect selected components. When we account for exposure, we consider the actual components that are exposed to the hazard.
- **Capacity:** It accounts for the strengths, attributes and resources available within a community, organisation or society to manage and reduce disaster risks and strengthen resilience.

A. Risk Modelling

Risk modelling usually follows four steps:

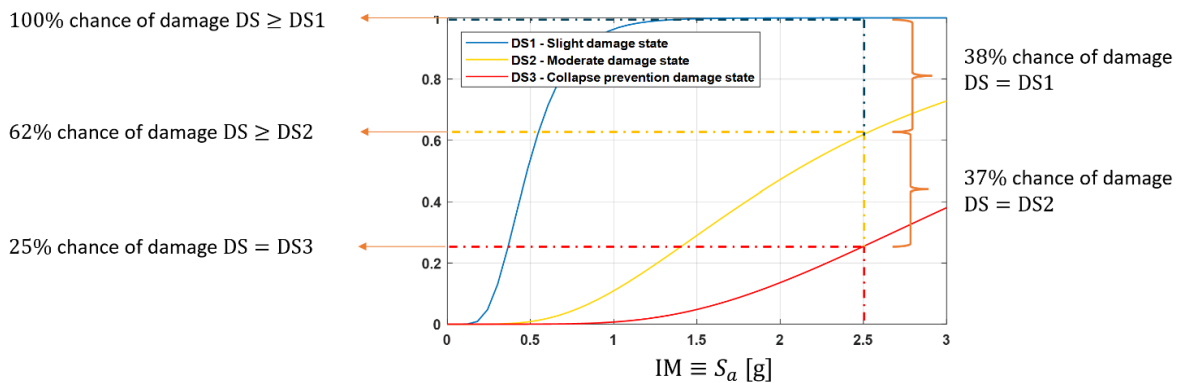
- First, we generate the events with their associated characteristics.
- Then, we need to translate these characteristics to local intensity measures. In general, there is no unified procedure to go from event characteristics to intensity measures. These are hazard-specific, and we will see a few examples in the rest of the session. These first two steps fall into the “hazard” category.
- The effect of these local intensity measures must be translated into damage to the exposed assets. To go from intensity to damage, we use **fragility curves**.
- The damage then must be transformed into losses. The losses might be economic as well as societal. In some cases, we obtain curves to translate the curves directly into losses; in this case, we talk about **loss curves**.

8.4 Fragility Analysis

The figure below shows an example set of fragility curves. The fragility curves quantify the probability of reaching or exceeding a certain damage state conditioned on the intensity measure of interest. In this case, the intensity measure is the spectral acceleration of the structure. For a spectral acceleration of $S_a = 2.5g$, we have approximately a 25% chance that the damage state is greater than or equal to DS3 (in this case, because there is no higher damage state, this is also the probability that the damage state is exactly DS3), a 62% chance that the damage state is greater than or equal to DS2, and a 100% chance that the damage state is greater than or equal to DS1. We can also obtain the probability that the damage state is exactly DS2 or DS1 by looking at the differences between the different curves. For example, the chance that the damage state is exactly DS2 will be equal to $62 - 25 = 37\%$. Fragility curves provide the probability associated with uncertain phenomena (the failure of the system, the system belonging to a specific damage state). The uncertainty associated with these events is due to



the uncertainties that characterize the variables at play, including the system properties, which cannot be known with certainty.



Source: Tomorrow's Cities

Figure 76: Examples of fragility curves for different damage states

8.4.1 Uncertainties

In general, we can distinguish between two types of uncertainties: aleatory and epistemic.

4. **Aleatory uncertainties** are those that are inherent in nature. They cannot be influenced by the observer or the manner of observation. For example, when we flip a coin, there will be a 50-50 chance that it will result in heads or tails, regardless of how much we know about the coin or the external conditions. These uncertainties cannot be reduced by their nature.
5. **Epistemic uncertainties** are those that arise from our lack of knowledge, our deliberate choice to simplify matters, errors in measuring observations, and the finite size of our samples. For example, the uncertainty in the state of a building after the occurrence of an earthquake is uncertain mostly because we don't know exactly the properties of the building's components, and our models are not accurate enough to capture its behavior due to the earthquake. We can reduce these uncertainties by improving our models, taking more accurate measurements, and/or by using larger samples.

Sometimes, whether something is aleatory or epistemic is debatable. In the coin example, we could technically improve our knowledge about the coin and the external conditions and better predict whether it would be heads or tails. However, it would be so complicated to do so that we classify these uncertainties as aleatory.

A. Uncertainties in Engineering

Among the aleatory uncertainties, we have the variability inherent to the physical phenomenon of interest that cannot be removed (for example, the characteristics of an earthquake are uncertain by nature - to a certain degree).

Among the epistemic uncertainties we can account for:

- **Model Inexactness:** This type of uncertainty arises when approximations are introduced in the formulation of the probabilistic model. It has two essential components: error in the form of the model, and missing variables.
- **Measurement Error:** Parameters in a probabilistic model are assessed by use of a sample of observations. These observed values, however, could be inexact due to human errors in the measurement, and errors in the measurement devices or procedure.
- **Statistical Uncertainty:** The accuracy of one's inferences depends on the observed sample size. The smaller the sample size, the larger is the uncertainty in the estimated



values of the parameters. If additional data cannot be gathered, then one must properly account for the effects of this uncertainty in all predictions and interpretations of the results.

- **Human Error:** Is the unavoidable process of making errors in the design, construction and operation of facilities by human beings.

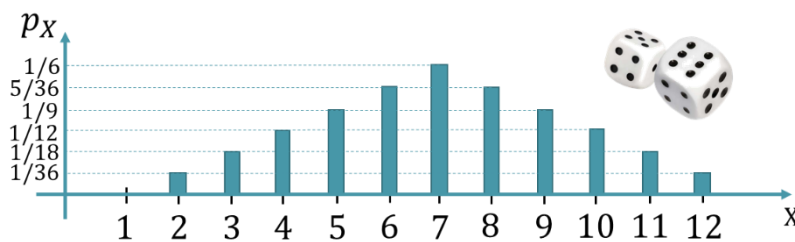
8.4.2 Random Variables

We usually model random quantities in our problems using random variables. A random variable is a mathematical formalization of quantities or objects which depend on random events. It is a mapping between the possible outcomes of an event and a measurable space (usually real numbers).

For example, the outcome of a dice roll can be mapped to the numbers from 1 to 6, or the outcome of a coin flip could be mapped to the numbers -1 or 1 (for example, heads could be -1 and tails could be 1, although there is no specific rule). Finally, we could assign the height of people in a room to the corresponding number on the real line (e.g., 1.60 m will be assigned to number 1.60). In the first two examples, we have a finite number of outcomes (numbers from 1 to 6 for the dice, heads or tails for the coin). In the last example, we have an infinite number of outcomes (any real number provided by our measuring tape, assuming that it has infinite precision). We use discrete random variables in the first case and continuous random variables in the second case.

A. Distribution of Random Variables

To quantify the probability of the different outcomes of the random variables (which are now numbers) we use distributions. The figure below shows the distribution of a discrete random variable associated with the result of the roll of two dice. The height of the bars is equal to the probability of that outcome. Rolling a 6 has a probability $p_x(6) = 1/6$, while rolling a 12 has a probability $p_x(12) = 1/36$. The function $p_x(x)$ is called the **probability mass function (pmf)**.

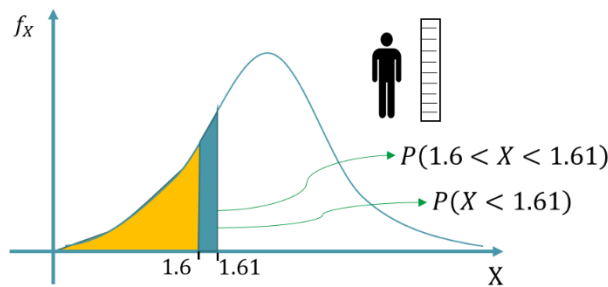


Source: Tomorrow's Cities

Figure 77: Probability Mass Function associated with the result of the two dice roll

For continuous random variables, we have an infinite number of outcomes, so the probability of obtaining exactly one number is 0. In this case, we need to use a **Probability Density Function (PDF)**. A pdf is a continuous function from which we can obtain the probability that we are interested in. For example, using the pdf in the figure below, if we want to know the probability that a person is between 1.60 m and 1.61 m tall ($P(1.6 < X < 1.61)$) we need to compute the area below the curve between these two numbers (green area). If we want to know the probability that the person is shorter than 1.60 m ($P(X < 1.60)$) we need to compute the area below the curve between $-\infty$ (the leftmost side) and 1.60 (yellow shaded area).





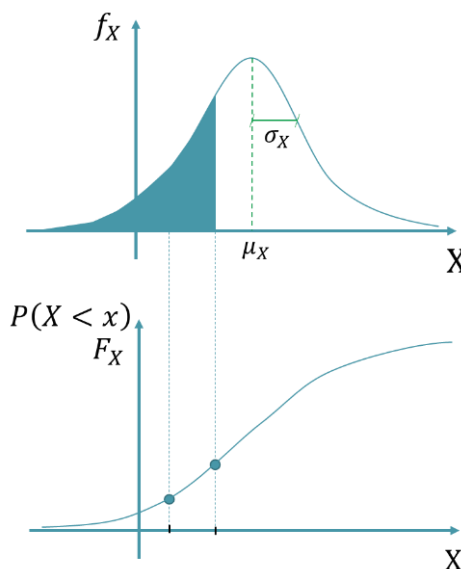
Source: Tomorrow's Cities

Figure 78: Probability Density Function of the height of a person

Probability Density Functions:

When we define a PDF, we need to provide:

- **Its shape**, by saying what type of distribution it follows (there exist several distributions typically used such as Normal, Lognormal, Gamma,...).
- **A measure of its location**, which usually corresponds to its **mean** (sometimes we also use the **median of the mode**).
- **A measure of its dispersion**, which usually corresponds to its standard deviation.
- Sometimes we might be interested in plotting the probability that a random variable is lower than a certain number. In other words, for each value, we want to indicate the area below the pdf between $-\infty$ and that value. These types of curves are called **Cumulative Distribution Functions (CDF)**. They always start at 0 and end at 1, and they usually do so in an S-shape. Because of these properties, they are usually used to fit fragility functions.



Source: Tomorrow's Cities

Figure 79: Cumulative Distribution Function (CDF)

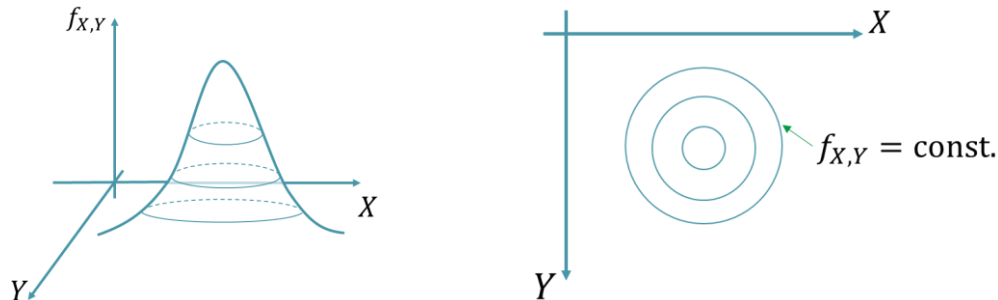
Multidimensional Probability Density Functions:

When we have more than one random variable, we can write their joint PDF. In the case of two random variables, these functions typically have a bell shape. In this case, we need to provide as many location and dispersion parameters as the number of variables (for the 2D case, two mean values and two standard deviation values). In addition, we also need to provide a



parameter that quantifies how the two variables are correlated to each other. Typically, this is done with a correlation coefficient.

- One way of obtaining fragility curves is to look at a 2D joint PDF where the random variables are the capacity and the demand of the system.



Source: Tomorrow's Cities

Figure 80: 2D Probability Density Function

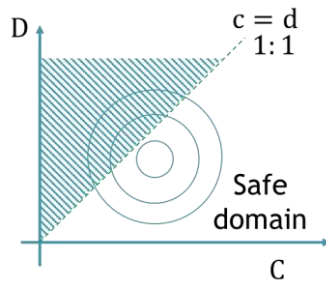
8.4.3 Capacity and Demand

- The capacity and the demand quantities depend on the type of problem that we are looking at. Below are a few examples in different fields of engineering.
- In structural, geotechnical and mechanical engineering, the capacity could be the ability of a member to take a force or deformation, while the demand could be the actual force or deformation imposed by a load.
- In construction and project management, the capacity could be the allowable time for completion of the work, while the demand could be the actual time spent/required to complete the project.
- In environmental engineering, the capacity could be the allowable value of a pollutant, while the demand could be the actual value of the pollutant.
- In hydraulics and hydrology engineering, the capacity could be the height of a dam or a levee, while the demand could be the water height due to the annual rainfall.
- In transportation engineering, the capacity could be the traffic volume that a highway or airport can offer, while the demand could be represented by the traffic needs.
- In sales (outside of engineering), the capacity could be the amount of a product in the store, while the demand could be the amount of that product requested by customers.

8.4.4 Reliability Analysis

In each of the examples in the previous section, failure occurs whenever the capacity of the system is lower than the demand on the system. Let us look at the joint pdf of capacity and demand. The line $c = d$ divides the domain into two separate sections. The part where $c > d$ is the safe domain, while the part where $c \leq d$ is the failure domain. The probability that the demand exceeds the capacity is equal to the volume below the pdf in the failure domain (this is the 2D equivalent of computing the area below the pdf). If we have the pdf, we can compute this volume with an integral. However, in most scenarios, we do not have the analytical expression for the pdf, but we can simulate realizations of capacity and demand. In this case, we can use Monte Carlo simulation to compute the probability of failure.





Source: Tomorrow's Cities

Figure 81: Joint PDF of capacity and demand, and definition of failure and safe domain

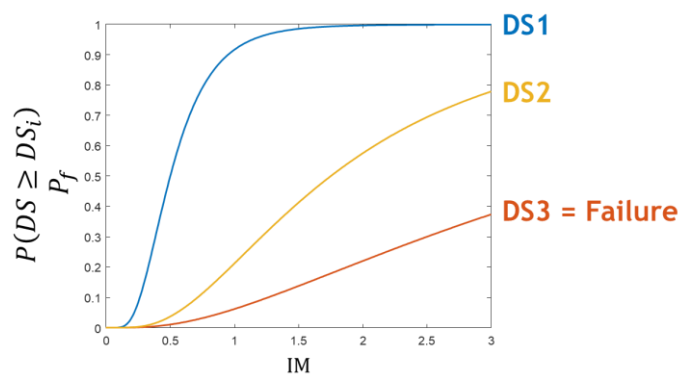
8.4.5 Monte Carlo Simulations

In Monte Carlo simulations, we simulate many pairs of capacity and demand (it is possible to do this with proper software, assuming that we know the distribution of the variables that affect capacity and demand) and count how many times the capacity is lower than the demand. Each of these realizations will result in failure. We can then estimate the probability of failure as the ratio between the number of realizations that resulted in a failure and the total number of realizations. As we increase the total number of realizations, the precision of our estimate is expected to increase. However, a computer will take longer to perform additional simulations. We need to reach a compromise between computational resources and precision.

Sometimes, the data points may not come from simulations, but rather they could be true realizations of the capacity and demand (which we might have observed in the field). In this case, an empirical estimate of the probability of failure can be obtained in the same way (by dividing the number of failures by the total number of observations). This is less common in practice due to the very low chance of observing failures in the field.

8.4.6 Fragility Curves

By repeating the analyses for different levels of intensity measures, we can obtain the fragility curves that were mentioned at the beginning. Specifically, if we count the failures, we will obtain the fragility curve associated with the failure of the system. However, the threshold for the demand does not need to be necessarily the one associated with failure. We can define lower thresholds for lower damage states and count how many times the demand exceeds those thresholds. This will provide us with additional fragility curves associated with other damage states. We will see some examples of damage states in seismic hazard analysis.



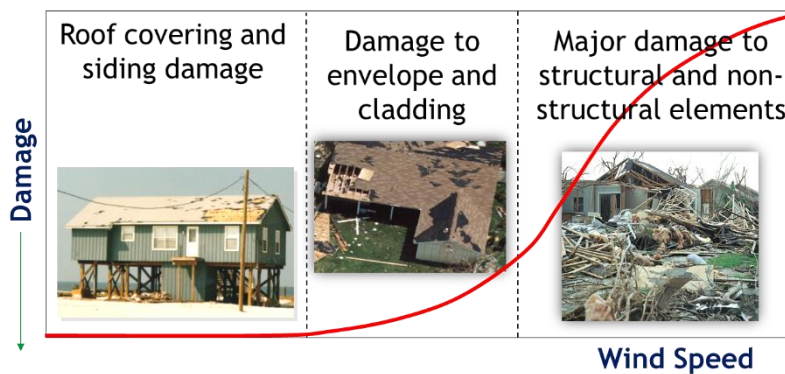
Source: Tomorrow's Cities

Figure 82: Fragility curves



8.4.7 Damage/ Vulnerability Curves

The damage/vulnerability curves look very similar to fragility curves, in that they typically have an S-shape. However, in this case they provide directly the expected damage associated with a certain intensity measure. A very common quantity to display on the y-axis of these curves is the damage ratio. The damage ratio is the ratio of repair cost to replacement value. If the damage ratio exceeds 1, then it would be more convenient to replace the asset rather than repairing it. Also in this case, it is important to specify the damage scale (just like in fragility curves). Because these curves typically do not come with uncertainty bounds, fragility curves are typically preferable (as they provide the uncertainties associated to each of the damage states). Both fragility and damage curves can be used to estimate the expected damage to an entire portfolio of buildings (i.e., an entire community). The characterization of the building stock is fundamental for such a task. In other words, fragility/vulnerability curves should be provided for each of the building types that we expect to find in our portfolio. These “building types” are typically called archetypes, and we will see some examples in the flood vulnerability section.



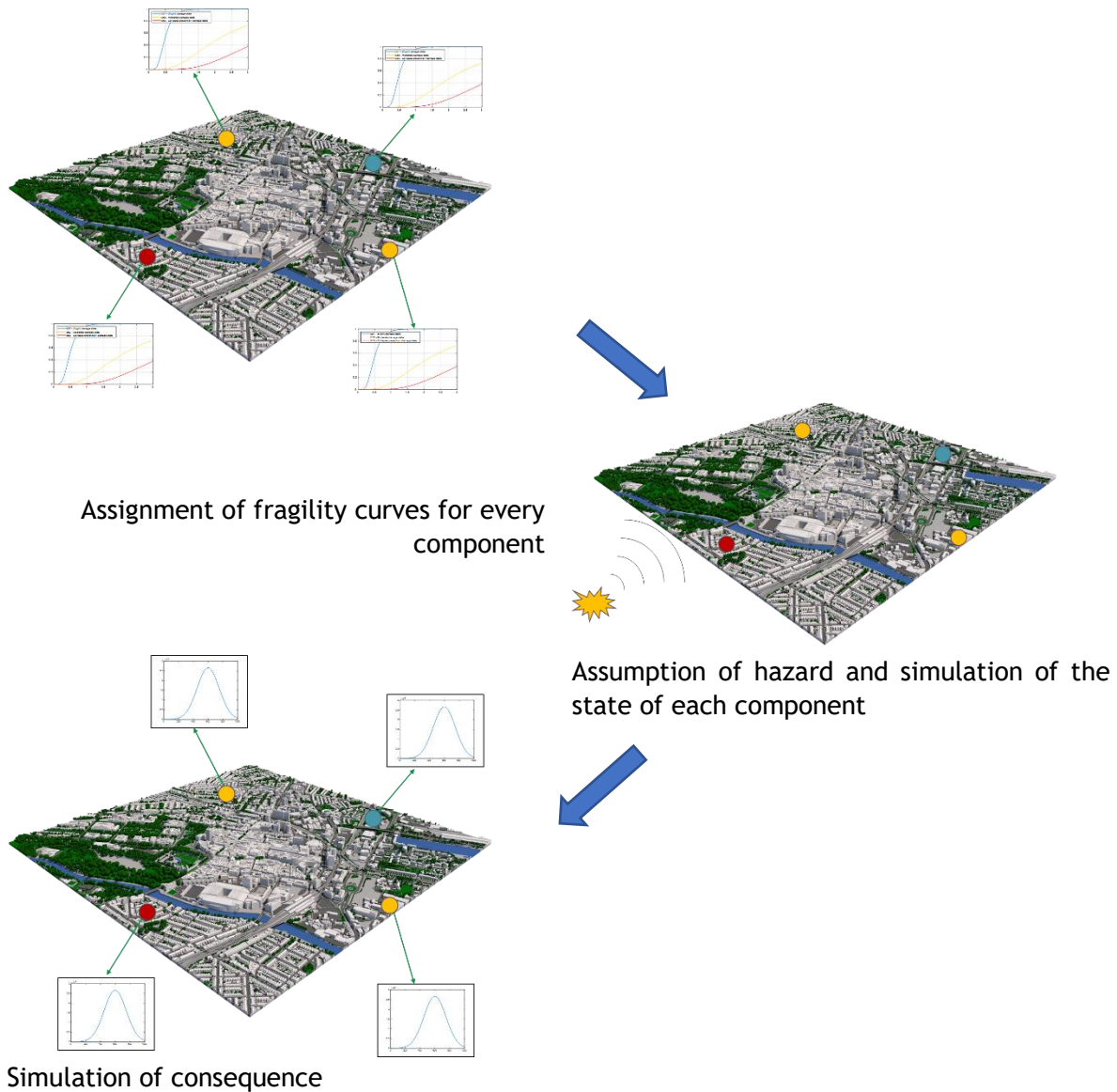
Source: Tomorrow’s Cities

Figure 83: Example of damage curve for wind hazard

8.4.8 Portfolio Assessment

To perform a portfolio assessment, we need to assign each of the components of our system to one of the archetypes. This will provide us with fragility/vulnerability curves for every component. We can then simulate the occurrence of a shock with given characteristics. We translate the event characteristics into intensity measures for the buildings using the hazard-specific procedure for that hazard (we will discuss earthquake and flood). Then, we can estimate the most likely damage state for each of the components (or provide the probability of each damage state). Finally, if we have costs or consequence associated to each of the damage states, we can obtain the expected total consequences due to the occurrence of the hazard. If we repeat this analysis for different hazard characteristics, we can obtain curves that provide the expected consequences/losses for the entire portfolio as a function of the hazard characteristics. We can call these loss curves. If, instead, we only look at a single realization of the hazard, we are performing a scenario analysis.





Source: Tomorrow's Cities

Figure 84: Portfolio Assessment

8.5 Fragility/ Vulnerability Curves for Earthquakes

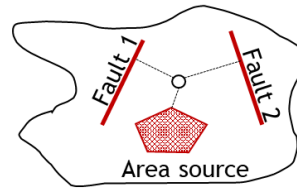
This chapter goes over a few details about the vulnerability analysis for earthquakes. Here we will be discussing the determination of the demand and the capacity of the structures and their use in analytical approach to obtain fragility curves.

8.5.1 Steps in Probabilistic Seismic Hazard Analysis (PSHA)

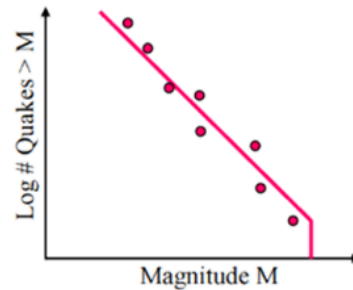
Probabilistic Seismic Hazard Analysis is in general made up of following steps:



1. We need to identify all sources capable of producing damaging ground motion. These could be modeled as both linear sources (faults) or area sources

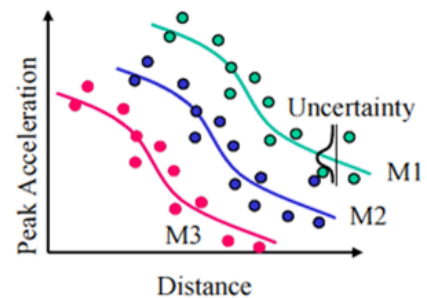


2. We need to characterize the earthquake occurrences and the distribution of earthquake magnitudes. Different magnitudes are associated with different rates of occurrence, usually quantified with occurrence curves. We will discuss these curves in more detail in the multi-hazard session.

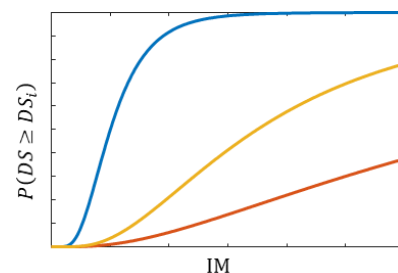


3. We need to characterize the distribution of the source-to-site distances associated with potential earthquakes.

4. We need to predict the resulting distribution of ground motion intensity as a function of earthquake characteristics. This is done with Ground Motion Prediction Equations (GMPEs) and will be discussed in more detail in the following section.

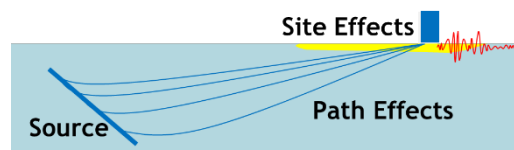


5. We need to combine the uncertainties in earthquake size, location and ground motion intensity to obtain the probability of the different damage states.



8.5.2 Ground Motion Prediction Equation (GMPE)

A GMPE is used to translate the earthquake characteristics into local intensity measures that describe the motion of the ground at the site of interest. They mathematically describe the rate of decay in ground motion with distance, accounting for the so-called path effects (due to the soil through which the waves propagate) and site effects (due to the soil at the site of interest).



Source: Tomorrow's Cities

Figure 85: Path and site effects on ground motion

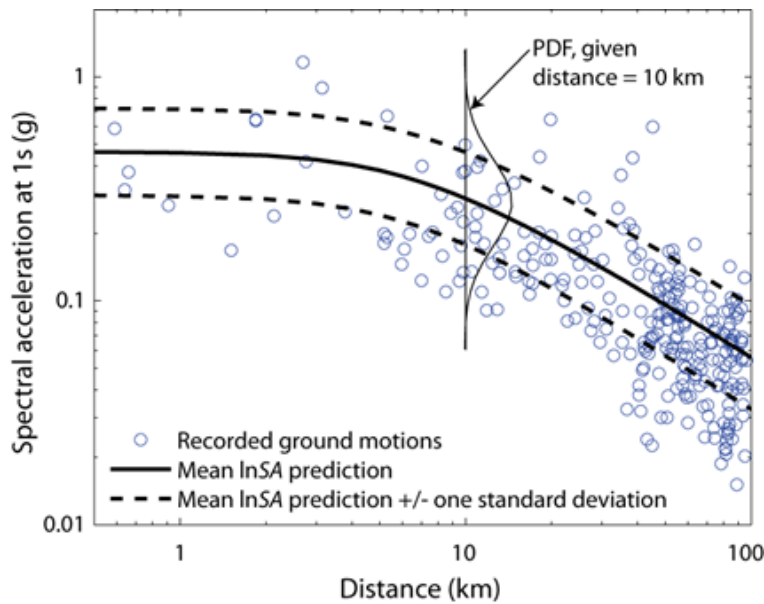


Below is an example of a GMPE commonly used in practice.

$$\log(Y) = c_1 + c_2 * M + c_3 * (M_{ref} - M)^2 + (c_4 + c_5 * M) * \log(R) + c_6 * R + \text{site effects} + \text{faulting mechanisms} + \text{basin effects} \dots + \text{error}$$

In the equation above, Y is the ground motion intensity measure (which could be peak ground acceleration, peak ground velocity, spectral acceleration...), M is the magnitude of the earthquake, R is the source-to-site distance, M_{ref} is a reference magnitude, and $c_1 - c_6$ are coefficients obtained empirically from the real or simulated ground motion data. The equation has additional terms to account for site effects, fault mechanisms and basing effects. Finally, the error term accounts for the aleatory uncertainty in the earthquake phenomenon (which we assume to not be able to reduce with additional modelling).

The GMPEs are developed by regression analysis of recorded strong motion databases and are typically updated as additional strong motion data become available. They are updated approximately every 5 years using statistical methods such as Bayesian updating. The GMPEs for parameters that decrease with increasing distance (PGA, PGV) are called **attenuation laws**. The figure below shows an example of predicted spectral acceleration as a function of the distance of the structure from the source.



Source: Tomorrow's Cities

Figure 86: Spectral acceleration of a structure as a function of the distance from the earthquake source

Note that, even if we fix the distance from the source, there is still some uncertainty associated with the resulting spectral acceleration S_a . From the data points in the figure, we can approximate the PDF of the S_a conditioned on the distance.

8.5.3 Exposure

We now need to estimate how our structures will respond to the ground motions that we have obtained from the previous step, and how vulnerable they are to the subsequent excitations. In other words, we need to find the capacity of and the demand on these structures. Typically, buildings are grouped according to their main structural characteristics, namely construction material, resisting mechanism, and height. Each of these categories affects both the capacity and the demand. In fact, the building characteristic not only affects the resistance of the structure (stronger material, better-designed resisting mechanism) but also how much of the



ground excitation is transformed into structure displacements and accelerations, i.e., its demand. Indeed, we will discuss how to predict and quantify this transformation later.

8.5.4 Building Damage Estimation

There are different ways of coming up with the fragility/vulnerability curves for the structures:

- Empirical: From post-earthquake surveys
- Judgement-based (heuristic): Based on expert opinion
- Analytical: From analyses of sets of building models under increasing ground motion severities
- Hybrid: A combination of sources
- The differences among these methods are mostly in terms of time and computational effort required, and accuracy of the assessment. Empirical methods take less effort but are less precise, while analytical methods take more effort but provide better estimates. Judgmental and hybrid functions fall in the middle.
- The following table summarize the advantages and disadvantages of each method in developing fragility functions:

Table 9: Characteristics of different methods on fragility functions development

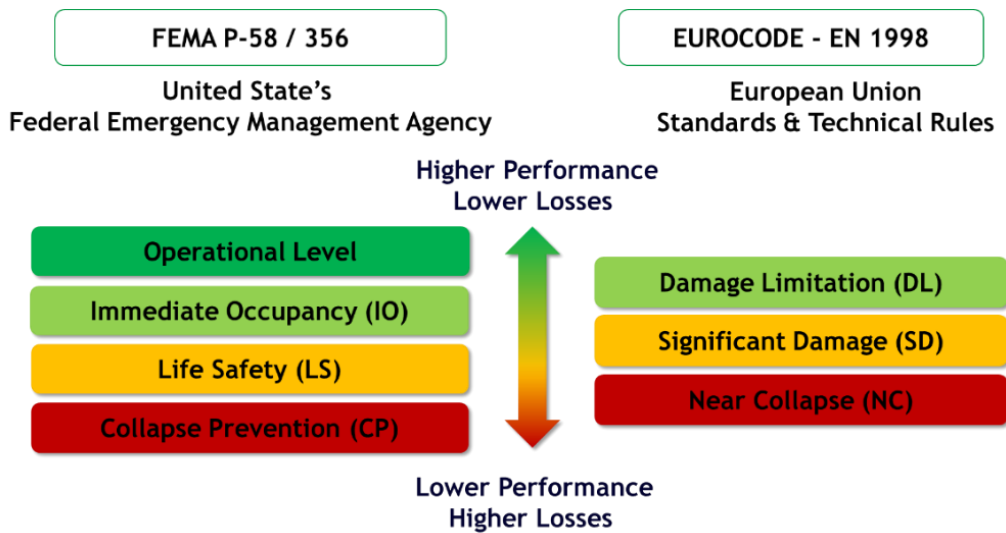
CATEGORY		CHARACTERISTICS
EMPIRICAL	Advantages	<ul style="list-style-type: none"> • Based on post-earthquake survey or on expert opinion • Most realistic
	Disadvantages	<ul style="list-style-type: none"> • Highly specific to a particular seismo-tectonic, geotechnical and built environment • The observational data used tend to be scarce and highly clustered in the low-damage, low-ground motion severity range • Include errors in building damage classification • Damage due to multiple earthquakes may be aggregated
CATEGORY		CHARACTERISTICS
JUDGEMENTAL	Advantages	<ul style="list-style-type: none"> • Based on expert opinion • The curves can be easily made to include all factors
	Disadvantages	<ul style="list-style-type: none"> • The reliability of the curves depends on the individual experience of the experts consulted • A consideration of local structural types, typical configurations, detailing and materials inherent in the expert vulnerability predictions
CATEGORY		CHARACTERISTICS
ANALYTICAL	Advantages	<ul style="list-style-type: none"> • Based on damage distributions simulated from the analyses • Reduced bias and increased reliability of the vulnerability estimate for different structures
	Disadvantages	<ul style="list-style-type: none"> • Substantial computational effort involved and limitations in modelling capabilities • The choices of the analytical method, idealization, seismic hazard, and damage models influence the derived curves and have been seen to cause significant discrepancies in seismic risk assessment



CATEGORY	CHARACTERISTICS	
HYBRID	Advantages	<ul style="list-style-type: none"> • Compensate for the scarcity of the observational data, subjectivity of judgemental data, and modelling deficiencies of analytical procedures • Modification of analytical or judgement-based relationships with observational data and experimental results
	Disadvantages	<ul style="list-style-type: none"> • The consideration of multiple data sources is necessary for the correct determination of vulnerability curve reliability

8.5.5 Damage State Definition

Damage state scales are used to classify the buildings based on the damage that they have experienced during the earthquake. These scales differ across countries and regulations. For example, the United States Federal Emergency Management Agency (FEMA), classifies buildings into four damage states: Operational Level, Immediate Occupancy (IO), Life Safety (LS), and Collapse Prevention (CP). The Eurocode from the European Union, instead, only considers three different damage states: Damage Limitation (DL), Significant Damage (SD), and Near Collapse (NC).



Source: Tomorrow's Cities

Figure 87: Damage scales across various standards

- The FEMA classification selects its four damage states based on usability and operability of the building. Here is a qualitative description of each of the damage states:
- **Operational level:** The building will stay functional and very minor repairs are required.
- **Immediate Occupancy (IO):** The building's spaces and systems are expected to be reasonably usable and operational.
- **Life Safety (LS):** There is an extremely low probability of threat to life safety, either from structural damage or the failure of non-structural components.
- **Collapse Prevention (CP):** The building is expected to not be stable under vertical loads and need major repairs.
- The qualitative descriptions are not enough for an inspector to classify the building to a specific damage state. Therefore, FEMA P-58 also provides detailed descriptions of the



damage to the building for each state. These descriptions are fundamental for the development of empirical fragility curves based on data collected during inspections. The following table provides such descriptions.

Table 10: Qualitative description of building-specific damage states (FEMA P-58)

Performance Level		Immediate Occupancy (IO)	Life Safety (LS)	Collapse Prevention (CP)
Concrete Frames	Primary	Minor hairline cracking; limited yielding possible at a few locations; no crushing (strains below 0.003).	Extensive damage to beams; spalling of cover and shear cracking (<1/8" width) for ductile columns; minor spalling in nonductile columns; joint cracks < 1/8" wide.	Extensive cracking and hinge formation in ductile elements; limited cracking and/or splice failure in some nonductile columns; severe damage in short columns.
	Secondary	Minor spalling in a few places in ductile columns and beams; flexural cracking in beams and columns; shear cracking in joints < 1/16" width.	Extensive cracking and hinge formation in ductile elements; limited cracking and/or splice failure in some nonductile columns; severe damage in short columns.	Extensive spalling in columns (limited shortening) and beams; severe joint damage; some reinforcing buckled.
Unreinforced Masonry Infill Walls	Primary	Minor (<1/8" width) cracking of masonry infills and veneers; minor spalling in veneers at a few corner openings.	Extensive cracking and some crushing but the walls remain in place, no falling units. Extensive crushing and spalling of veneers at corners of openings.	Extensive cracking and crushing; portions of face course shed.
	Secondary	Same as primary.	Same as primary.	Extensive crushing and shattering; some walls dislodge.

The table below provides a very qualitative classification by the Eurocode:

Table 11: Qualitative description of damage states (Eurocode)

Performance Level	Damage Limitation (DL)	Significant Damage (SD)	Near Collapse (NC)
Observed Damage	The building is considered as slightly damaged. Sustain minimal or no damage to their structural elements and only minor damage to their non-structural components.	Building is considered as significantly damaged. Extensive damage to structural and non-structural components.	Building is considered as heavily damaged. Experience a significant hazard to life safety resulting from failure of non-structural components.

The following is a classification proposed by Dolsek and Fajfar in 2008. It uses the same damage scale as the Eurocode, but it provides a more quantitative classification between the states.



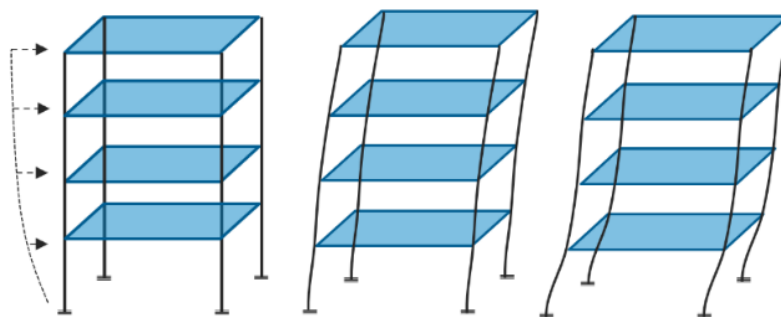
Table 12: Qualitative description of damage states (Dolsek and Fajfar, 2008 [14])

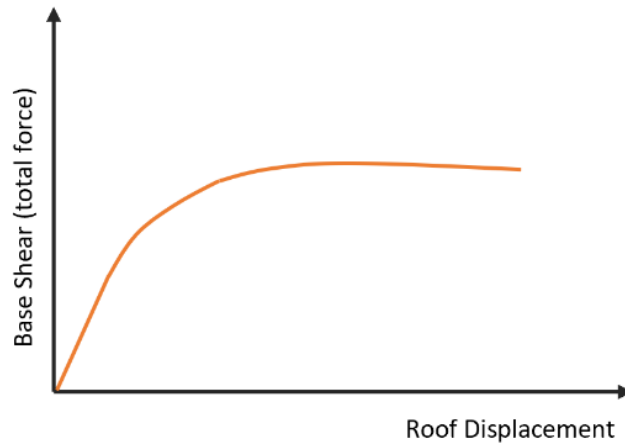
Performance Level	Damage Limitation (DL)	Significant Damage (SD)	Near Collapse (NC)
Observed Damage	For the case of infilled frames: limit state is attained at the deformation when the last infill in a storey starts to degrade. For the case of bare frames: this limit state is attained at the yield displacement of the idealized pushover curve.	The most critical column controls the state of the structure: the limit state is attained when the rotation at one hinge of any column exceeds 75% of the ultimate rotation.	The most critical column controls the state of the structure: the limit state is attained when the rotation at one hinge of any column exceeds 100% of the ultimate rotation.

8.5.6 Analytical Method of Development of Fragility Curves

A. Capacity

The classifications in the previous sections are particularly suitable for the development of empirical fragility curves. Let us now discuss briefly the procedure that is most commonly used to develop analytical fragility curves. To obtain analytical fragility curves, we need to quantify both the capacity of the system and its demand. A pushover analysis allows us to obtain a capacity curve which represents a building's stiffness, strength, and ductility. In a pushover analysis, a structure is pushed gradually under some lateral load (usually with a displacement-controlled procedure), and the amount of force and displacement is monitored at each step. The figure below shows the typical shape of a pushover curve. The base shear (which is numerically equal to the total force applied on the building) is plotted against the roof displacement. After an initial phase where the response of the system is elastic (linear part), the force stops increasing as the displacement increases. This is when parts of the building start to reach plasticity and the internal forces are redistributed. The curve is interrupted when the building collapses.

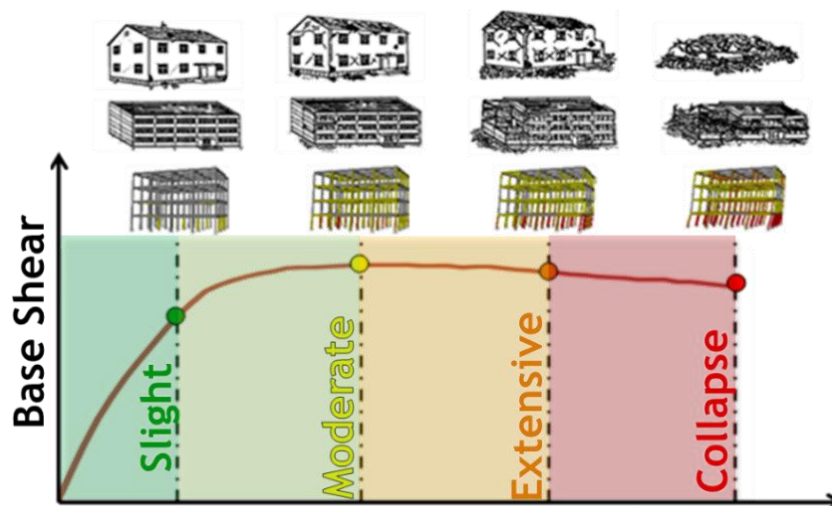




Source: Tomorrow's Cities

Figure 88: Typical pushover analysis

The capacity curve obtained with the pushover analysis can be used to define thresholds between the different damage states. For example, it could be assumed that the building switches from slight damage to moderate damage at the end of the elastic (linear) phase, while it could be assumed that the building switches from moderate to extensive damage when the peak of the capacity curve is reached. With this procedure, we can classify a building to a specific damage state based on the maximum displacement of the roof. We can then compare the actual displacement caused by the earthquake with these thresholds to estimate the damage caused by the earthquake.



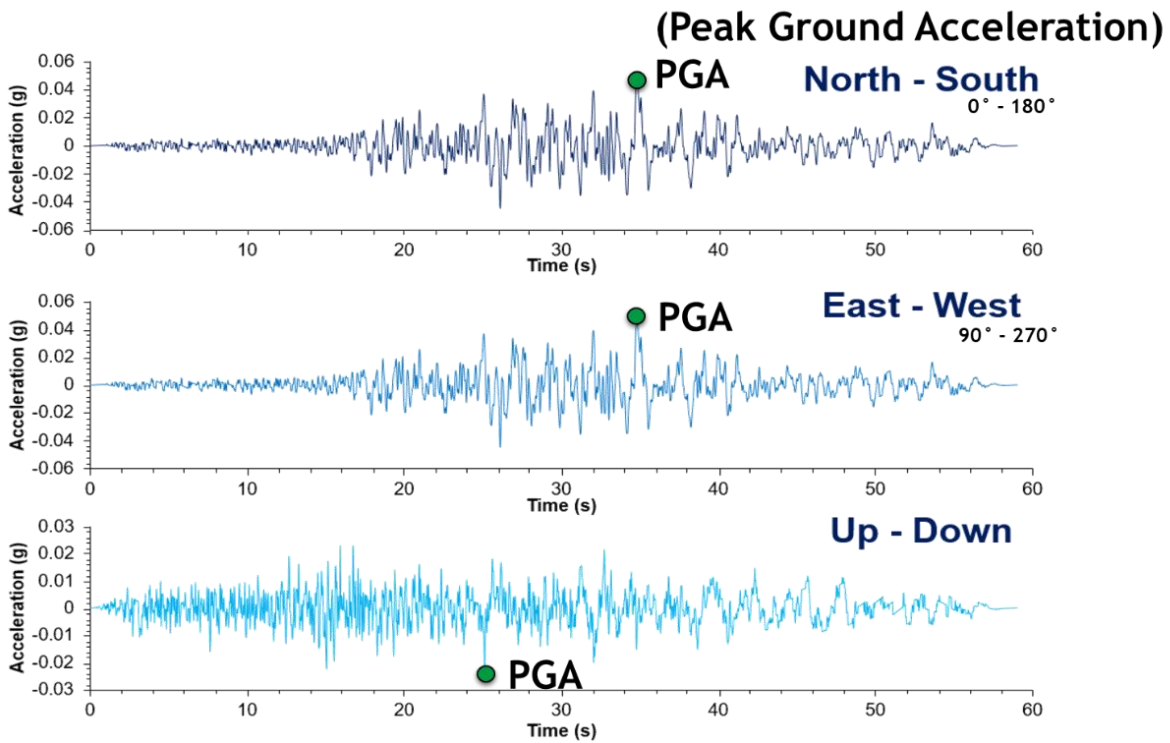
Source: Tomorrow's Cities

Figure 89: Thresholds between different damage states

B. Demand

We now need to find the maximum roof displacement caused by the occurrence of the earthquake. We start from the ground motion. We can either use the GMPEs, or we can look directly at the recorded ground motion. A common parameter to quantify the ground motion is Peak Ground Acceleration (PGA), which is just the maximum absolute value of the accelerogram.





Source: Tomorrow's Cities

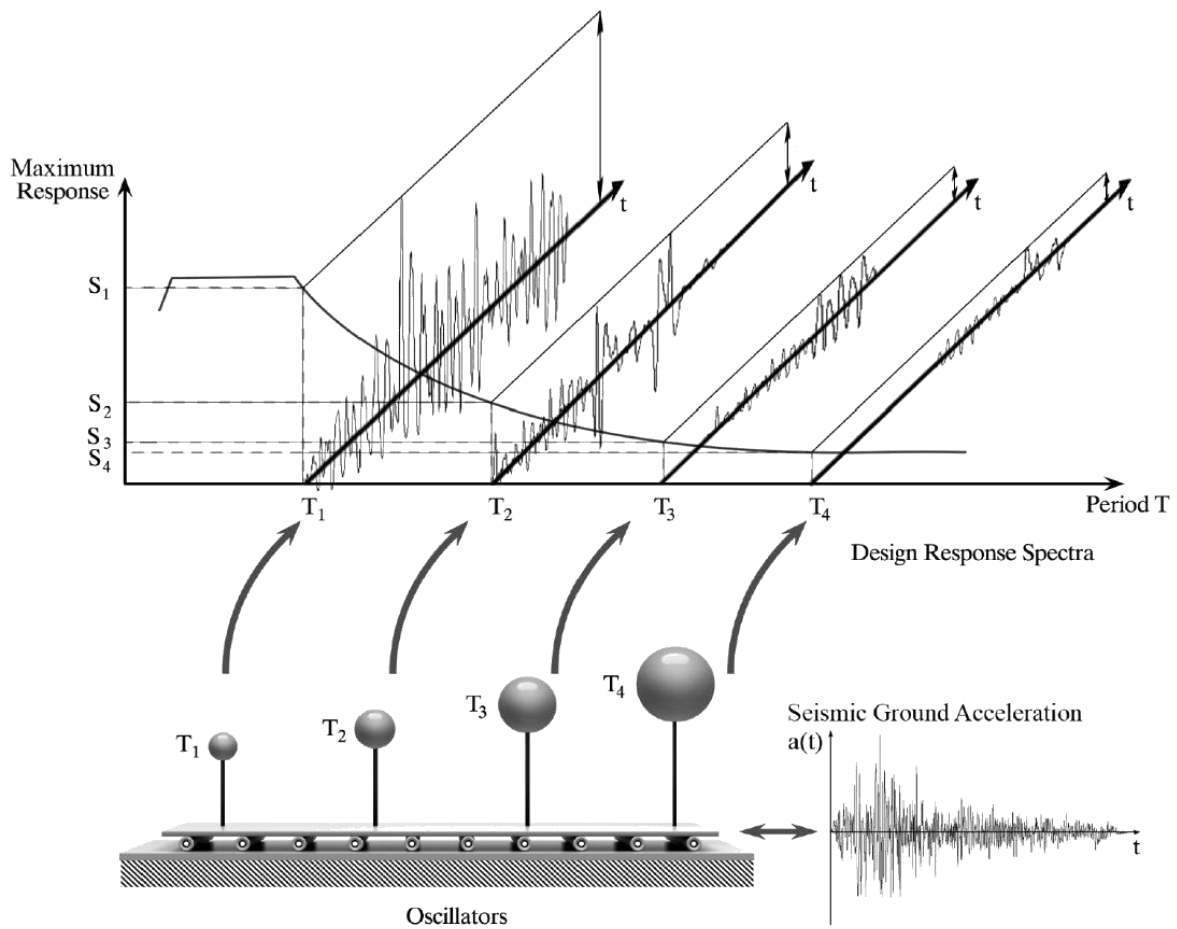
Figure 90: Recorded ground motion and Peak Ground Acceleration (PGA)

However, different structures subject to the same ground motion can react in drastically different ways. This depends on the natural period(s) of the structure. Complex structures have multiple natural periods, but structures with a single-degree-of-freedom (SDOF) only have one. These structures are typically simplified with a single mass at the top of a massless pole. In general, a lower natural period corresponds to a higher frequency of vibration.

By looking at the response of all possible SDOF structures subject to the same seismic excitation, we can obtain the so-called **response spectrum**. The response by several SDOF structures is recorded, the maximum acceleration of every time-history (i.e., **the spectral acceleration**) is then plotted against the natural period of each structure.

The following figure shows the procedure to obtain the response spectrum. The typical shape of the spectrum is also shown. Typically, there is a plateau for natural periods that are expected to “resonate” with the ground motion. Resonance describes the phenomenon of increased amplitude that occurs when the frequency of the seismic ground motion (or a Fourier component of it) is equal or close to the natural frequency (or one of the natural frequencies) of the system on which it acts.



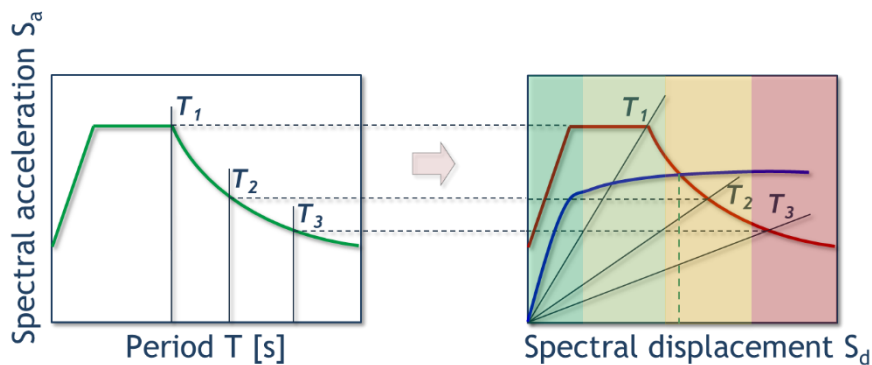


Source: Tomorrow's Cities

Figure 91: Procedure to obtain the response spectrum

We can now convert the response spectrum from acceleration to displacement measures, using the following relationship:

$$S_a = \omega^2 \cdot S_d = \left(\frac{2 \cdot \pi}{T}\right)^2 \cdot S_d$$



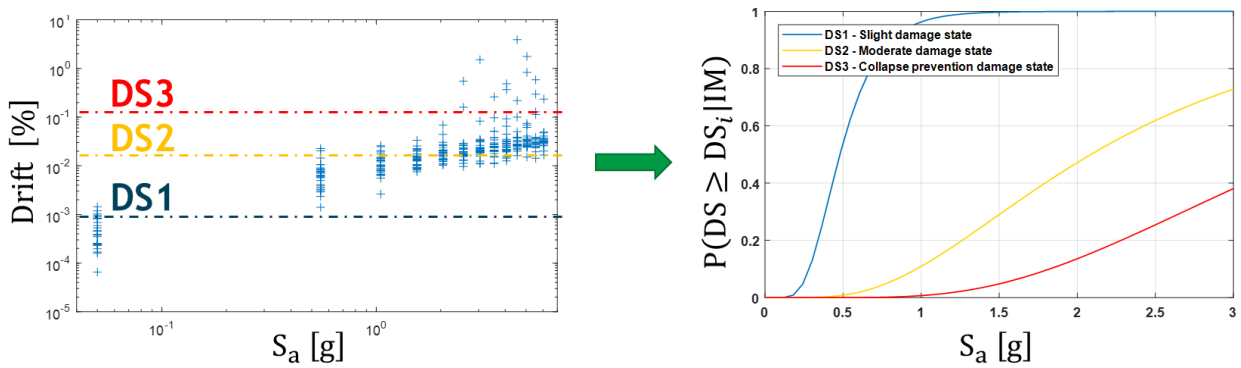
Source: Tomorrow's Cities

Figure 92: Determination of maximum displacement



The actual displacement of the structure is then obtained as the intersection between the pushover curve obtained and the response spectrum in terms of displacement. *(This is a simplification of the actual procedure. In reality, both the pushover curve and the spectral displacement curve need to be appropriately modified before we can take their intersection. For details about how to translate the pushover curve into the capacity curve and the spectral displacement curve into the demand curve - accounting for plasticities of the system - see the Eurocode EN-1998.)* Once we have the maximum displacement of the structure, we can compare it with the thresholds defined from the pushover curve to assign the structure to a damage state.

We now need to repeat our analysis for different values of intensity measures to obtain the fragility curves. One way of doing this is with incremental analysis. In incremental analysis, we consider several ground motions, and we progressively scale them to match defined intensity measures (e.g. $S_a = 0.05g, 0.1g, \dots, 3g$). For each ground motion and for each intensity, we estimate the damage state of the structure. From the simulations we can obtain the probability of falling into each of the damage states, and subsequently draw fragility curves.



Source: Tomorrow's Cities

Figure 93: Generation of fragility curves

8.6 Fragility/ Vulnerability Curves for Floods

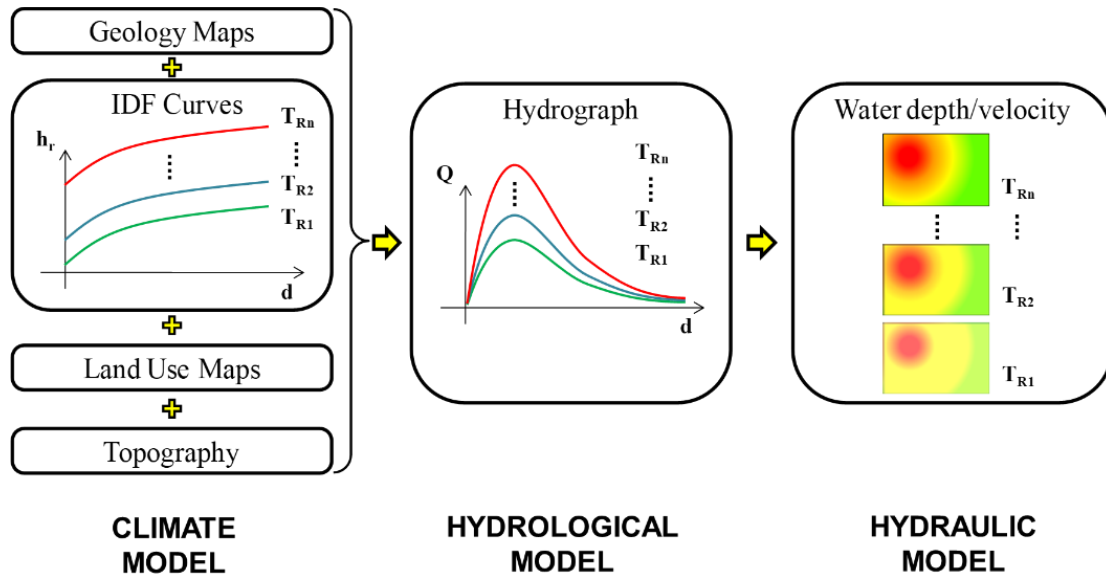
A flood is a condition of high water in which water has spilt over its natural or artificial banks onto normally dry land, such as a river inundating the land around it (its floodplain). One third of economic losses due to natural disasters in the European Union are due to floods (over 50 billion in 1998-2009). Floods are the most frequent and costly natural hazards along with windstorms, and accurately estimating the losses due to floods can help prevent such disastrous consequences.

8.6.1 Analytical Method of Development of Fragility Curves

A. Demand

Computing the demand of a flood requires several steps. First, we need a **climate model** to estimate how much rain is going to fall in the different locations that we are interested in. The most important tools in climate models are the intensity-duration frequency curves, which associate different event characteristics to certain return periods (we will talk more in detail about this type of curves in the multi-hazard session). Climate models also incorporate additional information coming from geology maps, land use maps and topographical maps. We then need to translate the rain into flow discharge (which is how much water flows at a specific river section at a given time instant). This is done with a **hydrological model**. Finally, we can use a **hydraulic model** to obtain the distribution of local intensity measures associated with different return periods (e.g., water height at a certain location as well as its duration).

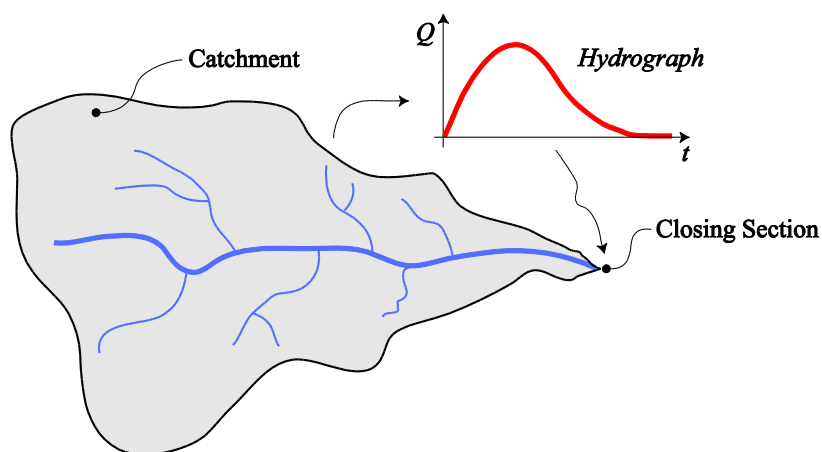




Source: Tomorrow's Cities

Figure 94: Determination of demand due to flooding hazard

To compute the discharge along the river over time following rainfall, we need to consider the entire catchment area (or drainage basin) of the river. This term refers to the topographical area from which a watercourse, or a water course section, receives surface water from rainfall (and/or melting snow or ice) - i.e., the land area that contributes water to given cross-section along a river network. The rain that falls at any point of the catchment area will follow a certain path to reach the water course, and will take a certain amount of time to reach the section of the river that we are interested in. The computation of hydrograms takes these paths (and the time required to follow them) into account (with a rainfall-runoff method) to plot the total flow discharge as a function of time. The area under the hydrograph is equal to the total discharge volume for the basin under study.



Source: Tomorrow's Cities

Figure 95: Hydrograph calculation

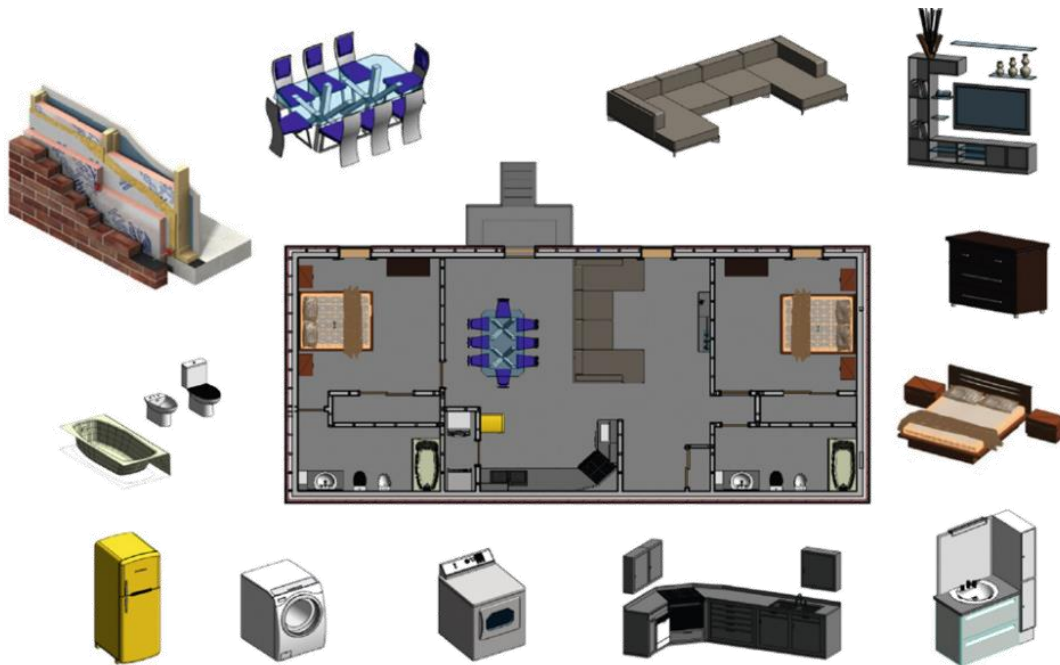
From hydrographs, we can obtain the amount of water that is expected to reach a certain river section at any time. By repeating the analysis for different rainfalls, we can obtain peak discharge and total water volume for different return periods. Finally, by accounting for other factors such as the topography in proximity of the water sections, we can obtain the local



intensity measures - demand - that we need to perform reliability analysis. These quantities could be the height of the water at different locations, the duration of the flood, and the velocity of the water flow.

B. Capacity

To estimate the probability of the different damage states of our system, we also need capacity values. We are going to focus on the method developed by Nofal et al. in 2020. This method focuses on the non-structural damage and looks at the damage of the components within the household. As, a content inventory for each household is required to run these analyses. These inventories include furniture and appliances that are expected to be damaged by the occurrence of a flood.



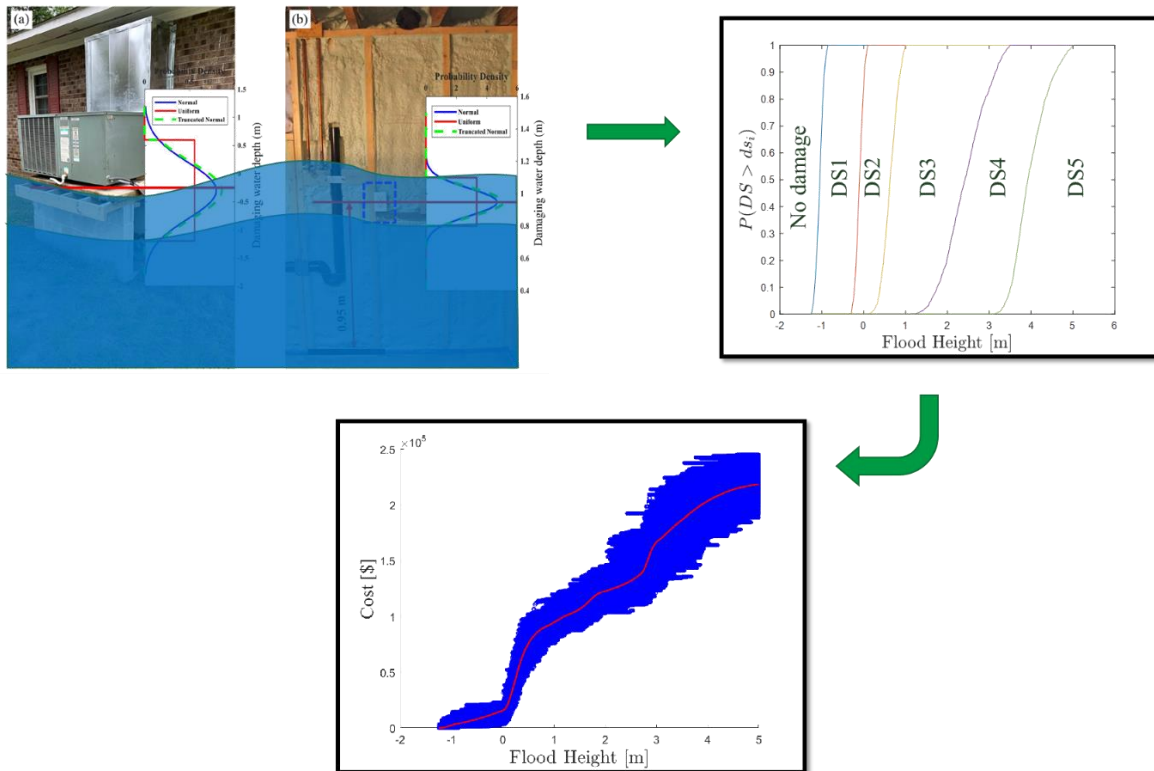
No.	Code	Foundation
1	S24	Crawlspace Base Insulation
2	S25	Flooring Insulation
3	S26	Entrance Stair
4	S16	Decking (Floor Beams/Joists +Plywood Subflooring)
5	S17	Wood Flooring/Tile flooring
6	S21	HVAC Pipes/Ducts
7	S22	AC Unit
8	S23	Heating Unit
9	S435	Baseboard
10	S437	Carpet
11	S41	Refrigerator
12	S42	Stove
13	S44	Washer
14	S45	Dryer
15	S46	Water Heater
16	S47	TV

Source: Nofal, O. M., van de Lindt, J. W., & Do, T. Q. (2020). Multi-variate and single-variable flood fragility and loss approaches for buildings. *Reliability Engineering & System Safety*, 202, 106971. [15]

Figure 96: Content inventory for a household



The capacity of each component is then assumed to simply be equal to their height (how high above the floor they are expected to be placed). In our incremental analysis and/or Monte Carlo simulation, we simulate different water heights, and we count how many times the components fall below or above the water level. In the simplified analysis that only considers the water height (Nofal et al. also have done a multidimensional analysis that also considers flood duration), a component is expected to fail as soon as the water reaches its height. By assigning different components to different damage states, we are then able to compute the fragility functions for each of these damage states. Nofal et al. also have assigned a certain replacement cost to each component, that is then used to obtain the expected cost due to a given flood height.



Source: Nofal, O. M., van de Lindt, J. W., & Do, T. Q. (2020). Multi-variate and single-variable flood fragility and loss approaches for buildings. *Reliability Engineering & System Safety*, 202, 106971. [15]

Figure 97: Component based flood damage estimation

The described procedure can be used to obtain fragility and loss curves for a single building. The analysis at the household level can be extended to entire communities by performing a portfolio analysis. In these portfolio analyses, buildings are assigned to given archetype based on their typology and content. A content inventory is provided for each archetype, and the analyses are repeated for each household in the community. Because portfolios of buildings and content inventories are currently only available for developed countries, within tomorrow's cities we are trying to develop them for developing countries.



SESSION 9: VULNERABILITY MODELLING – MULTI HAZARD

9.1 Objectives

By the end of the session, the participants will be able to:

- Assess the importance of multi-hazard analysis as more than just the sum of single hazard analyses.
- Differentiate between Level I and Level II interactions among hazards.
- Recognize the input required for a proper multi-hazard analysis.
- Use the knowledge gained in the session on single hazard vulnerability within the multi-hazard context.
- Evaluate the impact of different hazard scenarios (i.e., a sequence of hazardous events during the life cycle of the system).

9.2 Structure of Session 9

Structure
1. Introduction
2. Hazard Interactions: Level I Interactions
3. Hazard Interactions: Level II Interactions

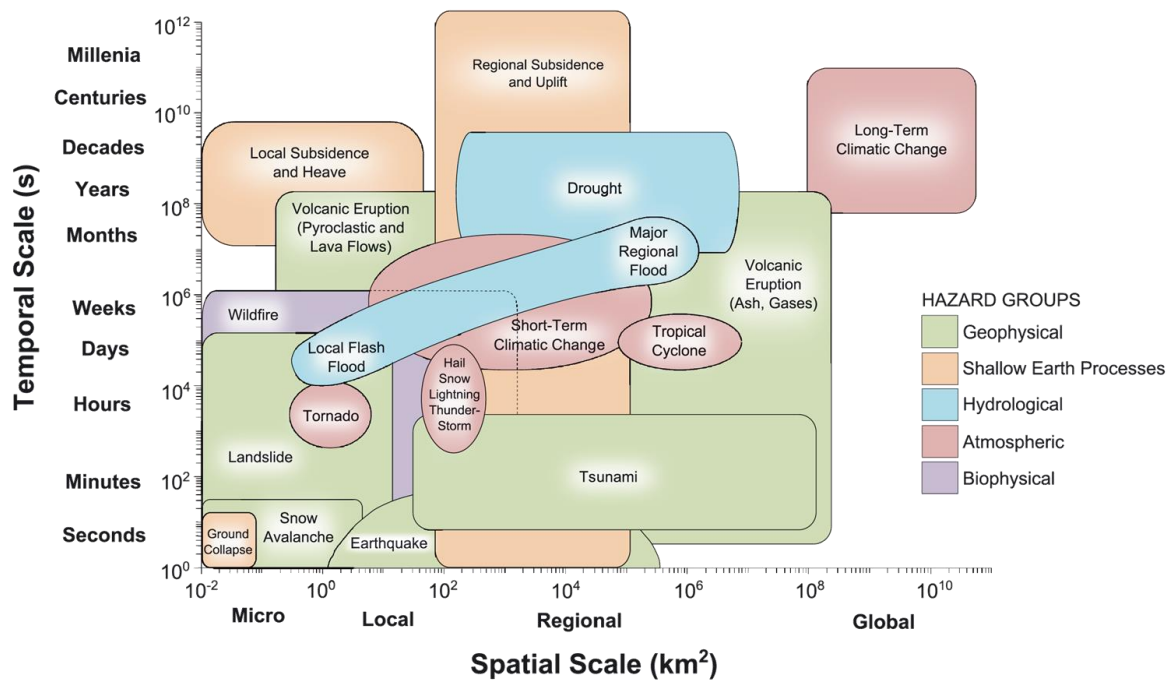
9.3 Introduction

There is growing concern about the vulnerability of infrastructure due to the occurrence of multiple hazards. The losses caused by cascading hazards might be significantly higher than the losses caused by individual hazards. In fact, the second hazard acts on a system that has already been damaged by the first, and the community served by the infrastructure is unprepared to face the consequences of a second hazard while still dealing with the effects of the first. For example, in the case of earthquakes, between 25% and 40% of losses and deaths have been reported to result as a consequence of a secondary effect, e.g., tsunami, liquefaction, fire and others [16] A famous, recent example of the disastrous consequences that could be caused by cascading hazards is the Tohoku earthquake which occurred in Japan in 2011. The earthquake caused a violent tsunami, which in turn damaged the Fukushima power plant. The effects were enormous and are still felt to this day.

9.3.1 Hazard Interactions

Whether hazards interact with each other depends on how close (both in time and space) they occur. The figure below [17] depicts the spatial and temporal scale of several hazards. Both scales span several orders of magnitudes. For example, ground collapse or a snow avalanche act at a micro-scale (very localized) and within the span of seconds, while a volcanic eruption acts at a regional scale, and its duration could be from a few minutes to months and even years. Long-term climate change can have effects on a global scale, and act over the course of decades and even centuries. Hazards do not interact if they occur in different locations, or extremely far away in time.

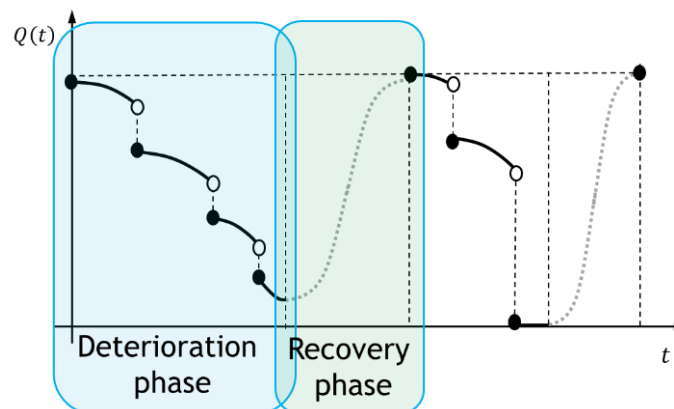




Source: Gill, J. C., & Malamud, B. D. (2014). Reviewing and visualizing the interactions of natural hazards. *Reviews of Geophysics*, 52(4), 680-722. [17]

Figure 98: Spatial and temporal scale of several hazards

We can visualize the effects of hazards when we plot a performance measure of the system over time. In general, we can separate it into two phases. In the deterioration phase, the performance of the system decreases over time (due for example to gradual deterioration processes such as corrosion). In the recovery phase (which is typically initiated whenever the performance falls below a certain threshold) the performance of the system decreases over time. The occurrence of hazards can cause a sharp decrease in the performance of the system, regardless of whether they happen in the deterioration or the recovery phase. In the literature, some works look at hazard occurrences as additional deterioration processes, called shock occurrences because they act instantaneously.



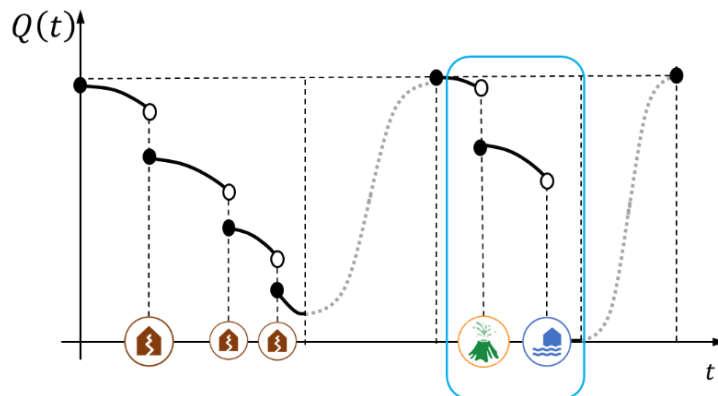
Source: Tomorrow's Cities

Figure 99: Performance measure of the system over time

If we look at the decrease in the performance of the system, we can tell that dependent hazards can have severe consequences. For example, the occurrence of multiple seismic shocks in a mainshock-aftershock sequence causes several jumps in the performance of the system. These



jumps are very close in time due to the interactions between the hazard occurrences. However, even hazards that occur independently could cause unintended interaction in terms of consequences if they happen close to each other (in time and space).



Source: Tomorrow's Cities

Figure 100: Performance measure of the system over time for independent hazard

A. Four Examples

The following examples show a few scenarios where the occurrence of multiple hazards caused severe consequences (*these examples are available in Gill and Malamud 2014 [17]*):

- **Mount Unzen and Mount Mayuyama, Japan, 1972:** The Japanese volcano Mount Unzen erupted in 1792, triggering the collapse of the adjacent volcano, Mount Mayuyama. This collapse, in the form of a large landslide, resulted in large volumes of material being deposited in a nearby ocean, which in turn triggered a tsunami. The tsunami crossed the ocean and devastated communities on the opposite Japanese shoreline, killing more than 15,000 people.
- **Alaska, USA, 1792:** An earthquake with a moment magnitude 9.2 occurred in the Prince William Sound region of Alaska in 1964. This earthquake triggered both submarine and subaerial landslides and a tsunami, and both regional uplift (or ground heave) and regional subsidence. These secondary hazards also triggered or increased the probability of further tertiary hazards, such that the submarine landslides (secondary) triggered further tsunami waves (tertiary), and regional subsidence (secondary) resulted in (and continues to result in) an increased probability of flooding (tertiary). Finally, the subsidence, together with the various stages of tsunami waves, caused serious flooding, leading to the loss of many lives.
- **Mount Pinatubo, Philippines, 1991:** Mount Pinatubo in the Philippines, an active stratovolcano, erupted in June 1991. Volcanic activity gradually increased at the volcano, with the eruption reaching its climax between 15 and 16 June 1991. This explosive eruption triggered many small earthquakes, both before and during the eruption. These earthquakes were likely triggered by subterranean magma propagation. The volcanic eruption also triggered pyroclastic density currents and ejected significant quantities of ash, debris, gases, and aerosols into the atmosphere and surrounding environment. The volcanic eruption resulted in the ejection of 17 megatons of sulfur dioxide and ash into the stratosphere. The eruption of Mount Pinatubo in 1991 coincided with Typhoon Yunya, which brought about intense rainfall. The combination of this rainfall and thick ash deposits triggered lahars and structural failures due to the additional mass exerted by the wet ash. Lahars blocked the Mapanuepe River, causing flooding of the Mapanuepe Valley. The volcanic blast also created a caldera at the summit of Mount Pinatubo, which filled with water during the seasonal rains. This water



and the deposited pyroclastic material continued to pose a threat to local communities after the eruption had finished, due to the potential for flooding, lahars, and landslide events.

- **Guatemala, 2010:** Tropical Storm Agatha hit the Pacific coastline of Guatemala on 29 May 2010. The storm brought strong winds and torrential rains. This heavy rain triggered mass movements, flooding across Guatemala City and contributed to a ground collapse event. This collapse occurred due to a pseudo-piping phenomenon in the Quaternary volcanic ash and pyroclastic density current deposits underlying Guatemala City. In this pseudo-piping process, subterranean water washes out the finer material within the pyroclastic deposits, followed by the coarser material eventually being eroded out and the formation of underground voids. The roofs of these subterranean voids can then collapse, resulting in ground surface deformation. The effects of Tropical Storm Agatha were exacerbated by the near-simultaneous eruption of Pacaya, a complex volcano located 30 km southwest of Guatemala City. Pacaya erupted 2 days prior to the onset of Tropical Storm Agatha on 27 May 2010. Ash and debris, ejected from Pacaya, covered much of Guatemala City. Reports suggested that the ash blocked parts of the drainage system, increasing the intensity of flooding during Tropical Storm Agatha. Furthermore, the combination of fresh ash, volcanic debris, and heavy rain, generated lahars and structural collapse.

B. Nomenclature

Before we proceed with the discussion of the mathematical framework to model interactions, we need to specify some important nomenclature to avoid confusion:

- By **event**, we mean the occurrence of a certain hazard belonging to any of the types being considered. I.e., the occurrence of an earthquake, the occurrence of a flood...
- By **event characteristics**, we mean the characteristics associated with the event that do not depend on the local effects and/or the physical impacts at the infrastructure level. For example, the magnitude and the rupture characteristics associated with an earthquake.
- We can then translate the event characteristics into **intensity measures** at the asset level (we will see how). The intensity measures account for the local effects and (sometimes) even for the physical assets that are present at the location of interest. For example, Peak Ground Acceleration and Spectral Acceleration in the case of earthquakes.

The occurrence of a hazard causes different impacts at different scales. We can separate site effects, physical impacts, network/systems disruptions, and social/economic consequences. The following classification is taken from Zaghi et al. (2016) [18]:

- **Site effects** essentially define the hazard and represent the actions produced by the hazard at a given location. They are to be understood in the context of causality of the physical impact. The existence of these effects does not depend on the presence of a physical component or a system of physical components. For example, the site effects of an earthquake include ground vibrations and liquefaction/ground settlement, which are independent of the existence of the physical component. Similarly, site effects of a tornado are excessive loads, uplift loads, and flying debris. Hazards that are caused or triggered by another hazard are not listed as site effects. For instance, a tsunami resulting from an earthquake is not considered as a site effect of the earthquake hazard; instead, it is regarded as an additional hazard.
- **Physical impacts** are modifications of the behavior and/or function of a physical component and are assumed to be directly caused by one or multiple site effects associated with hazards. They are not necessarily independent or mutually exclusive.

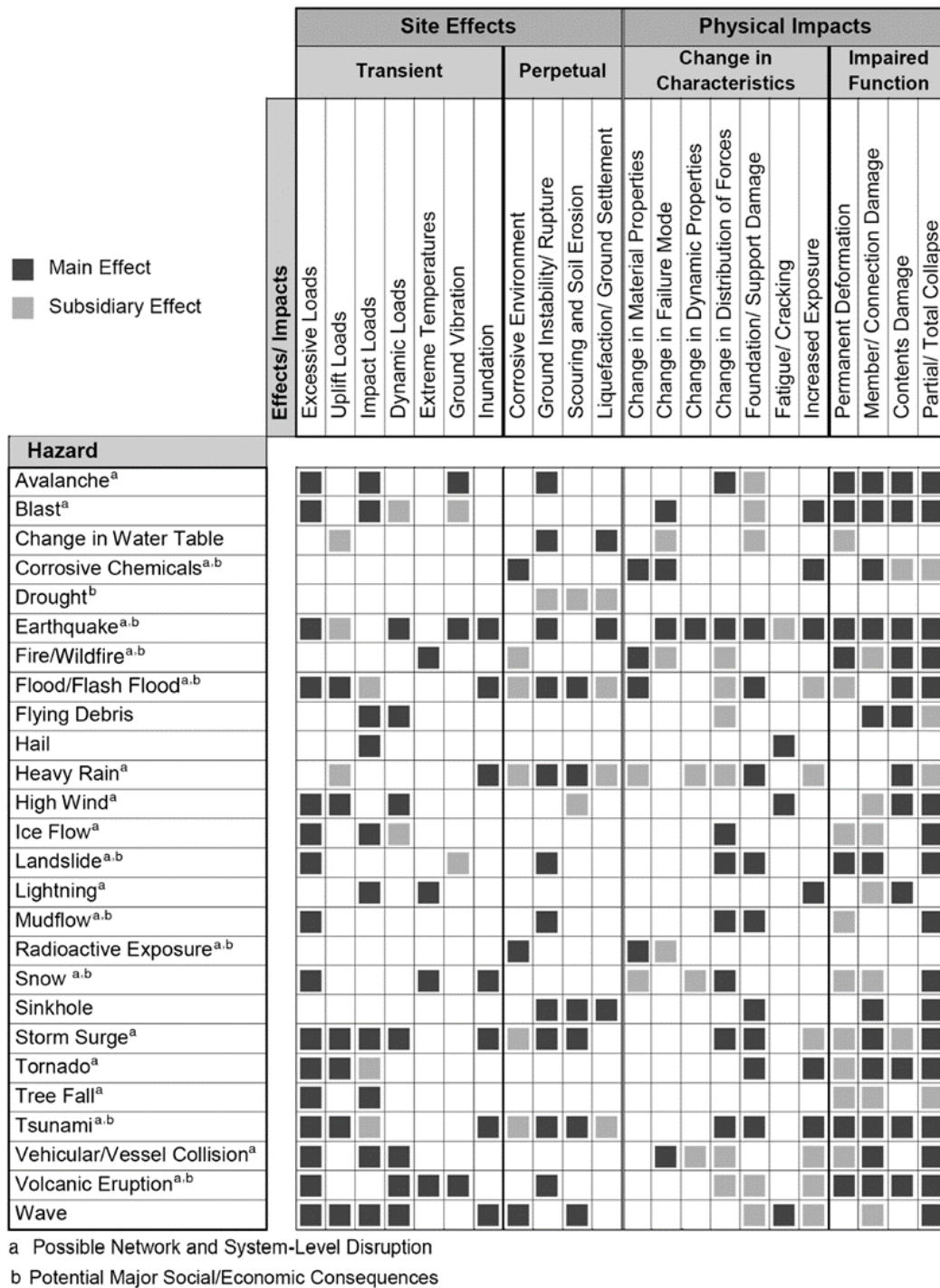


For example, the physical impacts of a flood hazard include foundation/support damage and change in material properties of a structure's elements (physical components) because of the hazard's site effects - that is, water overflow/accumulation and corrosive chemicals such as saltwater.

- **Network and system disruptions** are defined as interrupting or impairing effects on the function of a system or network at large scales. In the case of a significant storm surge, inundation of subway tunnels may cause a significant interruption of the public transportation system.
- **Social and economic consequences** recognize the role that affected structures and infrastructure systems play in societal functioning and human behavior. In the case of a tsunami, extensive damage to infrastructure may cause a mass migration of a local population.

The following figure, taken from Zaghi et al. (2016) [18] shows different hazards in a way that aids visualization of their effects and promotes understanding of their possible interactions through site effects and physical impacts. It presents possible main and subsidiary site effects and physical impacts of hazards (dark and light gray, respectively). The main effects/impacts are defined as those that are more probable and more damaging, whereas the subsidiary effects/impacts are those that are less probable or less severe.





Source: Zaghi et al. 2016 [18]

Figure 101: Site effects and physical impact of hazards

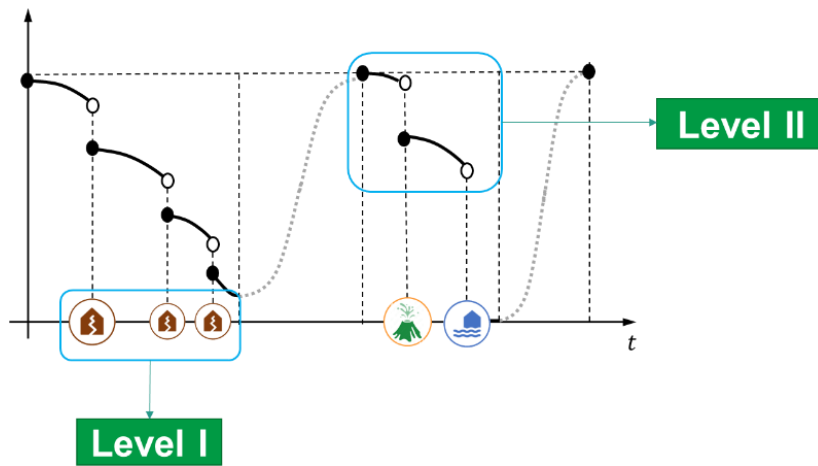
C. Types of Interactions

Finally, we classify interaction based on the distinction that was discussed above. Namely:

- Level I interactions are the natural interactions of the hazards that are independent of the physical components.
- Level II interactions are interactions that happen through the impact of the hazards on the physical components by:



- Changing the characteristics of the physical components.
- Impairing the functionality of the physical components.



Source: Tomorrow's Cities

Figure 102: Types of interaction

9.4 Hazard Interactions: Level I Interactions

9.4.1 Mathematical Modelling

A. Interaction Matrix

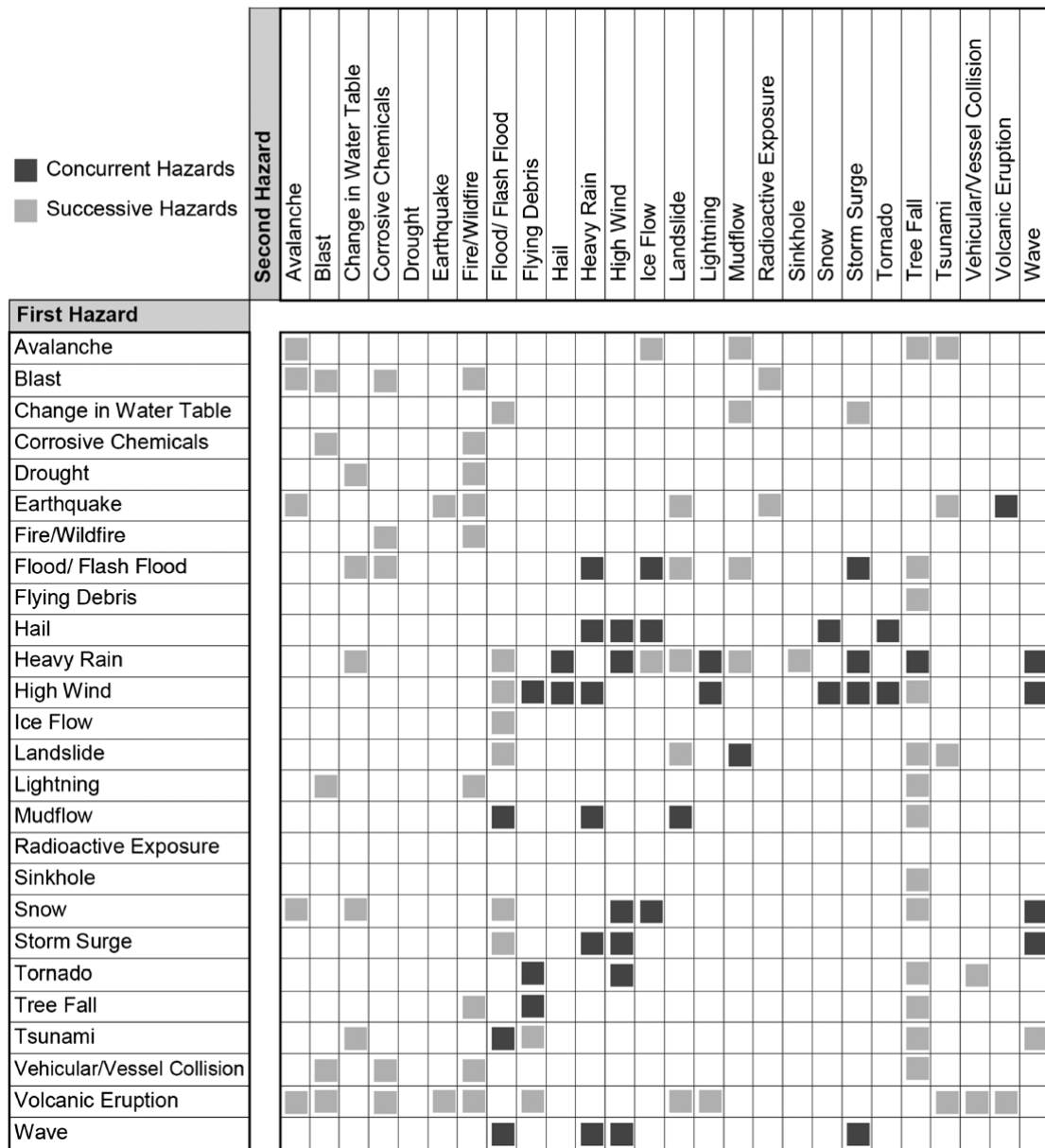
Hazards can be classified according to their level I interaction into two broad categories (Zaghi et al. 2016):

- **Concurrent hazards:** These hazards tend to occur at the same time and/or to overlap for a period of time. For example, storm surges, waves, and high winds co-occur during a hurricane.
- **Successive hazards:** Multiple hazards where one triggers, intensifies or broadens the region of the impact of another. Examples of successive hazards include earthquakes and tsunamis, earthquakes and avalanches, and heavy rainfall and landslides. Interactions between successive hazards can be furtherly decomposed as follows (Gill and Malamud 2014):
 - **Interactions where a hazard is triggered - Type A:** When a natural hazard triggers one or more secondary hazards almost immediately (for example, an earthquake immediately causes liquefaction).
 - **Interaction where the probability of a hazard is increased - Type B:** When a natural hazard alters the outlook of another, for a certain period of time (for example, the occurrence of a mainshock alters the underlying conditions that might cause the occurrence of aftershocks over time).

These distinctions are required in the mathematical models, as we will be discussing later.

The following figure is the interaction matrix available in Zaghi et al. (2016) [18]. The term first hazard denotes a hazard that occurs independently; the term secondary hazard denotes a hazard that may be concurrent with or successive to the primary hazard. In the figure, light and dark gray identify concurrent and successive hazards, respectively. Zaghi et al. did not further separate successive hazards into Type A and Type B because they were not concerned with the mathematical modelling of such interactions.





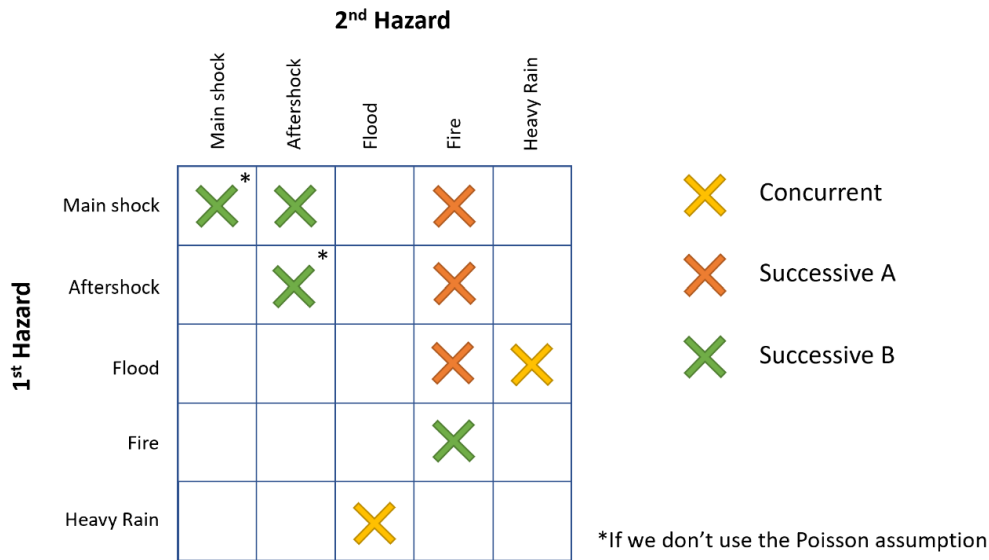
Source: Zaghi et al. 2016 [18]

Figure 103: Interactions through the nature of the hazard (level I interactions)

Shown below is a simplified version of the table in Zaghi et al. where we can observe the interactions specified in it. Floods and heavy rain might be happening at the same time due to the occurrence of another, major hazard (for example a hurricane). Hence, we classify them as **concurrent**. Fire might immediately follow other hazards such as seismic shocks and floods, due to exposed wires and other related consequences. As such, the interactions main shock/fire, aftershock/fire and flood/fire were classified as **successive Type A**. Mainshocks alter the underlying conditions around the fault and cause aftershocks to become more likely. As such, the interaction mainshock/aftershock is classified as **successive Type B**. The altered conditions of the fault also affect the occurrence of subsequent main shocks, which means that also the interaction main shock/main shock can be classified as **successive Type B**. This type of interaction is very often disregarded in the literature, and main shocks are usually assumed to occur independently from one another. The same applies to interactions between aftershocks (also classified as **successive Type B**); theoretically, the occurrence of every shock alters the



conditions of the fault and the probability of a subsequent shock. However, in practice, the occurrence of aftershocks is typically modelled accounting for the effects of the main shock only. Finally, because the occurrence of a fire might reduce the area that is susceptible to a subsequent fire, the interaction fire/fire is also classified as **successive Type B**.



Source: Tomorrow's Cities

Figure 104: Simplified interaction matrix

B. Occurrence rates

We now discuss a few mathematical quantities that are required to model the occurrence of the hazards in the formulation that we propose.

- A **rate** λ defines how many times we expect an event to occur (on average) in a certain unit of time. Its units are the inverse of time (e.g., months⁻¹ or years⁻¹). For example, a rate of $\lambda = 2 \text{ months}^{-1}$ means that we expect on average 2 event per month.
- The **return period** T defines how long we should wait (on average) between two successive events. Its units are time (e.g., months or years). For example, a return period of $T = 2 \text{ months}$ means that events happen on average 2 months apart. Rate and return period are directly correlated. In fact, the return period is the inverse of the rate (and vice versa).

$$T = \frac{1}{\lambda}$$

- The average number of events N in a certain reference time T_{ref} can be obtained by multiplying the rate for the reference time, i.e.,

$$N = \lambda T_{ref}$$

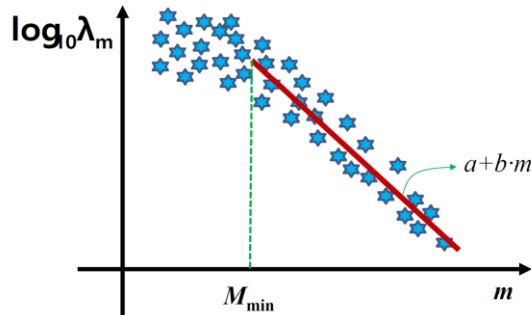
Rarer event characteristics (e.g., higher magnitudes) are typically associated with lower rates and higher return periods.

The figure below is a graph of the Gutenberg-Richter law, which relates the magnitude M of an earthquake and the logarithm of rate of earthquakes of at least that magnitude. The mathematical expression relating the two quantities is:

$$\log_{10} \lambda(M) = 10^{a-bM}$$



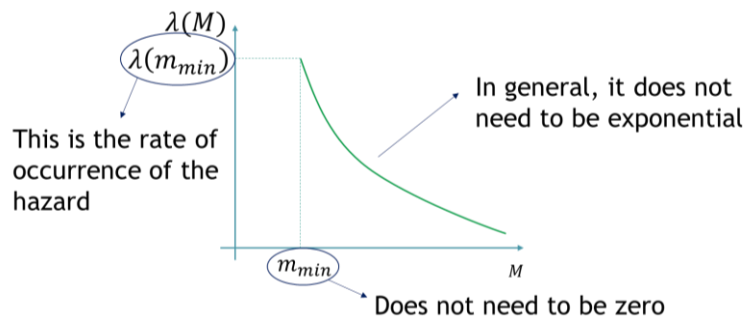
where the coefficients a and b depend on the region of interest. Values for these coefficients have been obtained with statistical analyses for different places around the world.



Source: Tomorrow's Cities

Figure 105: Gutenberg-Richter law

If we translate the curve in the natural scale, we obtain a curve that is exponentially decaying. Similar curves can be obtained for other events (not just earthquakes) for different event characteristics (not just magnitude). We refer to these curves as **occurrence curves**.



Source: Tomorrow's Cities

Figure 106: An occurrence curve

Note that the starting point of the x-axis does not need to be zero. It is instead the minimum magnitude m_{min} that is expected to have a recognizable effect on the system (for example, we are not interested in earthquakes that will never cause any damage). The rate associated to such magnitude, $\lambda(m_{min})$, is the rate of occurrence of the hazard. In other words, if the rate associated with earthquakes of magnitude 4 is λ_{min} , and 4 is the minimum magnitude that can cause damage on our system, then we can say that the rate of occurrence of earthquakes is 4.

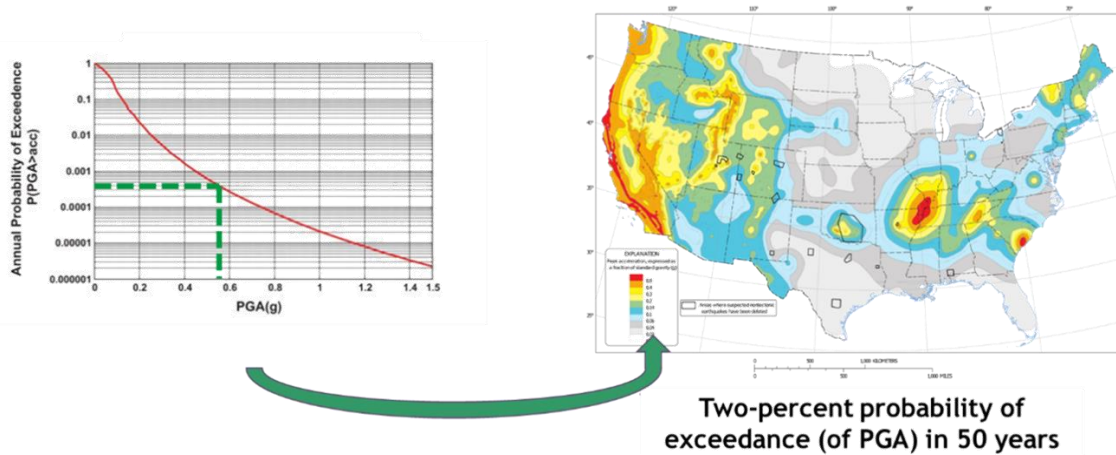
C. From Event Characteristics to Intensity Measures

Occurrence curves relate the event characteristics to their rate of occurrence. However, we have seen that sometimes we might need the local effect of hazards associated with certain event characteristics. In other words, we need to translate the event characteristics into intensity measures at the local scale. This is done typically using intensity predictions models that have been developed in the literature for several hazards. For example, we have seen in the session dedicated to vulnerability analysis for single hazards, that Ground Motion Prediction Equations (GMPEs) can translate magnitude and hypocentral distances into Peak Ground Velocity and Peak Ground Acceleration (site effects that do not involve the physical component) or Spectral acceleration (a quantity that accounts for the structure subject to the seismic excitation).



D. Occurrence Rates for Intensity Measures

Once we have transformed the event characteristics into intensity measures, we can obtain **hazard curves**. Hazard curves are very similar to occurrence curves, but they have intensity measures on the x-axis rather than event characteristics. From hazard curves we can obtain the intensity measure associated with given return periods for different locations and produce the hazard maps that can be found in several code regulations around the world. In general, sometimes we might need to generate the event characteristics, and sometimes we might need to generate the intensity measures. For example, the occurrence of an aftershock is influenced by the event characteristics of the main shock, but the occurrence of a landslide following an earthquake is affected by the intensity measure of the shock along the affected slope.

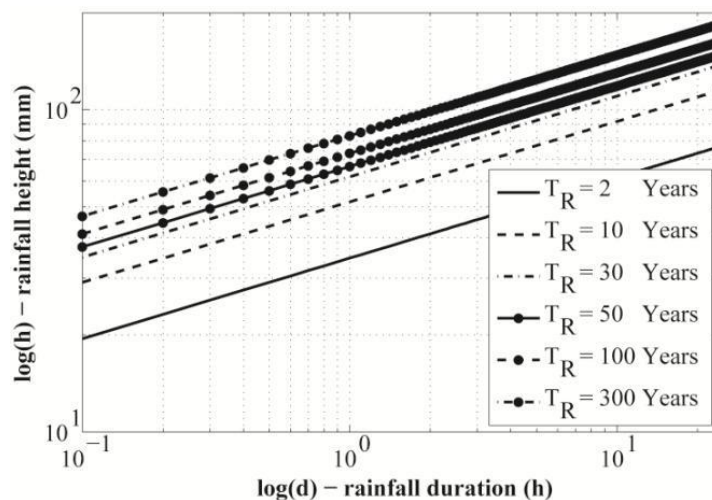


Source: Tomorrow's Cities

Figure 107: Earthquake hazard curve

E. Joint Occurrence/ Hazard Curves

When an event is associated with multiple characteristics and/or multiple intensity measures, occurrence/hazard curves become occurrence/hazard surfaces. For example, the figure below shows the return period associated with a combination of rainfall height and rainfall duration associated with a single rainfall event. We can use the rates and return periods obtained from these surfaces in the same way as the rates and periods obtained from the curves.



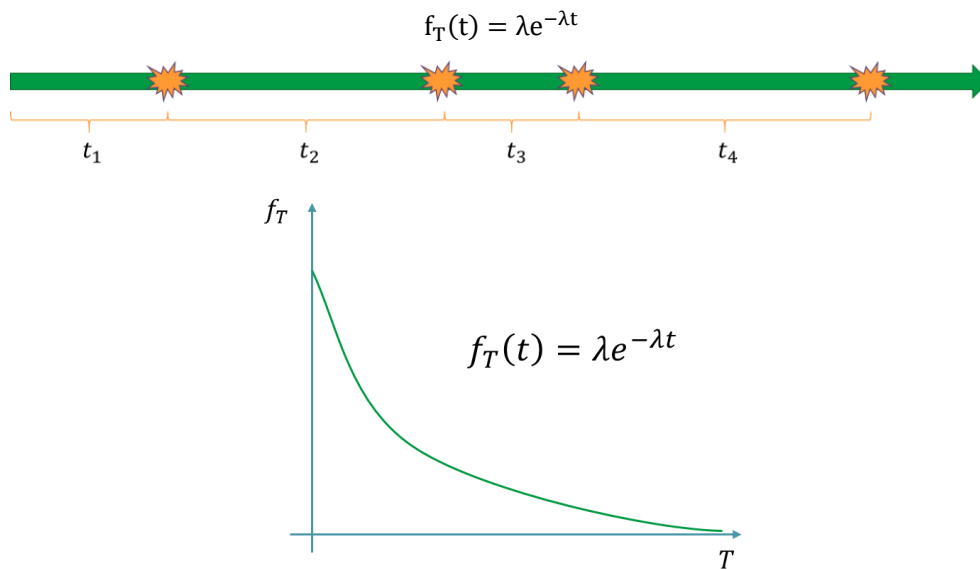
Source: Tomorrow's Cities

Figure 108: Hazard surface for a rainfall event (intensity measures are the rainfall height and duration)



F. Simulation of Events – Poisson Process

Now that we have the rates associated with single events, we need to simulate a scenario, i.e., a sequence of events with certain characteristics. In the proposed formulation, events are assumed to follow a Poisson process. This is a strong assumption which is, however, commonplace in practice. Events that do not satisfy the Poisson process assumption can be properly modified to obtain equivalent Poisson processes. In the Poisson process, the interarrival time follows an exponential distribution. In other words, the probability density function (pdf) of the interarrival times has the following expression:



Source: Tomorrow's Cities

Figure 109: Poisson process for simulation of a sequence of events

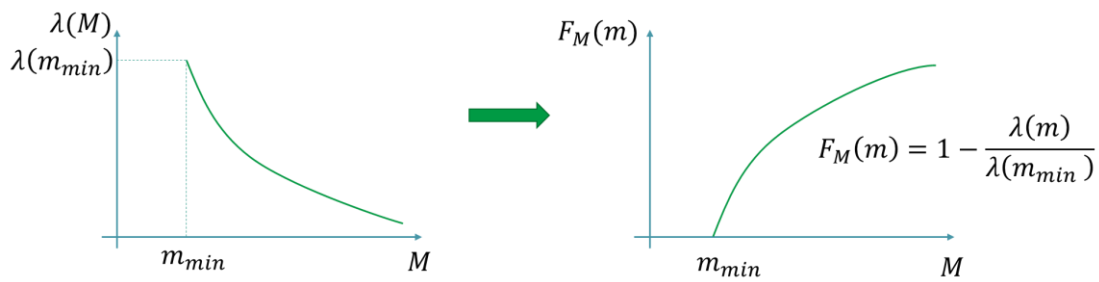
For additional details on how to interpret the pdf of a random variable, refer to the session on vulnerability analysis for single hazards. The parameter λ in the previous equation is the rate associated with the event that we are looking (i.e., the rate associated with the minimum event characteristic/intensity measure that will cause damage).

We can now simulate a sequence of events by simply simulating the inter-arrival times, i.e., randomly generating exponentially distributed numbers. Once we have the event occurrences, we need to obtain the corresponding characteristics/intensity measures. This is done with another random simulation of numbers, for which we need the distribution of the event characteristics/intensity measures. This is easily obtainable from the occurrence/hazard curves/surfaces. In fact, the Cumulative Distribution Function (CDF) of the event characteristic/intensity measure M can be obtained as follows:

$$F_M(m) = 1 - \frac{\lambda(m)}{\lambda(m_{\min})}$$

where $\lambda(m)$ denotes the rate associated with m (from the occurrence/hazard curve).





Source: Tomorrow's Cities

Figure 110: Generation of CDF of the event characteristic/ intensity measure M

In multi-hazard analysis, we do not have a single hazard event to simulate. Rather, we have multiple events that are all assumed to follow the Poisson process assumption. As long as these events are independent, we can use the theory behind competing Poisson processes to simulate their occurrence. For N competing types of hazards, each associated with the rate λ_i , the rate of occurrence of any hazard is just the sum of the rates, i.e.

$$\lambda = \sum_{i=1}^N \lambda_i$$

Once an event has been generated, the probability that it belongs to the i -th category can then be found as

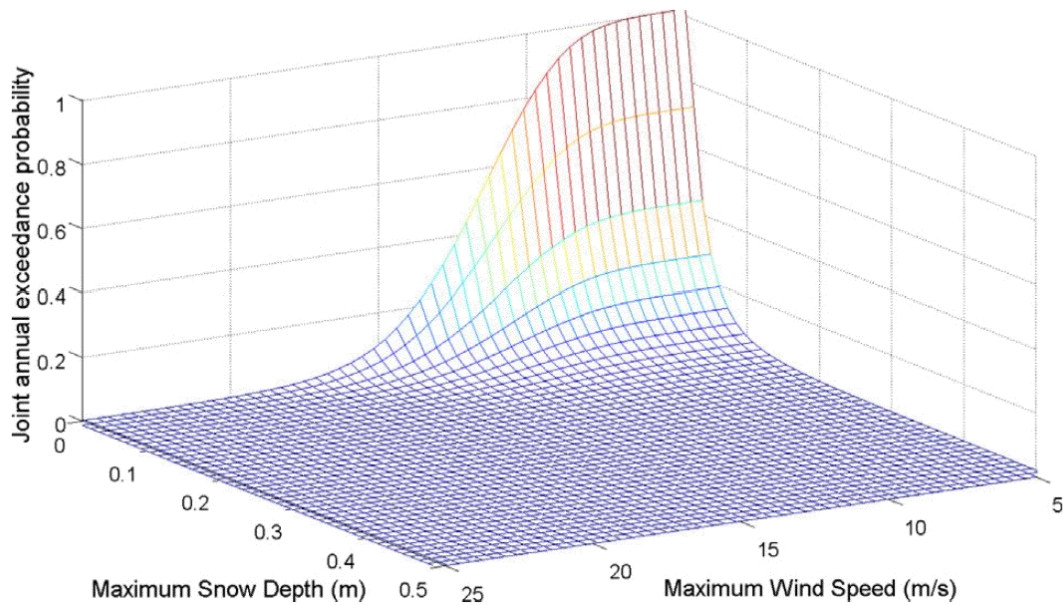
$$P(H = h_i) = \frac{\lambda_i}{\sum_{n=1}^N \lambda_n}$$

For example, if the occurrence of earthquakes has a rate $\lambda_1 = 2 \text{ years}^{-1}$, the occurrence of floods has a rate $\lambda_2 = 5 \text{ years}^{-1}$, and the occurrence of a tornado has a rate $\lambda_3 = 3 \text{ years}^{-1}$, then the occurrence of any hazard happens at a rate $\lambda = 2 + 5 + 3 = 10 \text{ years}^{-1}$, and the probability that a generic hazard is an earthquake is $P(H = h_1) = \frac{2}{2+5+3} = \frac{1}{5}$.

G. Modelling Secondary Hazards

The way we model concurrent hazards is very similar to how we model events associated with multiple hazard characteristics. In fact, also in this case we will have occurrence/hazard surfaces. However, on the axes, there will be the characteristics of multiple hazards, rather than the multiple characteristics of a single hazard.





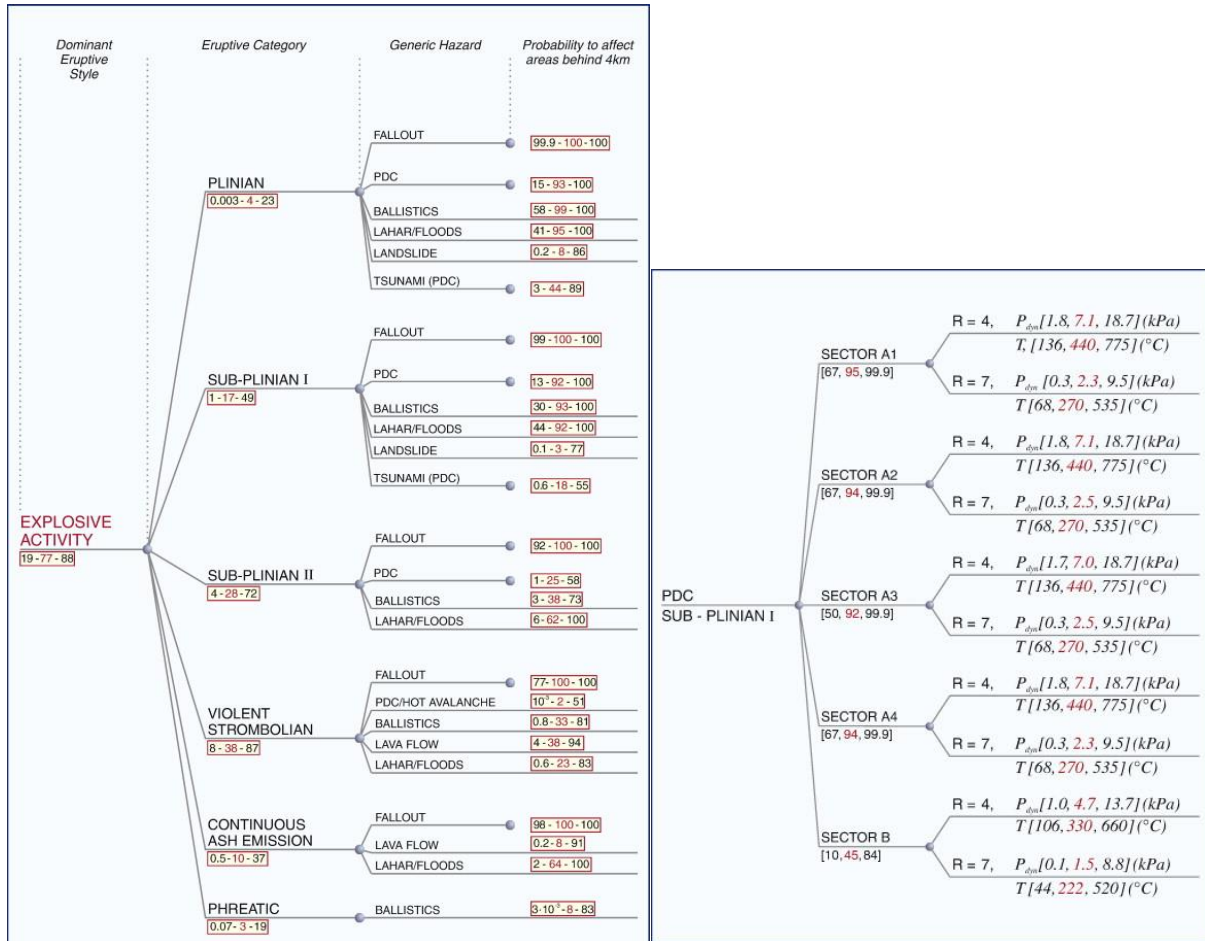
Source: Wang, Y., & Rosowsky, D. V. (2013). Characterization of joint wind-snow hazard for performance-based design. *Structural safety*, 43, 21-27. [19]

Figure 111: An example for modelling of concurrent hazard for wind-snow

As for the successive hazards, the modelling is different whether we are talking about type A or type B interactions (which is why we introduced this distinction in the first place).

First, let us look at the interactions when a secondary hazard is triggered (type A). In this case, after the occurrence of the primary hazard, we immediately simulate the occurrence of the secondary. There isn't a single, common procedure to model this type of interaction; the modelling must be tailored to what is available in the literature for the hazard of interest. For example, the figure below on the left, taken from Neri et al. (2008) [20], shows the probability that a secondary hazard (such as fallout, lahar/flood, landslide or tsunami) affects an area beyond 4km from the occurrence of a primary hazard, which in this case is a volcanic eruption of a specific category (i.e., Plinian or phreatic). Similar information is also provided for the characteristics of the secondary hazard; for example, the figure below on the right shows the variability in the dynamic pressure and peak temperature of a pyroclastic density current that follows a sub-plinian eruption.





Source: Neri, A., Aspinall, W. P., Cioni, R., Bertagnini, A., Baxter, P. J., Zuccaro, G., ... & Woo, G. (2008). Developing an event tree for probabilistic hazard and risk assessment at Vesuvius. *Journal of volcanology and geothermal research*, 178(3), 397-415. [20]

Figure 112: Probability of a secondary hazard given a specific type of volcanic eruption (left), and variability of the characteristics of the secondary hazard (right).

We can use information such as the one shown in the example above to obtain conditional probabilities and conditional distribution for the secondary hazards and their characteristics, respectively.

Finally, let us look at the interactions where the probability of a hazard is increased (Type B). These are the most complicated interactions to model because we need to redefine the occurrence/hazards curves based on the magnitude of the primary hazard. Also in this case, the specific modelling depends on what is available in the literature for the hazards of interest. For example, according to the modified Omori law, after a mainshock the rate of the aftershocks changes to the following:

$$v_{A|m}(m_A) = \frac{10^{a+b(m-m_{A,\min})} - 10^a}{(t+c)^p}$$

Where m is the magnitude of the mainshock, t is the time elapsed from the occurrence of the mainshock, $m_{A,\min}$ is the minimum intensity of a shock that would cause an effect on the system, and a, b, c, p are constants that depend on the site of interest. We can use the formula above to redefine the hazard curves for aftershocks that are expected to follow a main shock of magnitude m . In this case, because the new rate decays with time, the occurrence of aftershocks would follow a non-homogeneous Poisson process. We can transform this type of processes into an equivalent Poisson process that only lasts for a specified time after the



occurrence of the primary hazard (main shock). The corresponding curve will be a conditional occurrence/hazard curve. We also call memory the time that the system remembers the primary shock.

H. Required Inputs for Scenario Simulation

This is a brief recap of all the ingredients required to simulate a hazard scenario, i.e. a sequence of events.

- The taxonomy of the hazard interactions for the site of interest. See section 9.4.1-A for additional information.
- For individual hazards that act independently, we need their occurrence/hazard curves (if only one characteristic is associated with their occurrence) or surfaces (if multiple characteristics are associated with their occurrence). See section 9.4.1-B for a curve example and section 9.4.1-E for a surface example.
- For each interaction between concurrent hazards, we need their joint occurrence/hazard surface. See section 9.4.1-G for additional details.
- For Type A interactions, we need conditional probability and distributions for the secondary hazards and their associated intensities. See section 9.4.1-G for additional details.
- For Type B interactions, we need the conditional occurrence/hazard curves for the secondary hazard and the memory of the interaction. See section 9.4.1-G for additional details.

I. Scenario Simulation

We can now detail the procedure to generate a scenario of hazard events. In general, the system starts from a neutral state where the occurrence is defined by the hazard/occurrence rates/surfaces of individual hazards and concurrent hazards. We can use the theory of competing Poisson processes (section 9.4.1-F) to simulate the first hazard (or hazards in case of concurrent interactions).

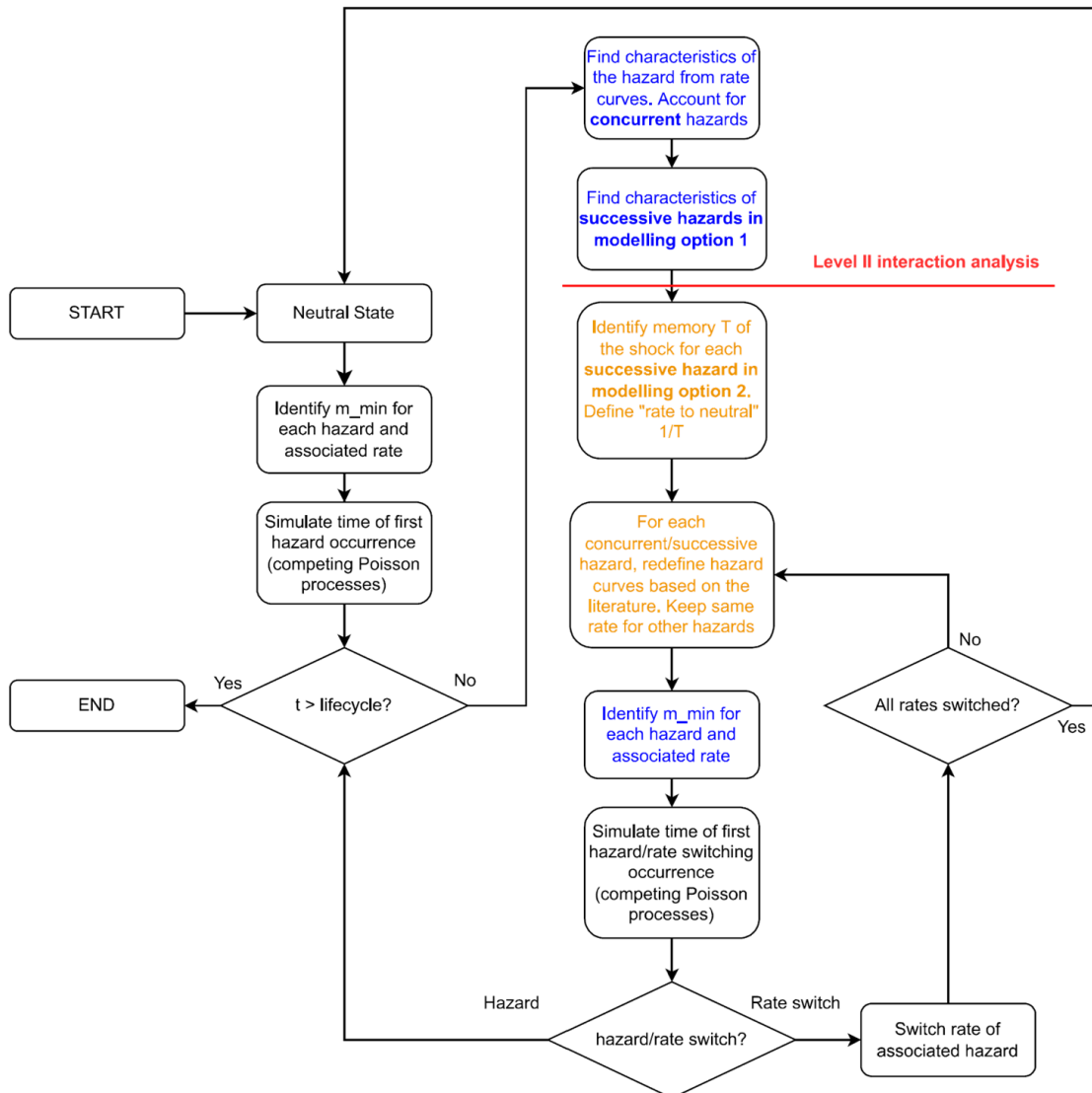
At this point, we can simulate the magnitude and/or intensity measure associated with the hazard using the formula in section 9.4.1-F for CDF (for the magnitude) and the procedures in section 9.4.1-D (if we need to obtain intensity measures from the magnitude). If the first event is the joint occurrence of two concurrent hazards whose magnitude/intensity measure is defined by a joint PDF, we can use it at this point. Right after the occurrence of the hazard, we then look at the taxonomy to identify the Successive Type A interactions. For each of these interactions, we simulate the secondary hazards based on conditional probability and distributions (section 9.4.1-G).

We then look again at the taxonomy to identify the Successive Type B interactions. For each of these interactions, we change the rates of the secondary hazards associated with them. We also identify the memory T of the interaction and add an additional possible event to the competing Poisson processes: a “rate switch” event associated with a rate $\xi = 1/T$. We can now simulate the following event in the scenario. This event could either be a new hazard occurrence or a rate switch.

- If the event is a hazard(s) occurrence, we repeat the steps highlighted thus far (simulate magnitude/intensity measures, simulate secondary hazards from Type A interactions, redefine rates of secondary hazards from Type B interactions, introduce new “rate switch” processes based on the memory of the Type B interactions).
- If the event is a rate switch, we change the rate associated with the hazard to the original value and remove the rate switch event from the pool of competing Poisson processes.



If the rates are all back to the original value, the system is back to its neutral state and the procedure can be repeated from the beginning. The procedure explained is summarized by the following flowchart.



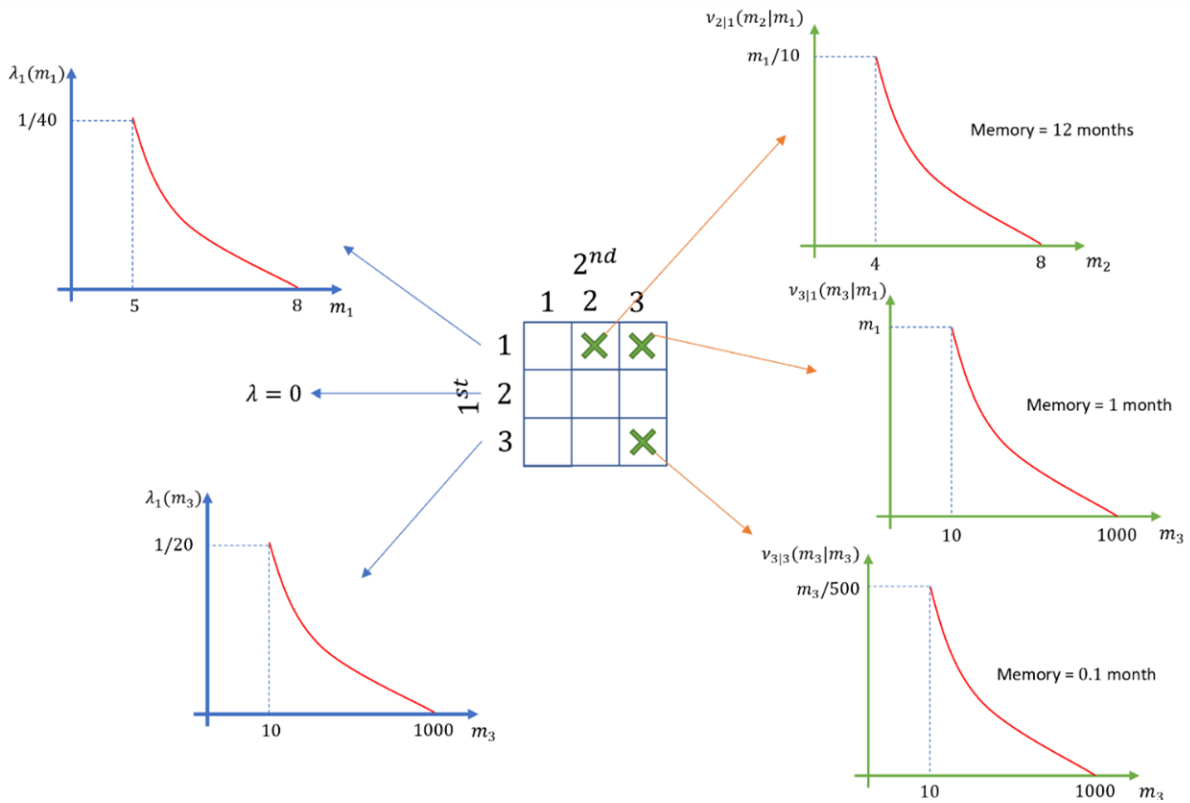
Source: Tomorrow's Cities

Figure 113: Flowchart summarizing the scenario simulation

Example of Scenario Simulation:

We now look at a simple example of a scenario simulation. The example only shows successive Type B interactions but can be extended to include concurrent hazards and successive Type A interactions. In the example, we consider three hazards. Hazard 1 and Hazard 3 can occur independently, while Hazard 2 only occurs as a secondary hazard. The figure below shows the taxonomy of the interactions of such hazards. The occurrence of Hazard 1 can modify the rates of Hazard 2 and Hazard 3, while the occurrence of Hazard 3 can modify the rates of Hazard 3 itself. The figure also shows the occurrence curves for the individual hazards and the conditional occurrence curves for the secondary hazards associated with each of the interactions. All the rates are expressed in months⁻¹.



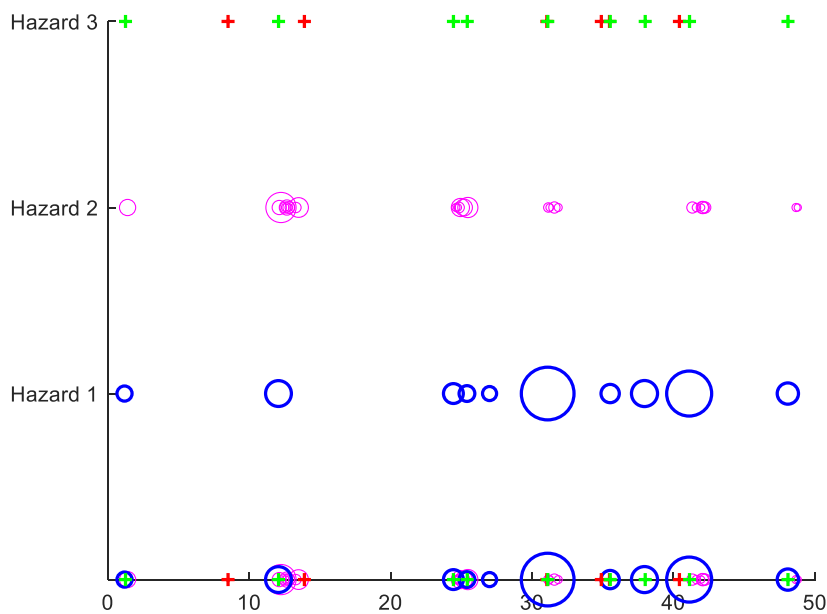


Source: Tomorrow's Cities

Figure 114: Data for the numerical example. Occurrence curves of primary hazards, interaction taxonomy, and conditional occurrence curves for each of the interactions.

Results:

We use the procedure described to simulate a scenario based on the input provided.



Source: Tomorrow's Cities

Figure 115: One scenario realization was obtained using the procedure in Figure and data above.



The figure shows the event occurrences as circles for Hazards 1 and 2, and as crosses for Hazard 3. For Hazards 1 and 2, the size of the circles is proportional to their magnitude/intensity. For Hazard 3, the occurrence is shown in red if the hazard occurred independently, and in green if the hazard occurred as a secondary hazard of a successive Type B interaction. We can see how Hazard 2 only occurs after the occurrence of Hazard 1 and keeps occurring for a certain after its occurrence (related to its memory). Simulating a scenario such as the one shown in the figure is extremely fast due to the assumptions that were made in our method. As such, multiple simulations can be performed. From these simulations, we can obtain important quantities which can then be used to select the most significant scenarios among the simulated ones, and/or be used to estimate the consequences on the affected assets based on the level II interactions. Examples of these important quantities are:

- (i) the probability of having a given number of hazards of a certain time in a given time span,
- (ii) the probability of hazard combinations,
- (iii) the distribution of the magnitude/intensity measures of the hazards and joint distributions for dependent hazards.

This concludes the discussion on Level I interactions. We now need to integrate the hazard occurrences obtained with this method with the consequences of these hazards on the assets affected. This is done via Level II interactions.

9.5 Hazard Interactions: Level II Interactions

9.5.1 Mathematical Modelling

Just like how we developed a taxonomy for Level I interactions, we can develop a similar one for Level II interactions. In general, hazards that tend to occur at the same time or very close to each other (due to Level I interactions) will also have correlated consequences (because there is no time to fix the disruption caused by the occurrence of the first hazard. However, hazards that do not have Level I interactions could have correlated consequences if they happen to occur very close to each other (think of the examples provided in Slides). Even hazards that occur at very different moments in time could interact with each other if there was no attempt to fix the system after the occurrence of the first hazard (either deliberately or because of negligence). This is why Level II interactions are, in general, possible between any two hazards, and should therefore be accounted for.

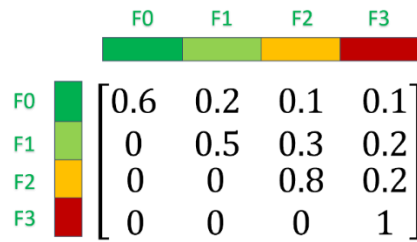
We propose two different ways of obtaining the consequences due to Level II interactions. The first one is a simulation-based method, and it consists of modeling the jump to different functionality states occurring when shocks are simulated within the framework for Level I interactions explained in the chapter. The second one is an analytical method that uses the important quantities obtained from the multiple scenario simulations. We will first focus on the simulation-based method.

A. Simulation-Based Method

Transition Probability Matrices:

A key component of the simulation-based method is transition probability matrices. A transition probability matrix defines the probability of going from one functionality level to another. The figure below shows an example of a transition probability matrix.





Source: Tomorrow's Cities

Figure 116: Example of transition probability matrix

The rows of the matrix represent the functionality level before, the occurrence of the hazards, and the columns represent the functionality level after the occurrence of the hazard. The entries of the matrix represent the probability of going from any functionality level to any other functionality level. For example, the entry (2,3) of the matrix (0.3 in the figure) is the probability that after the occurrence of the hazard a system in functionality state F2 moves to functionality state F3. Because the rows represent the probabilities of going from one state to any other state, the numbers along every row must sum up to one. These numbers can be obtained from the fragility curves of the system (see session on single hazard analysis). As such, these numbers will be a function of the magnitude/intensity measure of the hazard (such quantity is not shown in the figure for simplicity). Specifically, the numbers in the first row are obtained from the fragility curves of a system in pristine conditions (or functionality state F0), while the numbers in the other rows are obtained from state-dependent fragility curves, i.e. curves that quantify the probability of a damaged system to fall into even worse functionality states. Because we are talking about hazards, and the system is expected to fall into a worse state after the occurrence of a hazard (or stay in the same state), these transition probability matrices will all be upper triangular matrices.

In the single-hazard session, we have detailed a few examples of how to obtain fragility curves for different hazards. The values from these curves can be used to fill these transition probability matrices. However, the way we quantify damage across different hazards is in general different. For example, after the occurrence of an earthquake the damage might be quantified in terms of the structural conditions of the physical components (e.g., beams, walls, columns) whereas after the occurrence of a flood might be quantified in terms of the damage to the non-structural components (e.g., furniture and appliances). We need to make these scales comparable if we want to integrate this procedure into a formulation that looks at the interactions between different hazards.

The Unified Consequence Scale:

In these cases (when the original scales are not comparable) we intend to translate each scale into an equivalent consequence scale. For example, both the damage to structural components due to earthquakes and the damage to non-structural components due to flood could be translated into a scale that quantifies the accessibility of the building (e.g., how much the livelihood of the household is affected). There are different ways we could perform this translation:

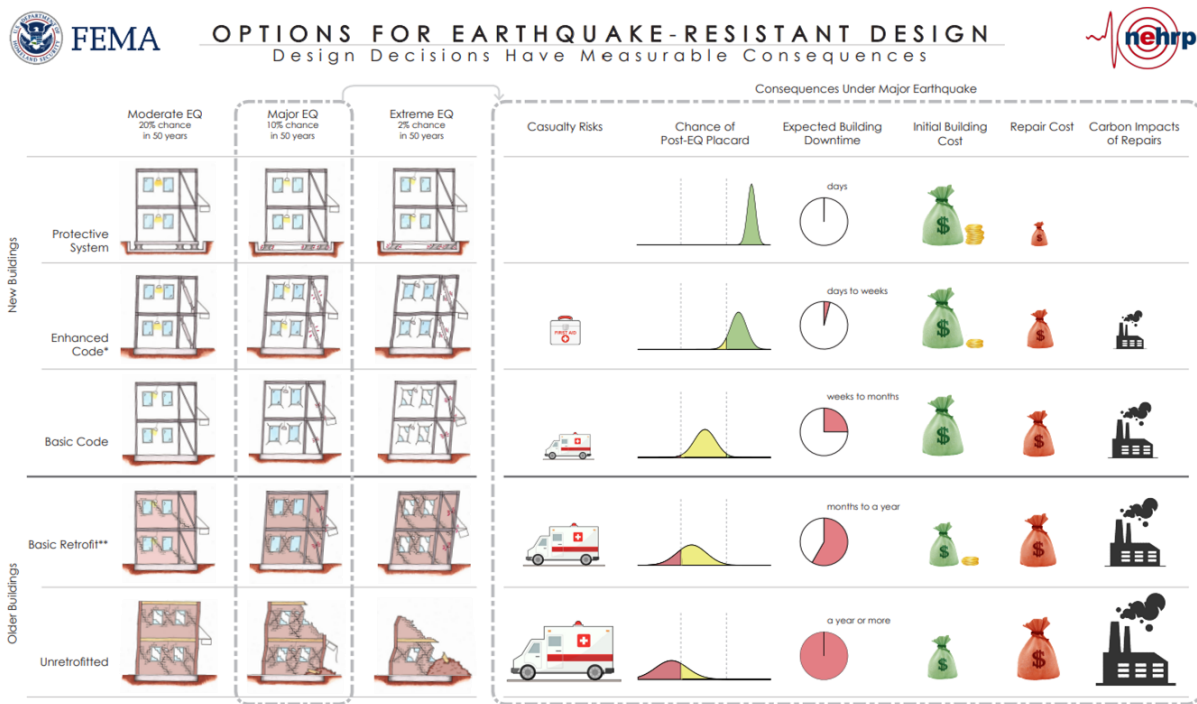
- In a deterministic sense, we could assign each of the states of the original scale to one value on the unified scale. Based on such value, we could then find the corresponding state in the unified scale.
- We could assign a probability of each of the states of the original scale to correspond to any state on the unified state. While more complicated, this approach allows us to account for the uncertainties that are inherent in the translation process.



Either way, we would then be able to quantify the consequences of every shock in terms of the same, unified scale. We would then be able to modify the original transition probability matrices into transition probability matrices where each row and each column correspond to the states of the unified scale. Note that, even if the row and columns of the transition probability matrices represent the same states, the entries of the matrices will still be hazard dependent (as well as dependent on the magnitude/intensity measure).

Example

As an example, let us look at the classification proposed by FEMA P-58 to quantify the damage and consequences following an earthquake. In FEMA P-58, we can identify 5 different damage states based on the conditions of the buildings following the earthquake. However, FEMA P-58 also provides alternative ways to quantify the consequences, including casualty risks, expected building downtime, repair costs and carbon impact of repairs. We could think of selecting one of these alternative scales as our unified scale. For example, the expected building downtime could be selected, as downtime is expected also as a consequence of other hazards. Downtime is also a good proxy of the losses in the building, and it could be used to quantify consequences in terms of the livelihood of the households (if we are looking at pro-poor frameworks). Fortunately, in this case the mapping between the original damage scale and the downtime scale is already provided by FEMA P-58.



Source: FEMA P-58

Figure 117: FEMA damage scales and measurable consequences

We now need to look at another hazard and quantify its consequences in terms of the quantity of our unified scale (downtime in this example). For example, in Nofal et al. (2020) [15] damage states are quantified in terms of the damage to the single components. Figure above shows the classification taken directly from the paper.



DS Level	Description	Damage Scale	Damage Ratio
DS0	Insignificant damage to components below first-floor elevation. Water enters crawlspace/basement and touches foundation (crawlspace or slab on grade). Damage to components within the crawlspace/basement including base insulation and stored inventory. Minor damage to garage interiors including drywall, cabinets, electrical outlets, wall insulation (Garage is below the FFE). No sewer backup into the living area.	Insignificant	0.0-0.03
DS1	Water touches floor joists up to minor water enters the building. Damage to carpets, pads, baseboards, flooring. Damage to the external AC unit (if the AC unit is not elevated) and the attached ductworks (if ductworks are in the crawlspace). Complete damage to the garage interior (if the garage is below FFE). No drywall damages with the potential of some mold on the subfloor above the crawlspace. Could have a minor sewer backup and/or minor mold issue.	Slight	0.03-0.15
DS2	Partial damage to drywalls along with damage to electrical components (base-outlets), water heater and furnace. Complete damage to major equipment, appliances, and furniture on the first floor. Damage to the lower bathroom and kitchen cabinets. Doors and windows may need replacement. Could have a major sewer backup and major mold issues.	Moderate	0.15-0.5
DS3	Damage to the non-structural components and interiors within the whole building including (but not limited) drywall damage to upper stories for multi-story buildings (e.g., attic, second story, etc.). Electrical switches and mid-outlets are destroyed. Damage to bathroom/kitchen upper cabinets, lighting fixtures on walls are destroyed with potential damage to ceiling lighting fixtures. Studs reusable; some may be damaged. Major sewer backup will happen along with major mold issues. Equipment, appliances, and furniture on the upper floors are also damaged (e.g., attic, second floor, etc.).	Extensive	0.5-0.7
DS4	Significant structural damage present (e.g., studs, trusses, joists, etc.). Non-structural components and interiors are destroyed including all drywall, appliances, cabinets, furniture, etc. Damage to rooftop units/components including roof insulation, sheathing and electro-mechanical systems (rooftop AC units, electrical systems, cable railing, sound system, etc.). Foundation could be floated off. The building must be demolished or potentially replaced.	Complete	0.7-1.0

Source: Nofal et al. 2020 [15]

Figure 118: Damage states following flood

There is no mapping provided in Nofal et al. (2020) to translate the damage states in Figure above into downtime for the households. However, the description of the damage states is detailed enough to allow us to estimate the downtime based on the damage to the components. For example, because DS0 includes damage to components within the crawlspace/basement including base insulation and stored inventory, as well as minor damage of garage interiors, we could estimate that the livelihood of the place is restored in a period ranging from days to weeks.

This is the procedure to follow to obtain the consequence of the different hazards in terms of the same quantities.

Deterioration and Recovery:

Deterioration and recovery can also cause changes from one state to another. However, while the changes that we have seen thus far are all triggered by an event (i.e., the occurrence of a hazard), the changes due to deterioration and recovery could occur at any time during the service life of the system. To model these phenomena, we introduced different points in time where we evaluate the probability that the system has jumped from one state to another due to either deterioration or recovery. The probability of these jumps is still quantified using transition probability matrices. However, these matrices do not depend on the intensity of any shock. Rather, they depend on the selected time interval. We could either have deterioration and recovery acting at all times, or we could separate a deterioration phase from a recovery phase. Note that, because the intent of recovery is to improve the condition of the system, the transition probability matrices for recovery will be lower triangular.



SESSION 10: VULNERABILITY MODELLING – MODEL SELECTION

10.1 Objectives

By the end of the session, the participants will be able to:

- Describe the concept of scoring, selecting and ranking physical impact models for multi hazard risk agreement.
- Apply the method of scoring and ranking of physical impact models.

10.2 Structure of Session 10

Structure
1. Physical Impact Models for Different Hazards
2. Characterization Procedure for Physical Impact Models
3. Example- Application on Tomorrowville

10.3 Physical Impact Models for Different Hazards

10.3.1 Earthquake Induced Ground Shaking

Earthquakes involve the sudden release of energy from a seismic source, causing ground motions that can generate a vibratory response in physical assets. This response can lead to damage, depending on the asset's dynamic structural characteristics (such as stiffness, strength, ductility capacity, hysteretic behaviour, strength degradation behaviour, plastic mechanism) and the nature of the ground shaking. Common damage mechanisms include brittle failure, plastic hinges, and support failures. Examples of these mechanisms include brittle failure in unreinforced masonry and adobe construction, plastic hinges and shear failures in reinforced-concrete buildings, and anchorage/connection failures in timber and steel constructions.

Typical Intensity Measures (IMs) accounts for certain measurement of the strength of the ground motion, for example, Peak Ground Acceleration (PGA) or Spectral Acceleration of the body's fundamental period [21]. More advanced methods follow the spectral shape of the ground motion, such as inelastic spectral displacement [22] and its duration [23]. Silva et al [24] has given more detailed description on selection of appropriate IMs. Economic losses (e.g., [25], [26], i.e., the cost to repair the physical damage), casualties (e.g., [27], and repair/recovery time (e.g., [28]) are the impact metrics that are most frequently incorporated in seismic vulnerability and damage-to-impact models. Debris cover [29] and environmental impact [30] are some of the recently introduced metrics.

10.3.2 Flooding and Mass Movement Hazards

Floods and other large-scale motions, such as landslides, lahars, and debris flows, are caused by gravitational forces. Intense rainfall, which is responsible for both floods and mass movements, is predicted to grow in intensity and frequency as a result of climate change (e.g., [31]). Strong morpho-dynamics are frequently present in these flows, which can cause transitional behaviors like erosion and the momentum and rheology of the flow are changed by deposition (for example, a dilute flash flood changing into a more concentrated debris flow when material is entrained).

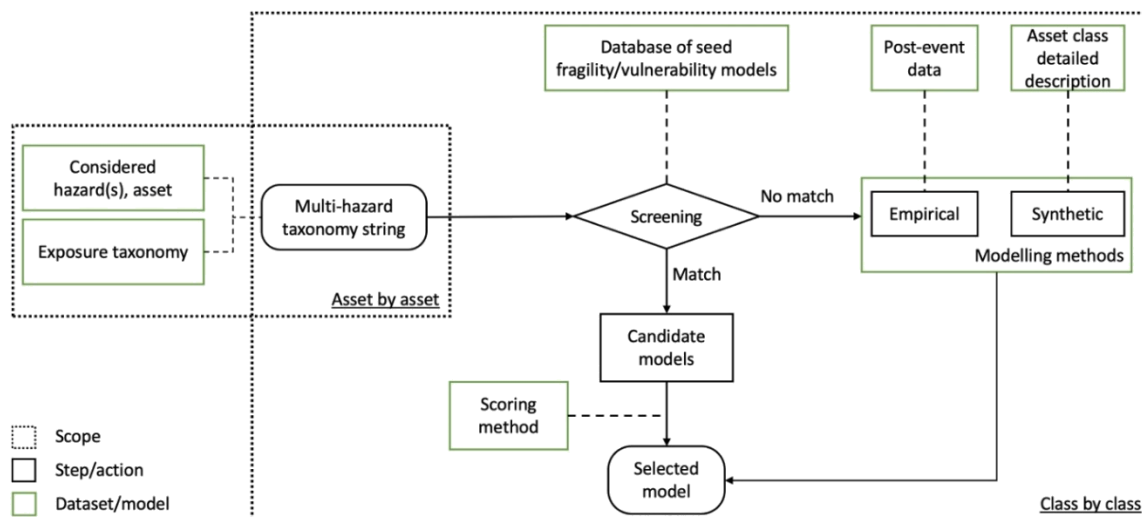


Flooding occurs when water levels rise in bodies of water, such as streams, rivers, or lakes, and the water overflows onto nearby land. In urban areas, this usually results in slow-moving water with a lot of pressure behind it. Flash floods are sudden, short-lived events that are caused by heavy rainfall or the sudden release of a large amount of water for example when dams or lakes burst [32]. They often have higher water flow rates in urban areas, where they can pick up loose debris and cause damage [33]. Debris flows are similar to flash floods and can cause same kinds of damage, and they are distinguished by their ability to carry large amounts of debris. Landslides are when large amounts of rock or soil move down a slope due to gravity. They can happen at widely different velocities.

10.4 Characterization Procedure for Physical Impact Models

The methodology for scoring, selecting and developing physical impact models starts after selecting one or more natural hazards, independent or interacting, relevant for a selected case-study area.

- Firstly, assets within the area of interest are grouped into classes according to a taxonomy model, which may require sets of general parameters specific to the identified asset class and hazards (e.g. occupancy, geometry parameters, design level).
- Next, the required asset class characteristics is codified in a multi-hazard taxonomy string and the minimum set of these parameters required for different hazard/ asset-class combinations.
- The taxonomy strings are then used to guide the hazard/ asset-class combination to relevant candidate impact models. The impact models are selected from interactive databases, model compendia or literature reviews, evaluating their simplicity, accuracy and data requirements of the overarching risk model.
- They are then scored and ranked according to a set of criteria to determine the most appropriate one.
- In case there is no satisfactory result, new physical impact models are developed based on an empirical or synthetic (analytical or numerical) approach.
- Multiple asset classes should be processed in parallel to determine whether physical impact models for different classed can be derived using a consistent methodology, which would lead to a desirable consistency in the damage/ impact estimations of the considered risk assessment.



Source: Gentile et al. 2022 [1]

Figure 119: Methodology to score and select physical impact models for a given asset class



The main goal is to obtain consistent evaluation and selection of a set of candidate physical impact models for use within multi-hazard risk modelling. It can also be beneficial for application to new physical assets to be constructed as part of a risk-informed urban development. Any values provided for relevant input parameters such as specific criteria, threshold values for screening, scoring schemes and weights are as recommendations and these can be adjusted by the users according to specific needs.

10.4.1 Preliminary phase: defining the exposure taxonomy string of the considered asset classes

In this step, the physical attributes of the asset classes of interest directly correlated with the physical impacts induced by relevant natural hazards are identified at the beginning. For instance, the lateral load resisting system attribute is used to determine earthquake and wind fragility (among other hazards), the presence of basement is relevant to flood fragility and the roof typology, and its features is a factor that influences hurricane fragility. The building occupancy type affects the likely distribution of its occupants during any particular day. For example, a school is likely to be full during certain hours on school days, predominantly by children. Moreover, the occupancy type also defines the components expected to present within a building. For example, industrial buildings house machinery.

A. Exposure Taxonomy String

Series of taxonomy strings are used to codify the attributes of a building/ infrastructure. It is a combination of alphanumeric labels that contain information on asset-class-specific attributes and are an ideal data format for storage within a database (e.g. GIS) to simplify interaction between the exposure and vulnerability modules of a risk model.

A taxonomy string should be general enough to consider multiple hazards, scales and asset classes. The Global Exposure Database for All (GED4ALL) [34] taxonomy is followed in the methodology as it facilitates links to many existing databases of physical impact models and thus best fits the above criteria. It is also referred to as Global Earthquake Model (GEM) taxonomy 3.0. It covers various assets such as buildings, roads, railways, bridges, pipelines, storage tanks, power grids, energy generation facilities, crops, livestock, forestry and socio-economic data and was developed considering hazards such as earthquakes, volcanoes, floods, tsunamis, storms, cyclones and drought.

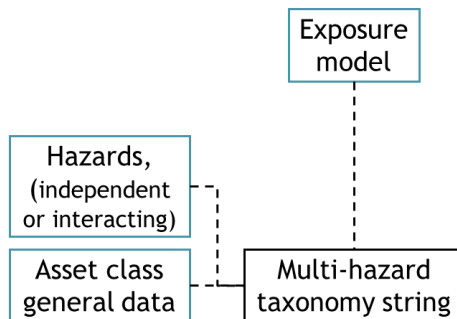


Figure 120: Considerations in Multi-hazard taxonomy string (GED4ALL)

The features of GED4ALL taxonomy strings are that it includes different attributes for different asset types and has three different levels of refinement/ detail i.e. from Level 1 and Level 3 facilitating accommodation of various degrees of available data. This flexibility eases the condition of data-scarce environment, particularly prevalent in developing countries. GED4ALL attributes for buildings and bridges, along with suggestions on those that are mandatory and



those that are optional regarding the physical impact modelling of different hazards are shown in Tables below.

Table 13: GED4ALL attributes for buildings exposed to various hazards

Attribute	OSM Key	EQ	FL	DF	TS	LA	FI	WI	VA
Direction	building:direction	O	O	O	O	O	-	O	-
Material of LLRS	building:lateral:material	R	R	R	R	R	O	R	R
Lateral Load Resisting System (LLRS)	building:lateral:system	R	R	R	R	R	O	R	R
Height	building:levels	R	R	R	R	R	R	R	R
Date of construction or retrofit	building:age	R	O	O	R	R	O	R	R
Surroundings	building:adjacency	O	O	O	O	-	O	-	-
Occupancy	Building	R	R	R	R	R	R	R	R
Shape of building plan	building:shape	O	O	O	O	O	R	R	-
Structural irregularity	building:irregularity	O	O	O	O	O	-	-	O
Ground floor hydrodynamics	ground_floor	-	-	O	O	-	-	-	-
Exterior walls	building:material	O	O	O	O	-	O	O	-
Roof shape	roof:shape	-	-	-	-	-	O	R	R
Floor system material	floor:material	O	O	O	O	O	O	O	O
Foundation	building:foundation	O	O	O	O	O	-	O	-
Fire protection	building:fireproof	-	-	-	-	-	R	-	-

OSM: OpenStreetMap; R: required; O: Optional; EQ: earthquake; FL: flood; DF: debris flow; TS: tsunami; LA: landslide; FI: fire; WI: wind; VA: volcanic ash

Table 14: GED4ALL attributes for bridges exposed to various hazards

Attribute	OSM Key	EQ	FL	DF	TS	LA	FI	WI	VA
General material	bridge:material	R	R	R	R	R	R	R	R
Super structure	bridge:structure	R	R	R	R	R	R	R	R
Deck characteristics	bridge:width;length;height	R	R	R	R	R	R	R	R
Deck structural system	bridge:support	O	O	O	O	O	O	O	O
Pier to deck connection	pier:connection	R	O	O	R	R	O	R	R
Pier to superstructure connection	pier:superstructure	O	O	O	O	O	O	O	O
Number of piers	bridge:total_piers	R	R	R	R	R	R	R	R
Shape of pier section	pier:shape	O	O	O	O	O	-	R	-
Pier height	pier:height	O	O	O	O	O	-	-	O
Spans	pier:span	R	R	R	R	R	R	R	R
Connections to the abutments	Abutment:connection	R	R	R	R	R	O	R	O
Bridge configuration	bridge:configuration	O	O	O	O	O	O	O	O
Level of seismicity	bridge:seismicity	O	-	-	-	-	-	-	-

Notations are as per Table above



Examples of GED4ALL taxonomy strings for various level are shown below:

Table 15: Examples of GED4ALL taxonomy strings

Level	GED4ALL taxonomy strings	Building attributes	Remarks
Level 1	CR/H:2/LWAL/RES	Two-storey reinforced concrete residential building with a wall lateral load resisting system	
Level 2	CR+CIP/H:2/LWAL/RES	Two-storey <u>cast in place</u> reinforced concrete residential building with a wall lateral load resisting system	Level 2 information includes data on material technology
Level 3	CR+CIP/H:2/LWAL/RES/ IRIR+IRPP:TOR+IRPS:REC	Two-storey cast in place reinforced concrete residential building with a wall lateral load resisting system and <u>with primary structural irregularity in the form of torsional eccentricity and secondary structural irregularity in the form of a re-entrant corner</u>	Level 3 information includes secondary information related to primary (Level 2) structural irregularities

Elaborative documentation for each asset class is provided at docs.riskdatalibrary.org/ged4all.html (last accessed June 2022).

10.4.2 Screening Phase: Selecting Candidate Physical Impact Models

The next step is identifying a list of candidate physical impact models among a given set of available options. For carrying out this task, the ideal resource would be an extensive database of single- and interacting multi-hazard physical impact models on multiple asset typologies consistent with the GED4ALL taxonomy. Although such a repository is not yet available, it is still under research.

The screening phase involves:

1. Defining three fundamental parameters: asset location, asset taxonomy string and considered hazards. To facilitate the model search, these parameters should be defined with different refinement levels.
2. Performing an automatic search in an interactive database of physical impact models. Multiple searches each for any combination of refinement in the above parameters should be performed, starting from their most-refined definitions. Each match found in these searches is taken as candidate model.
3. Performing a manual search in any non-interactive model compendium, literature review and regional/global models. Any match found should be taken as candidate model.
4. Performing a specific literature review for the most-refined definition of the above parameters that also considers specific user requirements (e.g. time-dependent models accounting material ageing, specific IMs). This promotes specificity of the model matches, whereas steps 2 and 3 promote the number of matches.
5. Screening the candidate models to determine a subset to be scored/ranked for quality of the successive phase. The users should consider the possibility of developing ad-hoc adjustments to improve the given model as a factor during screening. Screening is performed according to three criteria as presented in Table above along with a set of example qualitative acceptance thresholds for each, which can be modified appropriately according to user judgement for a considered application.



Table 16: Model screening criteria: minimum thresholds for acceptance [N_{ds} , R_{im} , N_{hp} are defined by the user; example values: $N_{ds}= 1$, $R_{im}=20$, $N_{hp}= 80$]

Screening criterion	Suggested acceptance threshold
Damage/impact appropriateness	Required DSs are defined (or N_{ds} DSs are missing). Required impact metric is modelled.
Required extrapolation	Required IM range is covered (or R_{im} % extrapolation needed)
Documentation	Documentation justifies N_{hp} % of the model's assumptions (e.g. damage scale, IM selection, fitting methods)

A. Available Interactive Databases of Candidate Models

There are several platforms that provide online or software tools for searching appropriate models using multiple key words and/or options. Some of the available interactive databases are listed in Table below.

Table 17: Available interactive databases

S.N.	Platform	Model	Hazard	Infrastructure
1	platform.openquake.org/vulnerability/list (last accessed June 2022)	GEM, [35]	Earthquake	Buildings
2	vulncurves.eu-risk.eucentre.it (last accessed June 2022)	ESRM, [36]	Earthquake	Buildings
3	thebridgedatabase.com/existing-fragility-curves/ (last accessed June 2022)	Stefanoiu et al., [37]	Earthquake	Bridges
4	clip.engr.oregonstate.edu (last accessed June 2022)	Alam et al., [38]	Earthquake, tornado	Lifeline utilities such as electric, water, wastewater and transportation systems
5	MS Windows-based fragility function manager, [131]	SYNER-G, [39]	Earthquake	Buildings, bridges, road infrastructure, oil and gas systems, and lifelines, including electric, water and wastewater
6	MS Windows based vulnerability module	CAPRA, [40]	Multi-hazards	Multiple asset classes
7	github.com/mattrighetti/fdm-repository-backend (last accessed June 2022)	Bombelli et al., [41]	Flood	Residential, commercial and industrial buildings, agricultural land and transport infrastructure
8	riskchanges.org/app/#/data-management/vulnerability (last accessed June 2022)	RiskChanges	Multiple hazards including wind, drought, fire, technological, earthquake, volcano	Various asset types



B. Available Non-interactive Databases and Model Compendia

Some of the short, extensive collection of physical impact model compendia and global models are provided in Table below.

Table 18: Available non-interactive databases and model compendia

S.N.	Platform	Model	Hazard	Infrastructure
1	ucl.ac.uk/epicentre/resources/gem-vulnerability-databases (last updated 2014 and last accessed June 2022)	Rossetto et al., [[42],[43]]	Earthquake	Buildings
2		Calvi et al. [43]	Tsunami	Buildings
3	github.com/eurotsunamirisk/etris_data_and_data_products (last accessed June 2022)	European tsunami risk service	Tsunami	Buildings
4		Martin and Silva, [44]	Earthquake	Buildings
5	publications.jrc.ec.europa.eu/repository/handle/JRC105688 (last accessed June 2022)	JRC, [45]	Flood	Various assets
6	publications.jrc.ec.europa.eu/repository/handle/JRC105688 (last accessed June 2022)	HAZUS	Flood	

10.4.3 Scoring and Ranking Phase: Selecting the Most Suitable Models

A. Use of Analytic Hierarchy Process (AHP) for Criteria Weights

Each of the four criteria: Relevance, Statistical Refinement, Model Quality and User Specific Requirement has a prescribed weight produced using the Analytic Hierarchy Process (AHP) [46] for consistent definition of the weights. AHP is a multi-criteria decision making model which has been successfully applied in engineering problems [47]. In this procedure, the fundamental steps include,

1. Step 1: Identifying the criteria and organizing goal, criteria and alternatives into hierarchy.

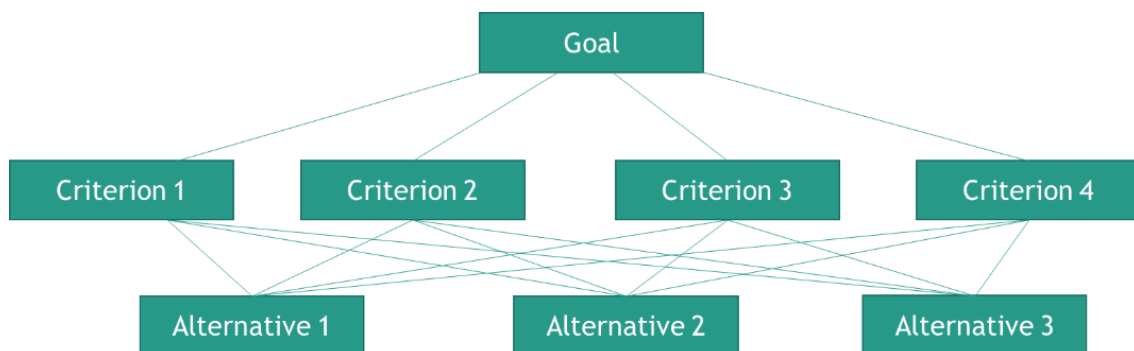


Figure 121: Organization into hierarchical structure

2. Step 2: Conducting pairwise comparisons between the relevant criteria at each level of the hierarchy.
3. Step 3: Calculating the relative importance (weights) of each criterion.



Example of application of AHP on Calculating Criteria Weights:

Let us take a simple example of determining appropriate weightage of criteria in selecting suitable daily meal package for a small office.

1. Step 1: For selecting suitable daily meal package, four criteria are identified below and then organized into hierarchy.

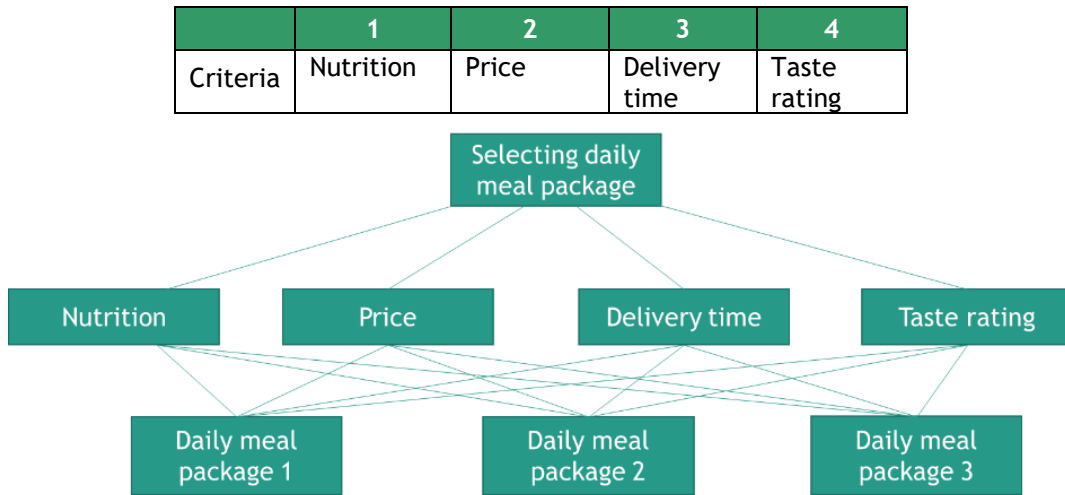


Figure 122: Hierarchical organization for selecting suitable daily meal package

2. Step 2: Pairwise comparisons between the relevant criteria at each level of the hierarchy is conducted:
 - a. First the relative importance (preference) of different criteria is determined with a set of scales.

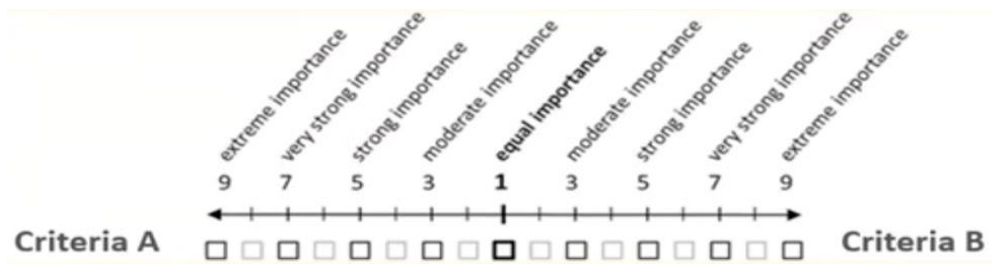


Table 19: Scale of relative importance

Preference Factor	Degree of Preference	Explanation
1	Equally important	The two domains contribute equally to the decision process
3	Moderately	One domain is slightly more important than the other
5	Strongly	One domain strongly dominates the other
7	Very strongly	One domain very strongly dominates the other
9	Extremely	One domain completely dominates the other in the decision process
2, 4, 6, 8	Intermediate	Used to represent compromises between the preferences in weights 1, 3, 5, 7 and 9
Reciprocals	Opposites	Used for inverse comparison



- b. Then matrix is created with preference factors as elements obtained from pairwise comparisons between different criteria.

Criteria	Nutrition	Price	Delivery time	Taste rating
Nutrition	1	2	3	7
Price	1/2	1	3	4
Delivery time	1/3	1/3	1	3
Taste rating	1/7	1/4	1/3	1

Reciprocals

Here, we can see that Nutrition is 2 times more important than Price and 7 times more important than Taste as expressed by the user.

3. Step 3: The relative importance (weight) of each criterion is calculated.
- a. The sum of the column of the matrix is calculated and each element is divided by their respective column sum.

Criteria	Nutrition	Price	Delivery time	Taste rating
Nutrition	1	2	3	7
Price	1/2	1	3	4
Delivery time	1/3	1/3	1	3
Taste rating	1/7	1/4	1/3	1
Column sum	1.98	3.58	7.33	15.00



Criteria	Nutrition	Price	Delivery time	Taste rating
Nutrition	1/1.98	2/3.58	3/7.33	7/15.00
Price	(1/2)/1.98	1/3.58	3/7.33	4/15.00
Delivery time	(1/3)/1.98	(1/3)/3.58	1/7.33	3/15.00
Taste rating	(1/7)/1.98	(1/4)/3.58	(1/3)/7.33	1/15.00



Criteria	Nutrition	Price	Delivery time	Taste rating
Nutrition	0.506	0.558	0.409	0.467
Price	0.253	0.279	0.409	0.267
Delivery time	0.169	0.093	0.136	0.200
Taste rating	0.072	0.070	0.045	0.067
Column sum	1.000	1.000	1.000	1.000

- b. Then the average value of each row is calculated which gives the respective weightage for each criteria.



Criteria	Nutrition	Price	Delivery time	Taste rating	Row average
Nutrition	0.506	0.558	0.409	0.467	0.485
Price	0.253	0.279	0.409	0.267	0.302
Delivery time	0.169	0.093	0.136	0.200	0.150
Taste rating	0.072	0.070	0.045	0.067	0.064
Column sum	1.000	1.000	1.000	1.000	1.000

The table below shows the resulting weightage calculated for each criteria:

Table 20: Calculated criteria weightage

Criteria	Criteria Weightage
Nutrition	48.5%
Price	30.2%
Delivery time	15.0%
Taste rating	6.4%

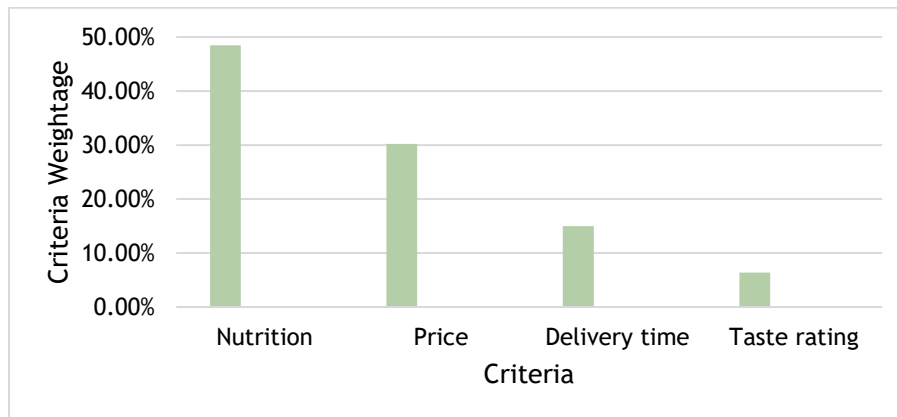


Figure 123: Graph showing criteria weightage calculated from AHP

B. Use of Technique for Order Preference by Similarity to an Ideal Solution (TOPSIS) for Scoring Attributes

Once the criteria weightage is determined, ranking of the models is done using Technique for Order Preference by Similarity to an Ideal Solution (TOPSIS) [48]. TOPSIS is used suitably for engineering decision-making problems e.g. [49]. Each attribute within a criterion is given a low (assigned 1), medium (assigned 2) or high (assigned 3) score. However, it is encouraged to test the sensitivity of the final result to these values and make alterations if required. The score of the given criterion is the minimum score among many of its attributes. For example,

Criteria: Relevance	
Attribute	Score
Geographical area	Low (1)
Intensity Measure	Medium (2)
Asset characteristics	High (3)
Criteria Score for Relevance	Low (1) - Lowest of the three



The weighted scores for a given criterion are used to define the ideal best and worst methods, and the most suitable model maximizes a trade-off between the distances from the ideal worst and best models.

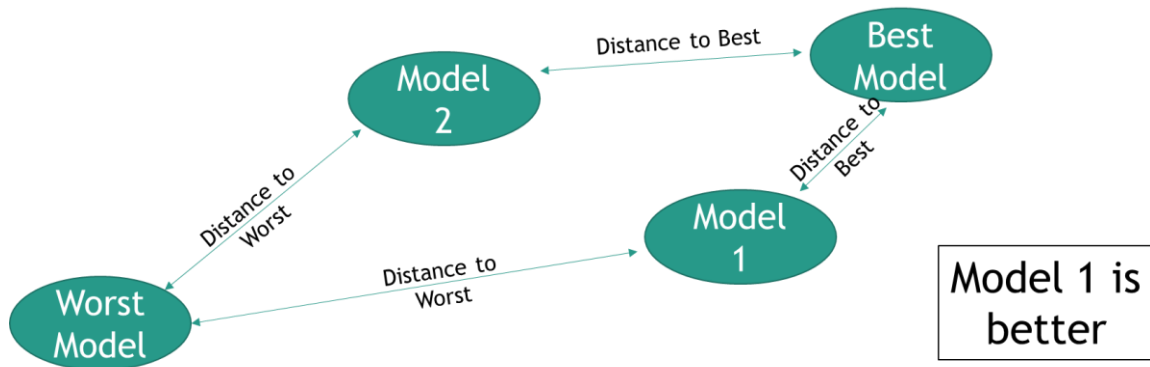


Figure 124: TOPSIS decision-making

Example of application of TOPSIS on Ranking for Selection:

Let us continue with the example taken in calculating criteria weightage for ranking and selecting suitable daily meal package for a small office.

- Step 1: Possible scores are given for each criterion. For all criteria, the definition of scores is arranged such that higher score corresponds to better result as shown below.

Nutrition	Price	Delivery time	Taste rating
Low (1)	High (1)	Slow (1)	Low (1)
Medium (2)	Medium (2)	Average (2)	Medium (2)
High (3)	Low (3)	Fast (3)	High (3)

- Step 2: Each criterion of the vendors of daily meal package is then scored 1, 2 or 3.

Vendors	Nutrition	Price	Delivery time	Taste rating
Vendor 1	1	3	2	3
Vendor 2	3	2	1	1
Vendor 3	2	2	1	1
Vendor 4	2	1	3	2

- Step 3: Then each score is normalised by dividing it by the sum of square roots of the scores within the criteria.

Vendors	Nutrition	Price	Delivery time	Taste rating
Vendor 1	1	3	2	3
Vendor 2	3	2	1	1
Vendor 3	2	2	1	1
Vendor 4	2	1	3	2
$\sqrt{\sum_{j=1}^n X_{ij}^2}$	4.24	4.24	3.87	3.87



Vendors	Nutrition	Price	Delivery time	Taste rating
Vendor 1	1/4.24=0.236	3/4.24=0.707	2/3.87=0.516	3/3.87=0.775
Vendor 2	3/4.24=0.707	2/4.24=0.471	1/3.87=0.258	1/3.87=0.258
Vendor 3	2/4.24=0.471	2/4.24=0.471	1/3.87=0.258	1/3.87=0.258
Vendor 4	2/4.24=0.471	1/4.24=0.236	3/3.87=0.775	2/3.87=0.516

4. Step 4: The normalised scores are multiplied by the weightages corresponding to each criterion. The weightage adopted for example are Nutrition - 48.5%, Price - 30.2%, Delivery time - 15% and Taste rating - 6.4%.

Weighted Normalised Decision Matrix

Vendors	Nutrition (48.5%)	Price (30.2%)	Delivery time (15%)	Taste rating (6.4%)
Vendor 1	0.485 x 0.236	0.302 x 0.707	0.15 x 0.516	0.064 x 0.775
Vendor 2	0.485 x 0.707	0.302 x 0.471	0.15 x 0.258	0.064 x 0.258
Vendor 3	0.485 x 0.471	0.302 x 0.471	0.15 x 0.258	0.064 x 0.258
Vendor 4	0.485 x 0.471	0.302 x 0.236	0.15 x 0.775	0.064 x 0.516

5. Step 5: The ideal best value and the ideal worst value in each criterion is determined.

Weighted Normalised Decision Matrix

Vendors	Nutrition	Price	Delivery time	Taste rating
Vendor 1	0.114	0.214	0.077	0.050
Vendor 2	0.343	0.142	0.039	0.017
Vendor 3	0.229	0.142	0.039	0.017
Vendor 4	0.229	0.071	0.116	0.033
V_j^+	0.343	0.214	0.116	0.050
V_j^-	0.114	0.071	0.039	0.017

V_j^+ = Ideal Best Value and V_j^- = Ideal Worst Value

6. Step 6: The distance of each vendor from ideal best value and ideal worst value are calculated.

Vendors	Nutrition	Price	Delivery time	Taste rating	S_i^+	S_i^-
Vendor 1	0.114	0.214	0.077	0.050	0.232	0.151
Vendor 2	0.343	0.142	0.039	0.017	0.110	0.239
Vendor 3	0.229	0.142	0.039	0.017	0.159	0.135
Vendor 4	0.229	0.071	0.116	0.033	0.183	0.139
V_j^+	0.343	0.214	0.116	0.050		
V_j^-	0.114	0.071	0.039	0.017		

$$S_i^+ = \text{Distance from Ideal Best Value} = \sqrt{\sum_{j=1}^n (V_{ij} - V_j^+)^2}$$

$$\text{and } S_i^- = \text{Distance from Ideal Worst Value} = \sqrt{\sum_{j=1}^n (V_{ij} - V_j^-)^2}$$

Example calculation of distance S_i^+ and S_i^- for Vendor 1:



$$S_i^+ = \sqrt{(0.114 - 0.343)^2 + (0.214 - 0.214)^2 + (0.077 - 0.116)^2 + (0.050 - 0.050)^2}$$

$$S_i^- = \sqrt{(0.114 - 0.114)^2 + (0.214 - 0.071)^2 + (0.077 - 0.039)^2 + (0.050 - 0.017)^2}$$

7. Step 7: The performance score of each vendor is calculated. Then the vendors are ranked based on this score.

Vendors	S_i^+	S_i^-	$S_i^+ + S_i^-$	$P_i = \frac{S_i^-}{S_i^+ + S_i^-}$	Rank
Vendor 1	0.232	0.151	0.383	0.39	4
Vendor 2	0.110	0.239	0.350	0.68	1
Vendor 3	0.159	0.135	0.293	0.45	2
Vendor 4	0.183	0.139	0.322	0.43	3

Conclusion: It is found that Vendor 2 ranks first with the highest performance score.

10.5 Example- Application on Tomorrowville

10.5.1 Description of the case study

To illustrate the application of the proposed methodology, the virtual urban testbed “Tomorrowville” is used. This is a synthetic urban area explicitly designed as a testbed for the TCDSE [3] of the Tomorrow’s Cities research programme. Although a fictitious urban settlement, Tomorrowville is based on digital elevation model of a real 500 ha area situated south of Kathmandu. It portrays the typical demographic, socioeconomic and physical features of urban landscapes in the Global south, specifically those of Kathmandu and Nairobi. This virtual testbed is susceptible to earthquakes, floods and debris flows [50].

Tomorrowville is characterized by spatially distributed information on its urban features, which includes land-used polygon information, building (physical) attributes, household (social) attributes, and individual/ person (social) attributes. These features are implemented in a GIS environment, which is described in detail in [51]. The physical impact models that are adopted are assigned to the buildings in the Tomorrowville GIS database using developed taxonomy strings, stored as attributes in the building layer. Accompanying it, a physical impact table consisting of the numerical definition of the physical impact model (for earthquakes, floods and debris flows) corresponding to each taxonomy string, is provided in a separate file (“vulnerabilityInventory”).

In order to explore the risk implications of different urban scenarios (conditional urban plans) in the context of TCDSE, various building layout have been created for Tomorrowville. These cases are shown in figure below. The first scenario (TV0_b0) reflects the present-day configuration of Tomorrowville, whereas TV50_total scenario represents one possible configuration of Tomorrowville 50 years in the future. A detailed description of the exposure layers in Tomorrowville is available in [51].



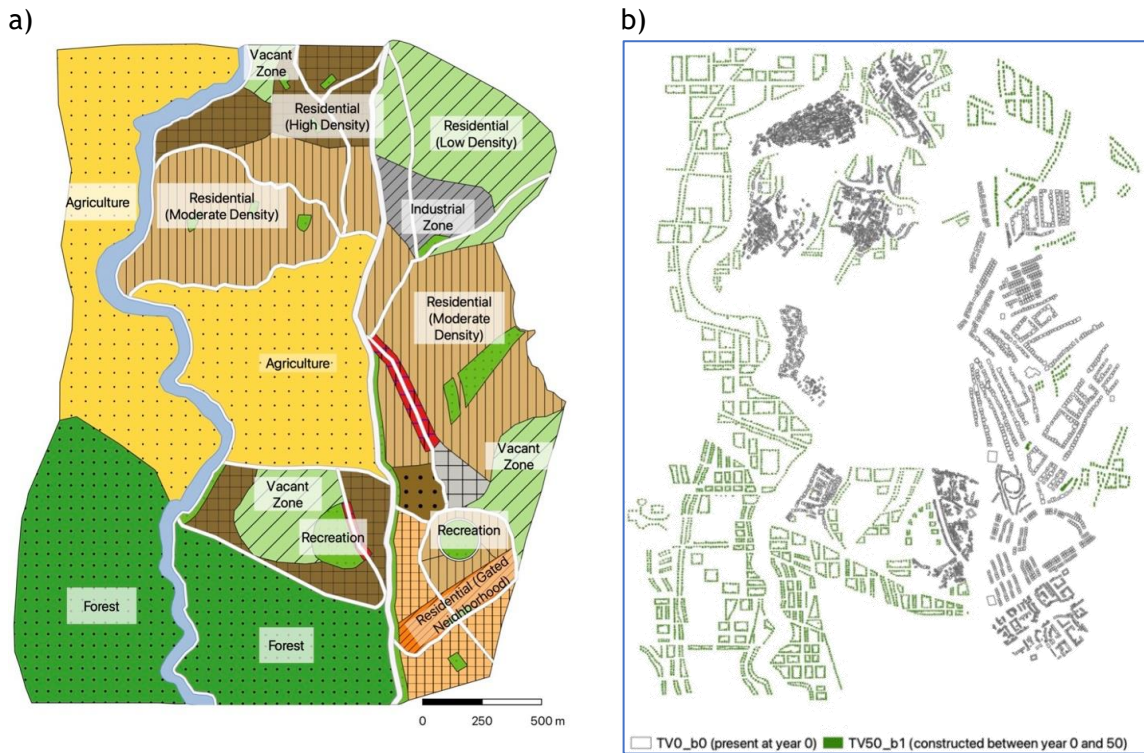


Figure 125: Methodology to score and select physical impact models for a given asset class

10.5.2 Exposure Characterization

In TV0_b0, the building attributes are generated algorithmically for 4,810 buildings (stored in the layer “buildingsTV0”) to be consistent with relevant statistical distributions of Nairobi and Kathmandu building data. However, due to the lack of detailed data available for this case study, a subset of GED4ALL attributes affecting physical impact modelling for the considered hazards: occupancy type, building material, lateral resisting system, height and code level are characterized. Each combination of these attributes constitutes a building class within Tomorrowville, which is mapped to a set of relevant physical impact models related to earthquakes, floods and debris flows using GED4ALL taxonomy strings. Ad-hoc simplified taxonomy strings are also defined to simplify communication among stakeholders and research of various backgrounds during the interdisciplinary environment of data-generation proves for Tomorrowville.

Table below shows the values adopted for different taxonomy attributes, along with their labels according to both GED4ALL and the simplified ad-hoc taxonomy strings.

Table 21: Adopted Exposure Taxonomy Attributes, considering the GED4ALL and the Simplified Ad-hoc Taxonomies

Attributes	Values	Label	GED4ALL taxonomy
Occupancy	Residential	Res	RES
	Commercial	Com	COM
	Industrial	Ind	IND
Material + Lateral	Adobe walls	Adb	MUR+ADO/LWAL
	Stone and mud (informal settlements)	StMin	MUR+ST+MOM/LWAL
	Brick and mud walls	BrM	MUR+CL+MOM/LWAL



Attributes	Values	Label	GED4ALL taxonomy
Resisting System	Brick and cement walls with flexible floor slabs	BrCfl	MUR+CLBRS+MOC/LWAL/--FWCN
	Brick and cement walls with rigid floor slabs	BrCri	MUR+ CLBRS+MOC/LWAL/-FWCN
	Masonry infilled reinforced concrete frames	RCi	CR+CIP/LFINF
Date of Construction (proxy for code level)	Pre 1994 (Low code)	LC	YPRE:1994 (and LFINF+CDL)
	Between 1994 and 2015	MC	YBET:1994:2015 (and LFINF+CDM)
	After 205	HC	YBET:2016:2022 (also LFINF+CDH)
Height	1-8 storeys	1s-8s	H:1-H:8

We can deduct various information based on these building attributes. Ordinary buildings in Tomorrowville are generally classified as residential (Res), commercial (Com), or industrial (Ind). Schools and hospitals are also present in Tomorrowville. The occupancy type, together with construction material and the number of storeys only affects the flood and debris flow vulnerability models for this application.

The combinations of building material and lateral load resisting system parameters within Tomorrowville that are possible are adobe wall buildings (Adb), informal settlements in stone and mud (StMin), brick and mud wall buildings (BrM), brick and cement walls with flexible floor slabs (BrCfl), brick and cement walls with rigid floor slabs (BrCri) and masonry-infilled reinforced concrete frames (RCi). The StMin buildings can either be one- or two-storey tall, while the Adb, BrM, BrCri, BrCfl buildings can reach up to four storeys. Lastly, the RCi buildings can be of one to eight storeys. Keeping in mind the physical impact models used for this application, the material affects earthquake, flood and debris flow models while the lateral load resisting system affects the earthquake models only.

The definition of building design codes associated with building classes in Tomorrowville (which only affect earthquake physical impact models in this case) is based on the advancement of seismic design codes in Nepal: low-code (LC) buildings are designed without any seismic code provisions; moderate-code (MC) buildings are built following construction practices in the period 1994-2015, and are therefore assumed to be compliant with the NBC 1994 code (Nepal National Building Code, [52]); high-code (HC) buildings are assumed to be compliant with the NBC 2015 code [52], and are designed with higher risk awareness of the designers after the 2015 earthquake in Nepal. RCi buildings can be assigned any of the aforementioned codes, while all the other building types are assigned low code due to poor code compliance assumed to be prevalent in the considered case-study. The above parameters are specifically distributed in each land-use polygon within the TV0-bo scenario. The distribution of occupancy type, height and code level of buildings in the TV50_total layer follows the corresponding assumptions adopted for TV0_b0.



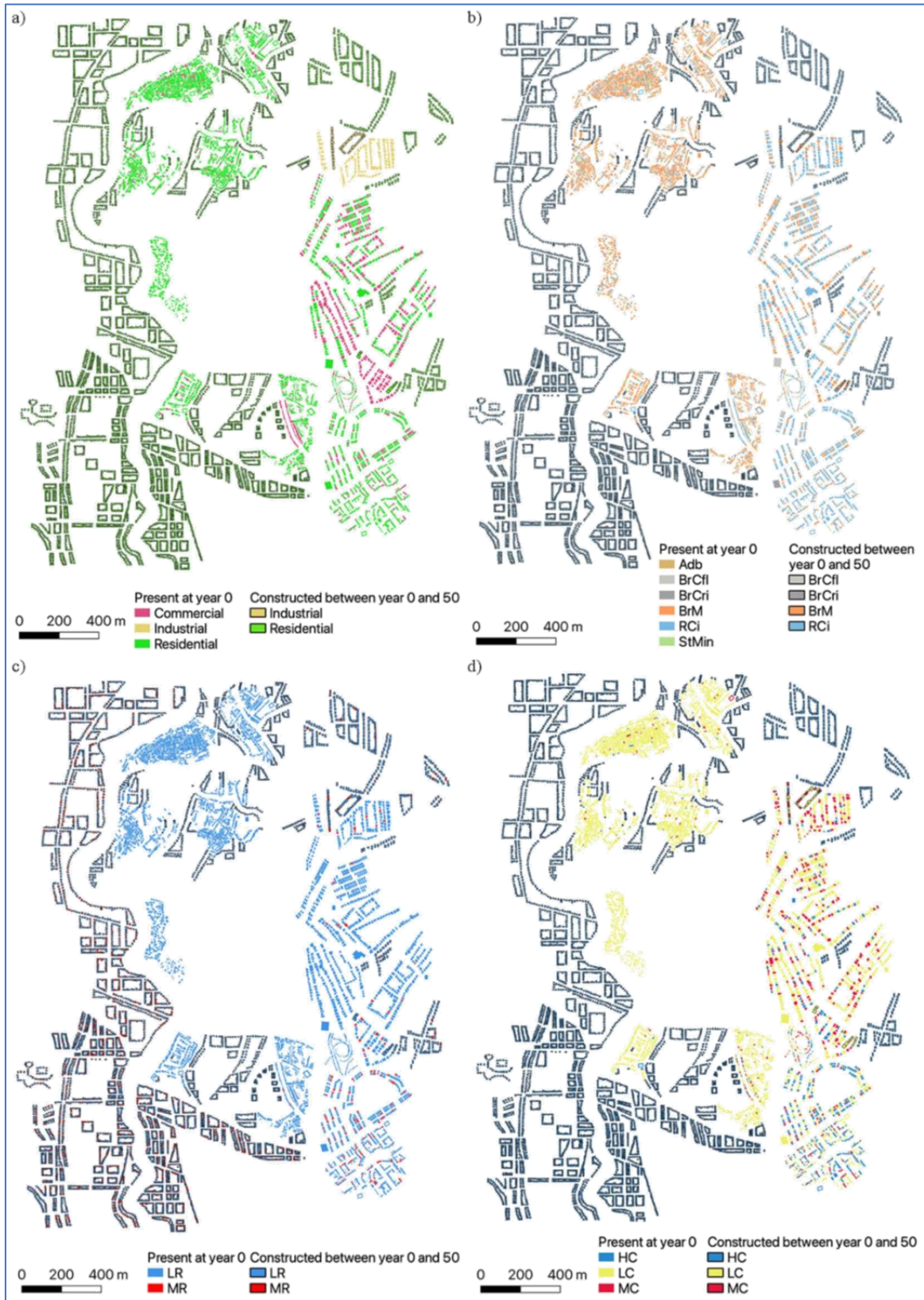


Figure 126: Building-class attributes of the TV50_total scenario in Tomorrowville: a) Occupancy type; b) Material and lateral load resisting system; c) Height; d) Code level



10.5.3 Modelling Choices and User Requirements for the Procedure

- The hazards considered for Tomorrowville are earthquakes, floods and debris flows.
- Fragility models are generally preferred (whenever available) over vulnerability models, since estimating damage enables greater flexibility in subsequently characterizing a wide array of impact metrics (e.g. casualties, human displacement) that may also relate to social impact.
- For this case study, it is reasonable to assume that flood physical impact models can also capture debris flow impacts as the low flow velocities and sediment concentration of debris flows within the shallow topography of building locations on the valley floor means that damage is primarily caused by inundation, rather than hydrodynamic stress and impacts from debris [50].
- Since the damage mechanism due to earthquakes (mainly displacement-related damage) is unrelated to the damage due to floods/ debris flows, the physical impact models of the building classes are considered independent. Thus, no multi-hazard fragility interaction is considered.
- For simplicity, time-dependent physical impact is also not considered. However, it can be approximated by scaling the parameters of the adopted physical impact models using properly calibrated factors (e.g. reducing the medians of a set of fragility functions).
- The crucial user-specific model requirement involves preferring sets of asset class-specific models (e.g. explicitly capturing the plastic mechanisms of a class) that are derived using consistent assumptions and modelling techniques and that can cover multiple asset classes within Tomorrowville. This maximizes the consistency of the damage estimations within the risk model, while capturing specific differences among the selected asset classes.
- Models using advanced IMs are also preferred over those adopting more conventional IMs.
- The adopted weights for TOPSIS for various criteria are as given below:

Table 22: Adopted Weights for TOPSIS

Criteria	Adopted weight
Relevance	25%
Statistical refinement	15%
Model quality	40%
User requirement	20%

The numerical values assigned to scores for the criteria are as:

Table 23: Values Assigned to Scores

Score	Value assigned
Low	1
Medium	2
High	3

This implementation of TOPSIS is available at github.com/robgen/rankFragilityVulnerability (last accessed June 2022).



10.5.4 Selected Physical Impact Models

An example building class of Reinforced Concrete with infill, medium code, 6 storied residential building, RCi+MC+6s+Res in the simplified taxonomy and CR+CIP/LFINF+CDM/H:6/YBET:1994:2015 according to GED4ALL, is used to describe the following procedure in detail.

For earthquake,

- Among the available databases (point 2 of the screening phase), the GEM vulnerability and the European seismic risk model databases produced only three candidate models: Akkar et al. [53], Erberik [54] and CR_LFINF_CDM-0_H6 in Crowley et al. [36].
- Among the model compendia (point 3 of the screening procedure), the HAZUS earthquake fragility model for mid-rise, moderate code reinforced concrete frames is a further match produced in this procedure step. Even though it refers explicitly to USA building classes, it is considered because it is commonly used for other regions.
- A literature review specifically concerned with Nepal building classes (point 4 of the screening procedure) returned the model by Gautam et al. [55]. The literature review was pursued by relaxing the constraint on the geographical location (i.e. targeting generic reinforced concrete building classes) but including some specific model requirements (used as a criterion in the ranking phase), particularly the explicit consideration of the building plastic mechanism (indirectly related to the seismic code) and the use of advanced IMs. As a result of the search, the study by Gentile and Galasso [56] is selected. The Gentile and Galasso models cover all the relevant concrete building classes in Tomorrowville.
- All the identified candidate models passed point 5 of the screening phase since they include adequate documentation (associated with international journal papers), an adequate damage scale covering four DSs and require no IM extrapolation for their specific use in Tomorrowville.
- The candidate models are then scored against the ranking criteria, as shown in table below. Although scoring only “medium” for “relevance”, the model by Gentile and Galasso, was selected since it scored “high” in all other criteria, finally resulting in a higher overall score according to TOPSIS.

For floods (and debris flows),

- The only available interactive database to perform a search according to point 2 of the procedure is the flood model database. A search within this database only produced the JRC, Asia, Concrete and Residential empirical vulnerability function as a candidate model.
- The model compendia search supporting point 3 of the procedure resulted in the same model as well as the HAZUS, six-storey, Concrete, Residential model. The JRC model can be consistently applied to all building classes in Tomorrowville, which is one of the user requirements.
- A literature review specifically concerned with Nepali building classes did not produce any relevant match. The empirical model in Tang et al. [57] for Thailand is identified as the country-level model closest to the geographic area relevant for Tomorrowville.
- The candidate flood models are then scored against the criteria and ranked according to TOPSIS (Table below). The JRC model was selected due to its highest score in the relevance criterion.



**Table 24: Model Ranking for the CP+CIP/LFINF+CDM/H:6/YBET: 1994:2015
(RCi+MC+6s+Res) building class**

Criterion: Attribute	Earthquake						Flood and debris flow		
	Akkar	Erberik	Crowley	HAZUS	Gautam	Gentile	JRC	HAZUS	Tang
<u>Relevance:</u>									
Geographical area	<u>Low</u>	<u>Low</u>	<u>Low</u>	<u>Low</u>	<u>High</u>	<u>Med</u>	<u>Med</u>	<u>Low</u>	<u>Low</u>
Asset characteristics	Med	Med	Med	Low	Med	High	Med	Med	Med
IM	Med	Med	Med	Low	Med	High	High	High	High
<u>Statistical refinement:</u>									
Uncertainties	<u>Med</u>	<u>Med</u>	<u>Med</u>	<u>Med</u>	<u>Med</u>	<u>High</u>	<u>Med</u>	<u>Med</u>	<u>Med</u>
First principles	High	High	High	High	High	High	High	High	High
<u>Model quality (empirical):</u>									
Impact observations	-	-	-	-	-	-	<u>Med</u>	<u>Med</u>	Med
IM observations	-	-	-	-	-	-	High	High	High
Constrained asset class	-	-	-	-	-	-	Med	Med	<u>Low</u>
Data quantity	-	-	-	-	-	-	High	High	Med
<u>Model quality (synthetic):</u>									
Fidelity to mechanics	<u>Med</u>	<u>Med</u>	<u>Med</u>	<u>Med</u>	<u>Med</u>	<u>High</u>	-	-	-
Aggregation level	Med	Med	Med	Med	High	High	-	-	-
<u>User requirements:</u>									
TOPSIS score	0	0	0	0	0.55	0.66	1	0.60	0
Ranking	3	3	3	3	2	1	1	2	3

As a result of the model selection procedure to all the building classes in Tomorrowville, 11 different earthquake fragility models are identified necessary.

- The fragility models in the study by Guragain [2] calibrated explicitly on Nepali building classes, are selected and applied for the Adb, BrM, BrCfl, BrCri, StMin components of the taxonomy string.
- The fragility models proposed by Gentile et al. [56] are used for all the RCi buildings, which are assigned based on height (LR, MR) and code-level (LC, MC, HC) components of the taxonomy string. Six different RCi building classes (i.e. combinations of LR/MR and LC/MC/HC) are present in Tomorrowville.



All the adopted earthquake fragility models are based on numerical simulations and use the same DS characterization i.e. slight (DS1), moderate (DS2), extensive (DS3) and complete (DS4).

For flood vulnerability functions, the JRC model is applied to all the building classes, considering the “Asia, Res” baseline function. The maximum damage of the baseline functions is modified by appropriate factors for RCi, Adb, BrM, BrCfl, BrCri and StMin buildings. The height modifier is then applied to these functions, leading to 48 unique flood/ debris-flow vulnerability functions across all considered building classes.



SESSION 11: NETWORK ANALYSIS

11.1 Objectives

By the end of the session, the participants will be able to:

- Use graph theory for modelling infrastructure.
- Define connectivity-based and flow-based analyses.
- Apply infrastructure performance assessment before and after the occurrence of a future hazard.

11.2 Structure of Session 11

Structure
1. Network Representation of Infrastructure
2. Types of Infrastructure Analysis
3. Infrastructure Performance Assessment in Post-Hazard Conditions
4. Exercises

11.3 Network Representation of Infrastructure

11.3.1 Motivations

The well-being and economic prosperity of societies depend on critical infrastructure and their provision of goods, services, and resources to communities. Critical infrastructure enables individuals to achieve valuable states and activities. For instance, while having access to energy and being mobile are directly reliant on the performance of the power and transportation infrastructure, food security and business activities could be indirectly affected by the reduction in the performance of critical infrastructure. Past events highlighted the vulnerability of infrastructure to disruptions caused by natural or anthropogenic hazards. There are also complex interdependencies among infrastructure. Such interdependencies can cause disruptions to propagate across infrastructure, resulting in multi-fold catastrophic consequences at several levels (e.g., individuals, households, and communities).

We need to be able to have tools that can simulate these impacts and make the best use of them to plan accordingly.

11.3.2 Graphs and Networks

We can represent infrastructure using graph theory. Graphs have been widely used in several fields, such as social science, neuroscience, and environmental engineering. Graphs are mathematical structures amounting from pairwise related objects called vertices (points or nodes) and the relation between a pair of nodes as edges (arcs, lines, or links.) Mathematically, a graph is written as $G = (V, E)$, where V is the set of nodes and E is the set of links.

Then, networks are defined as graphs in which the nodes and links possess attributes like names, hierarchy, functions, type, and state variables in addition to their topological identities (i.e., the pairwise relations that define the graphs.)

11.3.3 Infrastructure Modelling Definitions

Using a triplet of measures (capacity, demand, and supply), we can write the general expression for derived performance measures, i.e., a measure of how well the infrastructure is fulfilling



the stakeholders’ needs. The capacity of infrastructure is the measure of its ability to generate or transmit specific resources or services pertaining to the specific infrastructure’s purpose. The demand for infrastructure is the measure of its consumers’ needs in terms of the resources and services provided by the specific infrastructure. Lastly, the supply is the portion of the capacity that is mobilized by an infrastructure to meet an imposed demand. The following table provides additional definitions of the terminology typically used for infrastructure modeling. (**Original source:** Sharma, N., & Gardoni, P. (2022). “Mathematical modeling of interdependent infrastructure: An object-oriented approach for generalized network-system analysis.” *Reliability Engineering & System Safety*, 217, 108042. [58])

Table 25: Description of infrastructure modelling terms

Terms	Description
Base measures	The measures (for example, capacity and demand) are base measures if they are calculated using information limited to the specific infrastructure while assuming normal operations of all other interacting infrastructure. Base measures calculations do not consider the cascading effects coming from interdependencies.
Capacity	The capacity of infrastructure is the measure of its ability to generate or transmit the specific resources or services pertaining to the specific infrastructure’s purpose. The capacity of infrastructure is typically distributed both spatially over its various components and temporally. Infrastructure may have multiple capacity measures necessary to capture a variety of needs for resource/service generation and maintain operational safety
Demand	The demand on infrastructure is the measure of its consumers’ needs in terms of the resources and services provided by the specific infrastructure. Like capacity, demand on infrastructure may also be distributed spatially over its various components and temporally. Infrastructure may have multiple demand measures corresponding to the various capacities. Infrastructure failure can occur when infrastructure demand is more than its capacity. When the demand for infrastructure is less than its capacity, the control system should only mobilize a portion of its capacity.
Infrastructure	Shishko and Aster defined a system as “[t]he combination of elements that function together to produce the capability to meet a need. The elements include all hardware, software, equipment, facilities, personnel, processes, and procedures needed for this purpose.” We adopt the same definition also for infrastructure, as they serve the basic needs of modern society.
Network	A network is defined as a set of pairwise related objects where each of those objects has attributes other than the topology of their relations. Infrastructure can be mathematically represented by multiple interdependent network objects where individual network objects have specific capacity and demand measures, which serve a specific need in collectively attaining the purpose of the infrastructure. For example, a structural network object may serve the purpose of the physical integrity of infrastructure, while a flow network object may serve the purpose of a general commodity exchange.
Performance	The performance of infrastructure is defined as a measure of how well the infrastructure is fulfilling the stakeholders’ needs. Different stakeholders, such as the owners, the regulators, and the consumers, may have different requirements and infrastructure performance measures. The owners typically prioritize profitability and efficiency. The regulators represent the collective societal interests and prioritize quality, reliability, environmental protection, and economic justice. Consumers are typically concerned with the impact of the infrastructure services on their socio-economic activities, measured in functionality.
Supply	Supply is the portion of the capacity that is mobilized by an infrastructure to meet an imposed demand. The supply for a particular capacity and demand is



	not unique and depends on the control state variables. Different infrastructure may present different challenges to controlling supply. Control challenges may arise from infeasibility, inefficiency, cost, computation issues, legality, and ethics. Supply (along with capacity and demand) is needed to measure the infrastructure performance in terms of derived measures such as efficiency, reliability, and functionality.
--	---

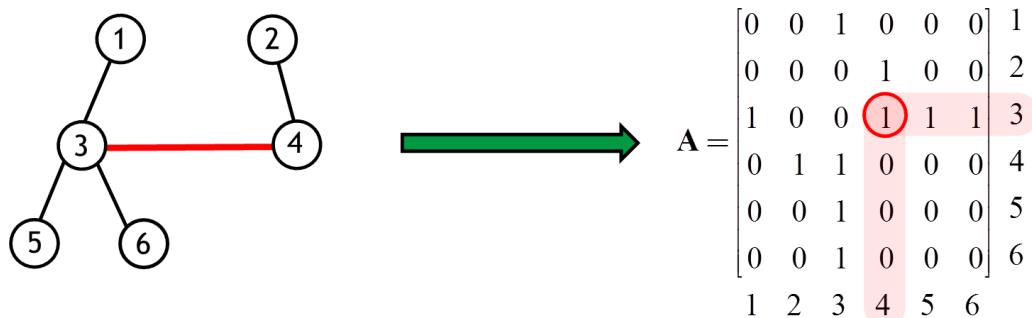
11.3.4 Need for Network Reliability

Components and systems are connected; for example, bridges may be part of a larger transportation network. We need to move from the reliability of a single component to the reliability of interconnected components at the network level.

However, network reliability analysis is challenging because (i) **the definition of network failure is complex**. It is given by a mix of physical damage and loss of functionality of the network elements. The major problems for networks come from the lack of connections and the limited accessibility, and (ii) **the network elements are heterogeneous**. Networks represent nodal components (such as cities, bridges, and water demand nodes) and links (such as pipes, highways, and electric power distribution lines) and links; some nodes or links may also have greater importance than others.

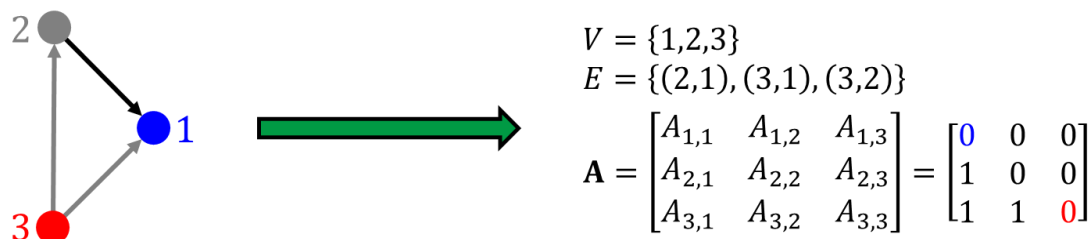
The first step in the network reliability analysis is to define the network topology. A network can be represented by a 0-1 table (*adjacency matrix*) with 0 on the diagonal and 1 if there is a link between node i and j .

Example:



Alternatively, we can use a set of nodes and a set of edges, including the relations among the nodes.

Example:



Because of the complexity of the problem, we need to rely on computing programming to deal with infrastructure and network analysis. *NetworkX* is a Python package for the creation, manipulation, and study of the structure, dynamics, and functions of complex networks



([NetworkX – NetworkX documentation](#)). Using two input files, we can construct a network in Python. The two input files can be stored in Excel sheets containing the nodes and edges list.

NODE_ID	POINT_X	POINT_Y	ID	FROM_NODE	TO_NODE	SLength	class
1	0	3.61	1	1	2	1.664	0
2	1	4.93	2	2	24	0.47	0
3	2	4.93	3	24	3	0.53	0
...
32	3.1	1	43	8	12	0.87	0

Example nodes list

Example edges list

Then, we pass these two input files to *Networkx* and build the network in Python (code below).

```

1. import pandas as pd
2. import networkx as nx
3.
4. def generate_network(list_of_nodes,list_of_edges,excel):
5.     if excel == 1:
6.         Nodes = pd.read_excel(list_of_nodes)
7.         Edges = pd.read_excel(list_of_edges)
8.     else:
9.         Nodes = list_of_nodes
10.        Edges = list_of_edges
11.        # Initialize Graph
12.        G = nx.Graph()
13.        try:
14.            # Add Nodes with Node ID and Coordinates
15.            for i in range(len(Nodes)):
16.                G.add_nodes_from([Nodes['NODE_ID'][i]],pos=(Nodes['POINT_X'][i],Nodes['
POINT_Y'][i]))
17.            del i
18.        except:
19.            print('Check node list - missing either NODE_ID, or POINT_X, POINT_Y')
20.        # Add Edges with length, and road type information
21.        try:
22.            for i in range(len(Edges)):
23.                e = (Edges['FROM_NODE'][i],Edges['TO_NODE'][i])
24.                G.add_edge(*e,ID=Edges.index[i],length=Edges['SLength'][i],road_type=Ed
ges['class'][i])
25.        except:
26.            print('Check edge list - missing either FROM_NODE, TO_NODE, SLength or class')
27.        return G
28.
29. list_of_nodes = 'Nodes_centerville.xlsx'
30. list_of_edges = 'Edges_centerville.xlsx'
31. excel = 1
32.
33. G_centerville = generate_network(list_of_nodes,list_of_edges,excel)

```

11.4 Types of Infrastructure Analysis

Infrastructure analyses can be classified into two categories, i.e., (i) topology-based approaches and (ii) flow-based approaches.

Topology-based approaches rely on measures of connectivity. They capture the connectivity of the considered infrastructure, which is generally a **necessary** condition for a fully operational



infrastructure. The concept of network failure in topology-based models is typically defined as the loss of connection after a disturbance between some nodes and the rest of the network.

Instead, **flow-based approaches** consider the specific flow of goods and services delivered by the considered infrastructure. They capture the ability of the critical infrastructure to provide essential goods and services to the community they serve. The concept of network failure in flow-based approaches is typically defined in terms of loss or reduction of functionality, which is the impossibility of the network to provide the required amount of goods and services.

11.4.1 Topology-based Approaches

Diameters and efficiency are measures of network connectivity. Two nodes are said to be connected if there is at least one path between them with a finite number of steps (links). The loss of connectivity can be considered a measure of network failure.

A. Definitions

Diameter δ is the average length of the shortest paths between nodes i and j – it is defined only for a connected network. **Efficiency** η is the average length of the inverse of the shortest paths between nodes i and j – it is always defined (between 0 and 1).

The adjacency matrix can also be weighted using a link weight matrix. For example, this can be done using the length of each link. Diameter and efficiency are then computed considering the length of each link.

Path is a sequence of edges that begins at a vertex of a graph and travels along the edges of the graph, always connecting pairs of adjacent vertices. **Shortest Path** is a path of the minimum weight (e.g., defined in terms of distance based on the link weight matrix).

B. Example Code to Compute δ And η Using the Network We Built During the First Part of this Session

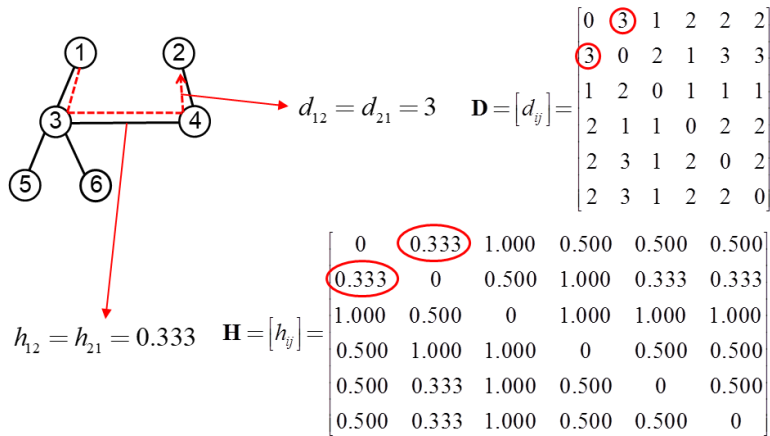
```

1. import networkx as nx
2. import numpy as np
3.
4. paths_length = dict(nx.all_pairs_dijkstra_path_length(G_centerville, weight='length'))
5. h_temp = 0
6. n = len(G_centerville)
7. for elem in paths_length.keys():
8.     val = np.array(list(paths_length[elem].values()))[1:]
9.     h_ij = 1/val
10.    h_i = np.sum(h_ij)
11.    h_temp += h_i
12.
13. h = h_temp/(n*(n-1))
14. delta = nx.average_shortest_path_length(G_centerville, weight='length')

```

To calculate the diameter and efficiency of a network, let us compute the matrices **D** and **H** of the shortest paths and of the inverse of the shortest paths. Each element $[d_{ij}]$ of the matrix **D** is computed considering how many steps (links) are needed to go from node i to node j . Then, the elements $[h_{ij}]$ of the matrix **H** are computed by taking the inverse of d_{ij} , i.e., $h_{ij} = 1/d_{ij}$. Then, the average of the values of the matrices **D** and **H** will provide an estimate of the diameter and efficiency of the network, respectively. For example, to go from node 1 to node 2, we pass through 3 links. Hence, $d_{12} = 3$, and $h_{12} = 0.333$.

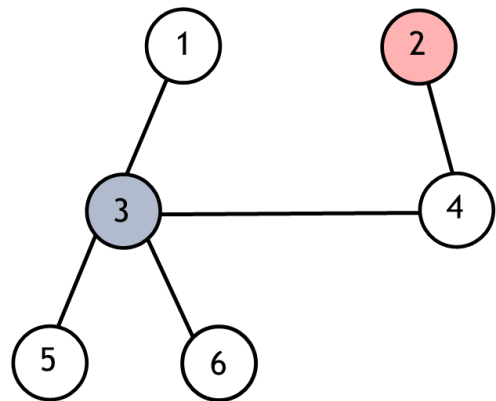




$$\delta = \frac{1}{n(n-1)} \sum_{i=1}^n \sum_{\substack{j=1 \\ j \neq i}}^n d_{ij} = \frac{56}{30} = 1.867$$

$$\eta = \frac{1}{n(n-1)} \sum_{i=1}^n \sum_{\substack{j=1 \\ j \neq i}}^n h_{ij} = \frac{19}{30} = 0.633$$

In graph theory and network analysis, indicators of centrality assign numbers or rankings to nodes within a graph corresponding to their network position. Applications include identifying the most influential person(s) in a social network, key nodes in urban networks, super-spreaders of disease, and brain networks.



As an example, degree centrality measures the number of edges that are incident to the vertex. Considering the following network, the degree centrality of node #3 is 4, and the degree centrality of node #2 is 1.

11.4.2 Flow-based Approaches

Flow-based methods track metrics of interest related to the flow of goods and services within the network. For example, in the case of transportation infrastructure, a traffic flow analysis is conducted to obtain the values of the travel time along the edges. Similarly, in the case of a potable water infrastructure, a hydraulic analysis is conducted to obtain the values of the water pressure at the distribution nodes as a metric of interest. Therefore, each network needs to be analyzed based on the specific features of the network itself, i.e., by solving the governing equations of the flow. Understanding the governing equations of the flow for each infrastructure is beyond the scope of this session. However, there are python packages that can be leveraged to solve infrastructure flow analyses - listed below.

Communities are composed of multiple layers of structures and infrastructure, including transportation, water, and electric power networks.

Each network needs to be analyzed based on the specific features of the network itself - solving the governing equations. There are available packages that can be used. For instance, we can use “SUMO” for the traffic flow analysis. Similarly, for the water flow analysis, we can use the python package “WNTR.” Lastly, we can use the python package PyPSA to run power flow analyses. In the following, there are more details on each package and the links to the relative web pages to access them.

Traffic flow analysis: Sumo.

“Simulation of Urban MObility” (SUMO) is an open-source, highly portable, microscopic, and continuous traffic simulation package designed to handle large networks. It allows for intermodal simulation, including pedestrians, and comes with a large set of tools for scenario creation. Available at: [SUMO Documentation \(dlr.de\)](http://sumo.dlr.de)

Water flow analysis: WNTR.



The Water Network Tool for Resilience (WNTR, pronounced winter) is a Python package designed to simulate and analyze the resilience of water distribution networks. WNTR has an application programming interface (API) that is flexible and allows for changes to the network structure and operations, along with the simulation of disruptive incidents and recovery actions. Available at: [Overview – WNTR 0.5.0.rc5 documentation](#)

Power flow analysis:

PyPSA. PyPSA is an open-source toolbox for simulating and optimizing modern power systems that include features such as conventional generators with unit commitment, variable wind and solar generation, storage units, coupling to other energy sectors, and mixed alternating and direct current networks. Available at: [PyPSA: Python for Power System Analysis – PyPSA 0.21.2 documentation](#).

11.5 Infrastructure Performance Assessment in Post-Hazard Conditions

There are three fundamental steps to running an infrastructure performance assessment in post-hazard conditions. First, we need information on the hazard (from Sessions 1-5 of this Module). Then, we need the inventory of the network elements, including the list of the vulnerable components to each hazard of interest. Lastly, we need performance-intensity measure curves, e.g., damage, fragility, or repair rates curves (from Sessions 7-9 of this Module).

We use the information from the hazard model to obtain the values of the intensity measure(s) at the site of the vulnerable components of the network.

Then, we combine this information with fragility functions and repair rates and obtain a representation of the damaged network (e.g., using Monte Carlo simulations to simulate if a network component fails). Such representation could result in a reduction in capacity and demand.

Lastly, we use topology-based or flow-based approaches **on the damaged network** to quantify the impact of the hazard.

Then, we need to look at the recovery of the physical components and translate it into changes in the network performance. For each time step, we simulate the recovery status. The status of each element depends on the damage level and its corresponding recovery function. To the new status will correspond a new functionality analysis. If the desired levels of functionality are not met, the network is not recovered, and we move to the next time step.

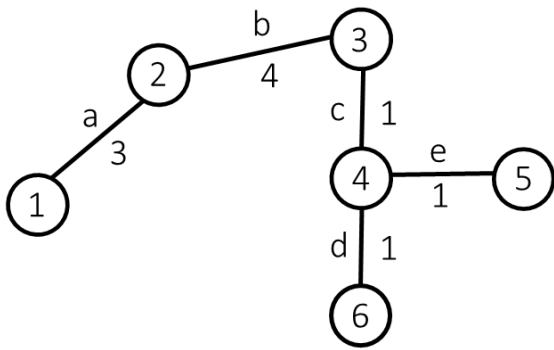
What we saw earlier translates visually in this figure here. At each step, we first quantify the damage state of each component. Then, the new status will correspond to a new functionality analysis. For instance, if we are interested in estimating the distance between points A and B, we see that right after a damaging event, the route is highly impacted (in fact, we will have to take a longer route. After a certain time from the occurrence of the damaging event, certain components are recovered, yet the route from A to B results in being impacted, and it is not the same as when the network is fully recovered. Lastly, in the end, when all the components are back functioning, the route from A to B is again the same as before the damaging event.

11.6 Exercises

11.6.1 Exercise 1: Infrastructure Representation – Adjacency matrix

Write the adjacency matrix representation of the following graph, both a) unweighted and b) weighted representation:





Solution a)

$$A = \begin{bmatrix} 0 & 1 & 0 & 0 & 0 & 0 \\ 1 & 0 & 1 & 0 & 0 & 0 \\ 0 & 1 & 0 & 1 & 0 & 0 \\ 0 & 0 & 1 & 0 & 1 & 1 \\ 0 & 0 & 0 & 1 & 0 & 0 \\ 0 & 0 & 0 & 1 & 0 & 0 \end{bmatrix}$$

Solution b)

$$A = \begin{bmatrix} 0 & 3 & 0 & 0 & 0 & 0 \\ 3 & 0 & 4 & 0 & 0 & 0 \\ 0 & 4 & 0 & 1 & 0 & 0 \\ 0 & 0 & 1 & 0 & 1 & 1 \\ 0 & 0 & 0 & 1 & 0 & 0 \\ 0 & 0 & 0 & 1 & 0 & 0 \end{bmatrix}$$

11.6.2 Exercise 2: Topology Metrics – Computing Diameter and Efficiency

Given the network in Exercise 1 (and the weights of each link), compute the values of c) diameter and d) efficiency

Solution c)

$$D = \begin{bmatrix} 0 & 3 & 7 & 8 & 9 & 9 \\ 3 & 0 & 4 & 5 & 6 & 6 \\ 7 & 4 & 0 & 1 & 2 & 2 \\ 8 & 5 & 1 & 0 & 1 & 1 \\ 9 & 6 & 2 & 1 & 0 & 2 \\ 9 & 6 & 2 & 1 & 2 & 0 \end{bmatrix}$$

$$\delta = \frac{1}{n(n-1)} \sum_{i=1}^n \sum_{\substack{j=1 \\ j \neq i}}^n d_{ij} = \frac{66}{30} = 2.20$$

Solution d)

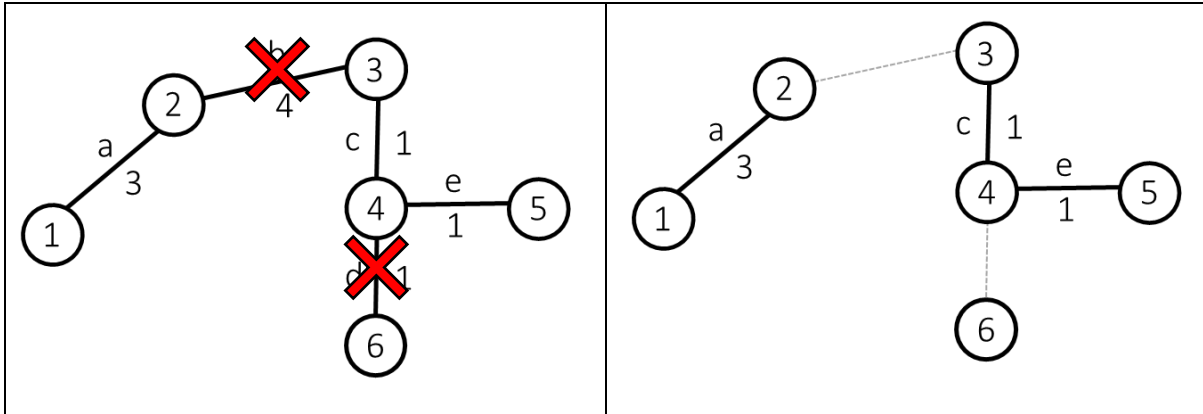
$$H = \begin{bmatrix} 0 & 0.333 & 0.143 & 0.125 & 0.111 & 0.111 \\ 0.333 & 0 & 0.250 & 0.200 & 0.167 & 0.167 \\ 0.143 & 0.250 & 0 & 1 & 0.500 & 0.500 \\ 0.125 & 0.200 & 1 & 0 & 1 & 1 \\ 0.111 & 0.167 & 0.500 & 1 & 0 & 0.500 \\ 0.111 & 0.167 & 0.500 & 1 & 0.500 & 0 \end{bmatrix}$$

$$\eta = \frac{1}{n(n-1)} \sum_{i=1}^n \sum_{\substack{j=1 \\ j \neq i}}^n h_{ij} = \frac{12.214}{30} = 0.407$$

11.6.3 Exercise 3: Infrastructure Performance Assessment in Post-hazard conditions – Changes in Network Performance

A hazard occurs in the region of interest, and links b and d are out of service. What are the new values of e) diameter and f) efficiency (Draw the damaged network for completion)?





Solution e) The new value of $\delta = \infty$ because the network is now disconnected. So, for example, the path from node #2 to node #3 will be ∞ . Consequently, taking the mean of the matrix D will result in an infinite value.

Solution f)

$$\mathbf{H}' = \begin{bmatrix} 0 & 0.333 & 0 & 0 & 0 & 0 \\ 0.333 & 0 & 0 & 0 & 0 & 0 \\ 0 & 0 & 0 & 1 & 0.500 & 0 \\ 0 & 0 & 1 & 0 & 1 & 0 \\ 0 & 0 & 0.500 & 1 & 0 & 0 \\ 0 & 0 & 0 & 0 & 0 & 0 \end{bmatrix}$$

$$\eta' = \frac{1}{n(n-1)} \sum_{i=1}^n \sum_{\substack{j=1 \\ j \neq i}}^n h'_{ij} = \frac{5.666}{30} = 0.189$$



SESSION 12: SOCIAL IMPACT

12.1 Objectives

By the end of the session, the participants will be able to:

- Identify the relevant inputs for social representation of vulnerability.
- Identify gaps in the social inputs for the TCDSE and explain ways in which these can be filled using qualitative and qualitative methods.
- Explain how SoVI is employed in the TCDSE.
- Discuss on the development of vulnerability proxies to assess changes to disaster risk over time.

12.2 Structure of Session 12

Structure
1. Social Vulnerability
2. Quantitative Methodology for Social Data Capture and Input
3. Utilizing Development Proxies to Inform Social Vulnerability and Impact

12.3 Social Vulnerability

Since the mid to late 1970s there was an emerging recognition that disasters did not impact upon individuals and communities in an equal way. Rather, the core observation was that some people were more vulnerable than others, and that these vulnerabilities could not be reduced to one's physical location. The core argument, then, is that disasters are themselves inherently social in origin, and thus to understand what leads to disasters, how there are variable impacts on individuals and communities, and indeed how to best engage with Disaster Risk Reduction, we need to address underlying social drivers of disasters. The UNISDR defines vulnerability as “the conditions determined by physical, social, economic and environmental processes, which increase the susceptibility of a community to the impact of hazards” (UNISDR 2009). We are interested here in social vulnerability.

12.3.1 Factors Shaping Social Vulnerabilities

- Physical factors (infrastructure)
- Social factors (class, genders, ethnicity, age, sexuality, etc.)
- Cultural factors
- Economic factors (structural economic impacts)
- Environmental factors
- Political and legal factors

12.3.2 Capturing Social Impact

The structure of capturing social vulnerability and practicability of measuring and integrating it into a modelling framework (of any kind) is a fluid process that is very much defined by the boundaries of the social and personal background of the population being modelled, collectively giving rise to a cultural makeup, composed of aspects including personal status and family situation to economic status and attitudes of risk sharing. Bringing such a potentially limitless combinations of cross scale variables into the context of a model requires a systematic approach towards bounding what is relevant, useful, and indicative.



Here, it is pertinent to state the meaning of social impact within the context of the TCDSE as a *'Fundamentally normative commitment to reduce vulnerabilities and improve the lives of populations.'* To go some way to addressing this, a requirement will be the **Effective development of means to:**

- Capture the demographics of urban spaces
- Measure & assess drivers of vulnerabilities
- Facilitate the reduction of vulnerability; and
- Support assessment of the impact of planning choices on vulnerabilities.

12.3.3 Process to Assess Social Impact

Shown in figure below is a suggested structure for approaching this in such a way. Composed of two units covering data input and methodology, the approach offers a format for apprehending the dynamics of change from a social perspective in relation to urban planning (this can however be adapted to consider specific hazard contexts to compliment the PHM methods you will have encountered in other parts of this module.) This brings us nicely onto the materials for Section 12.4, where we are introduced to the available data, the relevant process for gap identification and differentiated methodological approaches to align data availability with key gaps in social function. An important point to think about here will be how these gaps can be addressed by considerations of what is available against what can be modelled, in addition to how these can be aligned to meet the needs of a population in an area of interest.

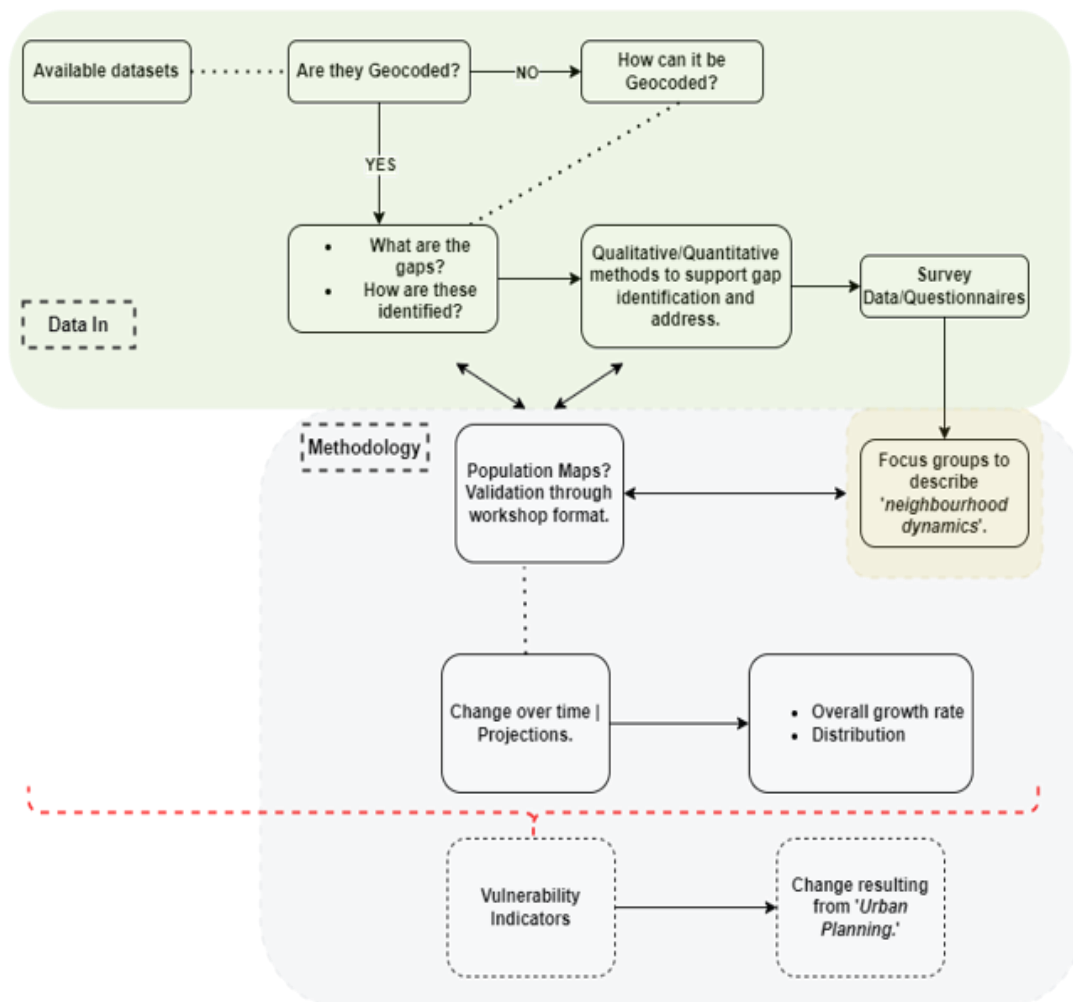


Figure 127: Structure of process to assess social impact



The overall aim here is to build on the modelling capabilities of the TCDSE and to best incorporate social components of areas of interest. This requires some thought about what makes up social data, which can consist of personal backgrounds of individuals as well as their social background. Personal status can be composed of factors like age, gender, mobility as well as cultural areas of difference and similarity and familial situation including marriage status and family structure. In terms of the data available to begin building a picture of this, household and individual levels of data may or may not be available through census and other formats. These can be of further use as they can support the composition of social background also by providing data on social position such as education level and employment, economic status from residence information and income. Details on social capital and risk sharing behaviours can be more difficult to assimilate as the former centres on patterns of contact and participation and so will largely need to be composed using survey and/or interview techniques and the latter is often presented through analysis of insurance data, which can be difficult to obtain.

Here we have identified some possible gaps in important inputs that, together, make up the social dimension of vulnerability and/or resilience and so they may or may not need to be considered when thinking about social impact. There are a number of approaches that can help reconcile these gaps through indexing and proxy development that can complement modelling approaches. Here we will begin by considering the methodological consideration for how we can do this in an efficient and useful way.

12.4 Quantitative Methodology for Social Data Capture and Input

In this section, we will be learning about how to orientate our thinking towards the quantitative elements of social data capture and input within the TCDSE.

Aim:

‘A fundamentally normative commitment to reduce vulnerabilities and improve the lives of populations.’

Key objectives:

- Measure and assess drivers of vulnerabilities.
- Facilitate the reduction of vulnerability, and
- Support assessment of the impact of planning choices on vulnerabilities.

Here, you will be able to:

- Consider the relevant inputs for social representation of vulnerability,
- Identify gaps in the social inputs for the computational platform,
- Address these gaps with a mixed methodological approach,
- Identify some data sources to support with rapid population of computational platform with socially representative data,
- Consider alternative approaches to address specific gaps in data rich/ data poor scenarios.

For this section, the outcomes will be:

1. Grasp of key ideas
2. An example methodology
3. Identification of data availability
4. Gap identification and address through modelling



12.4.1 Impact of Urban Planning on Social Vulnerability

We have the standard formulation of disaster risk being a function of vulnerability, exposure and hazard. Think through the ways in which Urban Planning can alter the social vulnerability component of this equation.

Vulnerable category	How might a proposed urban plan decrease the social vulnerability associated with the given category?	How might a proposed urban plan increase the social vulnerability associated with the given category?
Elderly		
Women		
Poor		
Disabled		

12.4.2 Keys Ideas and Example Methodology

When thinking about the data and methodology to address social vulnerability, we might think of the different quantitative methods at our disposal to address a specific question related to social impact and vulnerability. Using the Quantitative vs. Qualitative summary table below, complete the following:



QUANTITATIVE RESEARCH VERSUS QUALITATIVE RESEARCH

Quantitative Research uses statistics	Qualitative Research uses descriptions and observations
Data can be measured accurately	Data can be observed and not measured
Considered to be objective	Considered to be subjective
Uncovers measurable data to formulate theories and facts and uncover patterns	Helps to understand the underlying reasons, opinions, and motivations
Mainly uses hypotheses	Uses either hypotheses or research questions
Data collection methods are highly structured	Data collection methods are semi-structured or unstructured
The sample population is large	The sample population is small
	Pediaa.com

- **Prioritise** (by numbering the boxes 1 - 14) the key methodological points that you think will inform a methodology for informing social data input into the TCDSE.
- Refine these down to 7 points to give you a sense of a methodology for supporting with a social vulnerability data prioritisation and gap identification.
- Would you summarise your working methodology of being:



- Mixed?
- Mainly Quantitative?
- Mainly Qualitative?
- When thinking about the context of TC's, particularly around natural hazards
- What type of methodology do you think might be most important?
- Does your methodology from above address this need?
- How?
- If not, why not?

KEY QUESTION: What elements of this do you think would best support with the capture of social data and social vulnerability?

KEY POINT: Account for social vulnerabilities within the agent-based model and allowing the model to assess the impact of decisions on social vulnerabilities requires the deployment of metrics. Here, we are exploring which vulnerability index to deploy.

12.4.3 Identification of Data Inputs and Impacts

Ultimately the best approach towards addressing social vulnerability and characterising the social impacts as through a toolkit of mixed methods that both uncovers key data as well as helps to understand the underlying aspects of the social components for a given hazard scenario.

There are a range of data sources that can be used to inform the context of an event, including:

- **Population census:** Census data may include national level disaggregated socio-demographic and economic data (area, gender, occupation, education, etc.)
- **Ward level survey:** Local level disaggregated socio-demographic and economic data
- **Other relevant secondary sources:** Reports, Official records, Nepal Living Standard Survey, etc.
- Who/ where might you go to obtain this information from?

- Some instances might require the rapid assimilation of data to help prioritise potential areas of increased social vulnerability and/or risk. Some key sources for informing this scenario are:
 - Integrated Public Use Microdata Series (IPUMS) ([link](#))
 - UNICEF Multiple Indicator Cluster Surveys (MICS) ([link](#))
 - USAID Demographic and Health Survey Programme (DHS) ([link](#))
- Take a moment to familiarise yourself with these resources...
 - What do they offer in terms of **social** data availability?
 - How can this data be used to inform **potential impacts**?
 - What else might be required to support the capture of **social** vulnerability?
 - Can the data from these sources be used with the sources above to inform an accurate picture of vulnerability?
- Possible social impacts include: Casualties leading to breakdown of social groups, human displacement (permanent, temporary), business loss (industry, small traders, factories, restaurants, hotels, shops lost, etc.), job loss and/or impacts on income, agricultural loss (farmlands damaged, commercial farmhouse/animal sheds lost, livestock loss, food



production loss), infrastructure damage, loss of buildings (residential buildings, schools, hospitals, shelters), cultural damage (religious/cultural structures), environmental impacts.

- Which of these impacts might be best informed with the available data? What gaps are there? How might these be prioritised in terms of social need?

12.4.4 Gap Identification and Address through Modelling

Introducing new data using this approach is part of the validation process for informing social impact through vulnerability reduction (see figure below). The next step is to take this forward into the TCDSE and assess what elements of your methodology, data acquisition exercise and gap identification can come together to inform the social components of impact modelling and vulnerability capture.



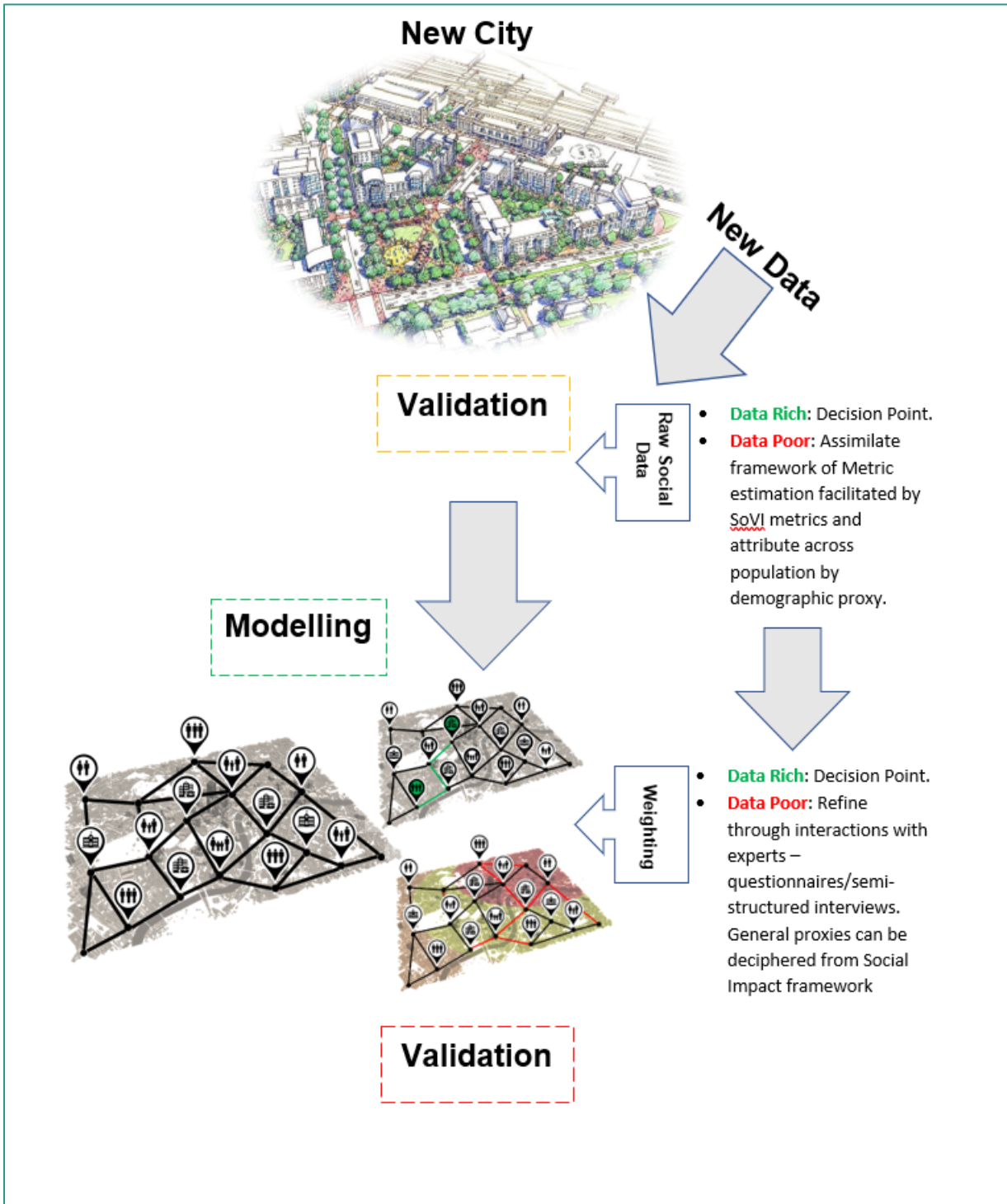


Figure 128: Impact modelling for gap identification

A. Exercise

Referring to the User Manual for the computational model, can you identify:

- The stage where your social data might be used to inform the model further?
- Will this be useful for informing social impact?
- How might this be enhanced?
- Social vulnerability does have points that cannot be captured through this process, particularly for data poor regions/areas. To assist with this, the Social Vulnerability



Indexing (SoVI) Method has been identified as a support mechanism to better address any further gaps.

- On the next page using the SoVI recipe pdf. and example, can you devise a summary Social Vulnerability matrix using the indicators you have identified as being important for input to the computerization to better identify areas of social impact?
- How might this change for data rich vs. data poor environments and how might this be reflected in the vulnerability weightings?

12.5 Utilising Development Proxies to Inform Social Vulnerability and Impact

For this section, the outcomes will be:

1. Grasp of methodological toolkit to develop proxy metrics.
2. Build a composite for weighing vulnerabilities.
3. Identification of trends to support proxy development.
4. Identification of key proxies to enhance social impact.

12.5.1 Assessing Changes to Vulnerability over Time

The drivers of social vulnerabilities are incredibly complex. They arise as a result of complex interactions of social, economic, political, and legal dynamics - as well as technology and education (to name but a few drivers). Modelling likely changes in any of these over a time scale of decades is not possible with any reasonable accuracy.

TCDSE effectively captures changes to the built environment. This provides a potential means of partially addressing change of social vulnerability over time. This slide provides a partial illustration of the complexity of the drivers of social vulnerability. To further complicate this, we need to recognize that changes in any one of these components will feed back into other drivers. We cannot assume that a positive change in one area will result in a straightforward reduction in overall social vulnerability for particular groups of people. This poses a further problem for attempts to model changes to social vulnerability over a time scale of decades. This would require an ability to account for alterations in each of these drivers. Consider the difficulty of predicting changes to the political dynamics informing an urban setting over a time frame of 20 years.

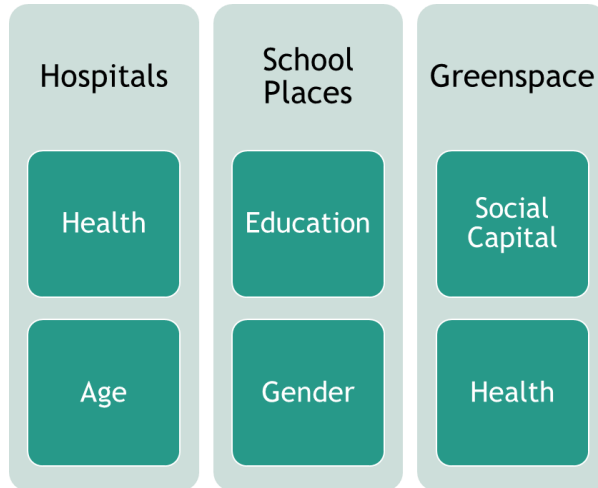
As such we are not able to model changes to social vulnerability in the future.

12.5.2 Assessing Social Impact using Changes to the Built Environment as Proxies

This is a useful approach for linking the previous materials covered to adaptive thinking for future development and dynamics that could, if untested, create increased impact factors for vulnerability and social impact.

In the example given in figure below, the table gives an outline of a vulnerability index that can be used to disaggregate such variables, as well as demonstrate the tangibility they might have with other well-known variables (as indicated by available data or through the framework of approaches developed through this session.)





Here, the approach would use changes in the built environment as an indicator of potential increase or decrease in disaster risk. This is not to capture change over time, which can be difficult to predict, but rather changes that may be presented because of urban planning and the well-documented relationship this has with positive and negative vulnerability indicators. An example of which might be more schools resulting in an increased volume of education and thus reducing overall vulnerability. As such, whilst the possible impact factor will remain, in this instance as a chance of 100%, there are various dependencies, centred around the nature of the hazard itself but also built environment proxies including health facilities, places of worship, school etc. that can be disaggregated to generate weightings that can, depending on their deployment within a model, or even conceptually through the matrix above, be used to reduce the overall vulnerability weighting for a specific indicator. This is a useful approach for linking the previous materials covered to adaptive thinking for future development and dynamics that could, if untested, create increased impact factors for vulnerability and social impact.

12.5.3 Applying the Built Environment Proxies

Each proxy is provided cardinal weighting (+ or -) depending on whether the change is seen as increasing or reducing the relevant component of the SoVI index. This change is relative to the baseline of the start of the implementation of the TCDSE (at present). i.e. Change in Built Environment = ± Disaster Risk. This is not to capture change over time, but rather change resulting from urban planning and the relationship this has to positive/ negative vulnerability indicators. For example, more schools = better education = a reduction in vulnerability....



SESSION 13: CHARACTERISING IMPACT METRICS

13.1 Objectives

By the end of the session, the participants will be able to:

- Discuss possible methods that can be used to identify the potential natural hazards.
- Identify data sources required to understand socio-economic and demographic context of the city.
- List out different impacts of the natural hazards.
- Discuss what an impact metric is.
- List examples of different types of impact metrics.
- Use methods of merging physical and social impacts of natural hazards, to characterize relevant impact metrics.
- Discuss how the computational platform computes impact metrics.

13.2 Structure of Session 13

Structure
1. Determining Relevant Natural Hazard Impacts for the City
2. How to Characterise Relevant Impact Metrics

13.3 Determining Relevant Natural Hazard Impacts for the City

The purpose of this lesson is to enable you to understand what methods can be used to identify the potential natural hazards, what data sources can be used to understand socio-economic and demographic context of the city and different impacts of the natural hazards to be considered.

13.3.1 Methods to Identify the Potential Natural Hazards

The potential methods to identify natural hazards can be Participatory Hazard Mapping (PHM) and field verification.

Participatory Hazard Mapping (PHM): The PHM can be conducted with potential stakeholders in the city e.g., past hazard victims, local residents, ward officials, teachers, farmers, etc., where participants are asked to locate natural hazards (experienced and potential) based on their knowledge within the given sketched boundary of the city. The process is then followed by field verification.

Field verification is done by observing the actual hazard/hazard prone sites with the help of PHM participants. GPS coordinates are also collected for records.

Example of experienced/potential natural hazards in a given city (fill in any more you can think of):

- Flood/inundation
- Landslides
- Earthquakes
- Fire (not natural in case of Khokana)

13.3.2 Possible Data Sources to Understand the Socio-economic and Demographic Context

To determine relevant natural hazard impacts, first it is imperative to understand the socio-economic and demographic context of the city.



Data sources that can be used:

- Research on local livelihood practices and risk of disaster
- CBS Data: Population census 2011, Nepal labour force survey, Nepal Living Standard Survey, etc. (may include national level disaggregated socio-demographic and economic data like gender, occupation, education, etc.)
- Ward/Municipal level survey: Local-level disaggregated socio-demographic and economic data (Income Tax Collection)
- Other relevant secondary sources: Reports, Official records (Examples: Baseline survey of LMC - 1999, Education International 2010)

13.3.3 List of Potential Impacts

Example of potential impacts:

- Casualty (number of deaths, seriously injured, minor injury)
- Human displacement (permanent, temporary)
- Business loss (cottage industry, small traders, factories, restaurants, hotels and shops lost)
- Job loss, daily wage
- Agricultural loss (farmlands damaged, commercial farmhouse/ animal sheds lost, livestock loss, food production loss)
- Infrastructure damage
- Loss of buildings (residential buildings, schools, hospitals, temporary shelters)
- Cultural damage (religious/cultural structures)
- Environmental impacts

13.4 Characterisation of Relevant Impact Metrics

The purpose of this lesson is to enable you to understand what impact metrics are, learn examples of different types of impact methods, and use methods for merging physical and social impacts of natural hazards, to characterise relevant impact metrics.

13.4.1 Impact Metric

Impact metrics are formal quantitative summaries of the Physical Infrastructure Impact and Social Impact module outputs.

A. Impact Metric Examples

List social impact metric examples:

.....
.....
.....
.....
.....
.....
.....
.....
.....

List economic impact metric examples:

.....
.....
.....
.....
.....
.....
.....
.....
.....



List environmental impact metric examples:

.....
.....
.....
.....
.....
.....
.....
.....
.....

13.4.2 Characterising Impact Metrics

A. Exercise 1: Characterising the Number of Orphans

Duration: 10 minutes

Tomorrowville 2050 is being planned, accounting for a M_w 7.5 earthquake that could occur 30km northeast at 1 pm on a working day. Explain how you would go about determining the number of orphans that may arise as a result of this earthquake event.

13.5 Use of Computational Platform to Compute Impact Metrics

The purpose of this lesson is to enable you to compute impact metrics with the computational platform. This lesson requires reference to an external user manual, which will act as the participants' workbook for the remainder of this session.



SESSION 14: END-TO-END DEMONSTRATION OF COMPUTATIONAL PLATFORM

14.1 Objectives

By the end of the session, the participants will be able to:

- Discuss the data formatting requirements of the computational platform
- Load appropriate data (related to visioning scenarios, hazard, and physical and social impact) into the computational platform.
- Initialize each successive calculation within the computational platform.

14.2 Structure of Session 14

Structure
1. Introduction
2. Computing Impact Using the Platform
3. TUTORIAL

14.3 Introduction

14.3.1 Background on the Computational Platform

The first version of the computational platform was developed as .m files in Matlab during the Tomorrowville demonstration. The code was then used as a backend to produce a user-friendly desktop application based on Matlab. The programming language of Tomorrow Cities desktop application is MATLAB® (R2022a). For simplicity this desktop application is called TCDA (Tomorrow Cities Desktop Application).

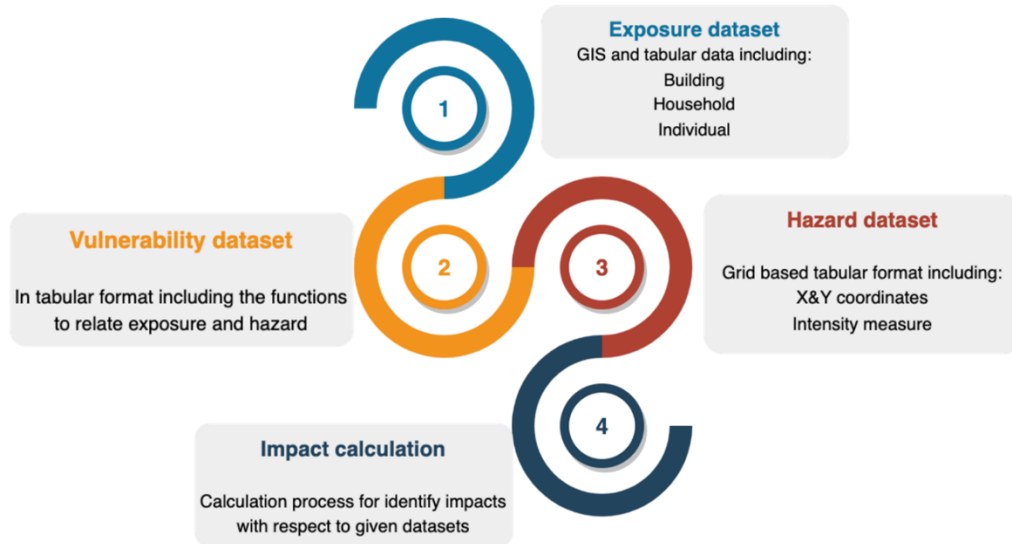
14.3.2 Installation Requirements

TCDA can only run on Windows(x64). For the installation of TCDA, the MATLAB Component Runtime (MCR) 9.12 is required. The MCR is a free redistributable that allows you to run programs written in a specific version of MATLAB without installing the MATLAB version itself. There is no harm in having MATLAB and the MCR installed simultaneously, or in having multiple versions of each one installed. *The installation guide is provided in the user guide for the application.*

14.3.3 Process of Computing Impact using the Platform

- Firstly, the exposure dataset is fed into the tool in the form of GIS and tabular data including information on buildings, households and individual.
- Next, the vulnerability dataset includes functions relating to exposure and hazard. They are provided as input.
- Then, grid based tabular hazard dataset including X and Y coordinates and intensity measures are also fed into the platform.
- Based on this information on exposure, hazard and vulnerability the platform calculates to identify impacts.





Source: Tomorrow's Cities

Figure 129: Process for computing impact

14.4 Computing Impact Using the Platform

14.4.1 Main Screen



Source: Tomorrow's Cities

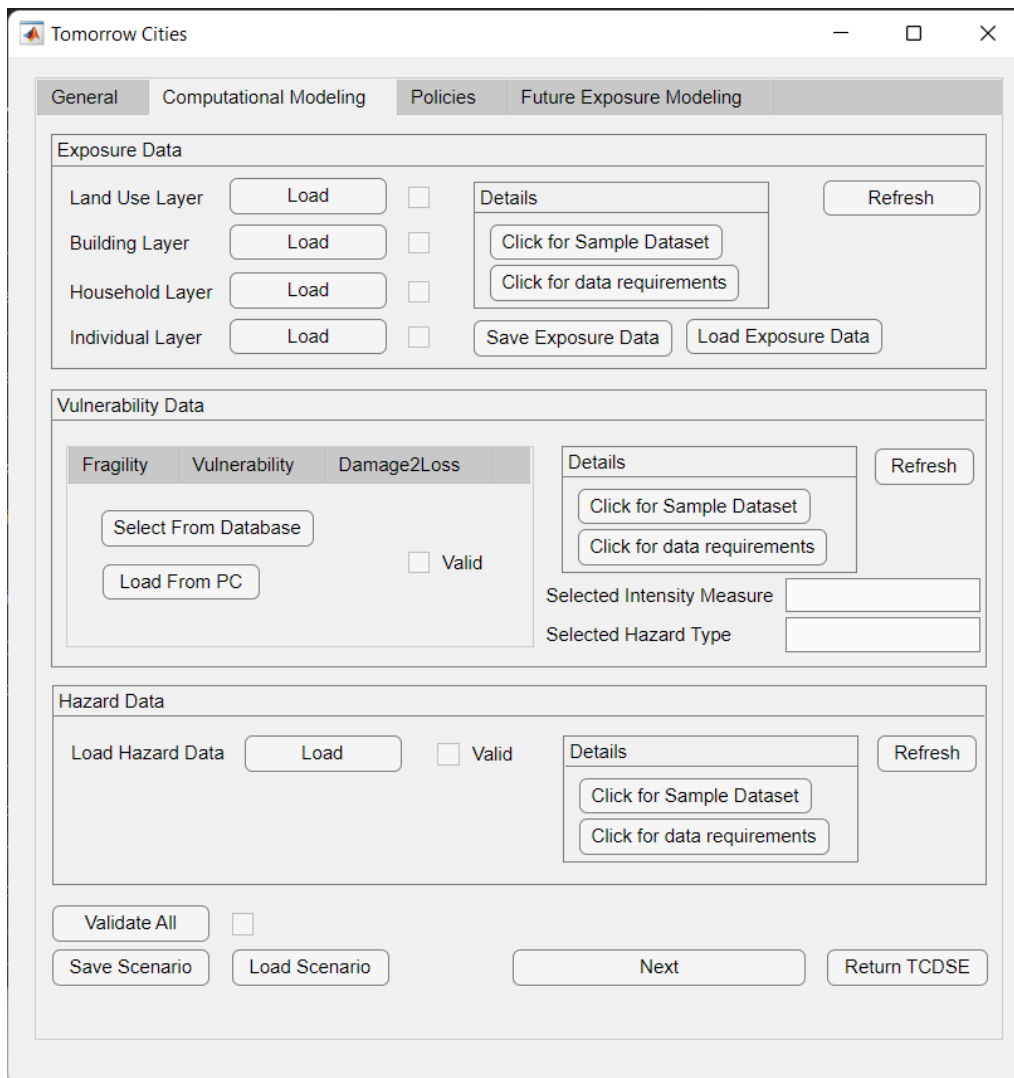
Figure 130: Main screen of the application



There are 2 different pushbuttons on the main screen. It would be better to give an explanation of every button briefly in this section. Push-button on the left side will open the Future Exposure Modeling screen which will help users to generate building, household and individual layer data just by providing land use data along with some probability distributions. Users will be able to generate synthetic data by using this program with their own customization. Computational Modeling screen can be opened with the push-button on the right side. This section will help users to calculate impact metrics by supplying exposure, hazard and vulnerability data.

A. Computational Modeling

When this button is pushed following screen will pop up:



Source: Tomorrow's Cities

Figure 131: Computational modeling page

In Figure above, there are three different panels for a user to interact with the application: Exposure Data, Vulnerability Data, and Hazard Data.

Exposure Data:

This panel provides loading section for different kinds of layers. For each layer data requirements are represented in the Details panel as can be seen in the figure below.

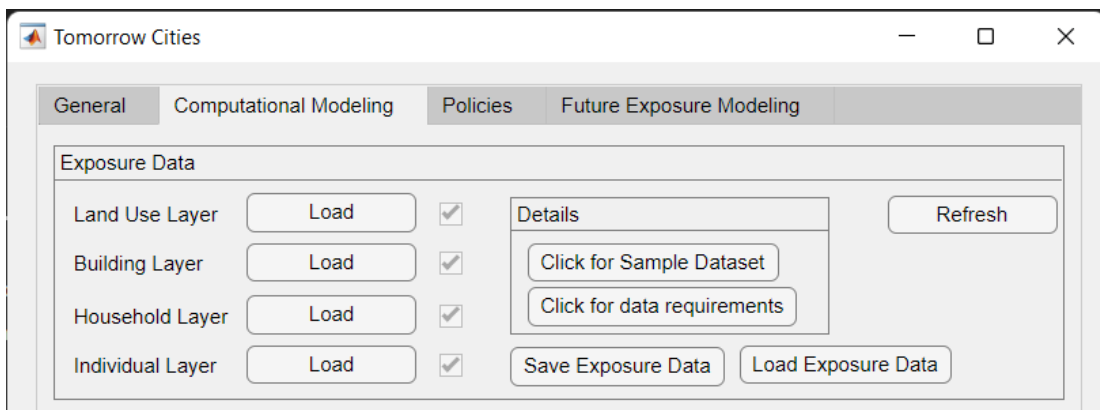


Land Use Layer	Building Layer	Household Layer	Individual Layer
zoneID	zoneID	bldID	hhID
LuF	bldID	hhID	indivID
densityCap	specialFac	nInd	gender
avgIncome	repValue	income	age
	nHouse	CommFacID	head
	residents		eduAttStat
	expStr		indivFacID

Source: Tomorrow's Cities

Figure 132: Exposure data requirements for every layer

Tooltips are given when the mouse is left stationary on the attributes of every layer. These attributes are checked every time the user load input layers, and warns user if requirements are not met. If there are not any problems with the data attributes, corresponding check boxes are ticked to let the user proceed to the next step as can be seen in below for all layers:

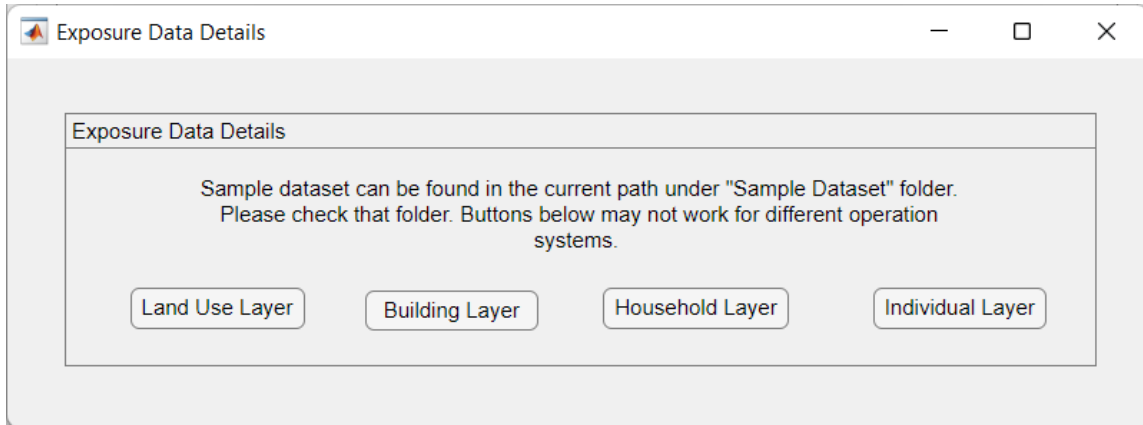


Source: Tomorrow's Cities

Figure 133: Exposure data validity for every layer

Following screen will pop up when the Click for Sample Dataset button is pushed in the Details panel:





Source: Tomorrow's Cities

Figure 134: Exposure data sample dataset for every layer

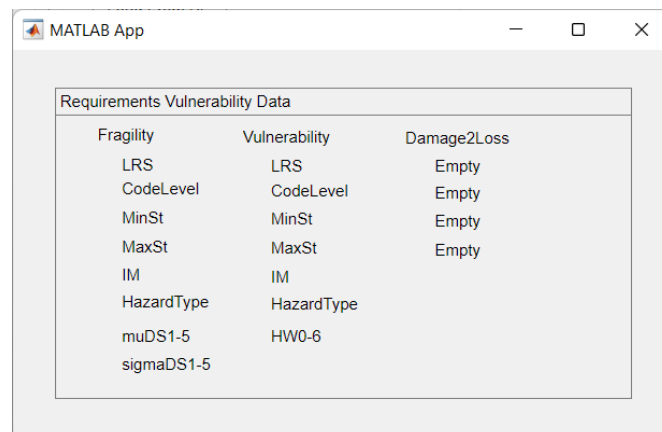
Note that pushing these buttons will open an excel file as an example. Other buttons in this panel will be described shortly below:

- **Save Exposure Data:** This button will allow user to keep all layers in a compact form which could later be used easily. In order to save exposure data, interrelations of all layers are checked beforehand. If there is any problem, the user will be warned and not allowed to save exposure data.
- **Load Exposure Data:** This button will help the user to load exposure data which is saved by this application before. Therefore, there is no need to check any data requirements nor interrelations between layers which will be a faster solution to load data.
- **Refresh:** User does not need to close the application, for changing the input layers data.

This button allows the user to refresh all the input layers once.

Vulnerability Data:

This panel provides loading section for different kinds of vulnerability data: Fragility, Vulnerability and Damage to Loss. Vulnerability data requirements are represented when clicking the Click for data requirements in the Details panel, which can be seen in Figure below:



Source: Tomorrow's Cities

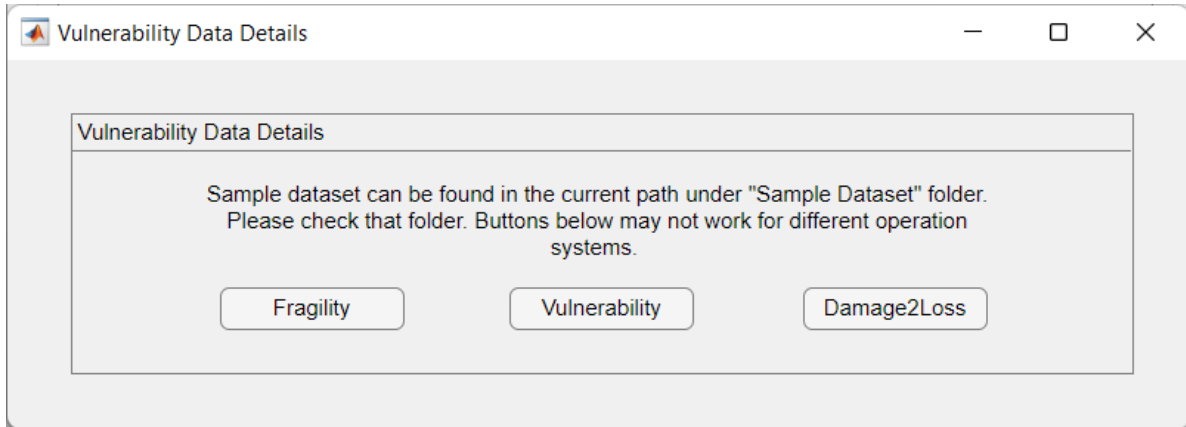
Figure 135: Vulnerability data requirements

Tooltips are given when the mouse is left stationary on the attributes of every layer.



These attributes are checked every time the user load vulnerability data, and warns the user if requirements are not met. If there are not any problems with the data attributes, corresponding check boxes (valid) are ticked to let the user proceed to the next step.

Following screen will pop up when the Click for Sample Dataset button is pushed in the Details panel:



Source: Tomorrow's Cities

Figure 136: Vulnerability data examples

Note that pushing these buttons will open an excel file as an example. Other sections in this panel will be described shortly below:

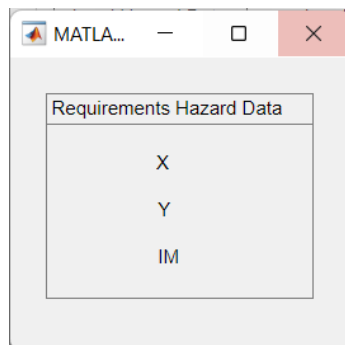
- **Selected Intensity Measure:** This is a string field to inform the user about the intensity measure which is obtained by utilizing the loaded vulnerability data.
- **Selected Hazard Type:** This is a string field to inform user about the hazard type which is obtained using the vulnerability data. This can be Earthquake, Debris Flow, Flood.
- **Refresh:** User does not need to close the application for changing the vulnerability data.

This button allows the user to refresh vulnerability data. Every time when using a new vulnerability.

data pushing this button is recommended.

Hazard Data:

This panel provides a loading section for hazard data. Hazard data requirements are represented in the Details panel as can be seen in Figure below:



Source: Tomorrow's Cities

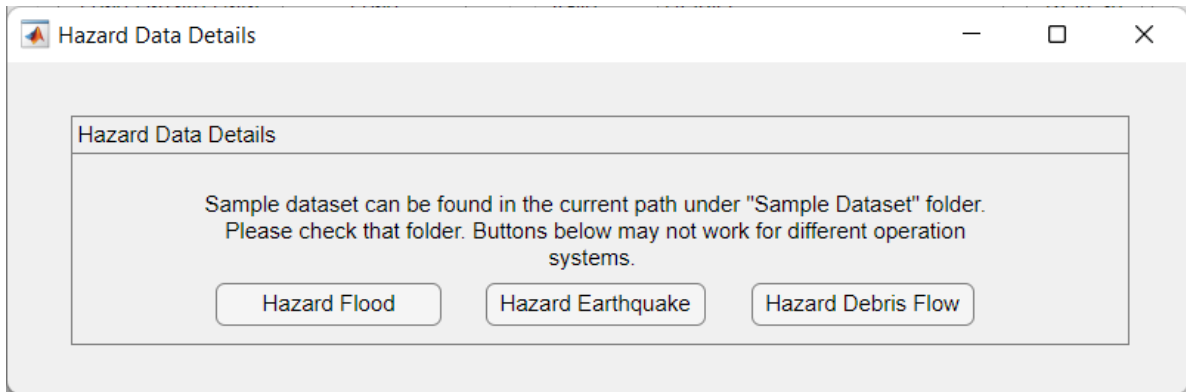
Figure 137: Hazard data requirements



Tooltips are given when the mouse is left stationary on the attributes.

These attributes are checked every time the user load hazard data, and warn user if requirements are not met. If there are not any problems with the data attributes, corresponding check boxes (valid) are ticked to let the user proceed to the next step.

The following screen will pop up when the Click for Sample Dataset button is pushed in the Details panel:



Source: Tomorrow's Cities

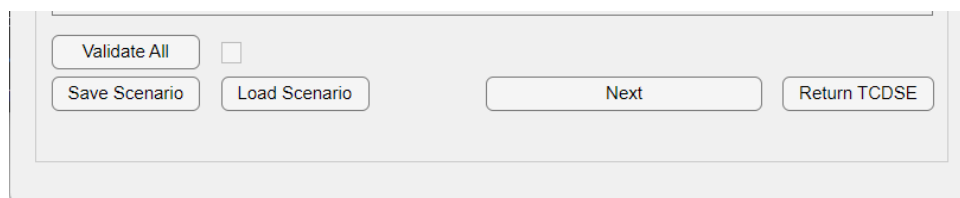
Figure 138: Hazard data examples

Note that pushing these buttons will open an excel file as an example. Other sections in this panel will be described shortly below:

Refresh: User does not need to close the application for changing the hazard data. This button allows the user to refresh hazard data. Every time when using a new hazard data pushing this button is recommended.

Other Buttons:

There are five push buttons at the bottom of the Computational Modeling page which will be described shortly as:



Source: Tomorrow's Cities

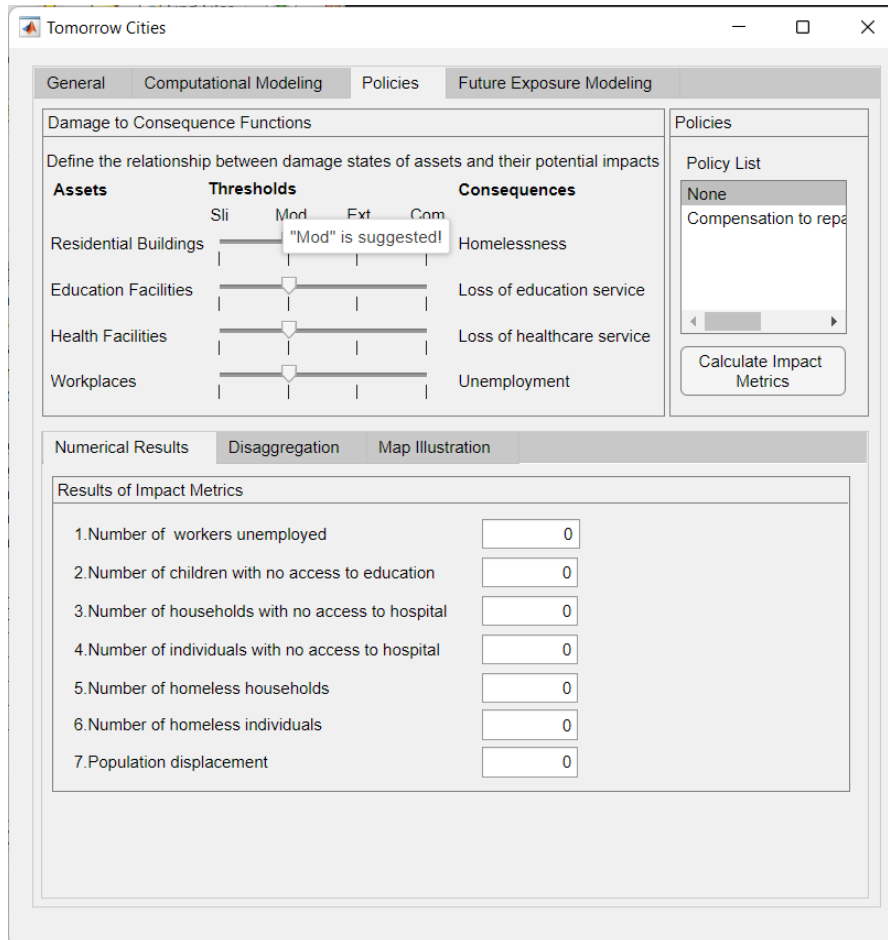
Figure 139: Other buttons

- **Return TCDSE:** Return the main page.
- **Next:** Proceed to the Policy page.
- **Validate All:** Not only exposure data should be validated, but also relations between vulnerability and exposure should be checked. Without validation, the user is not allowed to proceed to the next page. If validation successful, the checkbox near it will be ticked.
- **Save Scenario:** This button will allow user to save all input data.
- **Load Scenario:** User can load a scenario which is saved by this program.



B. Policies

After loading all necessary input files in the Computational Modeling page, the user will direct to the Policies page by clicking the Next button. The policy page has two main panels as can be seen in Figure below.



Source: Tomorrow's Cities

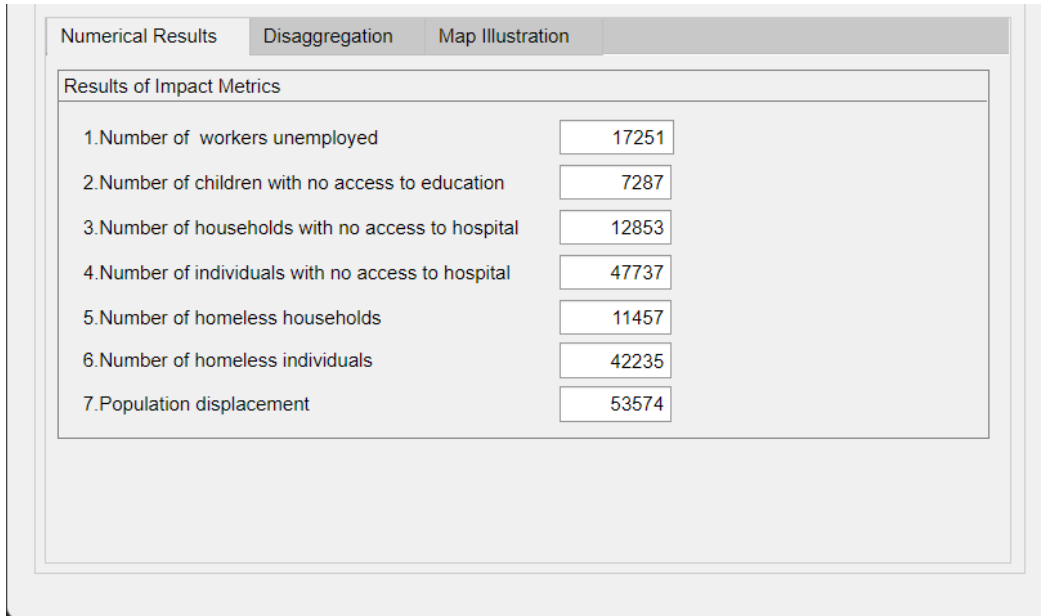
Figure 140: Policy page

Users can define the relationship between the damage states and corresponding consequences by using the sliders. By default, moderate or above damage states affect the consequences for earthquakes. These slides will become continuous for flood and debris flow. The policy list will be updated later on. For now, no policy is a default option. Calculate Impact Metrics button will trigger the computation of metrics which will be described in the next section.

Results:

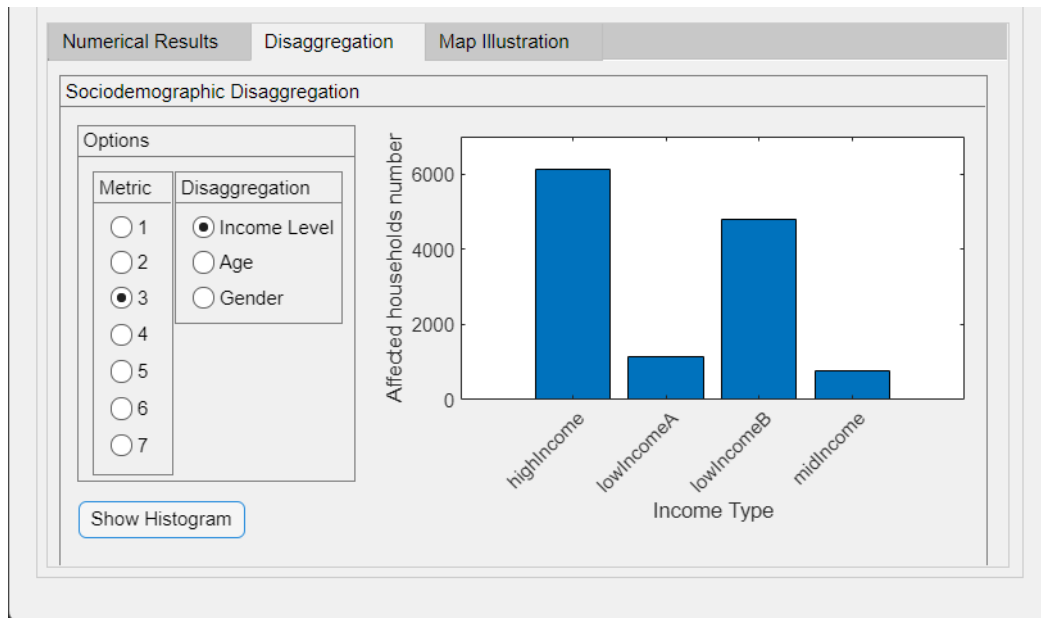
Numerical Results, Disaggregation and Map Illustration tabs are used to provide impact metric results with different perspectives. The numerical results tab shows the result of the metrics without any normalization. The disaggregation tab provides information in detail with respect to income level, age and gender for corresponding impact metrics. Map Illustration tab helps user to check the results on a map with different switch options on the left side. Users will be able to check normalized and absolute values of the impact metrics. In addition, root cause or residential places can be seen on the map. The gauge on the right side gives percentage/absolute information about the related impact metrics. List box can be used to choose different impact metrics, and the exact results can still be seen on the text box.





Source: Tomorrow's Cities

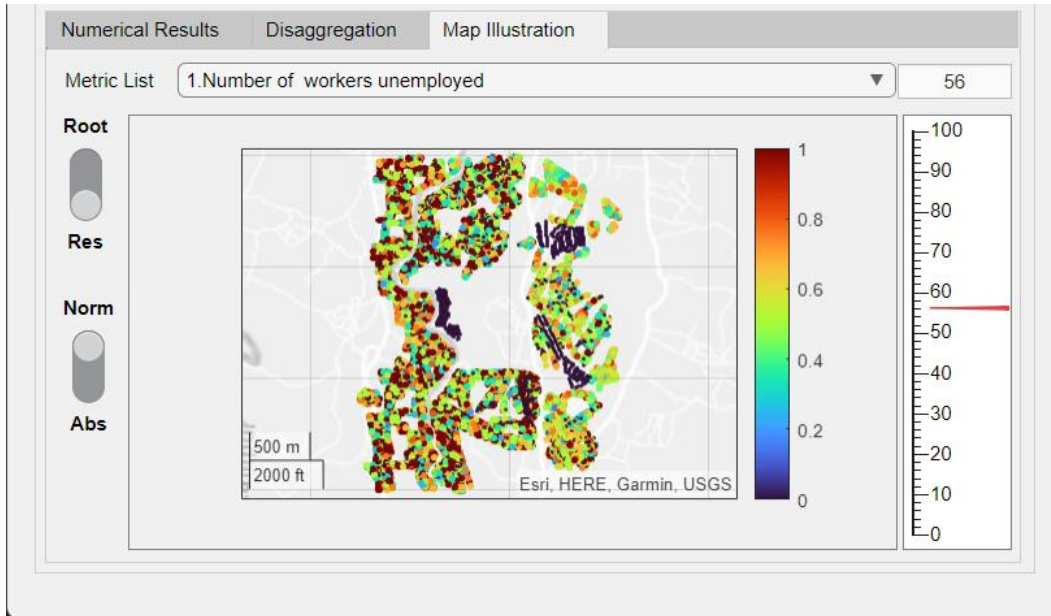
Figure 141: Numerical results example



Source: Tomorrow's Cities

Figure 142: Disaggregation example





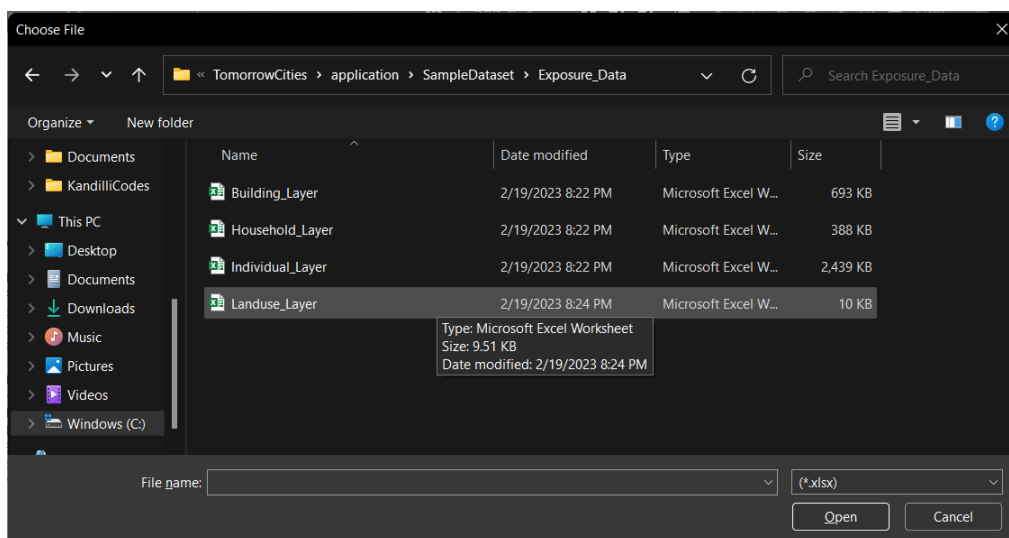
Source: Tomorrow's Cities

Figure 143: Map illustration example

14.5 TUTORIAL

This is a step-by-step tutorial for calculating the impact metrics. After the successful installation of the desktop application, run the program by double clicking. In order to avoid problems with file writing operations, you can open the program by right-clicking and giving it admin privileges.

In the main page, push the Computational Modeling button to proceed. In order to load exposure data, click Load button in the Exposure Data panel, and choose the appropriate layer in the following path *C:\Program Files \TomorrowCities \application\SampleDataset \Exposure Data*. This path could be different with respect to your installation folder; however, Load button will direct you to SampleDataset folder. At this step, you can even push the Save Exposure Data button to save them in a folder you want.



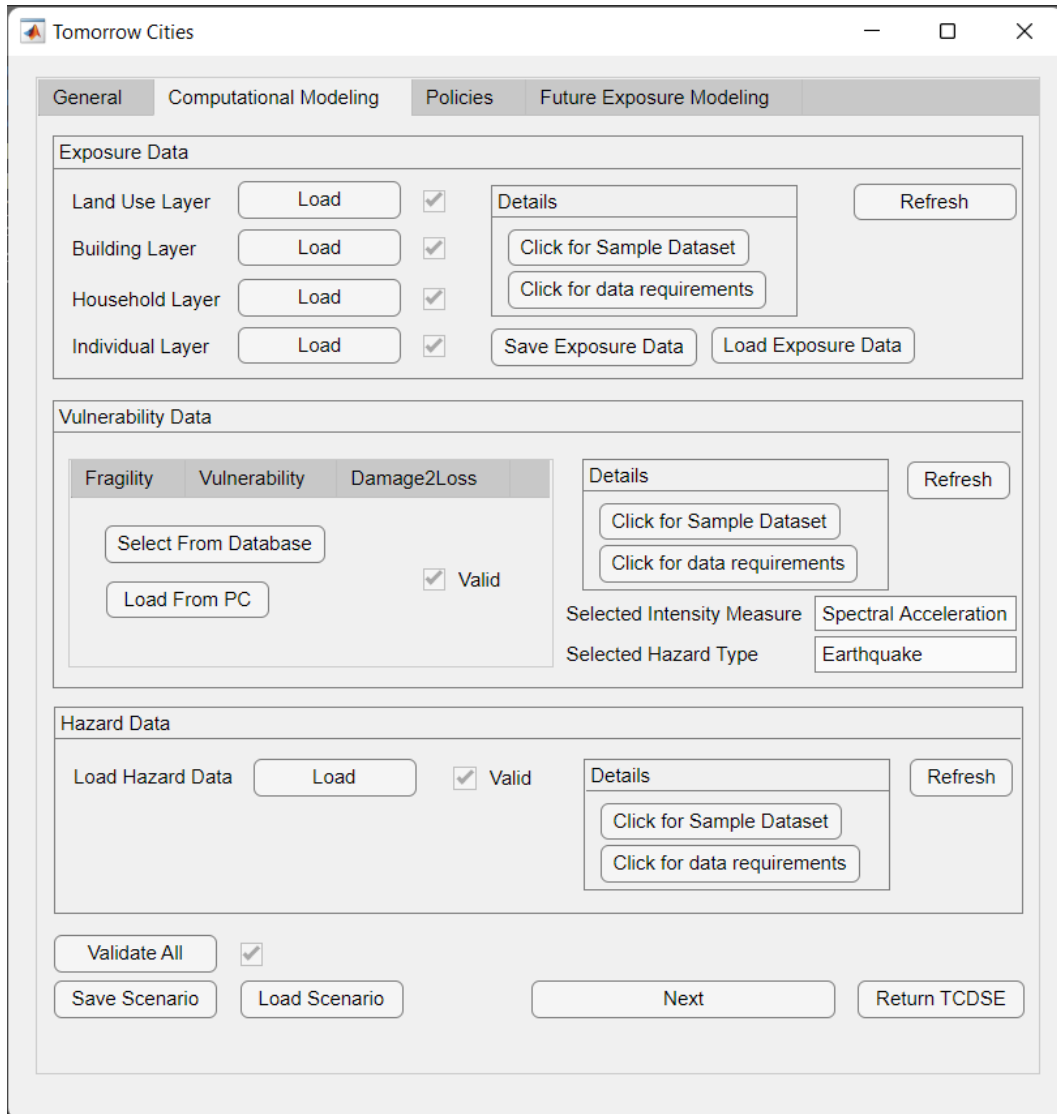
Source: Tomorrow's Cities

Figure 144: Loading exposure data from the corresponding path



In the Vulnerability Panel, choose Fragility tab and push Load From PC button and find out related fragility.xlsx file under the SampleDataset\Vulnerability Data folder. You will see Spectral Acceleration text in the Selected Intensity Measure textbox, and Selected Hazard Type textbox will be filled with Earthquake.

In the Hazard Data panel, open the SampleDataset\Hazard Data folder, and choose hazard eq.xlsx. Finally, push the Validate All button and click next. These steps will finalize the input sections in the computational modeling.

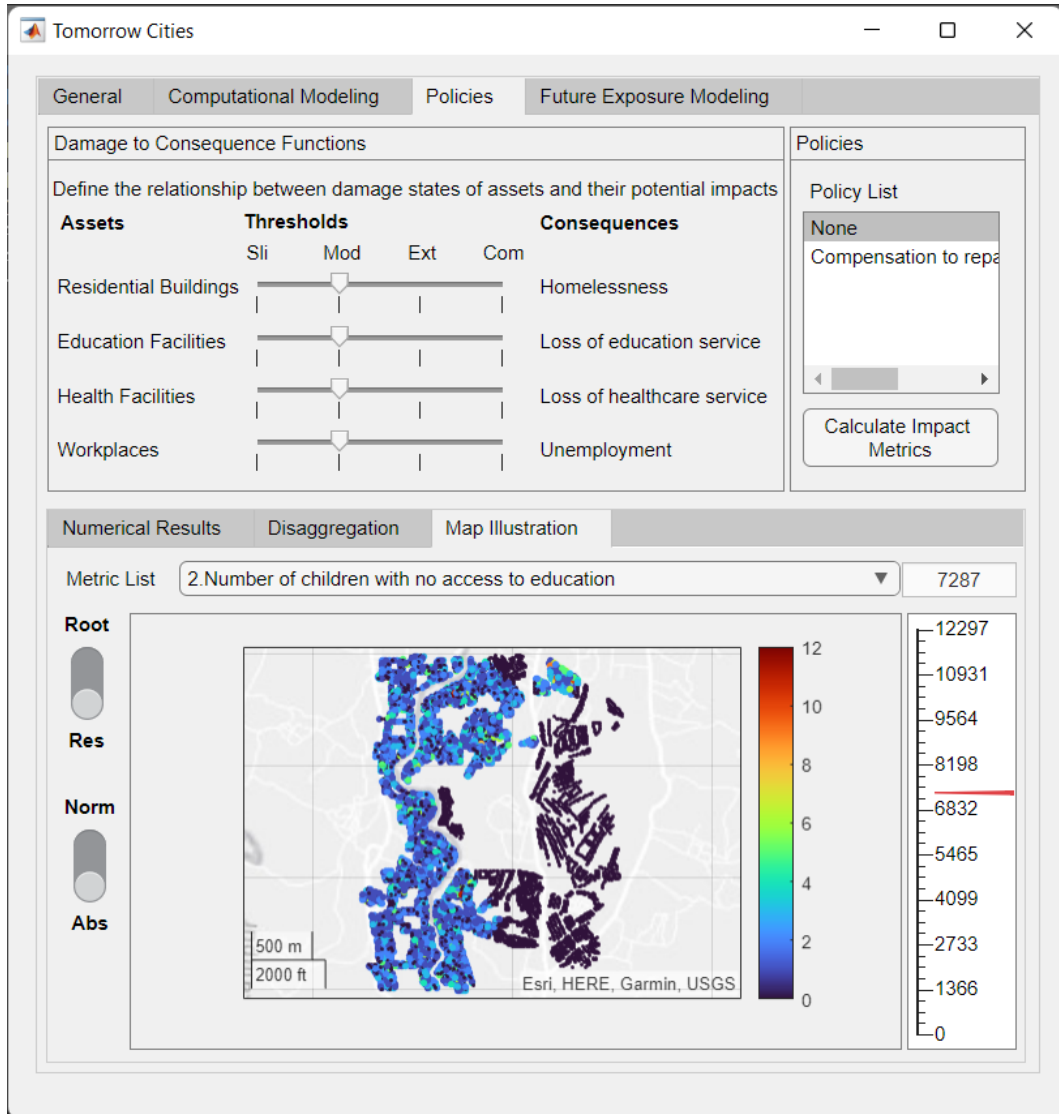


Source: Tomorrow's Cities

Figure 145: Loading data, and validate all

In the Policies screen, you do not need to change the sliders values, yet it is recommended to see the effect of different thresholds. Press Calculate Impact Metrics button and obtain the results of impact metrics. You can navigate through different tabs and learn details about social disaggregation or get information on a map. Finally, if you would like to see the effects of different thresholds, move the slider and press the Calculate Impact Metrics button. Results will be updated automatically. [59]





Source: Tomorrow's Cities

Figure 146: Policies screen



SESSION 15: LINKAGE OF MODULE 3 WITH OTHER MODULES

15.1 Objectives

By the end of the session, the participants will be able to:

- Recall the role of Module 3 within the broader context of the TCDSE.
- Explain how Module 3 relates to Module 2.
- Explain how Module 3 relates to Module 4.

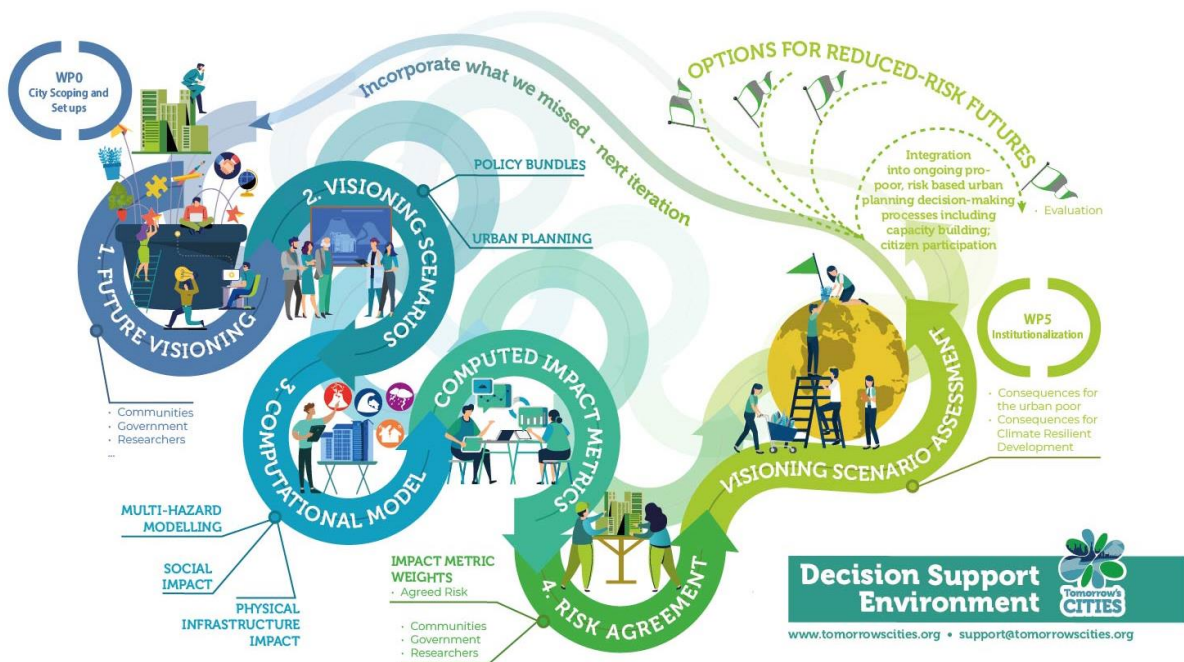
15.2 Structure of Session 15

Structure
1. Introduction
2. Linkage of Module 3 With Other Modules

15.3 Introduction

15.3.1 Recap of Module 3

In Module 3: Multi-hazard Physical and Social Impact Assessment we covered the core technical components of the TCDSE, which are the Computational Model and the Computed Impact Metrics that are obtained based on the calculations done within the various modules of the Computational Model.



Source: Tomorrow's Cities

Figure 147: Summary of Tomorrow's Cities Decision Support Environment

Please refer section 1.5 of Session 1: Introduction to Module 3 for details on each component of the TCDSE.



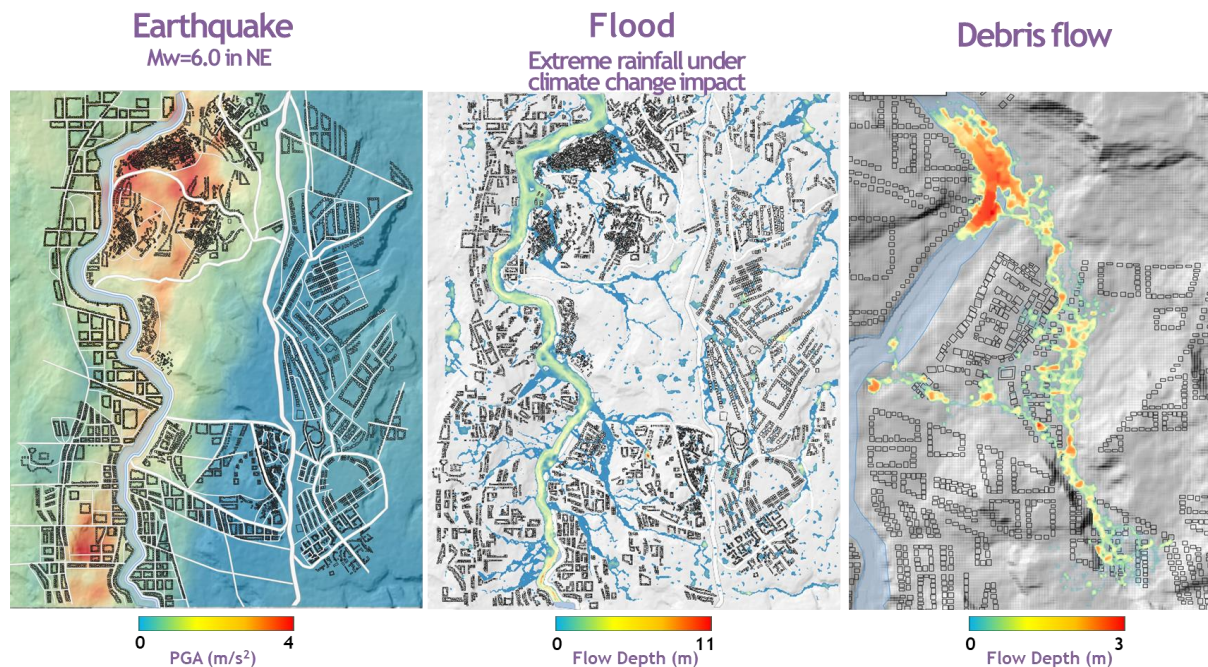
A. Computational Model

The Computational Model directly succeeds the phase of Visioning Scenarios of the TCDSE and it uses the information defined in Visioning Scenarios as an important input for its calculations. The outputs of the Computational Model are used to determine the Computed Impact Metrics, which subsequently act as key inputs to the Risk Agreement Module, which will be discussed in Module 4.

The Computational Model is composed of three modules:

B. Multi-hazard Modelling

Multi-hazard modelling involves modelling different types of natural hazards, to create a spatial map of hazard intensity measures associated with a specific hazard event, like the ones shown in the figure below. For instance, earthquake modelling might produce a map of peak ground acceleration values for a given earthquake. Module 3 covers various techniques and tools for modelling earthquakes, floods, debris flows, fires, landslides, as well as the effect of climate change. Not only that, but it also incorporates realistically contrived interrelationships between different hazards discussed in Session on Multi-hazard Vulnerability Modelling. For example, earthquake triggered tsunami and/ or liquefaction, wildfire followed by landslide. The outputs of this module serve as an input for intensity measures in the Physical Infrastructure Impact Module.



Source: Tomorrow's Cities

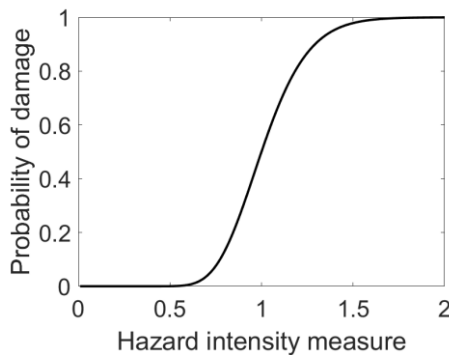
Figure 148: Scenarios for different hazards in Tomorrowville

C. Physical Infrastructure Impact

Module 3 also covers tools and techniques for modelling single- and multi-hazard effects on individual buildings. The hazard intensity measures output from the multi-hazard modelling process are input to various types of functions (for example, fragility functions) associated with the built environment in the physical infrastructure impact module, to determine the physical effects of the hazard event. Fragility models relate the probability of exceeding certain sets of damage level with relevant hazard intensity measures. In addition to physical effects of the



hazards, network level losses (such as infrastructure downtime) are also analysed as a part of a systemic approach for determining impact.



Source: Tomorrow's Cities

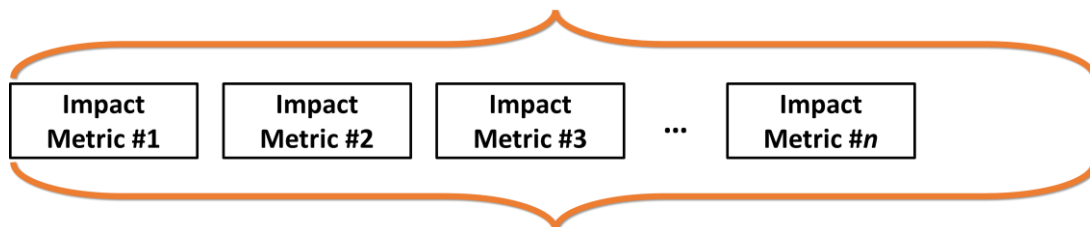
Figure 149: Typical Fragility Curve

D. Social Impact

Apart from physical effects, this module covers tools and techniques for modelling the effects of hazard event are integrated with social information (for example, that describes each person's daily dependence on the built environment) to characterise social impacts within the social impact module. The aim of Social Impact Module is to determine the differential impact on different social groups that the future multi-hazard scenarios might have in the city, particularly those that are most marginalised quantitatively and qualitatively.

15.3.2 Computed Impact Metrics

Outputs from the physical infrastructure impact and social impact modules are used to characterise formal quantitative or qualitative summaries of the impact of a natural hazard event on society, known as Computed Impact Metrics. These Impact Metrics are then used to compare and assess developed Visioning Scenarios in Stage 4: Risk Agreement of the TCDSE. Examples of Computed Impact Metrics include the number of people made homeless, the number of additional orphans, and the number of school days lost. These impact metrics can be economic, social, or environmental in nature.



Source: Tomorrow's Cities

Figure 150: Computed impact metrics for a visioning scenario

15.4 Linkage Of Module 3 With Other Modules

15.4.1 Linkage with Module 2

Firstly, the visioning scenarios covered in Module 2 act as important input to the first multi-hazard modelling module of the Computational Model. Specific characteristics of the urban form contained within the Visioning Scenarios can influence the values of the hazard intensity



measures output from the multi-hazard modelling module. For instance, flood depths may be increased by the presence of impermeable surfaces.

Furthermore, a Visioning Scenario contains complete information on what is exposed to the hazard intensity values output from the multi-hazard modelling module and therefore what (e.g., buildings, people, etc.) will be impacted by the occurrence of a hazard event. This information is also used to select appropriate impact models in the Computational Model. For instance, information on the height and construction material of a particular building stored within the building layer of the Visioning Scenario can be used to model the impact of an earthquake on that building, within the Physical Infrastructure Impact Module. Policy information captured in the Visioning Scenario can indicate the extent to which a particular level of damage to the built environment results in an impact on society. Finally, Visioning Scenario information can be used to guide the selection of relevant Computed Impact Metrics. For instance, the presence of a hospital within the building layer of a Visioning Scenario may suggest the use of a Computed Impact Metric that captures inaccessibility to hospital.

15.4.2 Linkage with Module 4

The Computed Impact Metrics, derived from the computational model, are presented to the stakeholders in Module 4, where they are tasked with prioritizing the metrics according to their preferences and their agenda. In other words, the stakeholders participate in activities to determine how important each metric is to them in a relative sense. Information on relative importance is translated into weightings. The corresponding weight is attached to each impact metric to convert it into a weighted impact metric. The weighted impact metrics are ultimately used to characterise “Agreed Risk”. Agree risk is a democratized measurement of the impact of a natural hazard event on society. It is a function of the objective values of the computed impact metrics that result from Module 3 and the subjective weights assigned to each metric that reflects stakeholders’ relative priorities.



REFERENCE

- [1] R. Gentile *et al.*, “Scoring, selecting, and developing physical impact models for multi-hazard risk assessment,” *International Journal of Disaster Risk Reduction*, vol. 82, p. 103365, Nov. 2022, doi: 10.1016/j.ijdr.2022.103365.
- [2] G. Ramesh, “Development of Earthquake Risk Assessment System for Nepal.” University of Tokyo(東京大学), Mar. 12, 2015. doi: 10.15083/00007589.
- [3] G. Cremen *et al.*, “A state-of-the-art decision-support environment for risk-sensitive and pro-poor urban planning and design in Tomorrow’s cities,” *International Journal of Disaster Risk Reduction*, vol. 85, p. 103400, Feb. 2023, doi: 10.1016/j.ijdr.2022.103400.
- [4] M. Pagani, V. Silva, M. Simionato, and K. Johnson, *OpenQuake Engine Manual*, Release 3.18.0. 2023.
- [5] B. Merz, J. Hall, M. Disse, and A. Schumann, “Fluvial flood risk management in a changing world,” *Nat. Hazards Earth Syst. Sci.*, vol. 10, no. 3, pp. 509-527, Mar. 2010, doi: 10.5194/nhess-10-509-2010.
- [6] L. Löschner, M. Herrnegger, B. Apperl, T. Senoner, W. Seher, and H. P. Nachtnebel, “Flood risk, climate change and settlement development: a micro-scale assessment of Austrian municipalities,” *Reg Environ Change*, vol. 17, no. 2, pp. 311-322, Feb. 2017, doi: 10.1007/s10113-016-1009-0.
- [7] J.-L. Kang, M.-D. Su, and L.-F. Chang, “Loss functions and framework for regional flood damage estimation in residential area,” *Journal of Marine Science and Technology*, vol. 13, no. 3, Sep. 2005, doi: 10.51400/2709-6998.2126.
- [8] N. S. Romali and Z. Yusop, “Flood damage and risk assessment for urban area in Malaysia,” *Hydrology Research*, vol. 52, no. 1, pp. 142-159, Feb. 2021, doi: 10.2166/nh.2020.121.
- [9] O. Hungr, S. Leroueil, and L. Picarelli, “The Varnes classification of landslide types, an update,” *Landslides*, vol. 11, no. 2, pp. 167-194, Apr. 2014, doi: 10.1007/s10346-013-0436-y.
- [10] M. C. Larsen and A. Simon, “A Rainfall Intensity-Duration Threshold for Landslides in a Humid-Tropical Environment, Puerto Rico,” *Geografiska Annaler. Series A, Physical Geography*, vol. 75, no. 1/2, p. 13, 1993, doi: 10.2307/521049.
- [11] E. A. Holcombe, M. E. W. Beesley, P. J. Vardanega, and R. Sorbie, “Urbanisation and landslides: hazard drivers and better practices,” *Proceedings of the Institution of Civil Engineers - Civil Engineering*, vol. 169, no. 3, pp. 137-144, Aug. 2016, doi: 10.1680/jcien.15.00044.
- [12] M. A. Moritz, M. E. Morais, L. A. Summerell, J. M. Carlson, and J. Doyle, “Wildfires, complexity, and highly optimized tolerance,” *Proc. Natl. Acad. Sci. U.S.A.*, vol. 102, no. 50, pp. 17912-17917, Dec. 2005, doi: 10.1073/pnas.0508985102.
- [13] A. F. Lutz, H. W. ter Maat, H. Biemans, A. B. Shrestha, P. Wester, and W. W. Immerzeel, “Selecting representative climate models for climate change impact studies: an advanced envelope-based selection approach: ADVANCED ENVELOPE-BASED CLIMATE MODEL SELECTION APPROACH,” *Int. J. Climatol.*, vol. 36, no. 12, pp. 3988-4005, Oct. 2016, doi: 10.1002/joc.4608.
- [14] M. Dolšek and P. Fajfar, “The effect of masonry infills on the seismic response of a four-storey reinforced concrete frame – a deterministic assessment,” *Engineering Structures*, vol. 30, no. 7, pp. 1991-2001, Jul. 2008, doi: 10.1016/j.engstruct.2008.01.001.
- [15] O. M. Nofal, J. W. van de Lindt, and T. Q. Do, “Multi-variate and single-variable flood fragility and loss approaches for buildings,” *Reliability Engineering & System Safety*, vol. 202, p. 106971, Oct. 2020, doi: 10.1016/j.res.2020.106971.



- [16] J. E. Daniell, A. M. Schaefer, and F. Wenzel, "Losses Associated with Secondary Effects in Earthquakes," *Front. Built Environ.*, vol. 3, p. 30, Jun. 2017, doi: 10.3389/fbuil.2017.00030.
- [17] J. C. Gill and B. D. Malamud, "Reviewing and visualizing the interactions of natural hazards: Interactions of Natural Hazards," *Rev. Geophys.*, vol. 52, no. 4, pp. 680-722, Dec. 2014, doi: 10.1002/2013RG000445.
- [18] A. E. Zaghi *et al.*, "Establishing Common Nomenclature, Characterizing the Problem, and Identifying Future Opportunities in Multihazard Design," *J. Struct. Eng.*, vol. 142, no. 12, p. H2516001, Dec. 2016, doi: 10.1061/(ASCE)ST.1943-541X.0001586.
- [19] Y. Wang and D. V. Rosowsky, "Characterization of joint wind-snow hazard for performance-based design," *Structural Safety*, vol. 43, pp. 21-27, Jul. 2013, doi: 10.1016/j.strusafe.2013.02.004.
- [20] A. Neri *et al.*, "Developing an Event Tree for probabilistic hazard and risk assessment at Vesuvius," *Journal of Volcanology and Geothermal Research*, vol. 178, no. 3, pp. 397-415, Dec. 2008, doi: 10.1016/j.jvolgeores.2008.05.014.
- [21] I. Zentner, M. Gündel, and N. Bonfils, "Fragility analysis methods: Review of existing approaches and application," *Nuclear Engineering and Design*, vol. 323, pp. 245-258, Nov. 2017, doi: 10.1016/j.nucengdes.2016.12.021.
- [22] N. Luco and C. A. Cornell, "Structure-Specific Scalar Intensity Measures for Near-Source and Ordinary Earthquake Ground Motions," *Earthquake Spectra*, vol. 23, no. 2, pp. 357-392, May 2007, doi: 10.1193/1.2723158.
- [23] A. C. Cornell, "Does duration really matter?" in: FHWA/NCEER Workshop on the National Representation of Seismic Ground Motion for New and Existing Highway Facilities.
- [24] V. Silva *et al.*, "Current Challenges and Future Trends in Analytical Fragility and Vulnerability Modeling," *Earthquake Spectra*, vol. 35, no. 4, pp. 1927-1952, Nov. 2019, doi: 10.1193/042418EQS1010.
- [25] G. Di Pasquale, G. Orsini, and R. W. Romeo, "New Developments in Seismic Risk Assessment in Italy," *Bulletin of Earthquake Engineering*, vol. 3, no. 1, pp. 101-128, Jan. 2005, doi: 10.1007/s10518-005-0202-1.
- [26] L. Martins and V. Silva, "Development of a fragility and vulnerability model for global seismic risk analyses," *Bulletin of Earthquake Engineering*, vol. 19, no. 15, pp. 6719-6745, Dec. 2021, doi: 10.1007/s10518-020-00885-1.
- [27] H.-Y. Noh, A. Kiremidjian, L. Ceferino, and E. So, "Bayesian Updating of Earthquake Vulnerability Functions with Application to Mortality Rates," *Earthquake Spectra*, vol. 33, no. 3, pp. 1173-1189, Aug. 2017, doi: 10.1193/081216eqs133m.
- [28] F. M. Al-Nammari and M. K. Lindell, "Earthquake recovery of historic buildings: exploring cost and time needs," *Disasters*, vol. 33, no. 3, pp. 457-481, Jul. 2009, doi: 10.1111/j.1467-7717.2008.01083.x.
- [29] D. N. Grant, "A mathematical form of probabilistic vulnerability model for loss and casualty ratios," *Earthquake Spectra*, vol. 36, no. 2, pp. 700-717, May 2020, doi: 10.1177/8755293019891719.
- [30] M. Caruso, R. Pinho, F. Bianchi, F. Cavalieri, and M. T. Lemmo, "Integrated economic and environmental building classification and optimal seismic vulnerability/energy efficiency retrofitting," *Bulletin of Earthquake Engineering*, vol. 19, no. 9, pp. 3627-3670, Jul. 2021, doi: 10.1007/s10518-021-01101-4.
- [31] D. Shrestha *et al.*, "Rainfall extremes under future climate change with implications for urban flood risk in Kathmandu, Nepal," *Int. J. Disaster Risk Reduc.*, 2022.



- [32] K. Ali, R. M. Bajracharyar, and N. Raut, "Advances and Challenges in Flash Flood Risk Assessment: A Review," *J Geogr Nat Disast*, vol. 07, no. 02, 2017, doi: 10.4172/2167-0587.1000195.
- [33] J. Douvinet, D. Delahaye, and P. Langlois, "Measuring surface flow concentrations using a cellular automaton metric: a new way of detecting potential impacts of flash floods in sedimentary context," *geomorphologie*, vol. 19, no. 1, pp. 27-46, Jun. 2013, doi: 10.4000/geomorphologie.10112.
- [34] V. Silva, S. Brzev, C. Scawthorn, C. Yepes, J. Dabbeek, and H. Crowley, "A Building Classification System for Multi-hazard Risk Assessment," *Int J Disaster Risk Sci*, vol. 13, no. 2, pp. 161-177, Apr. 2022, doi: 10.1007/s13753-022-00400-x.
- [35] C. Yepes-Estrada *et al.*, "The Global Earthquake Model Physical Vulnerability Database," *Earthquake Spectra*, vol. 32, no. 4, pp. 2567-2585, Nov. 2016, doi: 10.1193/011816EQS015DP.
- [36] Crowley *et al.*, *European Seismic Risk Model (ESRM20)*. IT: Eucentre, 2021. Accessed: Apr. 10, 2023. [Online]. Available: <https://doi.org/10.7414/EUC-EFEHR-TR002-ESRM20>
- [37] S. P. Stefanidou, E. A. Paraskevopoulos, V. K. Papanikolaou, and A. J. Kappos, "An online platform for bridge-specific fragility analysis of as-built and retrofitted bridges," *Bull Earthquake Eng*, vol. 20, no. 3, pp. 1717-1737, Feb. 2022, doi: 10.1007/s10518-021-01299-3.
- [38] M. S. Alam, B. G. Simpson, and A. R. Barbosa, *Defining Appropriate Fragility Functions for Oregon. A Report for the Cascadia Lifelines Program (CLiP)*. 2020.
- [39] K. Pitilakis, P. Franchin, B. Khazai, and H. Wenzel, Eds., *SYNER-G: Systemic Seismic Vulnerability and Risk Assessment of Complex Urban, Utility, Lifeline Systems and Critical Facilities: Methodology and Applications*, vol. 31. in Geotechnical, Geological and Earthquake Engineering, vol. 31. Dordrecht: Springer Netherlands, 2014. doi: 10.1007/978-94-017-8835-9.
- [40] CAPRA, *Integrating Disaster Risk Information into Development Policies and Programs in Latin America and the Caribbean, 2012*.
- [41] I. Bombelli, D. Molinari, P. Asaridis, and F. Ballio, "The 'Flood Damage Models' repository," in *Science and practice for an uncertain future*, Online: Budapest University of Technology and Economics, 2021, p. null-null. doi: 10.3311/FloodRisk2020.11.3.
- [42] T. Rossetto, I. Ioannou, and D. Grant, "Existing empirical fragility and vulnerability functions: compendium and guide for selection, Report 2015-1 .," *GEM Technical*, 2015, doi: <https://doi.org/10.13117>.
- [43] G. M. Calvi, R. Pinho, G. Magenes, J. J. Bommer, L. F. Restrepo-Velez, and H. Crowley, "Development of seismic vulnerability assessment methodologies over the past 30 years," *Journal of Earthquake Technology* 43, no. 43, pp. 75-104, 2006.
- [44] L. Martins and V. Silva, "Development of a fragility and vulnerability model for global seismic risk analyses," *Bull Earthquake Eng*, vol. 19, no. 15, pp. 6719-6745, Dec. 2021, doi: 10.1007/s10518-020-00885-1.
- [45] European Commission. Joint Research Centre., *Global flood depth-damage functions: methodology and the database with guidelines*. LU: Publications Office, 2016. Accessed: Apr. 10, 2023. [Online]. Available: <https://data.europa.eu/doi/10.2760/16510>
- [46] T.L. Saaty, *The Analytical Hierarchy Process*, McGraw-Hill, New York, USA, 1980.
- [47] R. Gentile and C. Galasso, "Simplified seismic loss assessment for optimal structural retrofit of RC buildings," *Earthquake Spectra*, vol. 37, no. 1, pp. 346-365, Feb. 2021, doi: 10.1177/8755293020952441.
- [48] CL. Ching, L. Hwang, and K. Yoon, *Multiple Attribute Decision Making: Methods and Applications A State-Of-The-Art Survey*. Springer Berlin Heidelberg, 1981.



- [49] N. Caterino, I. Iervolino, G. Manfredi, and E. Cosenza, "Comparative Analysis of Multi-Criteria Decision-Making Methods for Seismic Structural Retrofitting," *Computer-Aided Civil and Infrastructure Engineering*, vol. 24, no. 6, pp. 432-445, Aug. 2009, doi: 10.1111/j.1467-8667.2009.00599.x.
- [50] L. T. Jenkins *et al.*, "Physics-based simulations of multiple natural hazards for risk-sensitive planning and decision making in expanding urban regions," *International Journal of Disaster Risk Reduction*, vol. 84, p. 103338, Jan. 2023, doi: 10.1016/j.ijdrr.2022.103338.
- [51] E.Y. Mentese, G. Cremen, R. Gentile, M.E. Filippi, C. Galasso, J. McCloskey, *Risk-informed urbanisation scenario development through interdisciplinary and GIS-based processes, Int. J. Disaster Risk Reduc. (2022) under rev.*
- [52] *NBC, Nepal National Building Code, 201, 1994. Kathmandu, Nepal.*
- [53] S. Akkar, H. Sucuoğlu, and A. Yakut, "Displacement-Based Fragility Functions for Low- and Mid-rise Ordinary Concrete Buildings," *Earthquake Spectra*, vol. 21, no. 4, pp. 901-927, Nov. 2005, doi: 10.1193/1.2084232.
- [54] M. A. Erberik, "Fragility-based assessment of typical mid-rise and low-rise RC buildings in Turkey," *Engineering Structures*, vol. 30, no. 5, pp. 1360-1374, May 2008, doi: 10.1016/j.engstruct.2007.07.016.
- [55] D. Gautam, G. Fabbrocino, and F. Santucci de Magistris, "Derive empirical fragility functions for Nepali residential buildings," *Engineering Structures*, vol. 171, pp. 617-628, Sep. 2018, doi: 10.1016/j.engstruct.2018.06.018.
- [56] R. Gentile and C. Galasso, "Simplicity versus accuracy trade-off in estimating seismic fragility of existing reinforced concrete buildings," *Soil Dynamics and Earthquake Engineering*, vol. 144, p. 106678, May 2021, doi: 10.1016/j.soildyn.2021.106678.
- [57] J. C. S. Tang, S. Vongvisessomjai, and K. Sahasakmontri, "Estimation of flood damage cost for Bangkok," *Water Resour Manage*, vol. 6, no. 1, pp. 47-56, 1992, doi: 10.1007/BF00872187.
- [58] N. Sharma and P. Gardoni, "Mathematical modeling of interdependent infrastructure: An object-oriented approach for generalized network-system analysis," *Reliability Engineering & System Safety*, vol. 217, p. 108042, Jan. 2022, doi: 10.1016/j.ress.2021.108042.
- [59] D. Goktekin, *User Manual Tomorrow's Cities*. 2023.







UK Research
and Innovation



NSET
Disaster Resilient Communities in Nepal

Tomorrow's Cities is the UKRI GCRF Urban Disaster Risk Hub

"Tomorrow's Cities" is the UKRI GCRF Urban Disaster Risk Hub-one of twelve global interdisciplinary research hubs funded by an UK Research and Innovation Collective Fund Award

www.tomorrowscities.org

Key Contacts

Mark Pelling

Tomorrow's Cities
Director
mark.pelling@ucl.ac.uk

Hugh Sinclair

Tomorrow's Cities
Principal Investigator
hugh.sinclair@ed.ac.uk

Carmine Galasso

Senior Management
Team Member
c.galasso@ucl.ac.uk

Ramesh Guragain

Senior Management Team Member
Capacity Strengthening Lead
rguragain@nset.org.np